12-2008

'Fabrication and Characterization of Polymer Blends and Composites Derived from Biopolymers'

Suraj Sharma
Clemson University, ssharma@g.clemson.edu

FABRICATION AND CHARACTERIZATION OF POLYMER BLENDS AND COMPOSITES DERIVED FROM BIOPOLYMERS

A Dissertation
Presented to
the Graduate School of
Clemson University

In Partial Fulfillment
of the Requirements for the Degree
Doctor of Philosophy
Materials Science and Engineering

---

by
Suraj Sharma
December 2008

Accepted by:
Dr. Igor A. Luzinov, Committee Chair
Dr. Gary C. Lickfield
Dr. Philip J. Brown
Dr. Bogdan Zdyrko

ABSTRACT

This research focuses on fabricating blends and composites from natural polymers especially from proteins and natural epoxy, and describing the properties of plastics made from them. Specifically, plastic samples from partially denatured feathermeal and bloodmeal proteins, derived from the animal co-products (rendering) industry, were successfully produced through a compression molding process. The modulus (stiffness) of the material obtained was found to be comparable with that of commercial synthetic materials, such as polystyrene, but was found to have lower toughness characteristics, which is a common phenomenon among plastics produced from animal and plant proteins. Therefore, this study explored blending methods for improving the toughness. Plastic forming conditions for undenatured animal proteins such as chicken egg whites albumin and whey, used as a model, were established to prepare plastics from their blends with animal co-product proteins. The resultant plastic samples from these biomacromolecular blends demonstrated improved mechanical properties that were also compared with the established theoretical models known for polymer blends and composites. Moreover, plastics from albumin of chicken egg whites and human serum have demonstrated their potential in medical applications that require antibacterial properties.

Another natural polymer vegetable oil-based epoxy, especially epoxidized linseed oil, showed significant potential to replace petroleum-derived resins for use as a matrix for composites in structural applications. Moreover, the research showed the benefits of ultrasonic curing, which can help in preparing the out-of-autoclave composites.

DEDICATION

This work is dedicated to my wife Mrs. Kanta Sharma, my daughter Shriya Sharma, my parents Mrs. Leela Sharma and Late Mr. Purushottam Lal Sharma, my in-laws Retd. Lt. Col. Ramchandra Sharma and Mrs. Maina Sharma and to the rest of my family members for their love and support.

ACKNOWLEDGMENTS

I would like to thank my advisor Dr. Igor Luzinov for providing all his support and this opportunity to conduct the research. He was very understanding, and it was never stressful working under his tutelage. He was an excellent mentor who improved my productivity and honed my professional skills, greatly required for today's competitive job market. His critics not only helped me in my research but in other spheres of life also.

I would like to thank my committee members Dr. Gary C. Lickfield, Dr. Philip J. Brown, Dr. Bogdan Zydrko for their guidance, suggestions and encouragement. Dr. Lickfield was always available to advise me on any matter including research despite his busy schedule. I am greatly influenced by his caring attitude for my professional growth. Dr. Brown helped me to shape my skills desired for the professional growth, while providing his invaluable advice during my research. Dr. Zydrko provided his critical reviews, and was always available to help me during my research. I would like to specially thank Dr. Viktor Z. Klep, former member of Dr. Luzinov's group, for his guidance, help and suggestions. I would also like to acknowledge Dr. Konstantin Kornev for his advice and guidance.

I would also like to thank my current and past group members for maintaining a great work atmosphere at the lab: Dr. Karthik Ramaratnam, Dr. Yong Liu, Dr. Olha Hoy and her husband Mr. Taras Andrukh, Mr. Oleksandr Burtovyy, Dr. Volodymyr Tsyalkovsky, Dr. Ruslan Burtovyy and Mr. Zhenqing Li, Marius Chyasnavichyus and Ms. Fehime Vatansever. I would like to thank Ms. Kimberly Ivey and Ms. Robbie Nicholson for their assistance during the course of my research work.

I would also like to specially thank the under-graduate student James N. Hodges, who worked with me in my research work. I warmly thank Dr. Richard Aspland, Dr. Bhuvenesh Goswami, Dr. Stephen Foulger, and Dr. Michael Ellison for their wonderful teaching and guidance during my course work at Clemson University. And finally, I would like to thank the School of Materials Science and Engineering, CAEFF, and the ACREC for their financial support.

TABLE OF CONTENTS

Page

LIST OF TABLES

LIST OF FIGURES

List of Figures (Continued)

Figure **Page**

List of Figures (Continued)

Figure **Page**

List of Figures (Continued)

Figure **Page**

List of Figures (Continued)

Figure **Page**

List of Figures (Continued)

Figure **Page**

List of Figures (Continued)

Figure **Page**

CHAPTER 1

INTRODUCTION

Biodegradable materials from natural resources have become an intense research topic because of their availability from renewable resources. Though this research in general has become widespread, studies pertinent to plastics from animal co-product proteins (partially denatured) are limited. Therefore, this research is primarily focused on understanding the fundamental concepts involved in the fabrication and preparation of plastics and composites form these proteins. This research explored the potential of feathermeal and bloodmeal, animal co-product proteins to prepare plastics with characteristics that make these proteins suitable for various technical applications, where biodegradability is important. The study also extends to plastics from undenatured animal and human proteins since they are used as a model for these investigations and demonstrated first time their potential in medical applications, which requires increased biocompatibility. This study could open avenues for preparing typically non-recyclable articles, such as golf tees, flower pots, hunting bullets and discs, and in developing and modifying various medical devices, including, stents, and artificial arteries.

The depleting resources of fossil oils are also adversely affecting the thermoset resins, especially epoxy system used in high-performance applications. Therefore, biodegradable natural epoxy from modified vegetable oils can play a significant role to replace traditional epoxy system used mainly as matrix for composites. A literature review associated to protein plastics and epoxy systems (both natural and model) is

presented in **Chapter 2**. The general experimental procedures followed for most of the research reported here are discussed in **Chapter 3**.

In **Chapter 4**, model undenatured animal proteins were used to understand the fundamentals of plastic fabrication through a compression molding process. Albumins from chicken egg whites and human serum produced plastics with antimicrobial and shape memory characteristics, which are important for bioimplants and drug delivery devices. Unresolved issue of protein plastics, such as increased stiffness on storage, was specifically addressed through polymer blending in the following chapter.

In **Chapter 5**, blending technology was explored to develop plastics of desired properties, which is difficult to achieve using single component. Therefore, to address the issue of toughness, polymer plastic samples were prepared from the blends of undenatured chicken egg albumin and whey proteins, and from the blends of whey protein and natural rubber latex, through the compression-molding process.

Natural rubber latex, stabilized by protein in suspension, was used to produce polymer blends. The addition of dispersed rubber particles improved the toughness of the protein plastics. Thermal and mechanical characterizations were conducted to study the effect of blending. Moreover, protein-protein blends, which utilize their complimentary properties, were prepared to develop plastics of desired properties. The results were compared using “mixing rule” for polymer blends. Moreover, protein sequencing was used to determine reactive functional groups, such as amino, carboxylic and hydroxyl, of the amino acid residues.

Excessive availability of animal co-product (or rendered) proteins on a renewable basis has forced rendering industries to explore alternative uses, such as fuel, fertilizers, and plastics in addition to the traditional use as an ingredient for animal feed. Based on the investigations in **Chapters 4 and 5** with undenatured, animal proteins as a model for preparing plastics, a different approach was studied to prepare plastics from partially denatured, feathermeal protein as described in **Chapter 6**. This research explored the animal co-product protein, feathermeal, which is mostly used as a feeding ingredient in animal feed, to develop plastic. This partially denatured protein exhibited strong potential for various technical applications, which are difficult to recycle.

Feathermeal protein exhibited thermoplasticity and produced plastics having lower tensile strength and elongation properties, but higher stiffness than undenatured, protein plastics. In addition, stiffness (Young's modulus) was found to be comparable or more than that of commercial plastics, such as polystyrene and polycarbonate. To address plastic weaknesses, polymers blends were prepared using undenatured proteins, such as chicken egg whites albumin and whey, and a synthetic rubbery polymer, for example poly (glycidyl methacrylate)-co-(butyl methacrylate) copolymer. Moreover, these mechanical properties were compared with well-established, theoretical models for polymer blends and composites.

In **Chapter 7**, another co-product protein, bloodmeal, which is primarily used as an ingredient in animal feed, was successfully first time, transformed into plastics through the compression-molding process. The approach here involves direct compression molding of bloodmeal without adding any additional water. Detailed

investigations, including modeling of the mechanical properties, were conducted to prepare polymer blends using bloodmeal and undenatured whey and chicken egg whites albumin proteins to address the issue of toughness. In addition, whey modified natural fiber, hemp, was used to prepare biocomposites.

The research in **Chapter 8** reports that vegetable oil-based epoxy, especially epoxidized linseed oil, showed significant potential to replace petroleum-derived resins to be used as a matrix for composites in structural applications. Moreover, the research showed the benefits of ultrasonic curing, which can help in preparing the out-of-autoclave composites.

Thus, thermal and ultrasonic curing of vegetable oil based epoxy systems such as epoxidized linseed and epoxidized soybean oils, along with model one-part epoxy system, are investigated. In these natural epoxy systems, the addition of a latent curing agent, BPH (Benzylpyrazinium Hexafluoroantimonate), assisted in a full curing and developing a formulation with increased shelf life. In addition, ultrasonic curing, a non-traditional curing method, was studied to accelerate the curing process that may have potential in developing out-of-autoclave composites at low cost. Moreover, to investigate the thermal curing process, and the non-thermal and thermal effects of ultrasonic curing process, a model one-part epoxy system was used. An application of ultrasonic curing in preparing composites from carbon/epoxy prepreg system is illustrated in **Appendix I**, which details the possibilities and limitations of using Solidica's ultrasonic consolidation machine.

Therefore, this research adds to the existing knowledge about the fabrication of plastics from undenatured and partially-undenatured proteins, and natural epoxy system.

CHAPTER 2

LITERATURE REVIEW

This research focuses on fabricating blends and composites from biopolymers, with a particular emphasis on proteins and natural epoxies. Therefore, an overview of the theoretical considerations of creation of biodegradable materials from these biopolymers and the current methods practiced to fabricate plastics and composites is presented. In addition, the research pertinent to traditional epoxy-based composites and their fabrication using ultrasonic curing is also discussed.

2.1: Biodegradable plastic

Synthetic polymers, for example polyethylene and polypropylene, are not biodegradable and persist in the environment for many years after their disposal.[1] Their environmental impact is exacerbated by their extensive use in packaging materials, industrial products, medical devices, coatings and hygiene products. The issue becomes what to do with articles made from these materials once they are no longer useful.[2] Incineration represents one solution, but this process releases toxic substances into the environment. Another solution is recycling; poly(ethylene terephthalate) and high-density poly(ethylene) bottles, for example, can be recycled, e.g., as fibers for stuffing and as plastic lumber.

However, the dwindling availability of landfill sites, in addition to rising oil prices, has necessitated the development of biodegradable materials as substitutes for non-degradable plastics. Polymers from agricultural by-products[1] are especially attractive

as replacements for synthetic polymers,[3] the most important of these natural polymers being carbohydrates (starch, cellulose), proteins, and nucleic acids (DNA, RNA).[2] This third solution to the disposal or pollution problem arising from synthetic material is challenging because it is often the durability of plastics that makes them so useful.[2]

Biopolymers degrade, through the enzymatic action of bacteria, fungi, algae and other living organisms, into carbon dioxide, methane, water, inorganic compounds, or biomass and therefore do not persist in the environment. These types of biopolymers can be classified into three categories:[4]

- Those directly extracted from biomass;
- Those produced through chemical synthesis from biomass monomers;
- Those, such as microbial polymers, produced directly by natural or genetically modified organisms.

These categories are schematically presented in **Figure 2.1**. As this figure shows, biodegradable and green polymers can be converted into various forms including neat polymers, blended products, and composites.[1] For example, natural biopolymers have been employed for use in the manufacturing of plastic containers, exemplified by the use of a PHB (poly(3-hydroxybutyrate))-PHV(poly(3-hydroxyvalerate)) copolymer (BIOPOL) in the manufacturing of shampoo bottles.[2]

Bioplastics can be made using either a dry or a wet process.[5] The wet-process, which requires biopolymer dispersion in a film-forming solution, has been successfully applied to produce edible or biodegradable films and coatings. The dry-process, capitalizing on the thermoplastic properties of various biopolymers(primarily starch and

protein under lower water content conditions), has also been successfully applied to produce edible and/or biodegradable materials using such common melt processing technologies as extrusion, molding or rolling mill procedures. Since the use of solvents in the wet-process is not environmentally friendly, the dry-process of making plastics from starch, protein and lactic acid polymers is receiving increased attention.

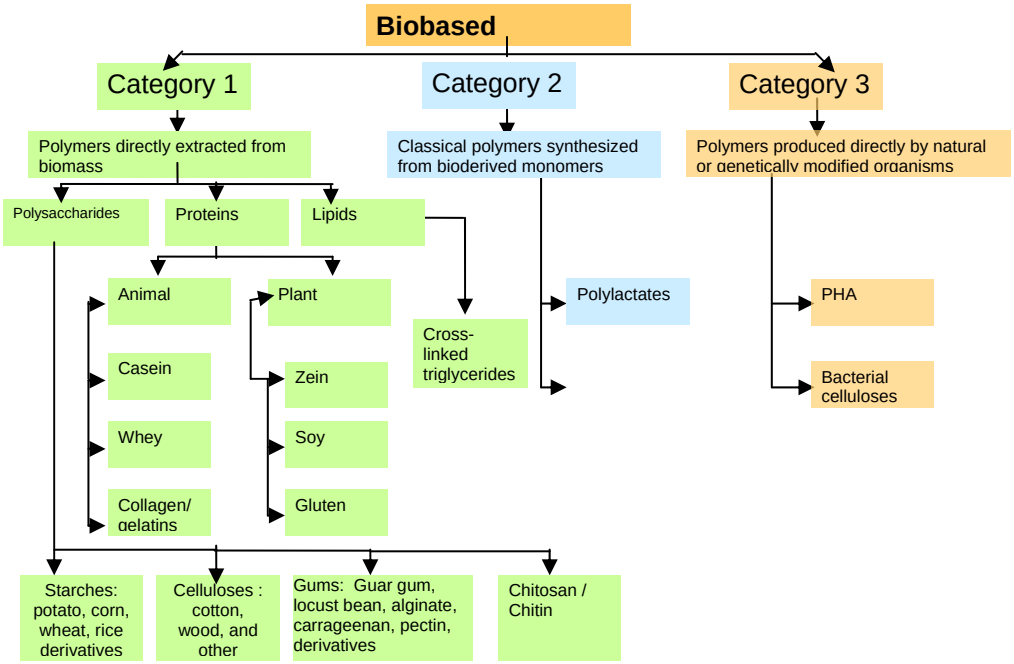

Figure 2.1. Schematic of biopolymers based on their origin and method of production.[4]

In particular, much research has been conducted that focuses on plastics made from lactic acid polymer. For example, Hermann et al.[6] used lactic acid derivatives to produce biodegradable composites with mechanical properties comparable to the more common glass-fiber reinforced ones, offering new materials for anisotropic and light-weight structural parts. In addition, Hu and Lim[7] developed polylactic acid composites

reinforced with biodegradable hemp fibers that showed improved mechanical properties. They also observed that alkali-treated hemp fibers produced composites of increased tensile and flexural strengths. In a similar study, Huda et al.[8] developed polylactic acid laminates, reinforced with kenaf fiber, having good mechanical and thermo-mechanical properties. However, the process for synthesizing lactic acid is costly, an expense that will probably continue to rise given the emphasis on corn as an alternative fuel.

A second area of research has focused on the development of thermoplastic starches (TPS) from maize, wheat, potato, or tapioca, which is subjected to a destructurization of intermolecular hydrogen bonding.[9] However, TPS-based bioplastics have significant disadvantages including inferior mechanical properties and high water absorption. To address these concerns, Carvalho et al.[10] mixed starch with natural rubber blends, developing a biodegradable starch-based plastic that had notably improved toughness.

One of the most important areas of current research involves using natural polymer proteins from animal and plants. These bioplastics have significant advantages over traditional plastics, especially in such areas as packaging. For example, soy protein has become an alternative to petroleum polymers in the manufacture of adhesives, plastics, and binders.[11,12] Studies have shown that plastics and polymer blends made from this protein exhibit increased strength and improved biodegradability. In addition, proteins are very versatile materials, originating from many sources, and because of the possible modifications, can exhibit a wide range of tuneabilities, allowing them to be easily tailored to fit a specific application. As a result, it is important to investigate the

development of material made from animal proteins, a renewable resource, especially abundant currently because of the outbreak of Bovine Spongiform Encephalopathy (BSE) or Mad Cow Disease.

A non-biodegradable synthetic polymer, epoxy is one of the most important petroleum-based thermoset polymers, and is widely used as a binder for high performance fiber-reinforced composites and laminates in various structural applications. However, processing of these is time consuming and expensive, requiring intensive research to substitute or partially replace them with natural epoxy originating from plant-based oils and to process them using unconventional methods, specifically ultrasonic curing.

2.2: Protein plastic

2.2.1: Protein denaturing and structurization of plastic

Protein, a group of complex organic compounds (heteropolymers), consists of combinations of polar and apolar amino acids in peptide linkages.[13] These amino acid residues are able to form numerous intermolecular bonds and interactions, resulting in a broad range of potential functional properties. [14] The amino acid sequence is the primary structure of the polypeptide protein chain, forming alpha helices and beta sheets, constituting the secondary structure. The three-dimensional conformation formed by a polypeptide chain is sometimes referred to as the tertiary structure, and if a particular protein molecule is formed as a complex of more than one polypeptide chain, then the complete structure is designated as a quaternary structure.

Proteins can be unfolded or denatured from their higher order structures when the disulfide bonds and weak non-covalent interactions holding the folded chain are broken.[15,16] Hawley[17] developed a thermodynamic description of the phase boundary of protein unfolding and was able to calculate the Gibbs free energy difference (ΔG) between the denatured and the native state of the protein, leading to an elliptical second order curve[18] for the given denaturating conditions (ΔG=0), as shown in **Figure 2.2**.

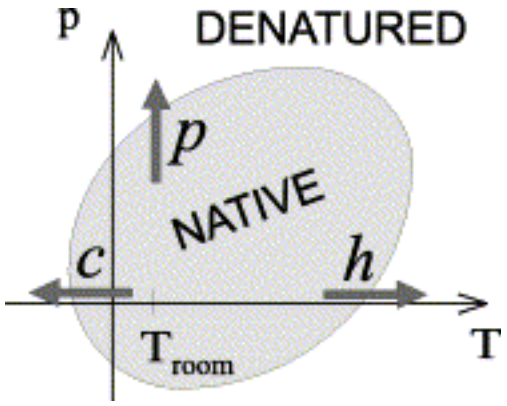

Figure 2.2. Schematic representation of the elliptic phase diagram of proteins. Where p--pressure, h--heat, and c--cold denaturations.[18]

This phase diagram can be divided into denatured and native regions. When the protein is in its native state, the effects of pressure and temperature result in an elastic (reversible) change, while at high pressure and high temperature, cooperative changes in the secondary structure produce a plastic or conformational effect, resulting in a change in the thermal expansion, the compressibility and the heat capacity of the proteins.[19]

The secondary structures, which are critical determinants in plastic formation, can be analyzed using FTIR and Raman spectroscopic techniques. For proteins distinct from synthetic polypeptides, the amide-I band is generally a broad composite, consisting of overlapping components of vibrational transitions associated with these secondary structures. It has been found that the intensity distribution across the amide-I bands (1700-1620cm^{-1}) of the IR can be resolved into components using Fourier deconvolution, correlating with the percentages of α-helices, β-structure, turns or any other type of secondary structure present.[20] The deconvoluted components can be classified based on an empirical comparison with the spectra arising from proteins known to contain only one major component (e.g., the α-helix of hemoglobin). Previous FTIR studies of various proteins confirmed that the deconvoluted amide-I band is comprised of a 1638 cm^{-1} and a 1687cm^{-1} band because of its β-sheet structure, a 1655 cm^{-1} band of α-helix or random coil structures, a 1670 cm^{-1} band of β-turns and a 1615 cm^{-1} band of intermolecular β-sheets due to protein aggregation.[21]

It has been found that higher order structures of proteins play an important role in the structurization of resulting plastics formed through thermal processing. During the heating of undenatured proteins, bonds of these higher order structures are weakened, resulting in a more flexible structure. If heating ceases at this stage, the protein should be able to readily refold, returning to its native structure. As heating continues, some of the cooperative hydrogen bonds that stabilize the helical structure will begin to break, and hydrophobic groups become exposed. The protein minimizes

its free energy by hiding the hydrophobic groups and exposing the polar groups at high temperatures, weakening the short-range interactions responsible for initial protein folding, and leading to a conformation different from the native protein. Moreover, the resulting structure of aggregated macromolecules resulting from cooling may not be of the lowest possible free energy because of kinetic barriers. Therefore, exposure of most proteins to high temperatures results in an irreversible denaturation.

2.2.2: Thermoplasticity of proteins

Proteins at approximately 100°C can be processed in the presence of a large amount of water or glycerol for such applications as coatings/films, adhesives and surfactants, or under low water contents through extrusion.[22] Water, low molecular-weight polyols, and oligosaccharides have been extensively used as plasticizers in the processing of protein plastics. Water, because of its high dielectric constant and capability of strong interactions with other polar molecules via hydrogen bonding, is important for the plasticizing effect, resulting in a reduction in the viscosity of the biopolymer-water mixtures and the fracture strength and elastic modulus of the bioplastic. These plasticizers shield the inter- and intra-molecular interactions, facilitate segmental molecular motion, and decrease internal friction in biopolymer materials.[23] This plasticization effect results in a reduction in the shaping or molding temperature of the thermoplastic process, imparts flexibility to the final material, and influences the functional properties as well.[24] Protein itself also contains plasticizing groups, the

efficiency of which is calculated using the Plasticizer equation introduced by Barone et al. [25] (**Equation 2.1**).

$$PE = \frac{(S + T + Y)}{C} \tag{2.1}$$

where S, T, Y, and C represent the weight % of amino acids serine, threonine, tyrosine, and cysteine, respectively, in such cysteine-containing proteins as the keratin found in avian feathers and feathermeal. This PE, which should be at least 2.5 to promote faster plasticization during thermal processing, signifies the number of mobile sites (i.e., S, T and Y amino acid residues) relative to the immobile sites (i.e., C amino acid residue) in protein macromolecules.

After plasticization, these proteins can be crosslinked using chemicals, heat and pressure to achieve the desired mechanical properties, through the formation of disulfide linkages, hydrogen bonds, hydrophobic interactions, and intra- and inter-molecular amine crosslinks.[14] Several plant and animal proteins, such as wheat and corn gluten, soy, pea, potato, casein, whey, collagen and keratin are available for producing plastic films. These proteins have good processability, both in the aqueous and melt media; good film forming properties; good mechanical properties in the resulting films, good adhesion to various substrates (coatings, adhesives), high resistance to UV, oils and organics, high barrier properties for O_2 and CO_2 gases, and good surface active properties.[26,27] Soy protein has been considered recently as an alternative to petroleum polymers in the manufacture of adhesives, plastics, and various binders.[11,28]

Paetau et al.[11] studied the preparation and processing conditions of soy plastic using compression molding. The strength of the plastic produced was comparable to

commercial polystyrene plastic. Based on their findings, it was observed that moisture, temperature and pressure were important factors in determining the mechanical and water resistance properties of this plastic. However, they could not resolve the problem of increased stiffness during storage and the lack of long-term stability, especially in the presence of water. Mo and Sun[29] studied the effects of storage time on the properties of soybean protein-based plastics. These plastics lost their toughness and became stiff and brittle over time. Sue and Jane[30] investigated the mechanical behavior of high protein content engineered soy plastics and compared these to commonly utilized petrochemical engineered plastics. They observed that the ductility and dimensional stability of soy plastics strongly depended on the level of moisture content or the level of plasticizer. **Figure 2.3** shows the dynamic mechanical spectra of various soy plastics compared to other engineered plastics.

Orliac et al.[31] developed biodegradable thermoplastics of suitable mechanical properties from sunflower protein isolates plasticized with glycerol and water through an injection molding process. Jerez et al.[32] developed bioplastics from hen egg whites and wheat gluten proteins for non-food applications through the compression molding process. In addition, they studied the effect of thermo-mechanical processing on the rheological properties of dough produced from egg white/glycerol and wheat gluten/glycerol, observing significant changes in the microstructure of the resulting plastics. According to their AFM study, an increase in pressure produced larger aggregates of macromolecules in a preferential direction, providing for the formation of higher molecular weight polymers through enhanced intermolecular crosslinking.

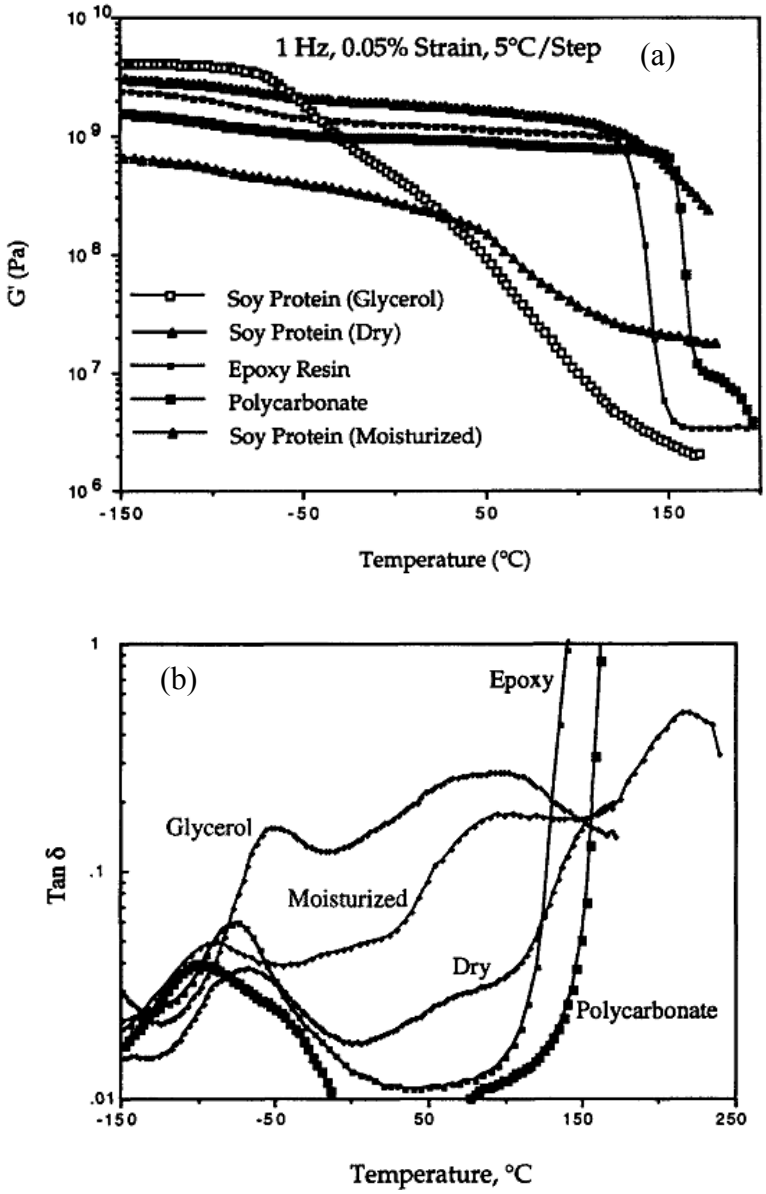

Figure 2.3. Dynamic mechanical spectroscopy (DMS) of polycarbonate, epoxy, and various forms of soy plastics: (a) Storage modulus, (b) Tan δ. Note: Soy protein (Glycerol): with 25 wt% of glycerol; Soy protein (Dry): with 5% moisture content; Soy protein (Moisturized): with 10% moisture content. (Reprinted with permission from Elsevier publications).

2.2.3: Modification of protein plastics

Different ways of modification have been studied to improve the mechanical and water stability of protein plastics. These modifications include: use of denaturants; plasticizers (e.g., glycerol and polyols); thermal processing variables, such as molding temperature and pressure; blending; fiber or filler reinforcement. For example, Mo and Sun[33] modified soy-protein with different concentrations of urea, a denaturing agent. They observed that the plastic from 2M urea-modified soy protein demonstrated an improved elongation, toughness fracture and water resistance. **Figure 2.4** shows the stress-strain curve at various urea concentrations.

Schilling et al.[34] used varying concentrations of glycerin, a plasticizer, to produce compression-molded plastics from soy protein. In general, they observed that raising the glycerin concentration increased the elongation and reduced the tensile strength, hardness, and elastic modulus.

Paetau et al.[11] studied the effect of preparation (for example, acid treatment) and processing conditions (such as molding temperature and moisture content) on the mechanical properties and water absorption of compression-molded plastics from soy protein. They observed that molding the material at 140°C resulted in soy plastic with higher tensile strength compared with those molded at lower temperatures. In addition, a moisture content greater than 10% resulted in plastic samples of increased extensibility.

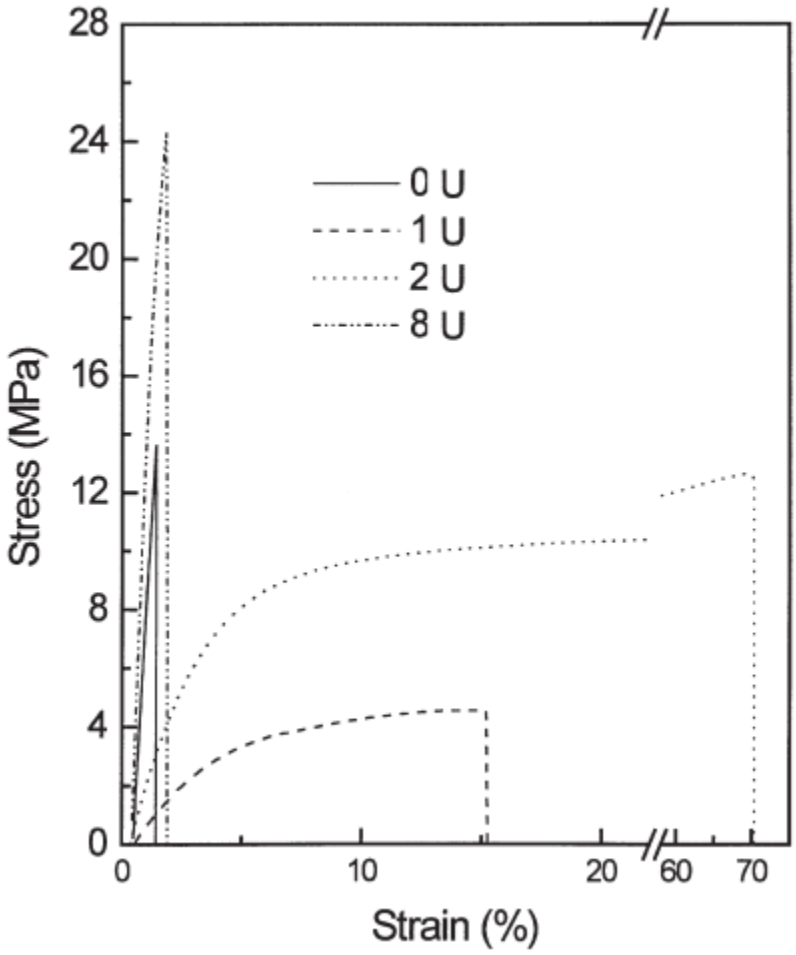

Figure 2.4. Mechanical properties of soy protein isolate (SPI) plastics molded at 120°C, 5.6MPa for 3 min from 0U: unmodified SPI; 1U: 1M urea-modified SPI; 2U: 2M urea-modified SPI; 8U: 8M urea-modified SPI. (Reprinted with permission from Springer publications).

To improve the toughness and water resistance properties of these protein plastics, blending and reinforcing have been found to be important methods that are receiving increased attention. The blends may combine the advantages of both components, exhibiting better characteristics than either component. In general, the blends can be divided into homogeneous (miscible, single phase) and heterogeneous (more than one phase). In a homogeneous blend, the components of the blend virtually lose a portion of

their identity. The final properties of a miscible blend usually follow the "mixing rule" (the arithmetical average of blend components). In a phase-separated blend, the properties of all blend components are present, and the final performance of the blend is dependent on the size of the structural elements and their adhesion. In general, a majority of immiscible blends are incompatible, demonstrating a negative deviation from the "mixing rule" because of gross phase morphology. These blends are in many ways useless if they are not compatibilized.[35]. Salmoral et al.[36] explored the compression molding process in preparing plastic exhibiting acceptable properties from blends containing chickpea proteins. Zhong and Sun[37] studied blends of soy protein isolate (SPI) and polycaprolactone (PCL) along with a compatibilizer, finding improved mechanical and water resistance properties. **Figure 2.5** shows the stress-strain curves of SPI/PCL blends with a 2 wt% of the compatibilizer. The SPI alone plastic showed brittle fracture, while ductile fractures were observed with an increased content of PCL.

Moreover, these researchers observed a water absorption of 165% at room temperature for 26 h study on pure SPI plastic. Addition of compatiblizer reduced the water absorption of SPI-only plastics to 74%, due to crosslinking reactions, while increasing the PCL content to 50% reduced the water absorption to 12%.

Wang et al.[38] developed plastics having mechanical properties similar to commercial thermoplastics such as polystyrene from the blends of soybean/poly (hydroxyl ester ether), a bisphenol A ether-based synthetic biodegradable thermoplastic polymer, and wheat gluten/poly(hydroxyl ester ether). Woerdeman et al.[39] studied blends

of wheat gluten protein and thiol-terminated, star branched (poly(ethylene glycol)) in the preparation of biodegradable plastics.

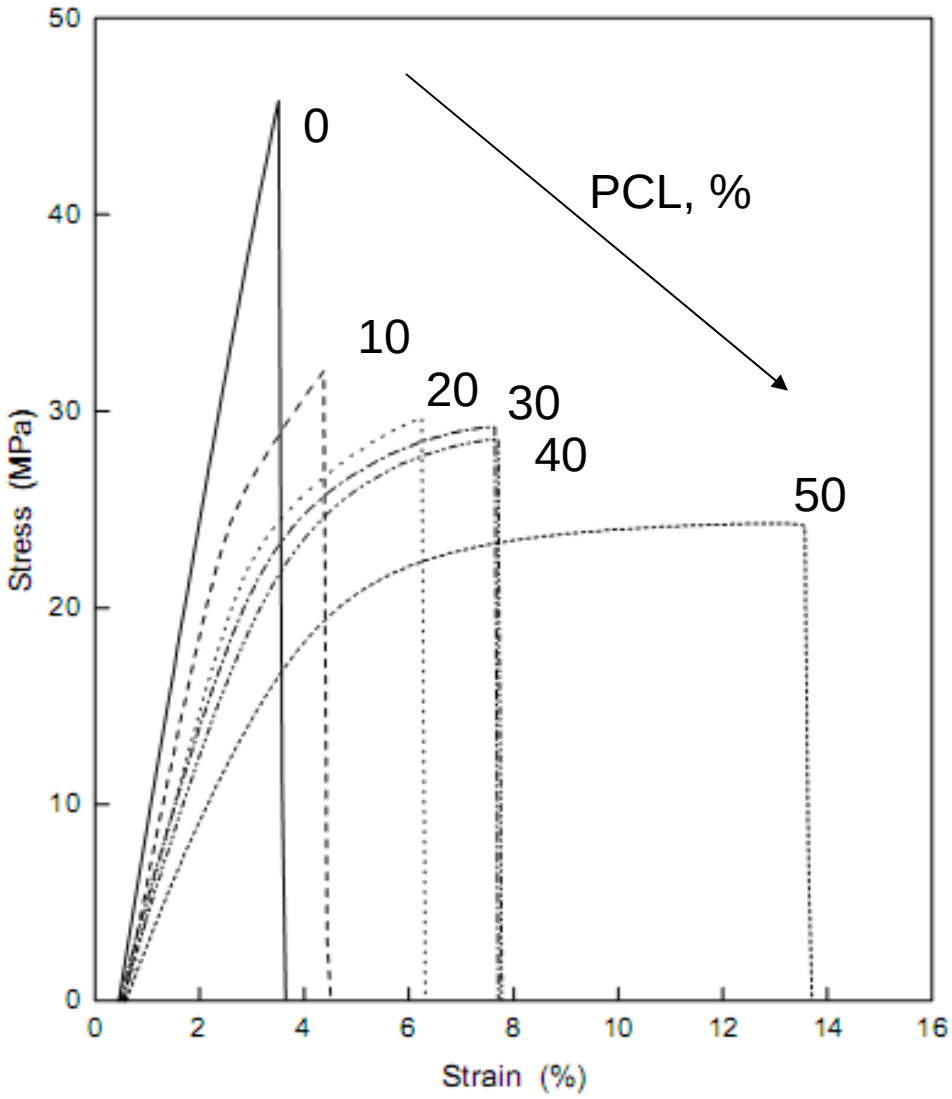

Figure 2.5. Typical stress-strain curves of the SPI/PCL blends with 2 wt% MDI. (Reprinted with permission from Elsevier publications).

Aithani et al.[40] developed injection-molded biodegradable plastics for packaging from the blends of corn gluten meal (a byproduct of the ethanol industries) and a

synthetic biodegradable polymer poly (ε-caprolactone). They used a combination of glycerol (plasticizer), ethanol (for processing), and guanidine hydrochloride (denaturant) to produce extrusion molded plastics of increased toughness.

Another method for improving mechanical and water resistance properties is by attaching various alkylating agents to these proteins, resulting in increased crosslinking. For example, Lens et al.[41] used caproaldehyde and lauraldehyde to attach hydrophobic groups to the amino groups of proteins, primarily from lysine, resulting in a strong gluten film with a swelling rate comparable to synthetic nylons. Bräuer et al.[42] used palmitic acid chloride and alkenyl-substituted succinic anhydrides to modify such proteins as wheat gluten, soy, corn zein and pea to become fusible and suitable for thermoplastic shaping. In addition, they found that 10wt.-% of plasticizing glycerol produced a flexible biodegradable material with reduced hydrophobicity.

Various reinforcements or fillers have also been explored to develop biocomposites with improved toughness and water resistance. For example, Wu et al.[43] developed inexpensive corn gluten meal composites of improved toughness, reinforced with wood fiber, by using compression and an injection-molding process. However, the wood fiber content did not affect the water resistance of these composites. In addition, Wang et al.[44] fabricated soy protein plastic reinforced with such fillers as chitin whisker, kraft lignin and hydroxypropyl lignin, exhibiting increased flexibility and improved water resistance.

Fillers, such as partially denatured proteins from animal co-products, available renewably at low cost, can play a significant role in the development of bio-based

plastics. However, limited studies have been conducted on these proteins. For example, Garcia et al.[45] developed plastics from the blends of meat-and-bone-meal and functional sodium caseinate. These plastics exhibited the characteristics of an amorphous hydrophilic polymer and, under different relative humidity, produced a range of materials of varying stiffness due to changes in the glass-transition temperature, a range similar to that showed by amorphous plastics produced from soy, wheat gluten, and gelatin proteins. In addition, plastic samples having more than 15% moisture exhibited higher elongation, and one with moisture less than 15% showed brittleness similar to that of a glassy material.

Moreover, various organic and inorganic fillers have been extensively used in the development of epoxy-based composites. These traditional thermoset polymers, frequently used for structural composites in aerospace, marine and transportation domains, are also derived from dwindling fossil fuels. Therefore, vegetable oil-based epoxies are receiving increased attention as more environmentally sound replacements.

2.3: Plastics from natural epoxy

Biodegradable materials are receiving increased attention due to their availability on a renewable basis and their environmental advantages. Depletion of non-renewable resources and dependence on petroleum-based polymers is causing a growing urgency to develop and commercialize new, environmentally compatible biobased polymers.[46] In this context, natural oils from agricultural resources, such as linseed oil and soybean oil, are useful in polymer material synthesis.[47] These natural oils can be functionalized by

epoxidation with organic peracids or H_2O_2 (hydrogen peroxide) and are considered as an inexpensive renewable material for the generation of thermoset epoxy.[48]

Thermoset composites from epoxy resins are often used in high-performance structural applications because they generally possess excellent properties, such as toughness and dimensional stability.[49,50]. These resins are generally used as the binding agent, offering attractive combinations of strength, ease of processing, and cost. For example, epoxy resin is widely used as the binder in the composites reinforced with carbon fibers used in aerospace applications.[51]

2.3.1. Epoxy resins

Typically, epoxy resins contain a characteristic oxirane structure or epoxide structure, as shown in **Figure 2.6** that can be converted into a cross-linked structure through a curing reaction. This curing can be achieved using anhydrides of carboxylic acids; compounds with active hydrogen such as polyamines, polyphenols, polyalcohol, polycarboxylic acids and polythiols; or catalysts such as Lewis acids and t-amines.[52] During the crosslinking process, two important phenomena of gellation and vitrification occur. The sudden and irreversible transformation from a viscous liquid to an elastic gel is called the gel point, the time at which the polymer no longer flows and, thus, is no longer processable. This gel point depends on the functionality, reactivity and stoichiometry of the reactants. For example, the gel point of a difunctional epoxy cross-linked with a stoichiometric amount of tetrafunctional amine having all hydrogens of equal reactivity is calculated to be α=0.577 (Flory, 1953).

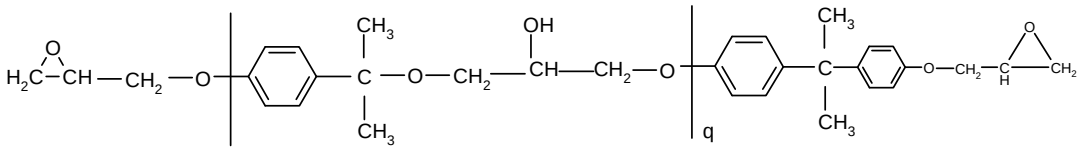

Figure 2.6. Chemical structure of an epoxy prepolymer. Note: $\overline{X_n}$ (of this compound) is = q+3. Compounds with q= 0.1-0.6 are liquid, those with q-2-12 are solids.

The second phenomenon, which may occur at any stage during cure, is the vitrification of the growing chains or network. This transformation from a viscous liquid or elastic gel to a glass begins to occur as the glass transition temperature becomes coincidental with the cure temperature. Vitrification has the potential to bring curing to an abrupt halt. However, it is a reversible transition, and curing can be resumed by heating epoxy to devitrify the partially cured thermoset. The onset of vitrification exhibits a shift from the chemical control to the diffusional control of the reaction and may be observed in the gradual decay of the reaction rate. Therefore, one-part epoxy is widely used for developing structural composites as these contain latent curing agents, activating the reaction at higher temperatures, allowing significant curing before vitrification. For example, a one-part epoxy system comprised of diglycidyl ether of bisphenol A (DGEBA), dicyandiamide (DDA) and accelerator Monuron has been extensively studied in the development of high-performance composites.

DDA has been used as a curing agent for epoxy resin in applications ranging from adhesives to composites and from printed circuit boards to powder coatings.[53] The most stable isomer of dicyandiamide has the cyano group on the imine nitrogen

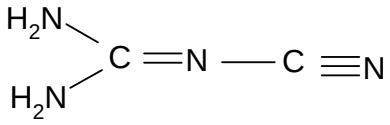

The other isomer is

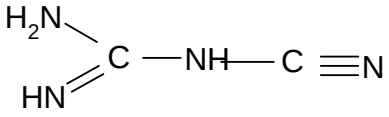

The DGEBA/DDA system can be cured at approximately 180ºC-200ºC. Moreover, the addition of such accelerators as aryldimethyl urea compounds (**Figure 2.7**) monuron (a), diuron (b), fenuron (c) and TDI-uron (d) results in a lowering of the curing temperature to approximately 130ºC. These compounds give the latency at room temperature necessary to formulate this single-component system.

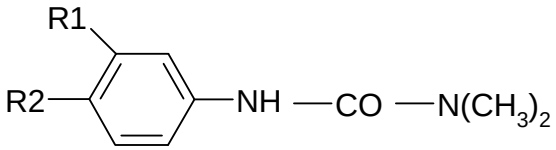

a: R1=Cl, R2=H; b: R1=Cl, R2=Cl; c: R1=H, R2=H; d: R1=CH_3, R2=NH-CO-N $(CH_3)_2$

Figure 2.7. Different aryldimethyl urea compounds

The synergistic effect of dicyandiamide and Monuron was investigated by Laliberte et al.[54] using DSC. The activation energies of these mixtures--epoxy resin+DDA, epoxy resin+DDA/Monuron, and epoxy resin+Monuron-- were found to be 39, 22, and 19 kcal/mol, respectively. The by-product of the resin+Monuron reaction is dimethyl amine. It was found that dimethylamine is able to dramatically enhance the reactivity of DDA. In

subsequent research, Barwich et al.[55] proposed the possible curing pathways of DGEBA/DDA/monuron system represented in **Figure 2.8**.

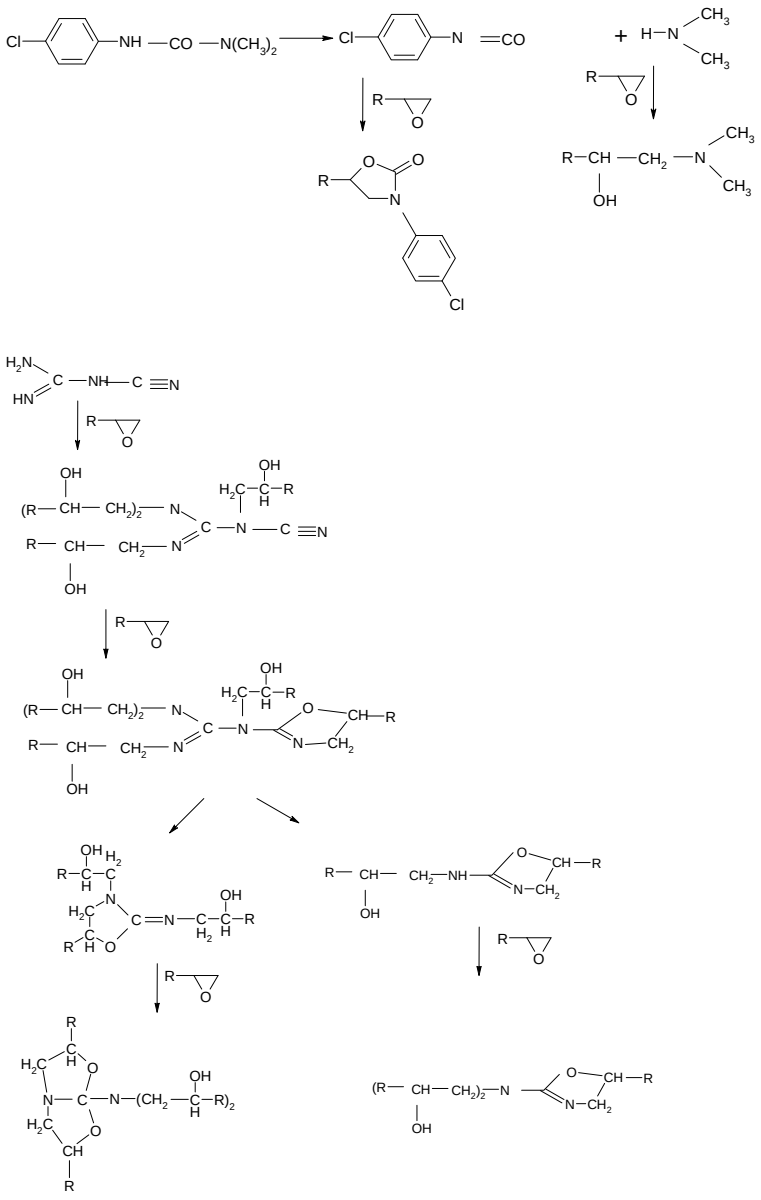

Figure 2.8. DGEBA/DDA curing pathways.

2.3.2: Ultrasonic curing

Another important aspect of these epoxy systems is the availability of a curing method at a minimum processing cost for the development of desired material. The traditional curing processes include oven heating, hot presses and platens, autoclave, infrared heating, and heating by electrical resistance heaters.[56] These conventional thermal energy processes, which conduct heat from the outside to the inside of the composite, can be hindered by the sample geometry and the relatively low thermal conductivity of the epoxy itself. The primary disadvantages of these processes, prohibitive in many technical applications, include high energy consumption, the time required to raise the temperature (slow heating), and the time needed to cool to a safe handling temperature.

Research has been conducted to investigate several unconventional epoxy curing methods for accelerating the curing process and reducing the total time of cure.[57] These processes can be classified as radiation curing using UV, gamma rays and electron beams; induction curing; dielectric curing using radio frequency and microwaves; and ultrasonic curing. For example, Crivello et al.[58] used high-energy radiation in the form of electron beam irradiation to develop carbon/epoxy laminates and wood-reinforced composites. Microwave heating has been the most common method studied because of its exceptional high heating rate; though a non-uniform electric field distribution in the material produces hot spots, which may degrade the material. The ultrasonic process cures the epoxy system from the inside of the bulk material, preventing hot spots and allowing uniform curing of composites.[59,60]

Ultrasound, generally considered to be approximately 20 kHz and higher, is propagated via a series of compression and rarefaction waves induced in the molecules of the medium through which it passes.[61] At sufficiently high power, the rarefaction cycle may exceed the attractive forces of the molecules in the liquid and lead to the formation of cavitation bubbles. These bubbles grow over a few cycles, taking in vapor or gas from the medium (rectified diffusion) until it reaches equilibrium size, matching the frequency of the bubble resonance to that of the applied ultrasound. This acoustic field experienced by the bubble is not stable due to the interference of other bubbles, resulting in a sudden expansion to an unstable size before collapsing violently and generating intense local heating and high pressures of approximately 5000°C and 1000 atm at heating and cooling rates of more than 10^{10} K/s.[62] These hot spots are responsible for producing the heat, which drives the high-energy chemical reactions. This behavior is schematically shown in **Figure 2.9**.

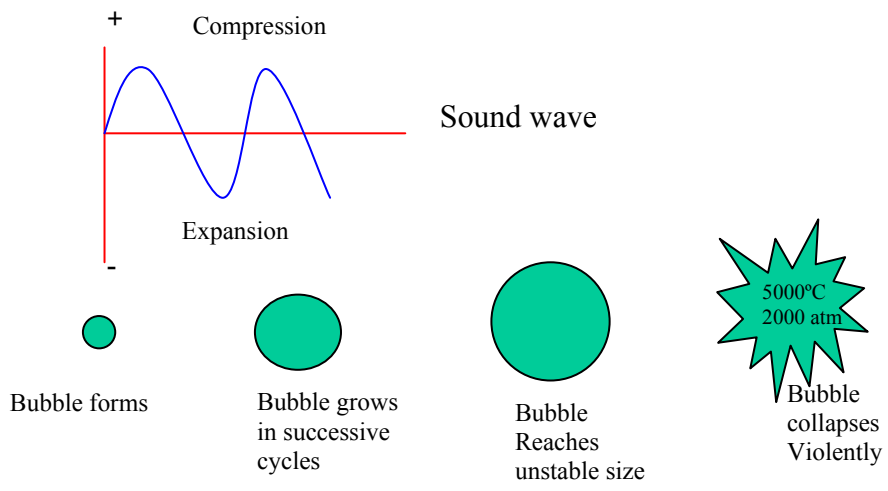

Figure 2.9. Schematic of cavitation effect.

Traditionally, heat and pressure are used to impregnate the reinforcement with matrix resin, thereby obtaining high quality prepegs, to consolidate their multi-layers of the prepegs, to debulk and deaerate the consolidated body, and to cure them.[63] These processing conditions for curing fiber-reinforced thermoset polymer composites can be provided by autoclaves of appropriate size, which are expensive and difficult to schedule. In contrast, the out-of-autoclave ultrasonic curing method generates both pressure and heating through viscoelastic dissipation.[64] Research has shown the benefits of using sonic energy in place of the traditional curing process of direct heating under pressure. These advantages include (1) the resin viscosity is reduced at a given temperature, producing better consolidation without resin advancement; (2) the time of resin curing is reduced by at least a factor of two, causing an increase in the manufacturing throughput; and (3) the sonic energy absorption tends to be self-limiting as curing advances, reducing the risk of over-curing and damage to the composites.[63]

The interaction of sonic energy with the uncured resins can produce both thermal and non-thermal effects due to micro-mixing, lower viscosity and higher diffusion rates. For example, the DSC technique in dynamic and isothermal modes has been used to study the kinetics of epoxy curing.[65] If the curing reaction is the only thermal event, then the rate of heat released during curing, $\left(\frac{dH}{dt}\right)$, can be directly proportional to the rate of reaction, $\frac{dc}{dt}$, based on **Equation 2.2:**

$$\frac{dc}{dt} = \frac{1}{\Delta H}\left(\frac{dH}{dt}\right) \tag{2.2}$$

where c represents the extent of the reaction.

Therefore, the DSC technique can be used to determine the curing kinetics of epoxy curing, representing by the n^{th} order (**Equation 2.3**) or the autocatalytic form (**Equation 2.4**), respectively:

$$\frac{dc}{dt} = k(1-c)^n \tag{2.3}$$

$$\frac{dc}{dt} = k(1-c)^n c^m \tag{2.4}$$

According to n^{th} order, the reaction rate is maximum at the time t=0 while for the autocatalytic form, it is maximum at some intermediate conversion, but the initial rate is zero. A study by Kamal[66] showed that, during the isothermal curing of epoxy system, the curing reaction showed a marked autocatalytic behavior. Kwan and Benatar[67] stated that the high and rapidly changing heat rate produced by ultrasonic curing makes the heating profile impossible to simulate by conventional heating methods. Therefore, they developed a chemical model through isothermal studies in DSC to determine the thermal effect on the reaction kinetics of epoxy.

In addition, Liu et al.[68] observed that the non-thermal effect of ultrasound streaming action accelerates the movement of epoxy resin molecules, enhancing the wettability between aramid fibers and epoxy resin. This effect markedly improved the interfacial shear strength and tensile strength of the epoxy-based composites reinforced with high-performance aramid fibers.

Roylance et al.[69] developed numerical simulation methods to understand the ultrasonic debulking or ultrasonic staging processes. According to the authors, insonification can induce very rapid localized heating, achieving temperatures well above the standard cure temperature in seconds, but the advancement of the cure may be slight. Therefore, ultrasonic curing, an out-of-autoclave process, has the potential to manufacture fast and inexpensive epoxy-based composites.

2.3.3: Natural epoxy

It has been shown that vegetable oils, containing a triglyceride structure with unsaturated fatty acid side chains, are considered one of the most important classes of renewable sources in the production of biobased plastics and composites.[70] Functionalized vegetable oils, for example epoxidized soybean oil (ESO), acrylated epoxidized soybean oil, linseed oil monoglyceride maleate, epoxidized linseed oil (ELO), epoxidized canola oil, and epoxidized castor oil, have been synthesized to prepare plastics and composites.[71,72,73,74] In addition, these natural epoxy have been blended with traditional epoxy resins to reduce the brittleness and the cost of conventional epoxy-based composites, currently being used in high-performance applications.[74,75]

The degree of unsaturation of vegetable oils and the types of curing agents play decisive roles in the development of plastics or composites with the required characteristics while still exhibiting biodegradability. For example, Xu et al.[76] studied the curing of ESO using the hardening agents, triethylene glycol diamine (TGD) and triethylene tetraamine (TETA), and found that the ESO/TETA system exhibited

viscoelastic properties similar to such synthetic plastics as polystyrene, polyethylene and polymethylmethacrylate. In addition, Miyagawa et al.[75]studied the diglycidyl ether of bisphenol F (DGEBF)/ELO system using the curing agent methyltetrahydrophthalic anhydride (MTPHA) to develop a flexible matrix system without phase separation. In a similar study, using the MTPHA curing agent, Boquillon fabricated an ELO-based composite reinforced with hemp fibers having mechanical properties appropriate for various technical applications. In addition, their findings were scaled up using such technologies as resin transfer molding (RTM) or beta-staged prepregs.[77] Wool and Lu[78] also synthesized bio-based thermosetting epoxy resins from linseed oil, the most molecularly unsaturated of all plant oils, resulting in properties comparable to the unsaturated polyesters used in sheet molding composites.

In summary, natural epoxies have shown the same potential as traditional epoxies for developing structural material. However, intensive research is required to mirror the properties of epoxy resins, which have been extensively used in prepegs and composite materials because of their versatile chemical structures, low volatility during curing, limited shrinkage, excellent adhesion, and chemical resistance.[79]

2.4: References

[1] Mohanty, A. K., Misra, M., and Hinrichsen. G. Macro. Mater. Eng. (2000), 276/277, 1.

[2] Hart, H., Craine, L. E., Hart, D. J., and Hadad, C. M., Organic Chemistry: A Short Course, 12 ed.,2007, Houghton Mifflin Company, Boston.

[3] Villar, M. A.; Thomas, E. L., and Armstrong, R. C., Polymer (1995), 36, 1869.

[4] Robertson, G. L., Food Packaging, Principles and Practice, 2nd ed., Taylor & Francis1, pp. 90.

[5] Cuq, B., Nathalie, G., and Guilbert, S., Polymer (1997), 38(16), 4071.

[6] Herrmann, A. S., Nickel, J., and Riedel, U., Polym. Degrad. Stab. (1998), 59, 251.

[7] Hu, R., and Lim, J-. K., J. Comp. Matl. (2007), 41, 1655.

[8] Huda, M. S., Drzal, L. T., Mohanty, A. K., and Misra, M., Comp. Sci. Tech. (2008), 68, 424.

[9] Baillie, C., Green Composites: Polymer Composites and the Environment (2004). CRC Press LLC, Boca Raton, FL.

[10] Carvalho, A. G. F., Job, A. E., Alves, N., Curvelo, A. A. S., and Gandini, A., Carbohydrate Polymers (2003), 53, 95.

[11] Paetau, I., Chen, C-. Z., and Jane, J-. L.lin. Ind. Eng. Chem. Res. (1994), 33, 1821.

[12] Zhong, Z., and Sun, X. S.,Polymer (2001), 42, 6961.

[13] Yada, R. Y., Proteins in Food Processing (2004), Woodhead Publishing, Chapter 2.

[14] Vaz, C. M., van Doeveran, P. F. N. M., Yilmaz, G., de Graaf, L. A., Reis, R. L., and Cunha, A. M., J. Appl. Polym. Sci. (2005), 97,604.

[15] Cuq, B., Nathalie, G., and Guilbert, S., Polymer (1997), 38, 4071.

[16] Abdelmoez, W., and Yoshida, H. Amer. Inst. Chem. Eng. (2006), 52, 2607.

[17] Hawley, S.A., Biochemistry (1971), 10**,** 2436.

[18] Smeller, L., Biochimica et Biophysica Acta (2002), 1595, 11.

[19] Smeller, L., and Heremans, K., Biochimica Biophysica Acta (1998), 1386, 353.

[20] Byler, D. M., and Susi, H., J. Ind. Micro. (1988), 3, 73.

[21] Subirade, M., Kelly, I., Gueguen, J., and Pezolet, M., Int. J. Bio. Macro. (1998), 23, 241.

[22] Vaz, C. M., Graff, D., Reis, R. L., and Cunha, A. M. NATO Science Series. Series II, Mathematics, Physics, and Chemistry (2002), 86, 93.

[23] Matveev, Y. I., Grinberg, V. Y., and Tolstoguzov, V. B., Food Hydrocolloids (2000), 14, 425.

[24] Pommet, M., Redl, A., Morel, M.- H., and Guilbert, S., Polymer (2003), 44, 115.

[25] Barone, J.R., and Schmidt, W. F., U.S. Patent No. 7,066,995 B1 (2006).

[26] de Graaf, L. A., and Kolster, P., Macromol. Symp. (1998), 127, 51.

[27] Lim, L. T., Mine, Y., and Tung, M. A., J. Agric. Food Chem. (1998), 46, 4022.

[28] Zhong, Z., and Sun, X. S., Polymer (2001), 42, 6961.

[29] Mo, X., and Sun, X., J. Polym. Environ. 92003), 11, 15.

[30] Sue, H.- J., and Jane, J.- L., Polymer (1997), 38, 5035.

[31] Orliac, O., Silveste, F., Rouilly, A., and Rigal, L., Ind. Eng. Chem. Res. (2003), 42, 1674.

[32] Jerez, A., Partal, P., Martínez, I., Gallegos, C., and Guerrero, A., J. Food Eng. (2007), 82, 608.

[33] Mo, X., and Sun, X., J. Amer. Oil Chem. Soc. (2001), 78, 867.

[34] Schilling, C. H., Babcock, T., Wang, S., and Jane, J. J. Mater. Res. (1995), 10, 2197.

[35] Koning, C., Duin, M. V., Pagnoulle, C., and Jerome, R., Prog. Polym. Sci. (1998), 23, 707.

[36] Salmoral, E. M., Gonzalez, M. E., Mariscal, M. P., and Medina, L. F., Ind. Crops Prod. (2000), 11, 227.

[37] Zhong, Z. and Sun, X. S., Polymer (2001), 42, 6961.

[38] Wang, C., Carriere, C. J., Willett, J. L. J. Polym. Sci.: Part B: Polym. Phys. (2002), 40: 2324.

[39] Woerdeman, D. L., Veraverbeke, W. S., Parnas, R. S., Johnson, D., Delcour, J. A., Verpoest, I., and Plummer, C. J. G., Biomacromolecules (2004), 5, 1262.

[40] Aithani, D., and Mohanty, A. K., Ind. Eng. Chem. Res. (2006), 45, 6147.

[41] Lens, J.- P., Mulder, W. J., and Kolster, P., Cereal Foods World (1999), 44, 5.

[42] Bräuerr, S., Meister, F., Gottlöber, R-. P., and Nechwatal, A., Macromol. Mater. Eng. (2007), 292, 176.

[43] Wu, Q., Sakabe, H., and Isobe, S., Ind. Eng. Chem. Res. (2003), 42, 6765.

[44] Wang, Y., Cao, X., and Zhang, L., Macromol. Biosci. (2006), 6, 524.

[45] Garcia, R. A., Onwulata, C. I., and Ashby, R. D., J. Agric. Food Chem. (2004), 52, 3776.

[46] Miyagawa, H., Mohanty, A. K., Drzal, L., and Misra, M., Nanotechnology (2005), 16, 118.

[47] Boquillon, N., and Fringant, C., Polymer (2000), 41, 8603.

[48] Park, S-., Jin, F-., and Lee, J-., Macromol. Rapid Commun. (2004), 25, 724.

[49] Mezzenga R, Boogh L, Manson J. A. E., Comp. Sc. Tech. (2001), 61, 787.

[50] Adachi T, Araki W, Nakahara T, Yamaji A, and Gamou M., J. Appl. Poly. Sc. (2002), 86, 2261.

[51] Williamson A., Encyclopedia of Materials Science & Technology (2001), Elsevier Sc. Ltd., pp. 90.

[52] Elias, H. G., Macromolecules-2 (Synthesis and Materials) (1977), Plenum Press, New York & London.

[53] Guthner T., Hammer B., J. Appl. Poly. Sc. (2000), 50, 1453.

[54] Laliberte B. R., Bornstein J., and Sacher R. E., Ind. Eng. Chem. Prod. Res. Dev. (1983), 22, 261.

[55] Barwich J., Guse D., and Brockmann H., Adhäsion (1989), 33, 27.

[56] Hahn O., and Ewerszumrode A., Welding in the World (1998), 41, 149.

[57] Berlan J., Rad. Phys. Chem. (1995), 45, 581.

[58] Crivello, J. V., Narayan, R., and Sternstein, S. S., J. Appl. Polym. Sci. (1997), 64, 2073.

[59] Petrie, E. M., Epoxy Adh. Form. (2006), McGraw-Hill.

[60] Boey, F. Y. C., Yap, B. H., and Chia, L., Polym. Test. (1999), 18, 93.

[61] Mason T. M., Chem. Soc. Rev. (1997), 26, 443.

[62] Suslick K. S., and Price G., J. Annu. Rev. Mater. Sci, (1999), 29, 295.

[63] Graham L. J., Ahlberg L. A., Cohen-Tenoudji F., and Tittmann B. R., Ultra. Symp. (1986), 1013.

[64] Roylance, M., Playerr, J., Zukas, W., and Roylance, D., J. Appl. Polym. Sci. (2004), 93, 1609.

[65] Ghaemy, M, Barghamadi, M, Behmadi, H., J. Appl. Poly. Sc. (2004), 94, 1049.

[66] Kamal, M. R., Polym. Eng. Sc. (1974), 14, 231.

[67] Kwan K. M., Cheng K., and Benatar A., Proc. Annual Tech. Conf.-Soc. Plas. Eng. (1998), 56, 1089.

[68] Liu, L., Huang, Y. D., Zhang, Z. Q., Jiang, B., and Nie, J., J. Appl. Polym. Sci. (2001), 81, 2764.

[69] Roylance, M., Player, J., Zukas, W., and Roylance, D., J. Appl. Polym. Sci. (2004),93, 1609.

[70] Lu, Y., and Larock, R. C., Macromol. Mater. Eng. (2007), 292, 1085.

[71] Boquillon, N., and Fringant, C., Polymer (2000), 41, 8603.

[72] Chakrapani, S., and Crivello, J. V., J. Macromol. Sci. (1998), 35, 1.

[73] Boquillon, N., Elbez, G., and Schönfeld, U., J. Wood. Sci. (2004), 50, 230.

[74] Espinoza-Perez, J. D., Wiesenborn, D. P., Tostenson, K., Ulven, C. A., and Tatlari, M., Amer. Soc. Agri. Bio. Eng. (2007), Paper Number: 076079.

[75] Miyagawa, H., Mohanty, A. K., Misra, M., and Drzal, L. T., Macromol. Mater. Eng.(2004), 289, 629.

[76] Xu, J., Liu, Z., Erhan, S. Z., and Carriere, C. J., J. Amer. Oil Chem. Soc. (2004), 81, 813.

[77] Boquillon, N., J. Appl. Polym. Sci. (2006), 101, 4037.

[78] Lu, J., and Wool, R. P., J. Appl. Polym. Sci. (2006), 99, 2481.

[79] Neville K., and Lee H., Epoxy Resins; Their Applications and Technology (1957), New York, McGraw-Hill.

CHAPTER 3

EXPERIMENTAL

The common experimental procedures followed in this research are presented here in this chapter, including a list of the chemical reagents, polymers, protein materials and epoxies used. The basic instrumentation techniques and general experimental procedures are also discussed.

3.1: Chemical Reagents

3.1.1: Methyl ethyl ketone (MEK):

MEK was obtained from Acros Organics. The MSDS name is 2-butanone, 99+% ACS grade. The catalog numbers are 14967-0000, 14967-0010, 14967-0025, and 14967-0250. The CAS number is 78-93-3.

3.1.2: Toluene:

Toluene was obtained from Acros Organics. The MSDS name is toluene, Reagent ACS. The catalog numbers are 424500-0000, 42455-0010, 42455-0250, and 42455-5000. The CAS number is 108-88-3.

3.1.3: Hexane:

Hexane was obtained from Mallinckrodt Chemicals. The MSDS name is hexane, ACS grade. The catalog numbers are AC2924, BPH292RS-115, H292500LC, and S800322MF. The CAS number is 110-54-3.

3.1.4: Ethanol:

Ethanol was obtained from Mallinckrodt Baker Inc. The MSDS name is reagent

alcohol, ACS. The catalog numbers are 5911, 6183, 7006, and 7019. The CAS number is 64-17-5.

3.1.5: Aerosil R805:

Aerosil ®R 805 was obtained from Evonic Degussa Corp. The MSDS name is aerosil® R 805. The CAS number is 92797-60-9.

3.1.6: Pyrazine:

Pyrazine was obtained from Sigma-Aldrich. The MSDS name is pyrazine, 99+%. The catalog number is P5603. The CAS number is 290-37-9.

3.1.7: Benzyl bromide:

Benzyl bromide was obtained from Sigma-Aldrich. The MSDS name is benzyl bromide. The catalog number is B17905. The CAS number is 100-39-0.

3.1.8: Sodium hexafluoroantimonate:

Sodium heaxafluroantimonate was obtained from Sigma-Aldrich. The MSDS name is sodium hexafluoroantimonate, tech. The catalog number is 237981. The CAS number is 16925-25-0.

3.1.9: Calcium chloride

Calcium chloride was obtained from Acros Organics. The MSDS name is calcium chloride, anhydrous, irregular granules 95%. The catalog number is 3000380010. The CAS number is 10043-52-4.

3.1.10 Natural rubber latex

Natural rubber latex was obtained from Chemionics Corp. The catalog number is P60CX7330.

3.2: Polymers Used

3.2.1: Poly (glycidyl methacrylate) [PGMA]-co- poly (butyl methacrylate) [PBMA] copolymer (Structure 3.1 for constituting monomers):

Random copolymer of GMA (glycidyl methacrylate) and BMA (butyl methacrylate), P(GMA-co-BMA) was synthesized in our lab. From proton NMR, the molar ratio of GMA and BMA was calculated as 2:1.07. This procedure was developed and carried out by Dr. V. Klep, School of Materials Science and Engineering, Clemson University.

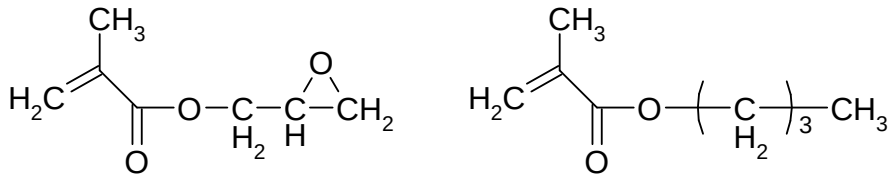

(S.3.1)

(Glycidyl methacrylate) (Butyl methacrylate)

3.3: Epoxy and curing agent used

3.3.1: One-part epoxy:

One-part epoxy adhesive system 2214 was supplied by 3M. This resin mainly composed of the bi-functional epoxy diglycidyl ether of bisphenol-A (DGEBA), the curing agent dicyandiamide (DDA) and the accelerator 3-(p-chloro phenyl)-1,1-dimethyl urea (Monuron).

3.3.1: Epoxidized soybean oil:

Epoxidized soybean oil, Vikoflex® 7170 was obtained from Arkema, Inc. The MSDS name is vikoflex® 7170 epoxidized soybean oil. The CAS number is 8013-07-8.

3.3.2 Epoxidized linseed oil:

Epoxidized linseed oil, Vikoflex® 7190 was obtained from Arkema, Inc., MN and, was supplied by Arkema, Inc. The MSDS name is vikoflex® 7190 epoxidized linseed oil. The CAS number is 8016-11-3.

3.3.3. N-Benzylpyrazinium Hexafluoroantimonate (BPH):

BPH, a latent curing agent, was synthesized by a known literature method.[1] Dr. Viktor Klep helped during the synthesis process.

3.3.4. Carbon/epoxy prepreg

The prepreg tape (DA409U/G35) was supplied by APCM Company. It contained 42% of unidirectional carbon fiber and 58% of one-part epoxy system (DGEBA/DDA/Diuron).

3.4: Protein material used

3.4.1. Animal co-product proteins:

Animal co-product proteins feather meal and blood meal were supplied by Fats and Proteins Research Foundation (FPRF), VA. **Table 3.1** shows the general composition of these proteins, including their amino acid compositions.

3.4.2. Whey Protein:

The whey protein isolate (BiPro™) was obtained from Davisco Foods Intl. It contained 91% protein.

Table 3.1. Nutrient Composition of Animal Proteins.[1]

Item	**Blood meal**[2]	**Feathermeal**
Crude Protein, %	88.9	81.0
Fat, %	1.0	7.0
Calcium, %	0.4	0.3
Phosphorus, %	0.3	0.5
Amino acids		
Methionine, %	0.6	0.6
Cystine, %	0.5	4.3
Lysine, %	7.1	2.3
Threonine, %	3.2	3.8
Isoleucine, %	1.0	3.9
Valine, %	7.3	5.9
Tryptophan, %	1.3	0.6
Arginine, %	3.6	5.6
Histidine, %	3.5	0.9
Leucine, %	10.5	6.9
Phenylalanine,%	5.7	3.9
Tyrosine, %	2.1	2.5
Glycines, %	4.6	6.1
Serine, %	4.3	8.5

[1] National Research Council, 1994
[2] Ring or flash dried

3.4.3. Chicken egg white albumin:

Albumin was obtained from Sigma-Aldrich. The MSDS name is albumin from chicken egg white, grade II. It contained at least 90% protein. The catalog number is A5253. The CAS number is 9006-59-1.

3.4.4. Human serum albumin:

The solution of Human serum albumin (HSA), contained 25% of HSA in phosphate buffer saline (PBS) (Source: Greiner Bio-One GmbH), was provided by Dr. Wen in Department of Bioengineering at Clemson University. HSA solution was freeze-dried for plastic fabrication.

3.5. Fiber used

3.5.1. Hemp fiber:

Hemp fiber was obtained from Hempline, Inc. The MSDS name is hemp fiber.

3.6: General Experimental and Characterization Techniques

3.6.1: Differential Scanning Calorimetry:

Differential Scanning Calorimentry (DSC) analysis was conducted using a TA Instrument (Model 2920) to determine the denaturing temperature (T_{den}) and the safe processing temperature window of the protein materials at a heating rate of 20°C min^{-1}. Data was analyzed using TA Instruments Universal Analysis 2000 version 3.9A software. The samples (6-8 mg in standard aluminum hermetic pans) were initially equilibrated at -60 °C and finally heated to 250 °C, a temperature below onset degradation. The glass

transition temperatures were obtained as the inflection point of the step transition. Temperature values of the endothermic peak maxima's were considered as the denaturing temperature.

3.6.2: Thermal Gravimetric Analysis:

Thermal Gravimetric Analysis (TGA) was conducted using a TA instrument Hi-Res TGA 2950. Data was analyzed using TA Instruments Universal Analysis 2000 version 3.9A software. Samples were heated at a rate of 20°C min^{-1} from room temperature to 400 °C under a nitrogen purge(40 mL min^{-1}).

3.6.3: Dynamic Mechanical Analysis:

Dynamic Mechanical Analysis (DMA) was performed using a DMS 210 Tensile Module (Seiko Instruments Inc., Japan) with specimen dimension of 40 mm × 10 mm and an effective gauge length of 20 mm. Samples were analyzed over a temperature range of 50°C to 225 °C at a heating rate of 2 °C min^{-1}, a frequency of 1 Hz and a deformation amplitude of 10 μm. Data were analyzed using EXSTAR6000 version 5.5 software.

3.6.4. Thermal Mechanical Analysis:

Thermal mechanical analysis of the cured samples were conducted using a TMA instrument (Model SS350, Seiko Instruments, Japan) at a compression load and a heating rate of 500mn and 2°Cmin^{-1}, respectively. Data were analyzed using EXSTAR6000 version 5.5 software.

3.6.5: Fourier Transform Infrared (FTIR) Spectroscopy:

FTIR spectroscopy was conducted using a Thermo-Nicolet Magna - IR™ 550 spectrometer (Thermo Nicolet, Waltham, MA) equipped with a Thermo Spectra-Tech

Foundation Series Endurance diamond attenuated total reflectance (ATR) accessory. Sample spectra were collected by performing 32 scans at a resolution of 4 cm^{-1} from 4000 cm^{-1} to 525 cm^{-1} and were ratioed against background spectra collected in the same manner. Data was analyzed using OMNIC E.S.P. v 7.2 software.

3.6.6: Scanning Electron Microscopy (SEM):

Scanning electron microscopy (SEM) images of fracture surfaces of plastic were obtained on Hitachi S3500N (Hitachi High-Technologies, Japan) microscope at an accelerating voltage of 20 kV. A Hummer®6.2 (Anatech Ltd., Hayward, CA) sputter coater was used to pre-coat the samples with a 4-5 nm layer of platinum for approximately 2 minutes with the pressure and voltage set to 70 milli-torr and 15 milli-amperes, respectively.

3.6.7. Static Mechanical Testing:

Tensile stress, percent strain-at-break, and Young's modulus were measured using the Instron testing system (Model 1125) from Instron Corp. Data were analyzed using Bluehill 2 version 2.4 software. The test was performed under controlled environment (20°C, 65% RH) according to the standard test method for tensile properties of plastics (ASTM D638-86) at 5 mm min^{-1} crosshead speed with a static load cell of 100 kN.

3.6.8: Moisture Testing :

A Sartorius MA50 moisture analyzer was used to analyze the moisture. For moisture testing, the samples were ground using liquid N_2. Moisture Content (MC) was determined by **Equation 3.1**:

$$MC = [(W_0 - W_{0d})/W_0] \times 100 \qquad (3.1)$$

where W_0 represents the initial weight of specimen; W_{0d} the weight of specimen after drying.

3.6.9. Preparation of plastics from animal co-product proteins and blends:

The feathermeal protein, as received, was mixed with hexane, stirred for 15 minutes, and filtered to extract soluble fatty and objectionable contents; this process was repeated three times. The defatted protein was then left overnight in a fume hood to dry and was later dried under vacuum at a temperature of 50°C for one hour, so as to ensure the complete evaporation of any residual solvent. The dried defatted feathermeal was manually ground and sieved using a stack of sieves (0.4 inch, 600 micron, and 300 micron pore opening). The received bloodmeal protein did not require fat removal process.

The proteins' moisture content was analyzed prior to molding. For whey or albumin/feathermeal and whey or albumin/bloodmeal blends, protein powders were mixed using a mechanical stirrer while adding water drop by drop to adjust the moisture content.

For feathermeal/rubbery copolymer blend, feathermeal powder was mixed with PGMA-co-PBMA polymer solution in MEK solvent and ultrasonicated for 60 min at 60°C, followed by rotary evaporation of solvent under nitrogen. The blend was left overnight in a fume hood. Finally, the sample was dried in an oven at 50°C or one hour under nitrogen environment to ensure complete evaporation of any residual solvent. The final modified protein powders was found to have bonded moisture content of 13%, which was appropriate for developing plastics.

Type I specimens (ASTM standard D638-03) were molded from 3.6g of feathermeal protein powder at 150°C and 3.6g of bloodmeal powder at 180°C in a hot press (Carver 60 Ton Economy Motorized Press). The mold and compression molding press are shown in **Figure 3.1**. The mold was at room temperature during material filling. After the molding, the mold and specimens were cooled to ≤ 70°C under pressure before they were taken off and allowed to cool further at ambient conditions. The pressure during molding was calculated on the basis of picture frame mold's area in contact with both top and bottom cover plates. This approach of calculating pressure experienced by the samples has been used by many researchers to prepare protein plastics.[2,3,4,5,6] Moreover, a picture frame mold, itself produce a uniform hydrostatic pressure.[6] Flash was removed by sanding the edges of the specimen with a grade-320 abrasive sandpaper. For whey/feathermeal and albumen/feathermeal blends, the samples were also molded at 150°C for 5 minutes, and were then cooled to ≤ 70°C under pressure before being taken off and allowed to cool further at ambient conditions. Bloodmeal composites reinforced with hemp fibers were processed at the similar processing conditions of neat bloodmeal plastic.

3.6.10. Preparation of plastics from undenatured animal and human proteins and blends.

3.6.10.1. Plastic from chicken egg white albumin, whey and HSA proteins:

The moisture content of the protein material was analyzed and adjusted prior to molding whey, albumin, or HSA by adding water drop by drop while mixing with a stirrer. Type-I specimens (ASTM standard D638-03) and DMA specimens were molded from 3.6g and 1.4g, respectively of these undenatured protein powders at 150°C and a

pressure of 20MPa for five minutes in a hot press (Carver 60 Ton Economy Motorized Press). The picture frame mold was at room temperature during material filling.

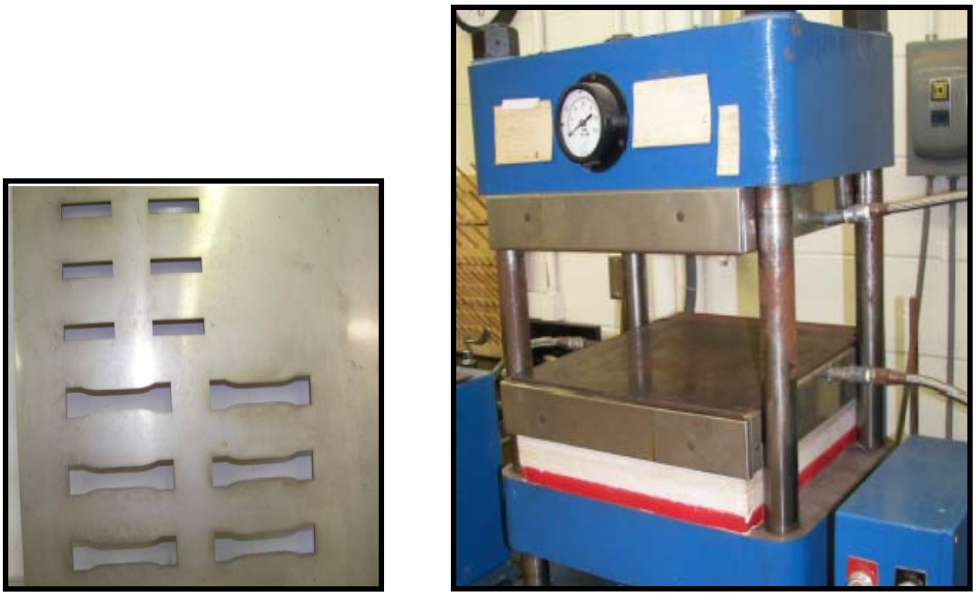

Figure 3.1. Picture frame mold and compression molding press.

3.6.10.2. Plastic from blends of chicken egg white albumin and whey proteins:

Whey and albumin proteins were dry-blended using a mechanical stirrer; water was then added to the mixture (up to 25% on dry weight of albumin and whey proteins) drop by drop. The mixture was kept overnight for equilibration with water. Samples were molded from these mixtures at 150°C and a pressure of 20MPa for five minutes in a hot press (Carver 60 Ton Economy Motorized Press), followed by ambient cooling and subsequent annealing overnight in an oven at 50°C. The picture frame mold used was at room temperature during material filling.

3.6.10.3. Plastic from blends of whey and natural rubber latex:

Whey and the natural rubber latex were mixed and stirred manually. Water was added until it reached 105% per protein weight. This mixture was then blended in a DSM microblender with a co-rotating twin screw extruder at an rpm of 100. Samples were molded with modified molding conditions of temperature--120°C, pressure--20MPa, holding time--5 minutes followed by ambient cooling and subsequent annealing in an oven at 70°C for 3 days.

3.6.10.4. Bacterial growth:

One colony of bacteria (S. aureus; Source: ATCC, VA; Cat.# ATCC-29213) was taken from a stock plate, placed in 5 ml of tryptic soy broth (Source: BD, NJ; Cat.# 211822), and incubated in a test tube for 18 hrs at 37°C with agitation. Subsequently, 1 ml aliquot of broth was centrifuged for 5 minutes at 1200 rpm, and then supernatant was aspirated. The pellet of bacteria was resuspended in 1 ml sterilized PBS (Source: Mediatech, Inc.,VA; Cat.# MT21-040-CV) and later added to 49 ml of PBS. Plastic samples were immersed in 5 ml of the bacteria suspension (2×10^7 bacteria/ml) and shaken at 100 rpm at 37°C. After 3 hrs, the samples were gently rinsed with sterile PBS three times. The viability of adherent bacteria on these plastic surfaces was investigated by staining them with 30 µl of SYTO 9 (Source: Invitrogen Corp., CA; Cat.# S-34854) at room temperature in the dark for 15 minutes and subsequently analyzing them under a Leica laser confocal microscope. The number of viable adherent S. aureus on each sample surface was counted and expressed relative to the surface area of the sample (CFU/cm^2). These bacterial growth experiments were conducted by Dr. Wen's research group in the Bioengineering Department at Clemson University.

3.6.11. One-part epoxy sample preparation:

Prior to curing, the epoxy adhesive, stored in a freezer, was allowed to warm to room temperature. For thermal curing, epoxy was cured in an oven at the desired temperatures. According to manufacturer, any of the following cure cycles would result in their full cure:

- 40 min @ 250°F (121°C)
- 10 min @ 300°F (149°C)
- 5 min @ 350°F (177°C)

However, epoxy should be cured at a slow heating rate (1-5°C/min) to prevent the thermal gradient in the cured parts, which results in stress-concentration; this is responsible for the early failure of the composite part.[7]

Figure 3.2 shows the schematic of the experimental setup for the ultrasonic curing process. It comprises a copper block, a Teflon insert, a thermal heater and thermo-controller, and thermocouples (TC). A Branson Ultrasonifier was used to generate the pulsed-ultrasound (0-100% pulse duration; one pulse of one second) of certain amplitude (20-40micron) at a constant frequency of 20 kHz. Epoxy samples, filled to a height of 5 mm, were subjected to pulsed-ultrasonic vibrations by immersing an ultrasonic horn a few millimeters into the resin. The temperature during epoxy curing was monitored with a thermocouple (TC) through a CALCOMMS^{TM} interface (CAL Controls Ltd., UK).

3.6.12. Thermal and Ultrasonic curing of ESO and ELO:

The required amount of curing agent BPH was dissolved in acetone and then epoxidized vegetable oil (ESO or ELO) was added, stirred for 10 min, and degassed for

60 min. The BPH was found to completely soluble in epoxy resins at room temperature. The formulated mixture was then poured into a Teflon mold to prepare samples for thermal and mechanical characterization. For thermal curing method, samples were cured at a temperature of 90°C for 1 hour, followed by a temperature of 180°C for 12 hours in an oven. For ultrasonic curing method, the required amount of BPH was dissolved in acetone and then ELO and 10wt.-% of Aerosil R805, a thixotropic agent, were added and hand mixed to produce a homogeneous viscous paste. Subsequently, this mixture was degassed for 60 min to remove acetone and entrapped air bubbles. The formulated mixture was then poured into a Teflon mold and covered with aluminum 3003 foil and cured using stationary ultrasonic horn producing a pulsed (50% pulse duration) ultrasound of an amplitude 40 micron at a preheating temperature of 100°C.

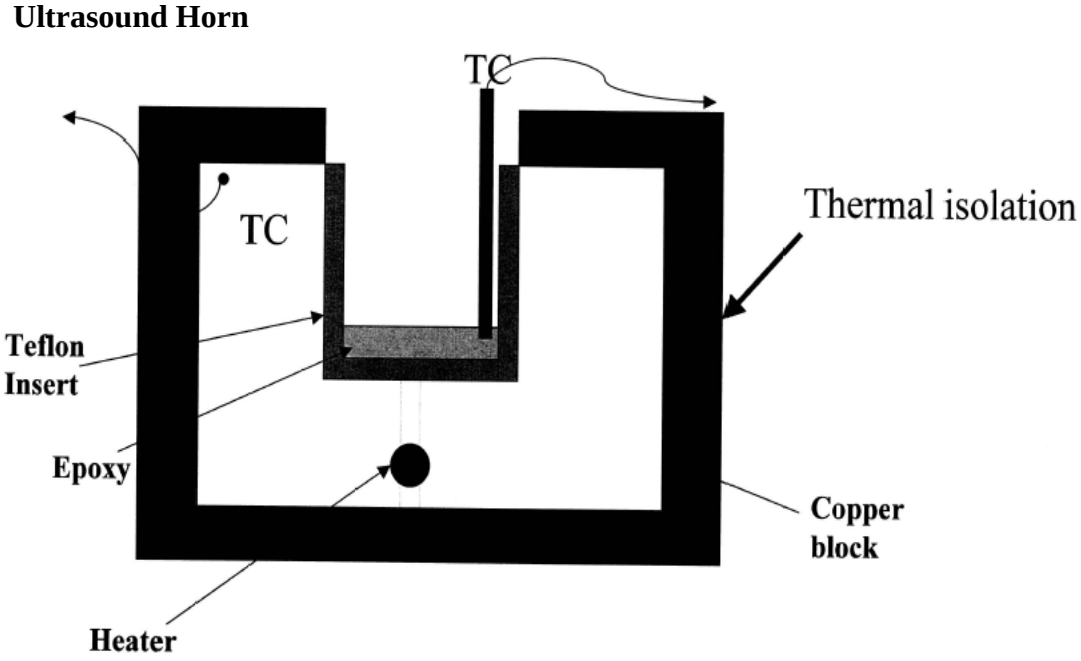

Figure 3.2. Schematic of ultrasonic curing. Note: TC--thermocouple.

3.6.13. Thermal, spectral and mechanical characterization of epoxy samples:

A TA instrument differential scanning calorimeter (DSC 2920) was used to monitor the exothermic crosslinking reaction. The total heat of the reaction (ΔH_T) for the uncured sample and the residual heat of the cured samples (ΔH_r) were measured from an individual dynamic scan running from 25ºC to 300ºC at a heating rate of 10ºC/min. The degree of conversion was calculated by **Equation. 3.2**:

$$\text{Degree of cure (\%)} = \alpha = \left(1 - \frac{\Delta H_r}{\Delta H_T}\right) \times 100 \qquad (3.2)$$

where ΔH_r represents the residual heat (J/g); and ΔH_T the total heat for the uncured sample (J/g).

From the dynamic run of the uncured epoxy system between 25ºC and 300ºC at a heating rate of 10ºC/min, isothermal temperatures of 100ºC, 115ºC, 125ºC and 135ºC (also observed during ultrasonic curing) were selected for developing a chemical model from the interval defined between 20ºC below the onset of curing and a point midway to the peak, maximum approximately 20-30ºC above the onset temperature of curing. The DSC cell was heated to the isothermal temperature, followed by the loading of the sample and the initiation of the curing. The typical isothermal curing curve comprises an initial baseline, an exothermic peak, and a final baseline (refer **Figure 8.13**).

Fourier Transform Infrared (FTIR) scans were collected using a Nicolet Magna 550 FTIR spectrometer equipped with a Nicolet Nic-Plan FTIR microscope. Samples were rolled out with a stainless steel rolling tool into the films on ZnSe IRtran plates, and 16 scans at a resolution of 4 cm^{-1} were collected for each sample. The dynamic

mechanical properties of the cured samples were analyzed using a DMTA instrument (Model DMS 210, Seiko Instruments). Dynamic mechanical analysis was conducted on the samples using a tensile fixture at a frequency of 1 Hz with a heating rate of $2°Cmin^{-1}$. Thermal mechanical analysis of the cured samples was conducted using a TMA instrument (Model SS350, Seiko Instruments) at a compression load and a heating rate of 500 mN and $2°Cmin^{-1}$, respectively.

3.7. References:

[1] Kim, M.., Lee, K.W., Endo, T., and Lee S.B., Macromolecules (2004), 37, 5830.

[2] Wang, Y., Cao, X., and Zhang, L., Macromol. Biosci. (2006), 6, 524.

[3] Paetau, I., Chen, C-. Z., and Jane, J-. L., Ind. Eng. Chem. Res. (1994), 33, 1821

[4] Sue, H.- J., Wang, S., and Jane, J.- L., Polymer (1997), 38, 5035.

[5] Mo, X., and Sun, X., J. Polym. Environ. (2003), 11, 15.

[6] Liu, W., Drzal, L. T., Mohanty, A. K., and Misra, M., Composites Part B: Engineering (2007), 3, 352.

[7] 3M Scotch-Weld™ Epoxy Adhesives, Technical Data, September, 1998.

CHAPTER 4

BIODEGRADABLE PLASTICS FROM UNDENATURED PROTEINS: ANIMAL AND HUMAN

4.1: Introduction

The importance of natural renewable based eco-friendly/biodegradable materials and the depleting sources of fossil fuels have led to the development of polymers from plant and animal by-products.[1] True biodegradable plastics can be reduced to single compounds by microorganisms and an important way of producing these plastics is by using natural polymers based on starch, proteins, and cellulose.[2] For example, soy protein has been recently considered as an alternative to petroleum polymers in the manufacture of adhesives, plastics, and various binders.[3,4] Proteins are very versatile materials, both in terms of their possible sources and their broad capacity for modification to meet the diverse requirements of specific applications.

Proteins can be a viable source of polymers for fiber, molded plastics, films, and an array of products currently supplied by the synthetic polymers industry. The major advantages are that proteins are derived from a sustainable resource, can be processed in much the same way as conventional synthetic polymers, are biodegradable, and are available at relatively low cost. Many researchers have developed plastics and biocomposites from animal and plant proteins and confirmed the benefits of these materials. For example, Paetau et al.[3] studied the preparation and processing conditions for making soy-plastics through a compression molding process. In another study, Salmoral et al.[2] developed plastic materials with acceptable properties by the

compression molding of blends containing either protein isolates or the defatted whole flour of chickpeas. In a study by Wang et al.,[5] plastic having properties similar to the commercial polystyrene thermoplastic was developed from blends of cereal proteins (soybean and wheat gluten) by using commercial extrusion and molding equipment. Similarly, biodegradable thermoplastics with improved mechanical properties were developed by Orliac et al.,[6] made from sunflower protein isolates with glycerol and water using an injection-molding process. In addition, Aithani and Mohanty[7] developed plastics out of corn gluten meal and its blends. Moreover, animal-based proteins, such as chicken egg whites,[8] whey,[9] feather keratin,[10] fish myofibrillar,[11] and meat-and-bone meal[12] have also been used to develop plastics.

It is common that bioplastics from protein biopolymers demonstrate low toughness and water stability. Extensive research is required to resolve these challenges and barriers. In this endeavor, studies have been conducted to utilize biomass-based plasticizer and various fillers, such as natural fibers[13,14] (e.g., hemp, pineapple leaf), natural rubber latex,[15] and basalt fiber[16] to improve the mechanical properties of bioplastics to make them comparable with petroleum-based plastics for their future substitution.

The primary objectives of this phase of research reported here were to develop plastics from animal proteins, such as albumin from chicken egg whites and whey, substituting them for synthetic plastic materials that are difficult to recycle, and to develop plastic from human serum albumin for bioimplants and drug delivery devices that would promote minimal bacterial growth and yield better wound healing response.

Another important objective was to investigate the thermal and mechanical characteristics of these plastics in order to understand the fabrication process, including the issues involved such as low toughness.

4.2: Materials

Protein materials from whey, albumin, and human serum albumin were used to develop biodegradable plastics. The whey protein isolate (BiPro, Davisco Foods Intl.) and albumin from chicken egg whites (A5253, Sigma-Aldrich) contained 91% and at least 90% proteins, respectively. The albumin and whey powders, as received, had a moisture content of 5.2% and 7.9%, respectively, which was primarily composed of bonded water. According to the supplier, the egg white protein was composed of 77% ovalbumin and 16% beta-Globulin. Ovalbumin has a molecular weight of 43 kD including 385 amino acid residues; beta globulin has a molecular weight of 76 kD including 686 amino acid residues.[17] Whey protein is composed of 50-55% Beta lactoglobulin (18 kD with 185 amino acid residues) and 20-25% alphalactalbumin (14 kD with 123 amino acid residues).[17] Natural rubber latex (70% solid, plus 30% water; pH: 10.8) samples were supplied by Chemionics Corp. The solution of Human serum albumin (HSA), which contained 25% HSA in phosphate buffer saline (PBS) (Source: Greiner Bio-One GmbH), was provided by Dr. Wen in the Department of Bioengineering at Clemson University. After freeze drying, the HSA (molecular weight~ 66,500D) was found to contain approximately 4% bonded water.

4.3: Results and discussion

4.3.1: Plastics from albumin and whey proteins

4.3.1.1 Fabrication of plastics

To achieve the first objective of developing plastics from undenatured animal proteins, whey and albumin proteins were studied to understand the general process of plastic fabrication. These two proteins are currently used in various technical applications, such as adhesives and coatings,[18,19] and are usually produced through the spray drying process. This process[20] transforms the feed from a fluid state (a solution, a suspension/slurry, or a thixotropic paste or melt) into a dried particulate form (powder, granules, or agglomerates) by spraying ("atomization") the feed into a hot drying medium. The spray is dried until the desired moisture content in the particles is obtained for the required form (as spheres, hollow spheres or cenospheres, fines, and agglomerates). The resulting product is then recovered from the air medium.

In addition to its use for whey and albumin, this process is widely used to produce other vegetable-based proteins, including soy beans, wheat gluten, peanuts, sunflower seeds, leaves, forage crops, and potato tubers, as well as animal-based proteins, such as bloodmeal, fishmeal, whey, and casein. SEM analysis was conducted to determine the particle size and shape of the spray dried whey and albumin used in this work. The SEM micrographs from **Figure 4.1** reveal the particle size of censospheres of approximately 20 microns.

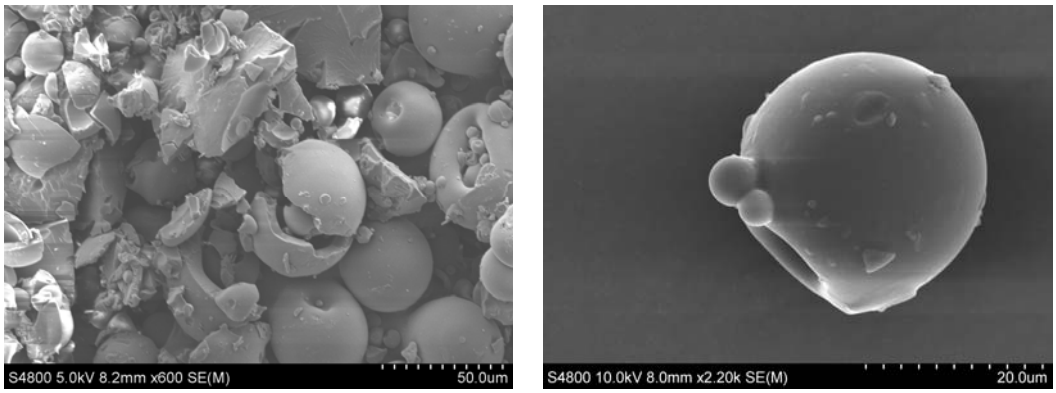

Figure 4.1. Scanning electron microscopy (SEM) micrographs of albumin (left) and whey protein (right) powders.

The albumin and whey powders, as received, had a moisture content of 5.2% and 7.9%, respectively. DSC measurements provide important information about the nature of water incorporated into these proteins. DSC and TGA thermographs for these proteins are shown in **Figure 4.2**. In fact, an endothermic peak around 0°C, which would correspond to the melting of crystallizable (unbound) water, was not observed. Thus, it was concluded that the water molecules situated in these biopolymers were bound to the protein macromolecules.[21]

The DSC thermograms in **Figure 4.2(a)** indicate that the albumin and whey proteins start denaturing at a temperature of 47°C and 78°C, respectively. The endothermic denaturing peak was observed at a temperature of 135° and 132°C for albumin and whey proteins, respectively. However, these temperatures are clearly not the degradation one, which onsets around 245° and 260°C for albumin and whey proteins, respectively, as can be seen in **Figure 4.2(b).**

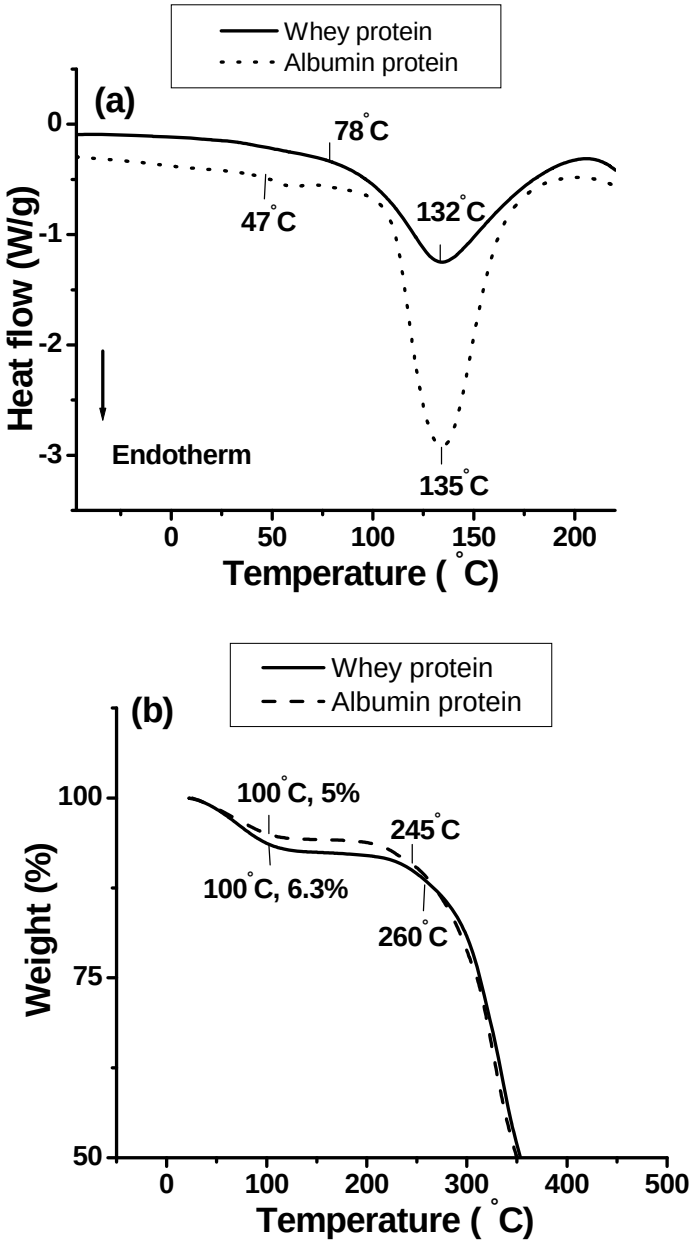

Figure 4.2. Thermal analysis of albumin and whey proteins powder: (a) DSC thermographs; (b) TGA thermographs.

Extensive previous research has found that to produce a plastic with acceptable performance from undenatured proteins, water or other molecules of low molecular

weight should be added to act as a plasticizer to improve the processability and thermoplasticity of the protein during molding.[3,22,23 25] It was observed that as received whey and albumin proteins used in this research did not produce plastic samples when compression molded. This can be seen from the SEM micrograph of brittle "white" albumin material shown in **Figure 4.3.** It was observed that some fusion of the protein particles occurred. However, it appeared that protein material has very high viscosity and, therefore, pressure and time of the compression molding in our experiment was insufficient to prepare plastic. The result indicates the importance of water as a plastisizer for developing bioplastics from these proteins.

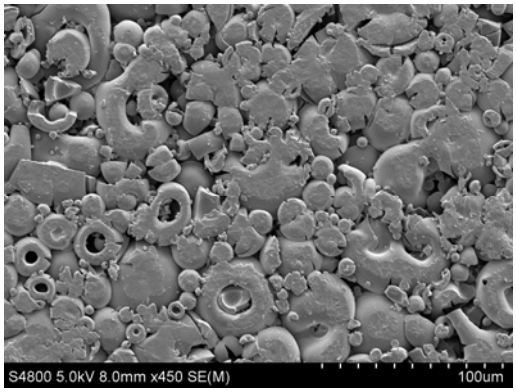

Figure 4.3. SEM micrograph of white brittle albumin material molded at a temperature of 150°C and a pressure of 20 MPa for 5 minutes.

Indeed, previous research has shown that at least 25-30% moisture content is necessary to make thermoplastics from plant- and animal-based proteins.[2,9] Therefore, trials to develop plastics from whey and albumin proteins were conducted at moisture

contents of 25% and higher. **Table 4.1** shows how increasing the water content beyond this optimal amount affects the processability and plastic forming ability.

Table 4.1. Effect of moisture content on plastic forming ability.

Moisture Content	**Consistency**	**Molding material**
25% water	Granular	Plastic
35% water	Agglomeration of granules	Difficult to make plastic
40% water	More viscous	Foam
50% water	Less viscous	Brittle foam

To further optimize the molding process, trials were conducted at pressures of 15, 20, 30, and 40 MPa while keeping the temperature constant at 150°C, and temperatures of 130°, 150°, 160°, and 180°C while keeping the molding pressure constant at 20 MPa. Many researchers have found that a pressure of approximately 20 MPa[2,3,26] is optimal for the development of plastics from these proteins. These temperatures cover the possible extent of denaturing (50% and higher) before degradation, as confirmed by the DSC thermographs of these proteins shown in **Figure 4.2(a).** The corresponding mechanical properties are shown in **Figure 4.4 (a,b)**, which leads to an optimal pressure and temperature of 20 MPa and 150°C, respectively based on tensile testing.

It was observed that the samples produced at temperatures of 130°C and 150°C exhibited a slightly yellow color, while the sample at 160°C had a brown color, indicating thermal degradation. Moreover, the samples produced at 180°C were dark orange, lacking

integrity. Molding pressures below 20 MPa were not sufficient to produce a plastic with acceptable mechanical properties. Other researchers have also found this pressure of approximately 20 MPa[2,3,26] and processing time of approximately of 5 min[3,4] optimal for the development of plastics from these proteins. Therefore, albumin and whey protein powders with 25% w/w of water were compression molded into dogbone and DMA samples at a temperature of 150°C and a pressure of 20 MPa for 5 minutes, followed by ambient cooling. The resulting plastic samples are shown in **Figure 4.5**.

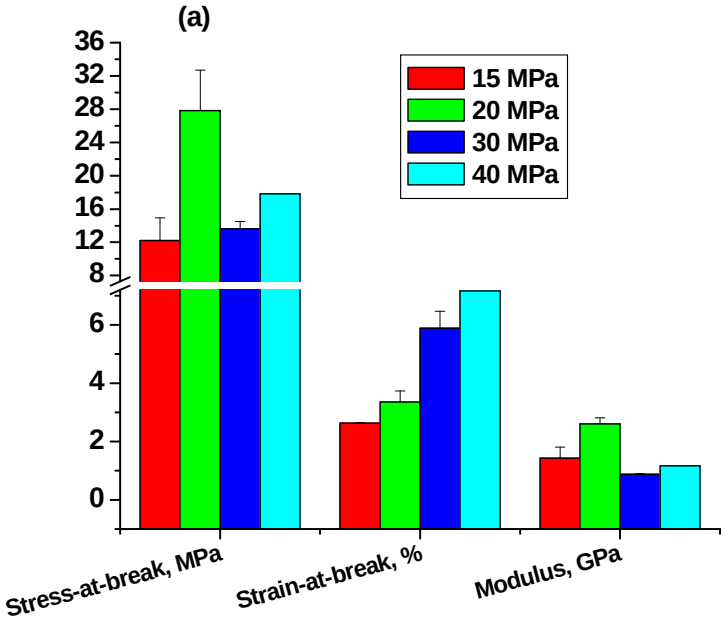

Figure 4.4(a). Mechanical properties of plastics produced from albumin protein, molded for 5 minutes, followed by ambient cooling: (a) variable pressures and a constant temperature of 150°C; (b) variable temperatures and a constant pressure of 20 MPa.

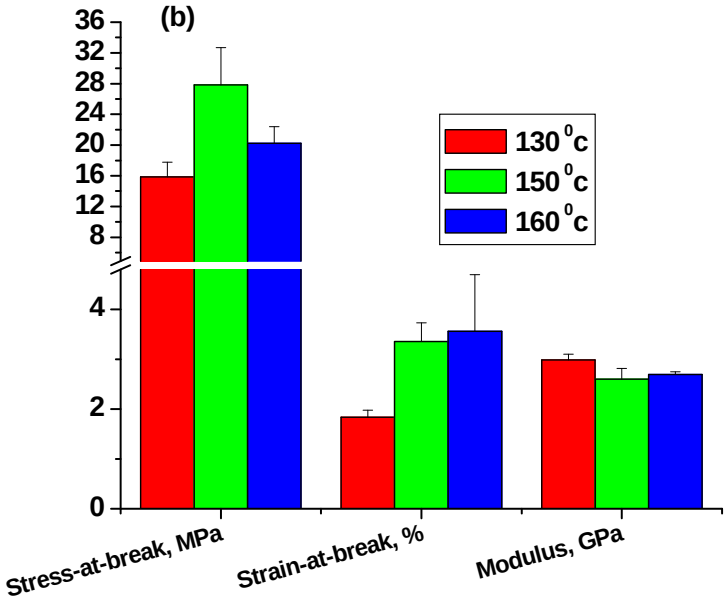

Figure 4.4(b). Mechanical properties of plastics produced from albumin protein, molded for 5 minutes, followed by ambient cooling: (a) variable pressures and a constant temperature of 150°C; (b) variable temperatures and a constant pressure of 20 MPa.

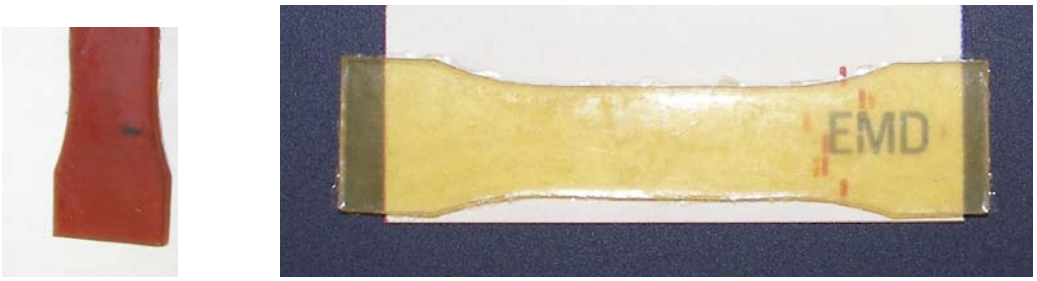

Figure 4.5. Dog bone sample from whey (left) and albumin (right) proteins.

It was observed that samples left for conditioning at room temperature (~27°C)showed an increase in modulus and stress-at-break and a decrease in strain-at-break over time due to the evaporation of the residual water content from the molded

samples. This behavior is attributed to the decrease in volume occupied by plasticizing water, resulting in the densification of the structure. The drying phenomenon and corresponding change in mechanical properties are illustrated in **Figure 4.6(a,b)**. After two days of an exponential drop in moisture content, the drying approached a steady state moisture content of approximately 7-8%.

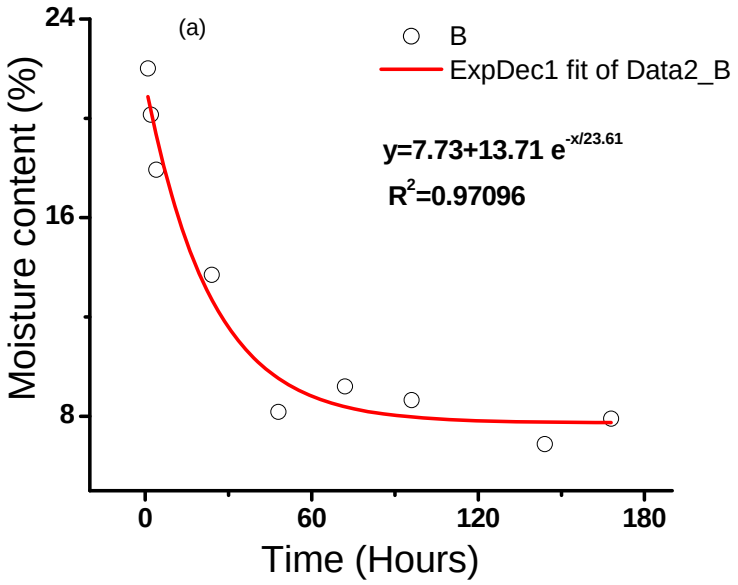

Figure 4.6 (a). Effect of conditioning at room temperature (~27°C) under fume hood on the moisture content of albumin sample molded at a temperature of 150°C and pressure of 20 MPa for 5 minutes.

Since the change in mechanical properties and moisture content of plastics during drying were dynamic events, it was hypothesized that this behavior might be due to the dynamic state of conformational change in the secondary protein structures. DSC experiments on these samples at different time intervals (one to five days) show some

evidence of these structures, as change in heat flow between 95° and 185°C can be seen in **Figure 4.7(a)**. After two days in this temperature range, heat flow does not change, indicating a more stable structure. In addition, this behavior of densification, which probably leads to compact beta sheets, is supported by slow evaporation of water, as shown from the TGA thermograph in **Figure 4.7(b)**.

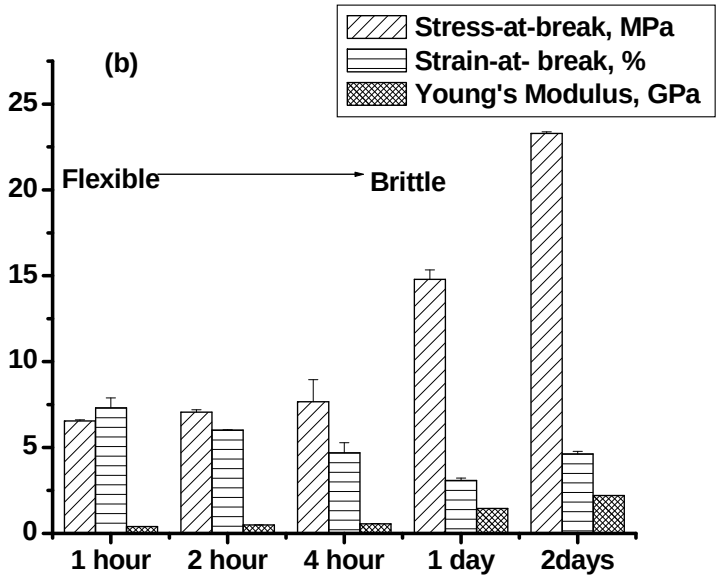

Figure 4.6 (b). Effect of ambient conditioning on the mechanical properties of albumin sample molded at a temperature of 150°C and a pressure of 20 MPa for 5 minutes.

During ambient drying, it was also observed that plastic samples began curling when left unconstrained, and **Figure 4.8(a)** shows out-of plane curling of unconstrained albumin plastic after two days. To prevent this, samples were constrained between glass plates. However, instead of out-of-plane curling, in-plane distortion of the constrained samples was observed after 14 days, as illustrated in **Figure 4.8(b)**.

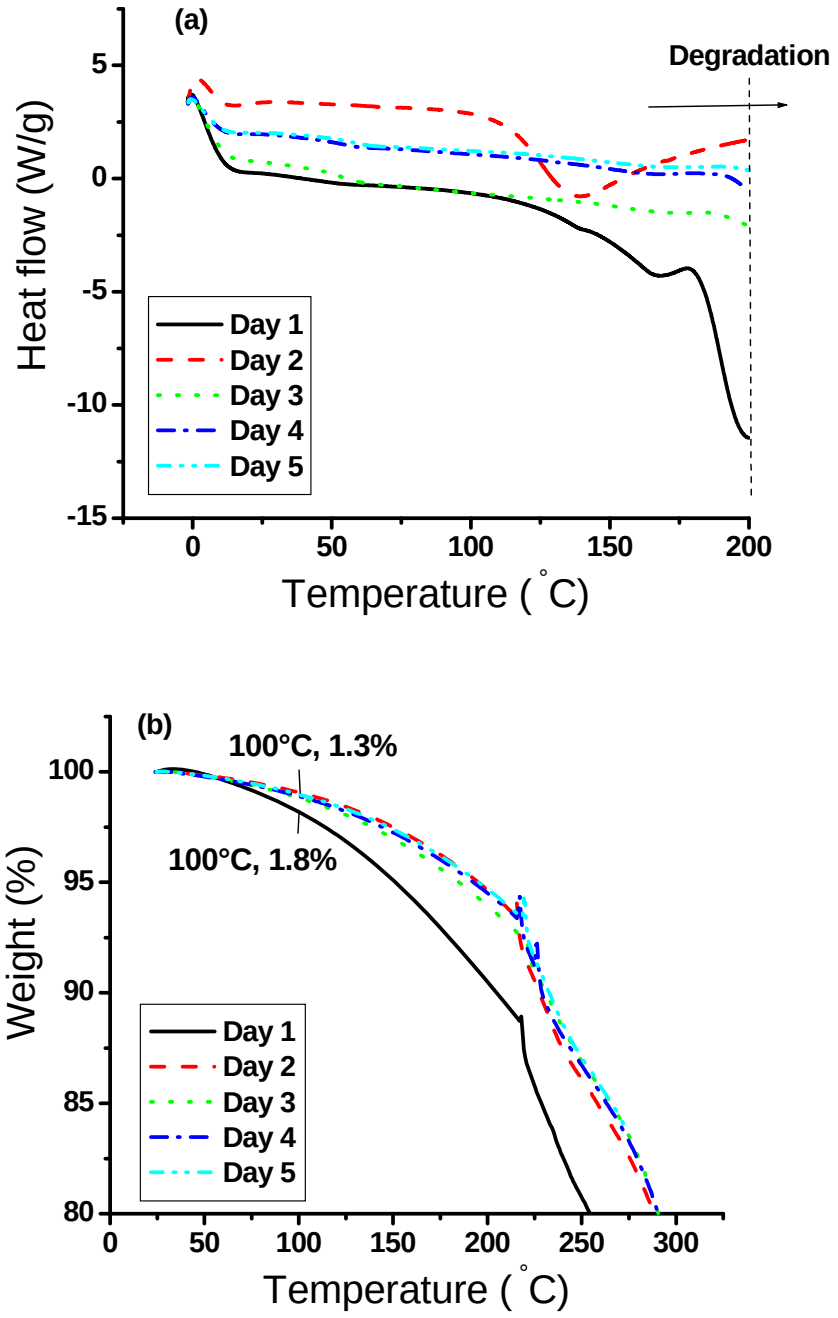

Figure 4.7. Effect of ambient conditioning on thermal properties of albumin plastic, molded at a temperature of 150°C and a pressure of 20 MPa for 5 minutes: (a) DSC thermogram, (b) TGA thermogram.

It is necessary to highlight that the albumin plastics showed a certain yellow color. It was suggested that, it occurred due to oxidation during molding process at high temperature.

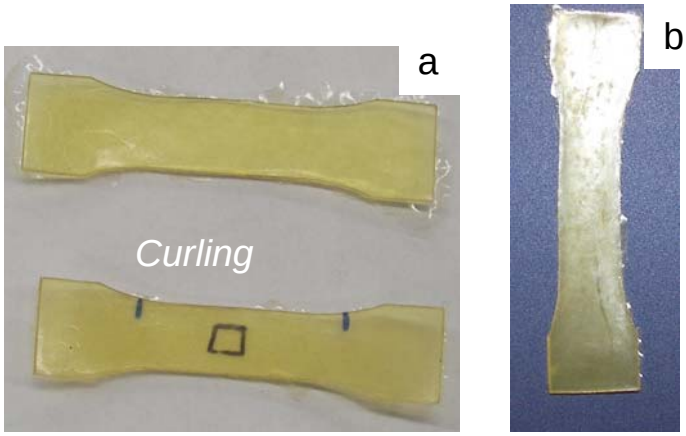

Figure 4.8. Effect of ambient conditioning on albumin sample: a) Out-of-plane curling after two days of unconstrained sample; b) In-plane bending after 14 days of constrained sample.

To accelerate the drying rate, kinetic experiments for moisture evaporation were performed using TGA at various isothermal temperatures, as shown in **Figure 4.9**. The residual moisture content of the plastic samples immediately after molding was 22% compared to 25% water content in the initial protein material. In addition, the drying rate (slope of curves) increased with an increase in isothermal temperature, as could be anticipated. The drying rate was 0.1% per minute at temperature of 50°C compared to 0.2% per minute at 120°C, assuming a linear drying.

However, when a sample was dried at 50°C for 4 hours in an oven, its residual moisture content was 7.4% compared to 3.7% using TGA. This difference was the result of the controlled, higher air flow in the TGA instrument compared to the air flow in oven

drying. To standardize the drying conditions, all plastic samples produced from undenatured proteins were subsequently annealed overnight at 50°C. In addition, all samples were left inside the molds during drying to prevent distortion. This drying procedure resulted in a residual water content of approximately 7.9% and 7.2% for whey and albumin plastic samples, respectively after overnight drying.

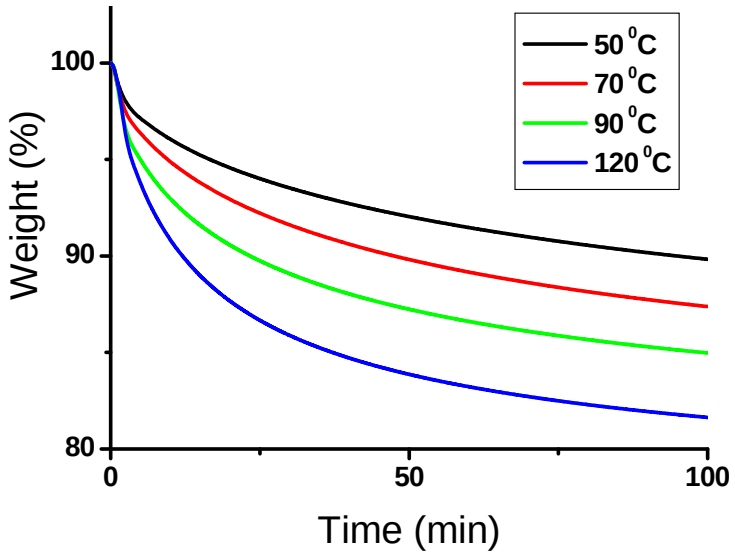

Figure 4.9. Effect of isothermal drying on moisture loss of albumin sample in TGA.

4.3.1.2. Mechanical properties

For mechanical measurements, samples were prepared under optimal conditions: molding temperature of 150°C, molding pressure of 20 MPa, holding time of 5mins, followed by ambient cooling and overnight drying in an oven at 50°C. For these samples, the stress-at-break, strain-at-break, and modulus were measured to be 19 MPa, 5.8%, and 1.4GPa for the whey plastics, and 16.7 MPa, 2.8%, and 2.4 GPa for the albumin plastics.

Figure 4.10(a) shows the typical stress-strain diagram and fracture micrograph for the tested dogbone samples made from the albumin plastic, indicating a ductile fracture. The first region, where stress (σ) increases linearly with strain (ε), is a region of elastic deformation; it is followed by plastic yield and strain hardening regions. This phenomenon of bond breakage in the yield region is reversible in nature, as can be observed from the cyclic loading testing of plastic samples in **Figure 4.10(b).** It appears that prior to the break, the biomacromolecules constituting the sample fold back when the sample is unloaded. This original mechanism of dissipating energy can be extremely useful if the plastic is subjected to a cycling loading during use.

Figure 4.11 shows the dynamic mechanical analysis of plastics made from these proteins. DMA technique[27] is used to measure the deformation of a material in response to vibrational or oscillating forces and determine the storage modulus (E', stiffness), the loss modulus (E"), and the mechanical damping or internal friction (Tanδ or loss factor). The loss tangent ($Tan\delta = \frac{E''}{E'}$), called internal friction or damping, is the ratio of energy dissipated per cycle to the maximum potential energy stored during a cycle. Metallic materials have small internal friction (0.001-0.004), while amorphous viscoelastic polymers (internal friction 0.1-0.3) are good damping materials that decrease undesirable vibration to safe limits by converting it into heat, which is dissipated within the damping materials rather than being radiated as airborne noise.

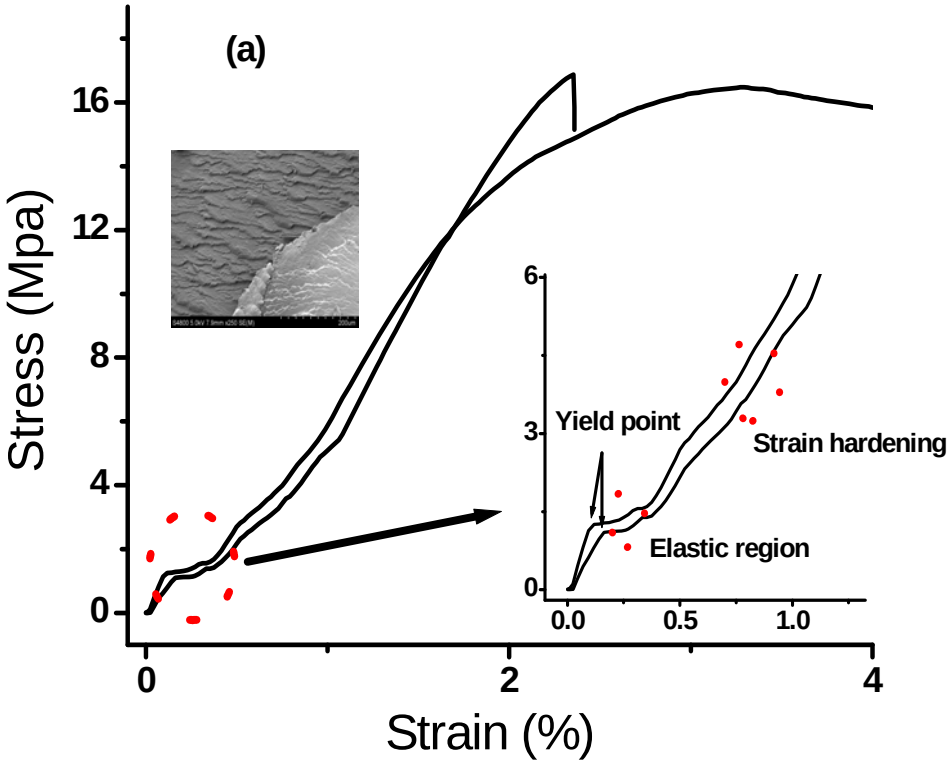

Figure 4.10 (a). Stress-strain curve for the compression molded albumin plastic, molded at a temperature of 150°C, and a pressure of 20 MPa for 5 minutes, followed by ambient cooling and then annealing overnight at temperature of 50°C.

Both albumin and whey plastics showed viscoelastic characteristics of an amorphous hydrophilic polymer. Hence, they have the ability to lose energy as heat (damping) and the ability to recover from deformation (elasticity). Moreover, whey plastic is stiffer than albumin plastic, as confirmed from the higher storage modulus (**Figure 4.11(a)**) over a temperature range of measurement and higher glass-transition temperature (peak of Tanδ curve in **Figure 4.11(b)**).

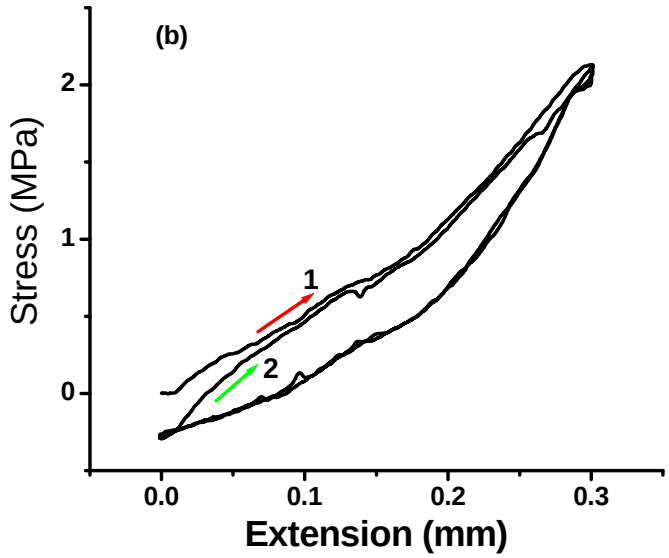

Figure 4.10(b). Cyclic loading testing of the albumin samples, molded at a temperature of 150°C, and a pressure of 20 MPa for 5 minutes, followed by ambient cooling and then annealing overnight at temperature of 50°C.

As scientific literature shows, protein plastic samples are very stable under room conditions and do not show significant degradation or other detrimental effects during storage. For example, previous research by Ye et al.[28] demonstrated the absence of bacterial development on wheat gluten plastic before it was put into soil. However, under favorable soil and water conditions, protein plastic surfaces showed growth of microorganisms whose number increased exponentially with time at the beginning of the degradation. In addition, the study conducted by Domenek et al.[29] observed that bioplastics from wheat gluten protein degraded after 36 days under aerobic fermentation and within 50 days under farmland soil.

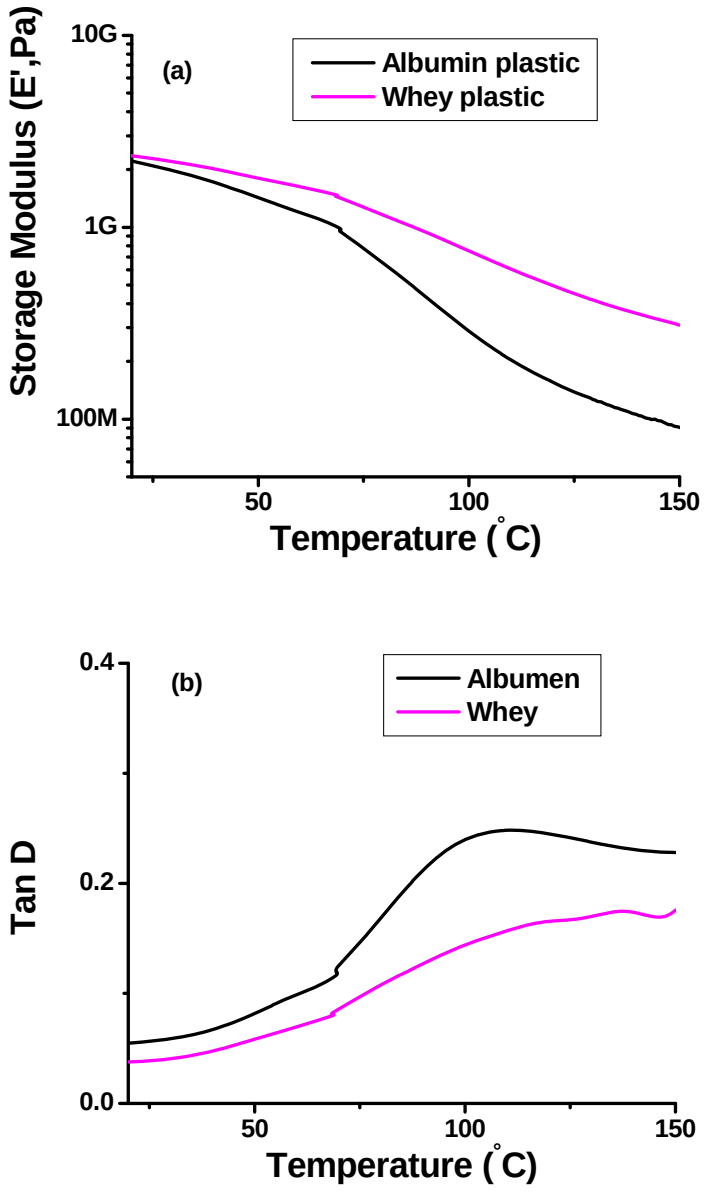

Figure 4.11. (a) Storage modulus; (b) Loss factor or Tan δ of the albumin and whey plastic samples, molded at a temperature of 150°C and a pressure of 20 MPa for 5 minutes, followed by ambient cooling and then annealing overnight at temperature of 50°C.

Therefore, in this research, plastics from undenatured animal proteins were expected to be biodegradable. During a short water absorption testing, albumin plastics demonstrated approximately 57% swelling in 24 hours and 59% in 48 hours. This swelling may result in favorable conditions for microorganisms to attack amide groups to cause biodegradation.

4.3.2: Plastics for medical implants and drug delivery

Protein plastics from various molding processes have a significant potential to impact the development of biomaterials for medical applications due to their benign properties. Past studies have shown the importance of blood-biomaterial interaction for medical devices like catheters, cannuales, guide wires, stents, shunts, vascular grafts, heart valves, heart and ventricular assist devices, oxygenators, and dialyzers.[30] It is important that these devices be biocompatible. If they are not, serious complications may result, including thrombosis, thromboembolism, the activation of circulating hemostatic blood elements, and the activation of inflammatory and immunologic pathways. Biocompatibility avoids these complications by allowing the host to respond appropriately to provide an improved healing response.

Research has found that interfacial reactions involving a physiochemical process such as protein adsorption occur with most biomaterials.[31] Specifically hydrophilic polymers, such as poly(vinyl alcohol), acrylic and methacrylic polymers and copolymers exhibit variable thrombogenicity but little capacity to retain the adherent thrombus. Surface grafted hydrogels have also been found to improve thromboresistance; as a

result, they can improve catheter lubricity and act effectively as reservoirs for drug delivery. Like hydrogels, in-vitro studies of hydrophilic polymer poly (ethylene oxide) surfaces indicate that they have reduced interaction with blood proteins and cells. Various biological and bioactive molecules used as coatings, such as phospholipids and heparin, also have been clinically shown to improve thromboresistance. However, the sterilization process required before implantation may cause deleterious effects to the coating.

To address the issue of biocompatibility, the research reported here produced plastic samples from chicken egg white albumin and human serum albumin to study their interaction with bacteria, which otherwise may produce inflammatory response.

4.3.2.1: Plastic from albumin

Plastic samples were prepared from egg white protein following the same protocol for molding used for egg white and whey proteins. These plastic samples were then sonicated for 10 minutes each in a bath of hexane, toluene, and alcohol to check their surfaces. It was observed that these solvents did not harm the samples. This cleaning process ensured that the samples were free of contaminants and pathogens. Subsequently, these samples were sent to Dr. Wen's research group in the Bioengineering Department at Clemson University for observation of bacterial growth during *in-vivo* and *in-vitro* experiments. The results of initial *in-vitro* study are reported in **Figure 4.12**, showing the absence of bacterial adhesion after the samples were immersed in a bath of bacterial solution for 3 hours compared to a control sample of titanium, which is the typical material used for implants.

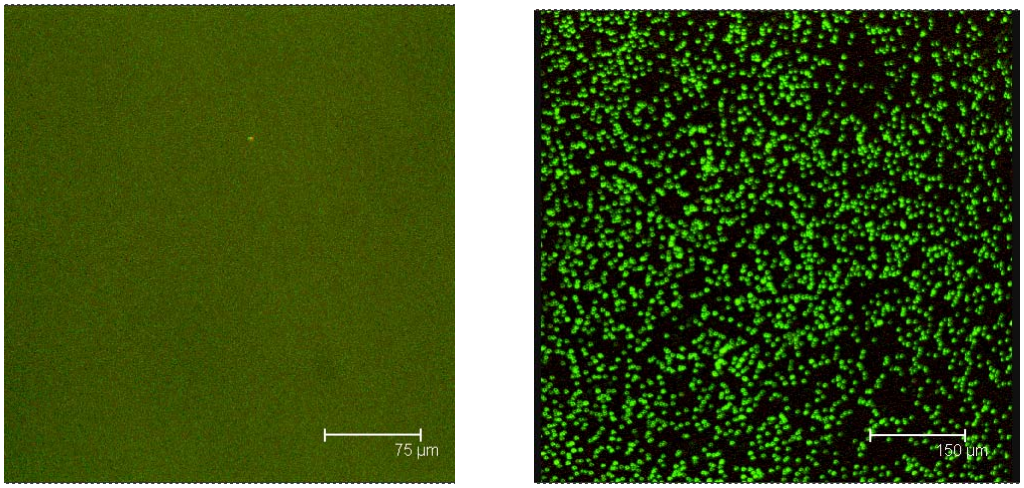

Figure 4.12. Bacteria cultured on albumin plastic sample (left) and titanium control sample (right).

One possible explanation of this finding could be the hydration around the material, which inhibits the bacterial adhesion. In addition, it has been found that albumin possesses good antibacterial activity over many bacterial strains, such as S. aureus, S. epidermidis, E coli, S. mutans, and S. mitis.[32] According to Tang et al.[33] and Kinnari et al.[34], this may be attributed to the fact that the albumin is an acidic protein with a net negative surface charge and reduced surface hydrophobicity and thus promoting repulsion between bacteria and surface.

4.3.2.2: Plastics from human albumin

A similar procedure for developing plastics from egg albumin and whey proteins was used to fabricate plastics made from human serum albumin protein. Plastic samples were prepared from a 25% human serum albumin (HSA) in phosphate buffer saline (PBS), which was purified and freeze dried, resulting in a residual bonded water content

of 5%. This non-crystallizable bonded water was not observed in the DSC thermograph at 0°C (**Figure 4.13 (a)).** However, this water was observed in the TGA measurement shown in **Figure 4.13 (b)**. In addition, DSC thermograms show the protein denaturing or unfolding at approximately 130-150°C. This is clearly not the degradation temperature, which occurs at approximately 250°C as can be seen from TGA thermographs**.** Based on these results, HSA powder with 25% w/w of added water was compression molded at a temperature of 150°C and a pressure of 20MPa for 5 minutes, followed by ambient cooling and overnight drying in an oven at 50^{o}C.

During the preparation of the plastic samples, the protein macromolecules denatured due to combined effect of heat, pressure, and time. HSA starts denaturing at a temperature of 86°C. In fact, the original endothermic peak due to the denaturation (150°C) was not detected for the plastic samples obtained (**Figure 4.13(a)**). The result may indicate that another type of folded structure is formed during the plastic preparation. TGA results showed that a different weight loss pattern was observed for the plastic samples (**Figure 4.13(b)**) in comparison to the original HSA material. Specifically, the first water weight loss occurred over a more extended temperature range: from room temperature to approximately 250°C. The slowdown of the water loss can be explained by the denser structure of the plastic sample as compared with the protein powder. The onset temperature of degradation (260°C), however, was virtually unaffected by the compression molding.

The mechanical properties of plastics produced from human serum albumin were compared to those of plastics produced from chicken egg white albumin, as shown in

Figure 4.14. HSA plastic exhibited increased strength, elongation, and modulus compared to egg white plastic. Past research has found that protein-based plastics are composed of a thermoset network, resulting from such factors as interaction due to hydrogen bonding in beta-sheets[35] and the formation of crosslinks[36] through the amino groups reaction. These crosslinks on thermal heating may form amide and ester links because of the reaction between the COOH and NH_2 side groups and the COOH and OH side groups of amino acid residues, respectively. The free COOH groups are primarily found in amino acids, such as aspartic and glutamic acid, while the OH groups are found in serine, threonine, and tyrosine amino acids; the NH_2 side groups are found in arginine and lysine amino acid residues. In addition, higher molecular weight of HSA protein suggests better mechanical properties than egg albumin.

However, the comparison of storage modulus (E') and loss factor (ratio of loss modulus to elastic modulus) of these plastics, as seen in **Figure 4.15,** did not demonstrate a significance difference. However, lower values of the loss factor between room temperature and 150°C, as well as the higher peak temperature (or glass-transition temperature) of HSA plastic may suggest a stronger network structure than egg whites plastic, probably because of the formation of multiple crosslinks.

Moreover, it was observed that HSA plastics swelled to 83% when immersed in DI water for 24 hours, becoming a flexible gel. If left under ambient conditions, HSA plastic sample returned to a dry state over a period of time.

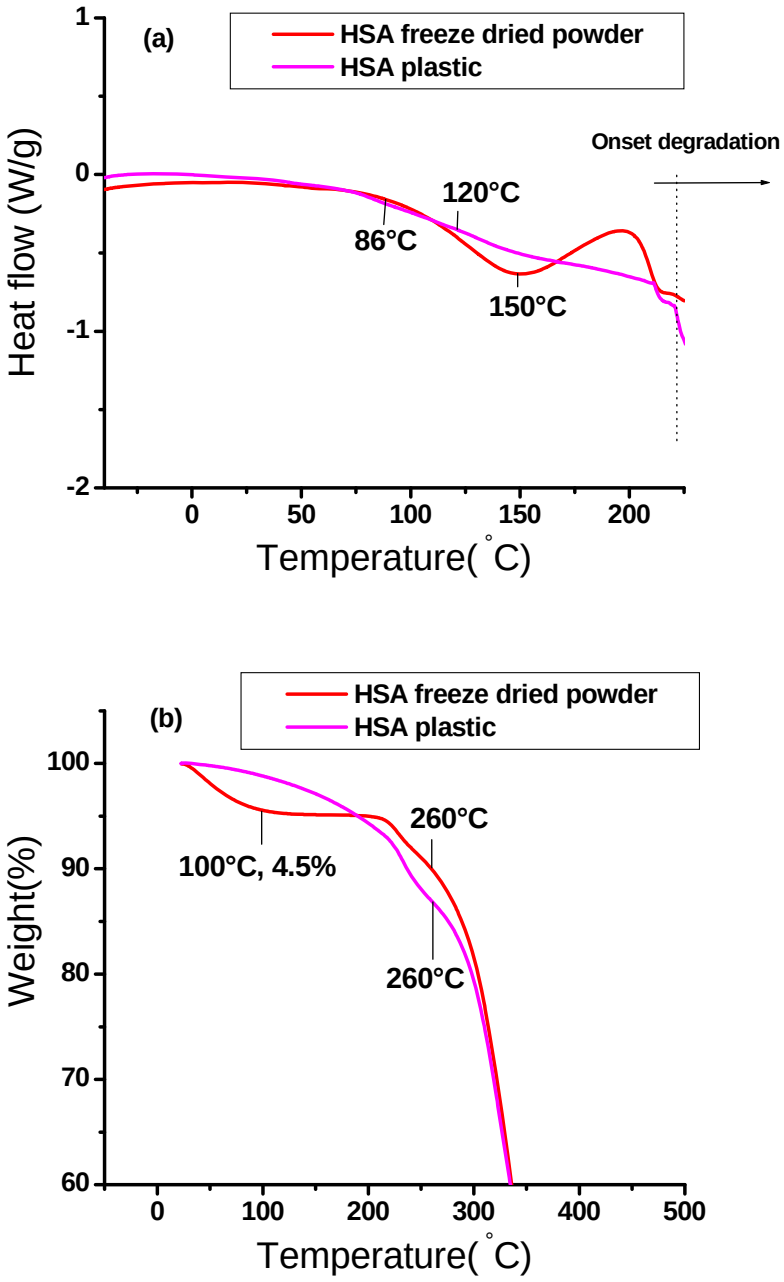

Figure 4.13. Thermal analysis of HSA protein powder and its plastic: (a) DSC thermographs; (b) TGA thermographs.

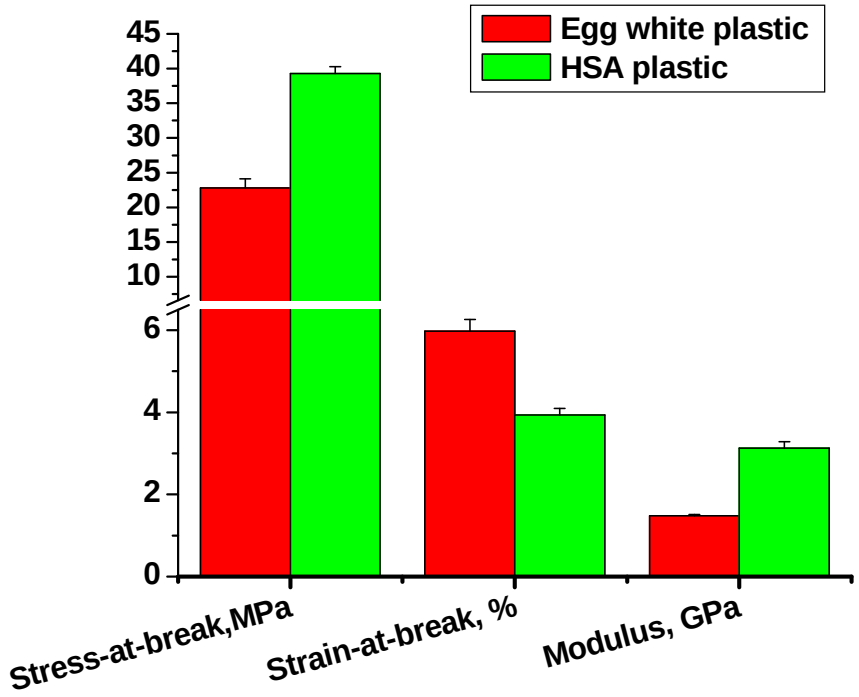

Figure 4.14. Mechanical properties of plastics produced from human serum albumin and egg white proteins, molded at a temperature of 150°C and pressure of 20 MPa, followed by ambient air cooling and annealing overnight at 50°C.

To observe the swelling kinetics in water within 24 hours period, TMA setup involving a quartz probe in compression mode was used as in **Figure 4.16.** As **Figure 4.17** indicates the initial swelling rate was fast, slowing until eventually approaching a steady state. This characteristic swelling, similar to that of hydrogels and poly (ethylene oxide) surfaces[30], may help in designing medical devices having an improved thromboresistance and biocompatibility while at the same time being flexible and biodegradable.

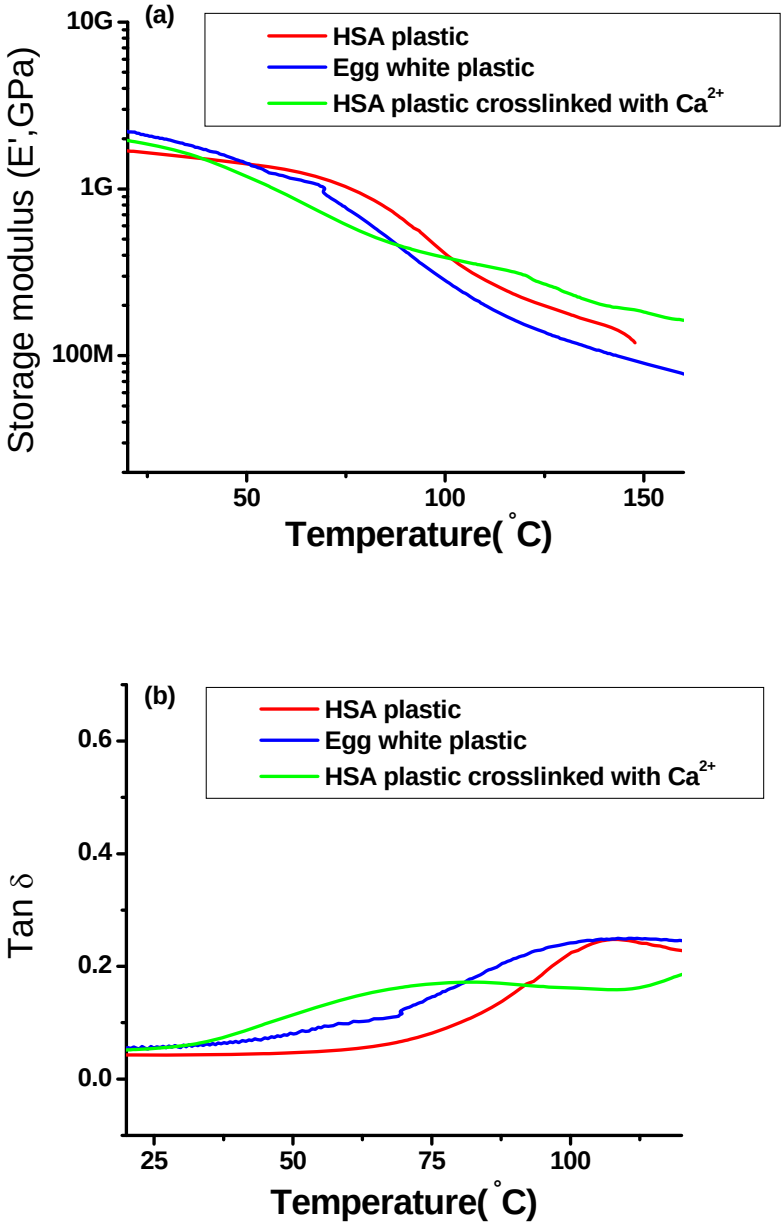

Figure 4.15. Dynamic mechanical properties of plastics produced from human serum albumin and egg white proteins, molded at a temperature of 150°C and a pressure of 20 MPa, followed by ambient air cooling and annealing overnight at 50°C: (a) Storage or elastic modulus, (b) Loss factor or internal friction.

Figure 4.16. Experimental setup of swelling kinetics of HSA plastics using thermomechanical analyzer.

To examine the change in modulus during swelling, the TMA setup shown in **Figure 4.16** was used. The change in the lateral deformation of a sample over time is shown in **Figure 4.18**. First, the depth of penetration of the dry sample was measured under a 50mN compression load. Subsequently, water was added to the Petri dish and the sample was allowed to swell without any load on the probe for approximately two hours. The depth of penetration of the resulting gelled material was measured at the same compression load of 50mN. The temperature during the entire process was the room temperature. The Young's modulus of this material was determined using **Equation 4.1,** as Yanni et al.[37] demonstrated there was a correlation between the data using TMA and the data from the accepted ASTM methods.[38]

$$E = \frac{3F}{4Dd} \quad \text{or } E = \frac{a}{d} \tag{4.1}$$

where: E represents the modulus, MPa; F the force, N; D the diameter of a circular, flat tipped probe, mm; and d the penetration depth, mm. Note: a represents the constant.

According to them, Young's modulus of a material may be determined as a function of temperature by following the penetration of a weighted probe into a sample as the sample is heated at a uniform rate. However, this is not an absolute method, which requires calibration for any material of interest.

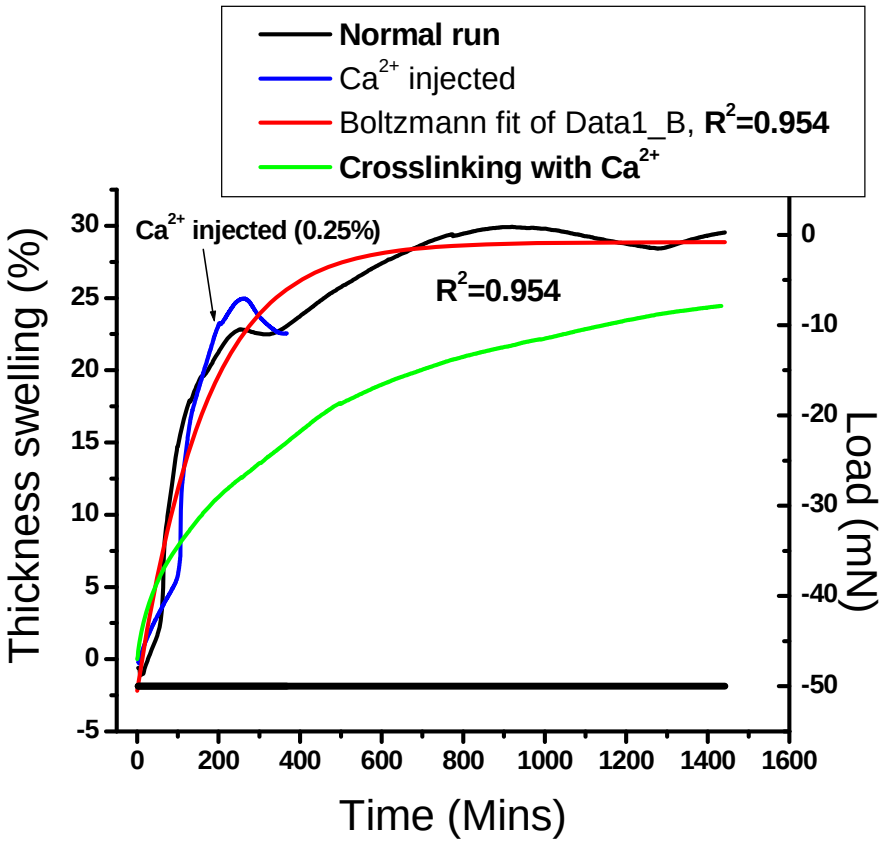

Figure 4.17. Swelling deformation measured during the swelling kinetics of plastics produced from human serum albumin protein, produced at a temperature of 150°C and pressure of 20 MPa, followed by ambient cooling and annealing overnight at 50°C.

The initial Young's modulus was 3.13 GPa, and the constant (a) was 18.3. As **Figure 4.18** shows, after being subjected to a swelling deformation, the modulus of the

plastic determined by **Equation 4.2** is reduced due to gelation. This trend continues until the gel system collapses after eight hours, reaching a stable gel system state.

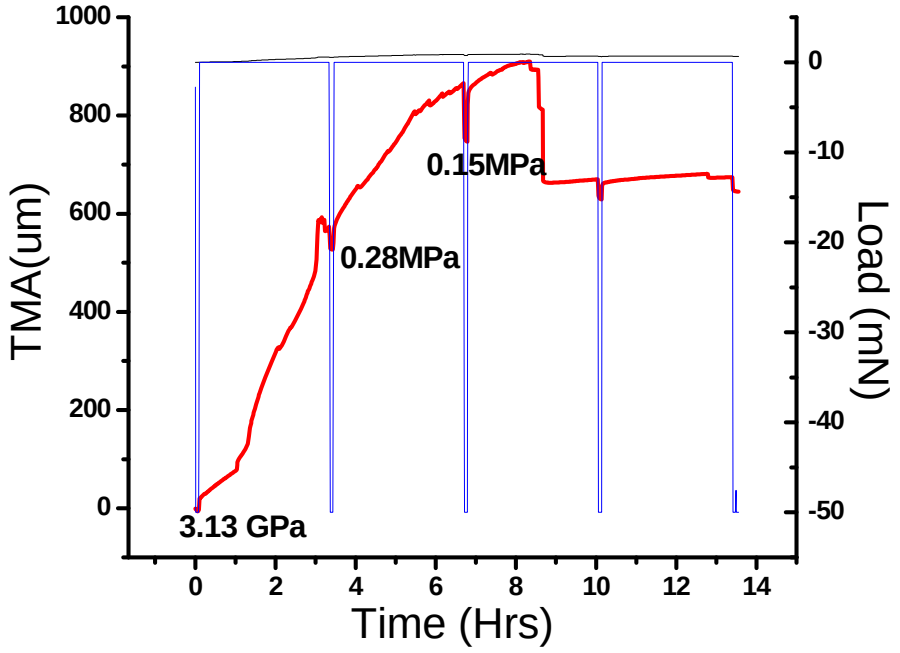

Figure 4.18. Modulus of plastics produced from human serum albumin protein, produced at a temperature of 150°C and a pressure of 20 MPa, followed by ambient cooling and annealing overnight at 50°C.

To modify the degree of swelling, calcium ions were added as a crosslinking agent. Calcium ions can interact with carboxylic units present in aspartic and glutamic amino acids residues and form ionic bridges between different chains of protein material. This method to modify mechanical properties and behavior of polymers containing carboxylic groups employing Ca^{2+} ions is known and used, for example, to alternate properties of alginate fibers.[39]

During one of the swelling experiments using the TMA probe, calcium ions (0.25%w/v of $CaCl_2$ solution) were injected, and as **Figure 4.17** shows, the system shrank as water molecules were replaced by calcium ions forming crosslinks with carboxylic units. To substantiate this effect of calcium ions on crosslinking, one sample of HSA plastic was swelled under water for two hours and then transferred to a calcium chloride solution (0.25%w/v) overnight. The sample was then dried under ambient conditions for three days before their swelling was measured using the TMA setup described earlier. There was found to be a significant drop in swelling, as can be seen in **Figure 4.17**, which is attributed to the new crosslinks formed by calcium ions. Thus, it is possible to vary the concentration and treatment time of calcium ions to alter the water resistance properties of these plastics.

4.4: Conclusion

Plastic samples made from pure, undenatured animal proteins of chicken egg whites, whey, and human serum albumin were successfully produced through the compression-molding process. These plastics were prepared under the optimal conditions: molding temperature of 150°C, molding pressure of 20 MPa, holding time of 5mins, followed by ambient cooling and overnight drying in an oven at 50°C. The water content in the protein material during thermal processing played a vital role in the development of these plastics. In addition, ageing (water evaporation) during storage lead to an increase in the plastic's mechanical properties of strength and stiffness (modulus). A reversible stress-strain property over the yield region was observed. These plastics

showed viscoelastic characteristics of an amorphous polymer. In addition, significant swelling of these plastics in water may produce favorable conditions for microorganisms to attack.

Plastic samples produced from chicken egg white albumin and human serum albumin demonstrated no bacterial adhesion when cultured with *S. aureus* bacteria. HSA plastics exhibited increased strength, elongation, and modulus compared to egg white plastics. There was found to be a significant drop in swelling of HSA plastics due to modification with calcium ions as crosslinks.

4.5: References:

[1] Kumar, R., Choudhary, V., Mishra, S., Varma, I. K., and Mattiason, B., Ind. Crops Prod. (2002), 16**,** 155**.**

[2] Salmoral, E. M., Gonzalez, M. E., Mariscal, M. P., and Medina, L. F., Ind. Crops Prod. (2000), 11, 227.

[3] Paetau, I., Chen, C. Z., and Jane, J. L. Ind. Eng. Chem. Res. (1994),33, 1821.

[4] Zhong, Z., and Sun, X. S. Polymer (2001), 42, 6961.

[5] Wang, C., Carriere, C. J., and Willett, J. L., J. Polym. Sci.: Part B: Polym. Phys. (2002),40, 2324.

[6] Orliac, O., Silveste, F., Rouilly, A., and Rigal. L., Ind. Eng. Chem. Res.(2003), 42, 1674.

[7] Aithani, D., and Mohanty, A. K., Ind. Eng. Chem. Res.(2006), 45, 6147.

[8]. Jerez, A., Partal, P., Martínez, I., Gallegos, C., and Guerrero, A. J. Food Eng. (2007),

82, 608.

[9] Sothornvit, R., Olsen, C. W., Mchugh, T. H., and Krochta, J. M., J Food Sci. (2003), 68, 1985.

[10] Barone, J. R., Schmidt, W. F., and Gregoire, N. T., J. Appl. Polym. Sci. (2006), 100, 1432.

[11] Cuq, B., Nathalie, G., and Guilbert, S., Polymer (1997), 38, 4071.

[12] Garcia, R.A., Onwulata, C. I., and Ashby, R. D., J. Agric. Food Chem. (2004), 52, 3776.

[13] Mohanty, A. K., Tummala, P., Liu, W., Misra, M., Mulukutla, P. V., and Drzal, L. T., J. Polym. Environ. (2005), 13, 279.

[14] Liu, W., Misra, M., Askeland, P., Drzal, L. T., and Mohanty, A. K., Polymer (2005), 46, 2710.

[15] Isobe, S., Sakabe, H., Yoshina, T., Wu, Q. X., Nagai, M., Tomita, T., and Yanai, N., Japanese Patent No. 2002-246346.

[16] Ye, Peng, Reitz, L., Horan, C., and Parnas, R., J. Polym Environ (2006), 14, 1.

[17] http://www.rcsb.org, Protein Data bank.

[18]. Audic, J-. L.; Chaufer, B.; Daufin, G. Le Lait 2003, 83, 417.

[19]. Jerez, A., Partal, P., Martínez, I., Gallegos, C., Guerrero, A., J. Food Engg. (2007), 82, 608.

[20] Masters, K., Spray Drying Handbook (1979). John Wiley & Sons Inc., New York.

[21]. Muffett, D. J., and Snyder, H. E., J. Agric. Food Chem. (1980), 28, 1303.

[22] Zhang, J., Mungara, P., and Jane, J., Polymer (2001), 42, 2569.

[23]. Cuq, B., Gontard, N., and Guilbert, S., Polymer (1997), 38, 4071.

[24]. Rouilly, A., Orliac, O., Silvestre, L., and Rigal, L., Polymer (2001), 42, 10111.

[25]. Matveev, Y. I., Grinberg, V. Y., Tolstoguzov, V. B., Food Hydrocolloids (2000), 14, 425.

[26] Sue, H.- J., Wang, S., and Jane, J.- L., Polymer (1997), 38, 5035.

[27] Murayama, T., Dynamic Mechanical Analysis of Polymeric Material (1978), Elsevier Scientific Publishing Company, Amsterdam- Oxford- New York.

[28] Ye, P., Reitz, L., Horan, C., and Parnas, R., J. Polym. Environ. (2006), 14, 1.

[29] Domenek, S., Feuilloley, P., Gratraud, J., Morel, M.-, and Guilbert, S., Chemosphere (2004), 54, 551.

[30] Hanson, S. R. In Handbook of Biomaterial Properties 1998, Black, J., and Hastings, G., Eds.; Chapman & Hall, London, Chap.C1.

[31] Williams, D. F. In Handbook of Biomaterial Properties 1998, Black, J., and Hastings, G., Eds.; Chapman & Hall, London, Chap.1.

[32] Qiu, Y., Zhang, N., An, Y. H., and Wen, X., Int. J. Art. Org. (2007), 30, 828.

[33] Tang, H., Wang, A., Liang, X., Cao, T., Salley, S. O., McAllister, J. P., and Simon Ng, K. Y., Collo. Surf. B: Bio. (2006), 51, 16.

[34] Kinnari, T. J., and Jero, J., Otolaryngology-Head and Neck Surgery (2005), 133, 596.

[35] De Graaf, L. A., J. Biotech. (2000), 79, 299.

[36] Vaz, C. M., De Graaf, L. A., Reis, R. L., and Cunha, A. M. In Polymer Based Systems on Tissue Engineering, Replacemetn and Regeneration 2002, Reis, R. L., and Cohn, D., Eds.; Kluwer Academic Publishers, Netherlands, Pg. 93.

[37] ASTM standard, E2347-04.

[38] Carter, O. L. et al., Thermomechanica Acta (1972), 4, 199.

[39] Goh, G. H., Heng, P. W. S., Huang, E. P. E., Li, B. K. H., and Chan, L. W., J. Anti. Chemo. (2008),62, 105.

CHAPTER 5

BIODEGRADABLE PLASTICS FROM BLENDS OF UNDENATURED PROTEINS

5.1: Introduction

One of the most efficient routes for obtaining plastics with enhanced properties is polymer blending, in which two or more polymers are combined in one polymeric material. For instance, blends of synthetic and natural polymers (e.g., polysaccharide, proteins) have been used to produce totally and partially degradable blends.[1] For a polyblend, a weakness in one component can, to a certain extent, be camouflaged by the strength in the remaining parts.[2] In a homogeneous blend, the components of the blend lose part of their identity. The final properties of a miscible blend usually follow the so-called "mixing rule" (the arithmetical average of blend components) (**Figure 5.1**).

In a phase-separated blend, the properties of all blend components are present, and the final performance of the blend is very dependent upon the size of structural elements and their adhesion at the interface.[2] In general, the majority of immiscible blends are incompatible and demonstrate negative deviation from the "mixing rule" because of gross phase morphology and low interfacial adhesion. These blends are in many ways futile if they are not compatibilized. In a few exceptional cases, some properties of a compatible blend may be better than those of the individual components. Namely, a synergistic effect, which is sometimes difficult to predict, is observed. The cartoon of mechanical performance of polymer blends is represented in **Figure 5.1**.

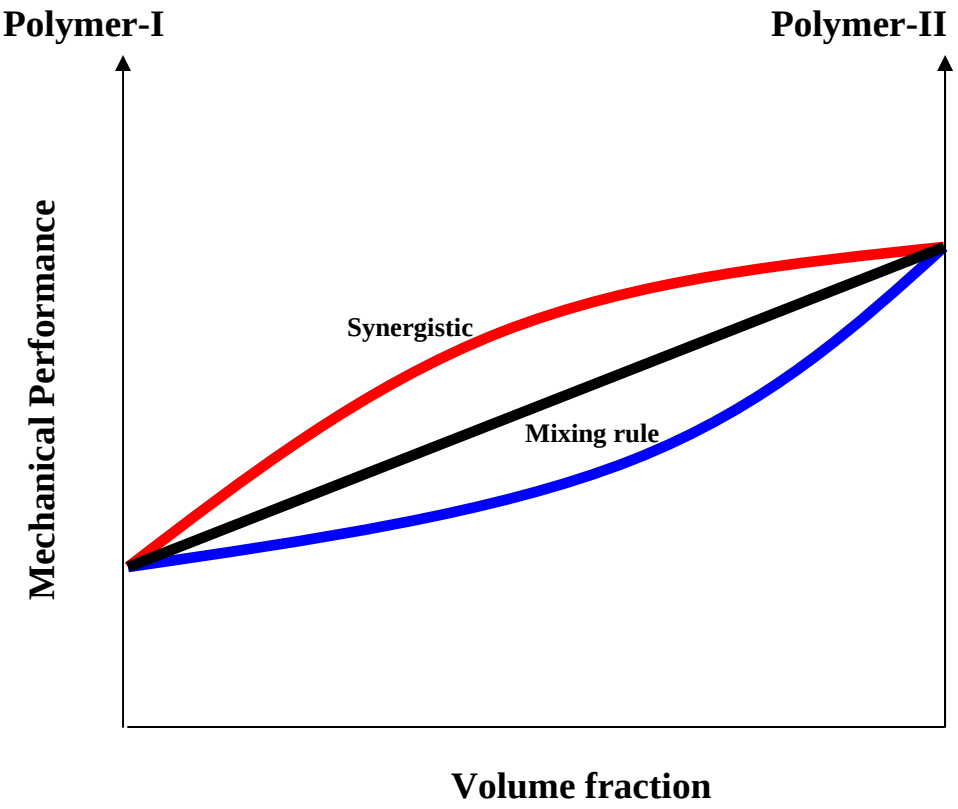

Figure 5.1. Mechanical performance of polymer blends.

Salmoral et al.[3] studied compression molding processes to prepare plastic with acceptable properties from the blends containing chickpea proteins, starch, and glycerol. In addition, Wu et al.[4] developed plastics from the blends of soy meal and natural rubber pellets of improved toughness and water resistance.

The blending of proteins with synthetic biodegradable polymers has also been studied to address the issues of water resistance and flexibility. For example, Zhong and Sun[5] prepared plastics with improved mechanical and water resistance properties from the blends of soy protein and synthetic biodegradable polycaprolactone, along with

methylene diphenyl diisocyanate (MDI) as a compatibilizer. Moreover, they used another synthetic polymer poly(ethylene-ethyl-acrylate) along with MDI to produce plastic with better properties than those demonstrated by the blends of soy protein and polycaprolactone.[6] In addition, Aithani et al. [7] developed injection-molded biodegradable plastics from the blends of corn gluten meal (a byproduct of ethanol industries) and polycaprolactone for packaging. Similarly, Mungara et al.[8] studied the blends of soy protein and biodegradable polyester along with polyvinylpyrolidone as a compatibilizer to produce plastics with reduced moisture sensitivity, resulting in a good shelf life and stability under ambient conditions.

In another study, Wang et al.[9] developed plastics having mechanical properties similar to commercial thermoplastics such as polystyrene from the blends of soybean and synthetic biodegradable polymer poly(hydroxyl ester ether) as well as wheat gluten and poly(hydroxyl ester ether) .

Protein-protein blends have also been studied for developing glues, fibers, and plastics. For example, Zhang et al.[10] extruded zein-soy protein to develop wet-spun fibers. The tenacity of these fibers was greater than that of soy protein fibers at 11% relative humidity. Kumar et al.[11], in a review, stated that soybean protein was mixed with animal blood to produce adhesive glue and found to be ideal for wood product assembly. In addition, soluble dried chicken blood blended with soy protein in a 1:1 ratio, crosslinked with dialdehyde starch, has been used for manufacturing interior-type plywood. Soybean-casein glues have also demonstrated composite performance for developing panels and flush door assemblies.[11]

The primary objective of this phase of research was to develop blends from whey and albumin proteins, and whey and natural rubber latex, to improve the flexibility or toughness of these protein-based plastics while minimizing the use of synthetic petroleum-based products. Traditionally, polyol plasticizers are used to impart flexibility to protein-based plastics. It has been found that these plasticizers can penetrate out of protein matrix and form liquid-like drops on the surface of a film at high relative humidity.[12] This phenomenon is called "leaching." In contrast, rubber is found to be a biobased and biodegradable[12,13] natural polymer, and has been used for improving the elongation properties of the material. The rubber particles are surrounded by protein anions, hindering the coagulation of the latex.[4,14,15] These proteins are decomposed rapidly by bacteria and enzymes when exposed to air, causing the rubber to partially coagulate. In the presence of air, crosslinking of the rubber occurs within the latex particles resulting in gel formation and subsequent degradation of the polymer chains.[15]

Furthermore, protein-protein blends provide an opportunity to use their complimentary properties to develop plastics of desired properties. Another important objective of this research was to investigate the thermal and the mechanical characteristics of these plastics in understanding the fabrication process.

5.2: Materials

Whey and egg albumin proteins, and natural rubber latex, were used to develop biodegradable blends. The whey protein isolate (BiPro, Davisco Foods Intl.) and albumin from chicken egg whites (A5253, Sigma-Aldrich) contained 91% and at least 90%

proteins, respectively. According to the supplier, the egg white protein was composed of 77% ovalbumin and 16% beta-Globulin. Ovalbumin has a molecular weight of 43 kD, including 385 amino acid residues; beta globulin has a molecular weight of 76 kD, including 686 amino acid residues.[16] Whey protein is composed of 50-55% Beta lactoglobulin (18 kD with 185 amino acid residues) and 20-25% alphalactalbumin (14kD with 123 amino acid residues).[16] Natural rubber latex (70% solid plus 30% water; pH: 10.8) samples were supplied by Chemionics Corp.

5.3: Results and discussion

5.3.1: Bioplastics from blends

5.3.1.1: Blends of whey and natural rubber latex

Natural rubber was the first biopolymer used in the rubber industry.[17] It is found to be biobased and biodegradable[12,13], a natural polymer, and has been used for improving the elongation properties of the material. Rubber latex is essentially a dispersion or emulsion of *cis*-1,4-polyisoprene in water, having particle size between 0.15 and 3.0μm. Other components of the rubber latex are 1-2% protein and phosphoproteins, 2% resins, 1% fatty acids, 1% carbohydrates, and approximately 0.5% inorganic salt. The rubber particles are surrounded by protein anions, which hinder the coagulation of the latex.[4,14,15] In addition, these proteins are decomposed rapidly by bacteria and enzymes when exposed to air, partially coagulating the rubber. Therefore, blends of whey protein and rubber latex were found in this work to be compatible for the development of plastic with improved mechanical properties.

By using a DSM microblender twin screw extruder, blends of whey protein and natural rubber latex were prepared according to the method described in the experimental section of this chapter. It was observed that at more than 20% of natural rubber content it was difficult to mix and extrude the blend due to the increased viscosity (rubber has a molecular weight in excess of one million[18]). In addition, it was observed that the blends required 105% of water per protein weight to obtain smooth processability during blending.

Results of thermal analysis of the blends using DSC and TGA techniques are shown in **Figure 5.2**. The DSC thermograms in **Figure 5.2(a)** did not demonstrate prominent endothermic peaks due to denaturing of the whey protein, indicating the plasticizing effect of water. However, an endotherm at 0°C due to unbound water can be observed. Extensive previous research has found that to produce a plastic with acceptable performance from undenatured proteins, water or other molecules of low molecular weight should be added to act as a plasticizer to improve the processability and thermoplasticity of the protein during molding.[19,20-22] This crystallizable water was not present when whey protein was added with 25wt.-% of water, as shown in **Figure 4.2(a)** of Chapter 4. The on-set of degradation did not change, as can be seen in **Figure 5.2(b)** (compare to **Figure 4.2(b)** of Chapter 4).

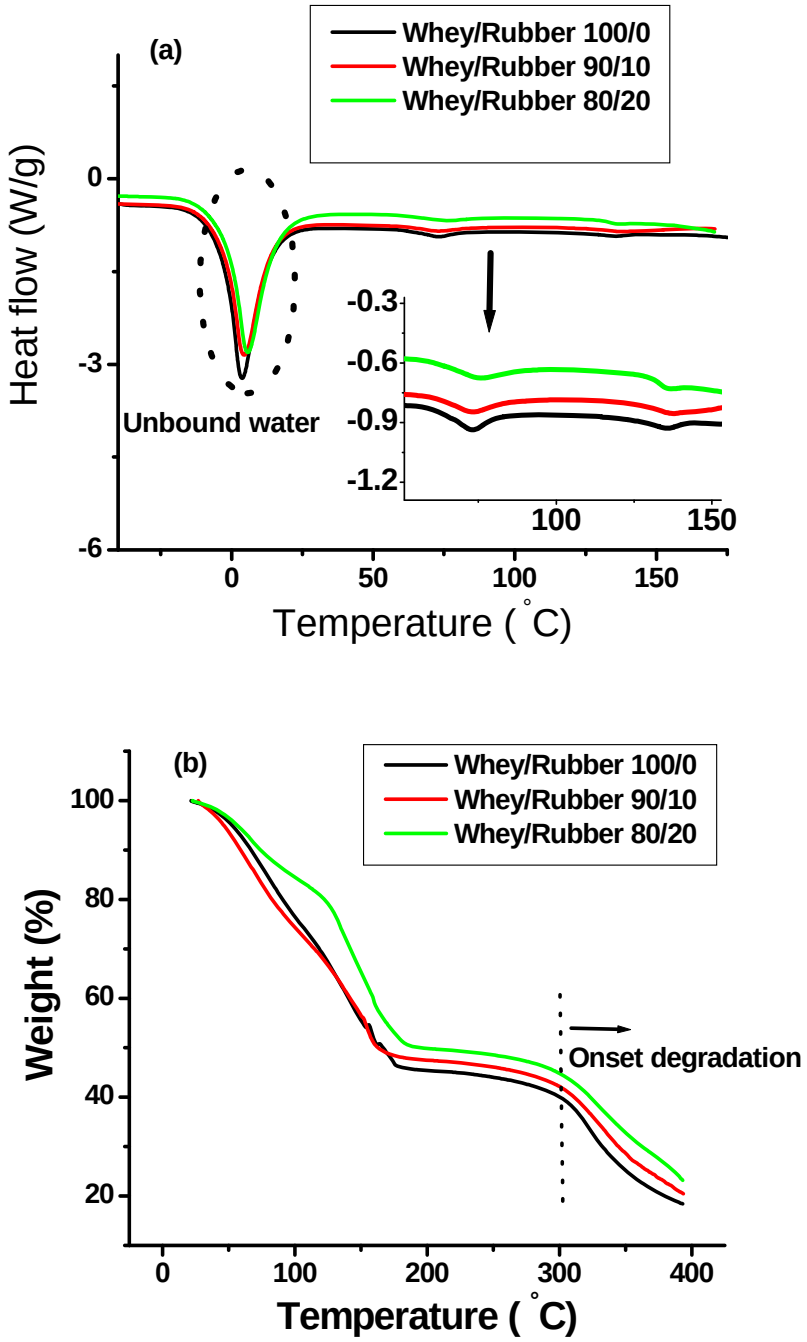

Figure 5.2. Thermal analysis of blends of whey and natural rubber: (a) DSC thermographs.; (b) TGA thermogram.

It was observed that plastic samples were not possible to prepare using molding conditions of whey plastic described in Chapter 3; i.e., temperature--150°C, pressure--20MPa, holding time--5 minutes, followed by ambient cooling and conditioning overnight at 50°C in an oven. In addition, higher water content (more than 25%) results in a foam-like material, lacking integrity. Therefore, samples were molded using the modified molding conditions of temperature--120°C, pressure--20MPa, holding time--5 minutes, followed by ambient cooling and subsequent conditioning in an oven at 70°C for 3 days. The dried sample contained residual moisture content of approximately 6%.

Figure 5.3 shows the results of thermal analysis of these plastics. The DSC thermograph shown in **Figure 5.3(a)** did not clearly indicate the presence of two phases. But, the dynamic mechanical and thermal analysis (DMTA), shown later, confirmed the two phases. This difference can be attributed to the higher sensitivity of DMTA than DSC. TGA results showed that a different weight-loss pattern was observed for the plastic samples (**Figure 5.3(b)**) in comparison with the original blend material. Specifically, the first (water) weight loss occurred over a more extended temperature range: from room temperature to about 220°C. The slowdown of the water loss can be explained by the denser structure of the plastic sample as compared with the protein powder (**Figure 5.2(b)**). The temperature of degradation, however, was not affected by the compression molding.

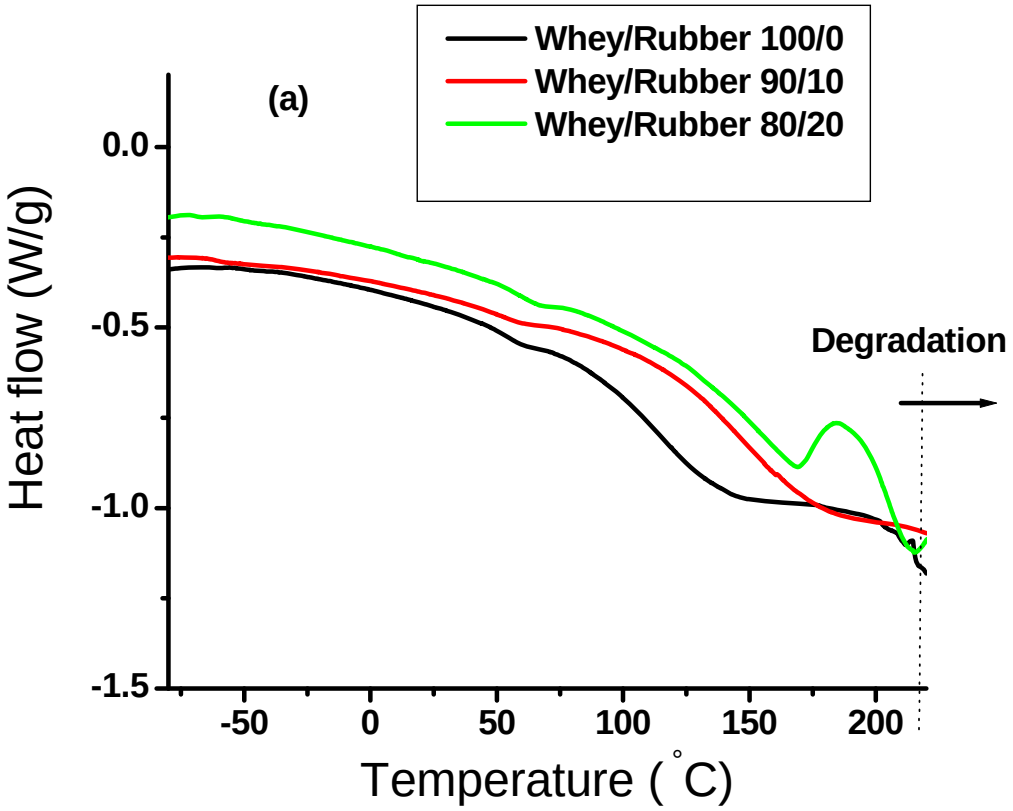

Figure 5.3(a). Thermal analysis of plastic samples from the blends of whey and natural rubber latex: (a) DSC thermographs.

The static and dynamic mechanical properties of the plastics at different blend ratios can be seen in **Figure 5.4**. The toughness properties, i.e., both tensile strength and elongation in **Figure 5.4(a)**, showed improvement compared to the neat whey plastic. This improvement in toughness can be attributed to strong interfacial adhesion between the protein and the natural rubber latex.[12]

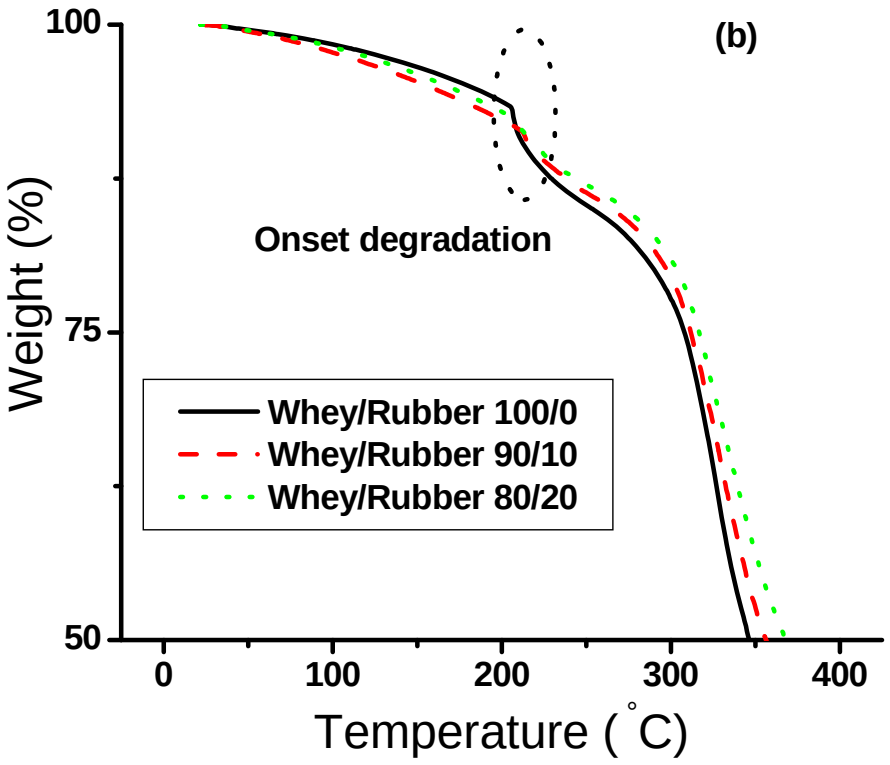

Figure 5.3(b). Thermal analysis of plastic samples from the blends of whey and natural rubber latex: (b) TGA thermographs.

It has been found that natural rubber latex particles contain, in addition to polyisoprene, about 2.5 to 3.5% protein on their surface.[18] In addition, **Figure 5.4(b)** demonstrates an overall depression in the storage modulus as the amount of rubber component increased to 20% in the blends. Past study with the blends of rigid polystyrene and synthetic rubber (styrene-butadiene-styrene block polymers) has also found that, by incorporating the rubber particles, modulus of composite reduces and can be predicted by theoretical models, such as Kerner equation and its modified form Halpin

and Tsai equation.[23] In addition, above a polystyrene volume fraction of 0.8, the rubber appears to be a dispersion of spherical particles in the polystyrene.

The height of Tan δ or loss factor peaks in **Figure 5.4(c)** increased with rubber content, confirming the improvement in toughness properties. Tan δ (ratio of the loss to the storage modulus) is also called the damping, and is an indicator of how efficiently the material loses energy to molecular rearrangements and internal friction.[24] In addition, the lower transition at approximately (-)75°C can be attributed to the rubber phase, and the one around 175°C to whey-rich phase.

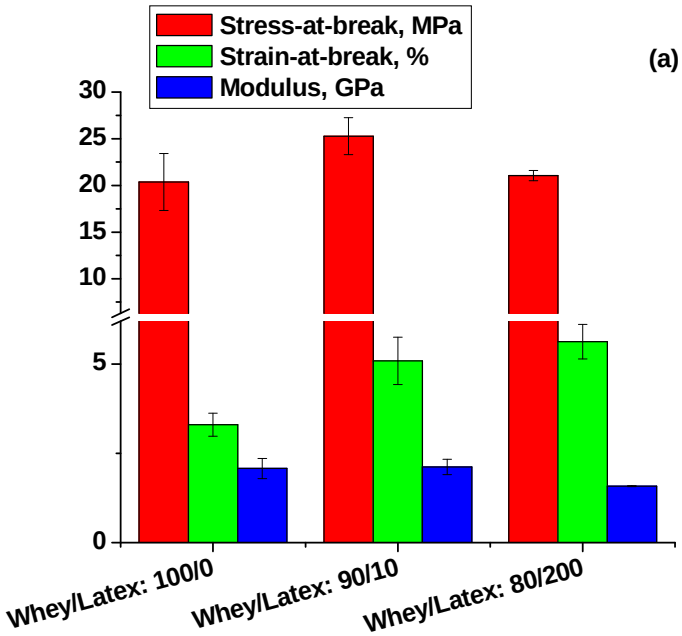

Figure 5.4(a). Mechanical properties of plastics produced from blends of whey and rubber latex, molded at a temperature of 120°C and a pressure of 20 MPa for 5 minutes, followed by ambient cooling and subsequently annealing in an oven at 70°C for 3days: (a)Tensile properties.

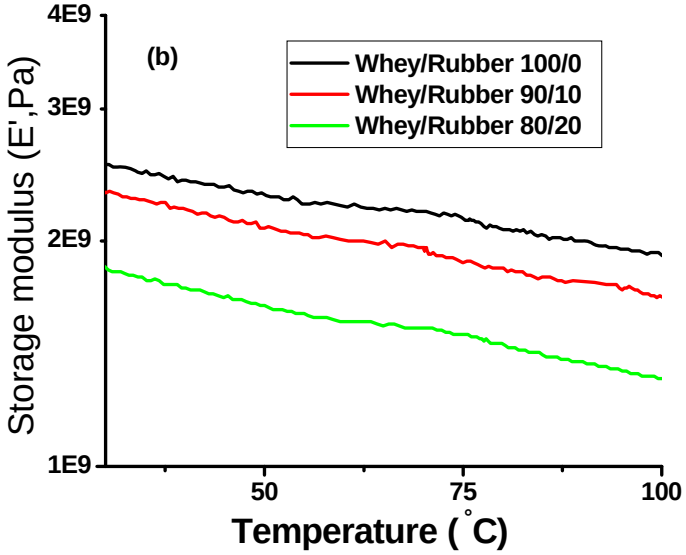

Figure 5.4(b). Mechanical properties of plastics produced from blends of whey and rubber latex, molded at a temperature of 120°C and a pressure of 20 MPa for 5 minutes, followed by ambient cooling and subsequently annealing in an oven at 70°C for 3days: (b)Storage modulus.

5.3.1.2: Blends of Undenatured proteins

Mixtures of whey/albumin at various w/w ratios were prepared to obtain the polymer blends. Specifically, the protein powders were dry-blended using a mechanical stirrer; water was then added drop-by-drop to this mixture (up to 25% on total weight of albumin and whey proteins). The powdery mixture set overnight to allow for the equilibration of the water distribution. The cartoon of these protein blends is shown in **Figure 5.5** and represents the basic concept of dry-blending of two proteins in this research.

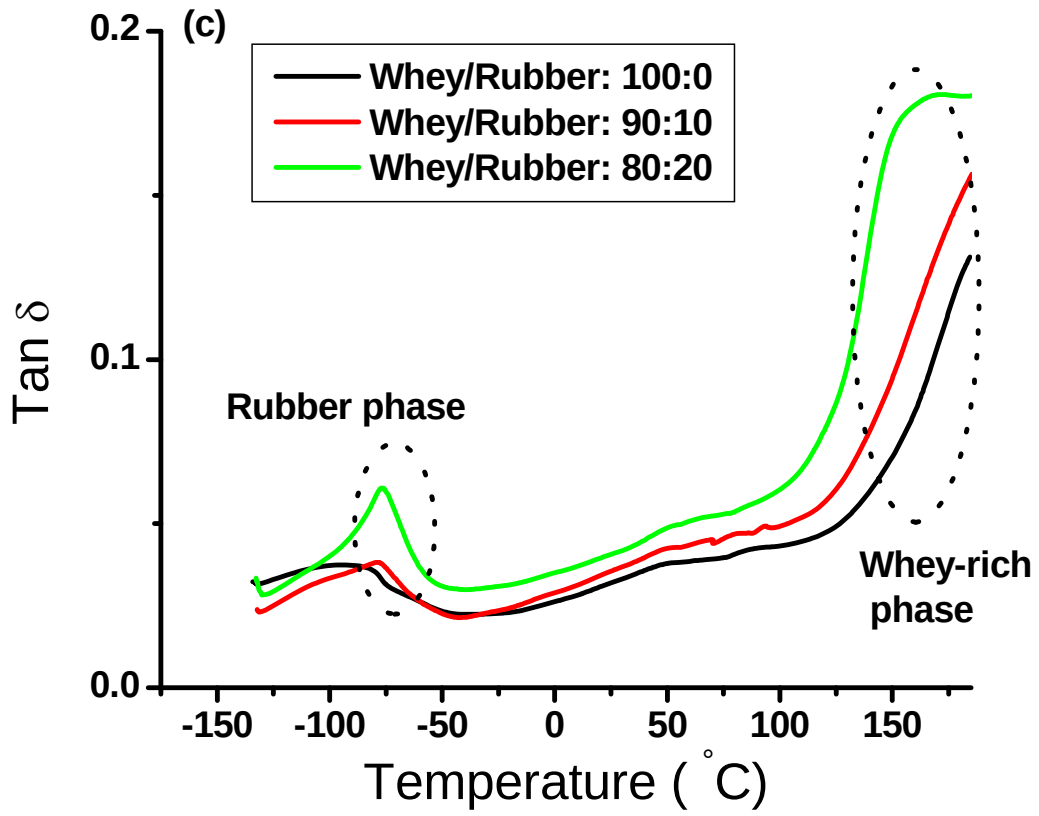

Figure 5.4(c). Mechanical properties of plastics produced from blends of whey and rubber latex, molded at a temperature of 120°C and a pressure of 20 MPa for 5 minutes, followed by ambient cooling and subsequently annealing in an oven at 70°C for 3days: (c) Loss factor or Tan δ.

The protein/protein blend is assumed to be compatible because these proteins contain complementary reactive functional groups (for example, amino, carboxy, and hydroxy). Because of the reactions between the functionalities at the phase boundary, strong interfacial adhesion should be readily achieved during molding at a temperature of approximately 150°C.

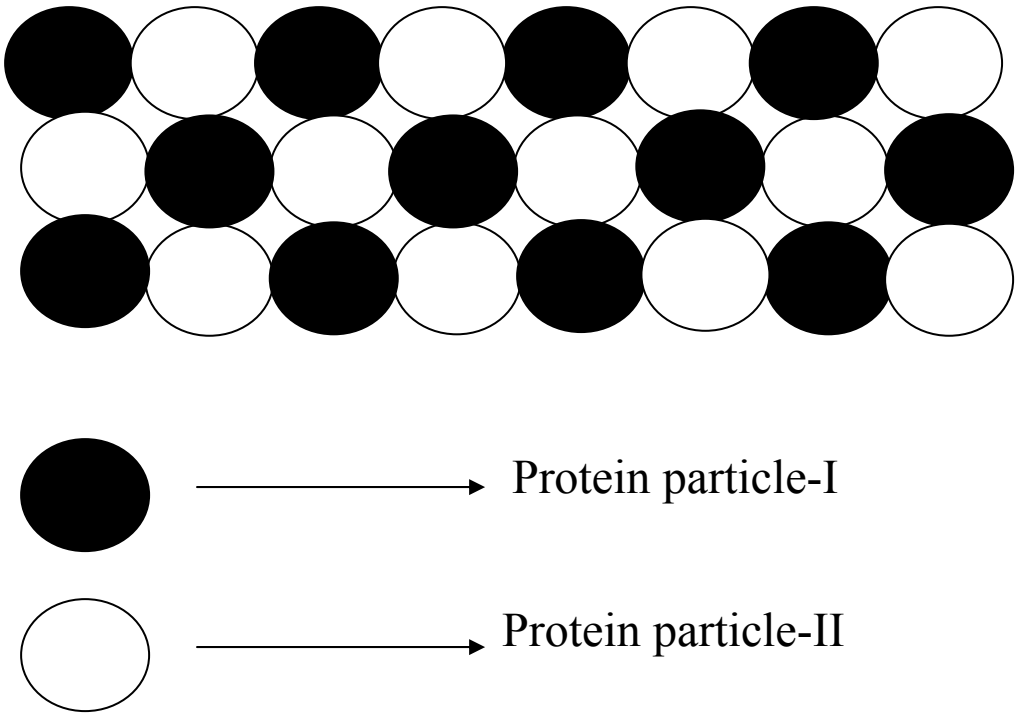

Figure 5.5. Schematic of dry-blending of proteins.

A DSC study of the protein mixture showed almost no crystallizable (unbound) water in the samples as shown in **Figure 5.6(a)**, suggesting the water molecules in the mixture were bound to the protein macromolecules through hydrogen bonding. Denaturing peak temperatures of blends were practically unchanged on mixing compared to whey or albumin proteins. This peak was approximately at 132°C. However, enthalpy of protein unfolding was found to be higher in blends than in individual protein components. This effect is difficult to explan straightforwardly. However, it can be supposed that formation of contacts between different (whey and albumin) proteins might be responsible for this behavior. The TGA analysis (**Figure 5.6(b))** shows the weight-loss of the blend protein samples. The first weight-loss occurred from room temperature to

approximately 100°C, a loss that was primarily caused due to water evaporation. The second weight-loss, suggesting significant degradation of the protein, was initiated at 225°C. Based on these results, the mixed protein powders were compression-molded using a Carver press at a temperature of 150°C and a pressure of 20 MPa for five minutes. Subsequently, samples were cooled under ambient conditions; this procedure was followed by overnight annealing at 50°C.

Figure 5.7 shows the thermal characteristics of these plastics, produced at various blend ratios. Phase separation can not be easily observed in the DSC thermograph of **Figure 5.7(a)**. However, **Figure 5.7(b)** shows the derivative heat flow, the peaks of which correspond to transitions such as glass-transition (Tg). These Tg of approximately 60°C is probably due to albumin-rich phase and of 120°C due to whey-rich phase (see **Figure 5.7(b)**). Moreover, a slow drying over a broad temperature, shown in the TGA thermographs of **Figure 5.7(b)**, confirms a dense structure of these plastic samples as compared to the original protein powders. The temperature of degradation, however, is not affected by the compression molding.

Figure 5.8 shows static and dynamic mechanical properties of these blended plastics of varying blend ratios. The behavior of these blends was modeled, employing known empirical mixing rule of polymer blends. At the lower proportion of either blend components, i.e. below 30% of either whey or albumin proteins, both strength and modulus followed the mixing rule or showed synergistic effect, as can be seen in **Figure 5.8(a)** and **Figure 5.8(c)**.

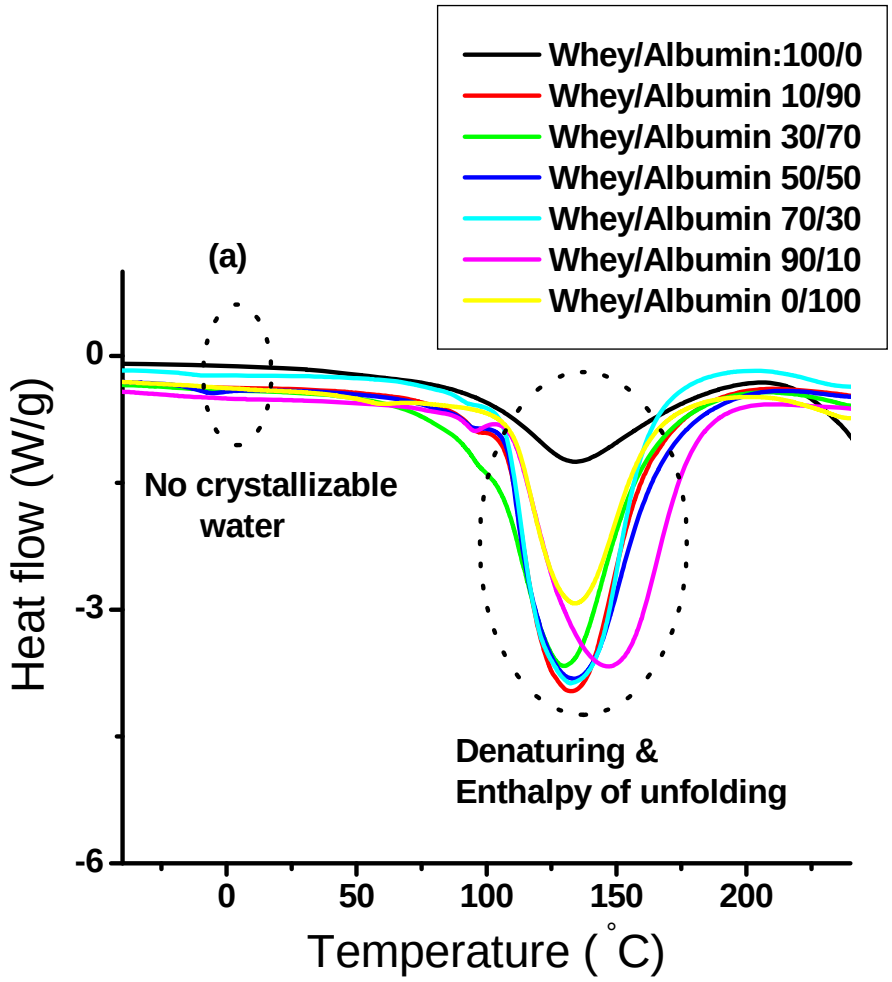

Figure 5.6(a). Thermal analysis of blends of proteins: DSC thermograms.

When the whey component was more than 70%, the plastic demonstrated a much higher strength and modulus than plastic with the albumin component above 70%. This result may be attributed to the higher effective complimentary reactive groups (COOH, OH, NH_2) in whey protein (9.6×10^{20} reactive groups per gram) than in albumin protein (6.2×10^{20} reactive groups per gram), leading to more crosslinks and resulting in a

stronger network structure. However, elongation properties in **Figure 5.8(b)** demonstrated the opposite behavior, which is common. At 50% of each component, there was a significant drop in strength and modulus. Thus, probably continuous morphology is in effect because of a considerable contribution from both components, resulting in a mismatch of mechanical properties and leading to failure, due to the component having a lower strength (albumin in this case).

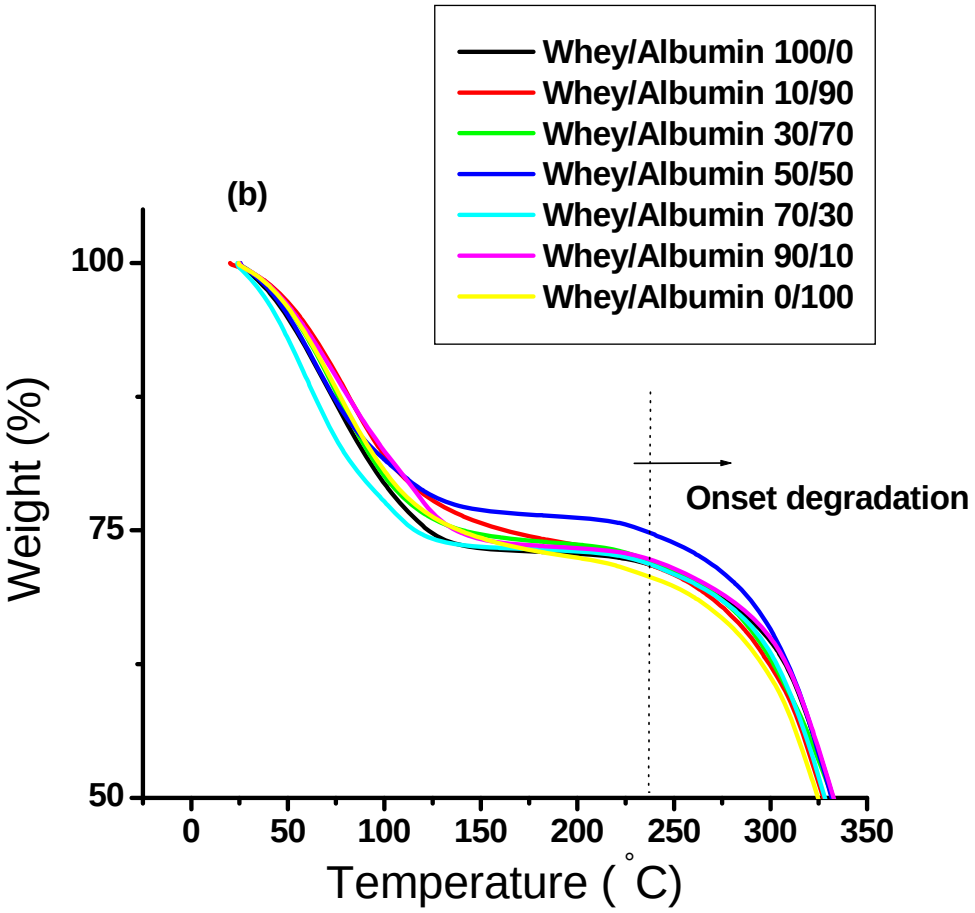

Figure 5.6(b). Thermal analysis of blends of proteins: TGA thermograms.

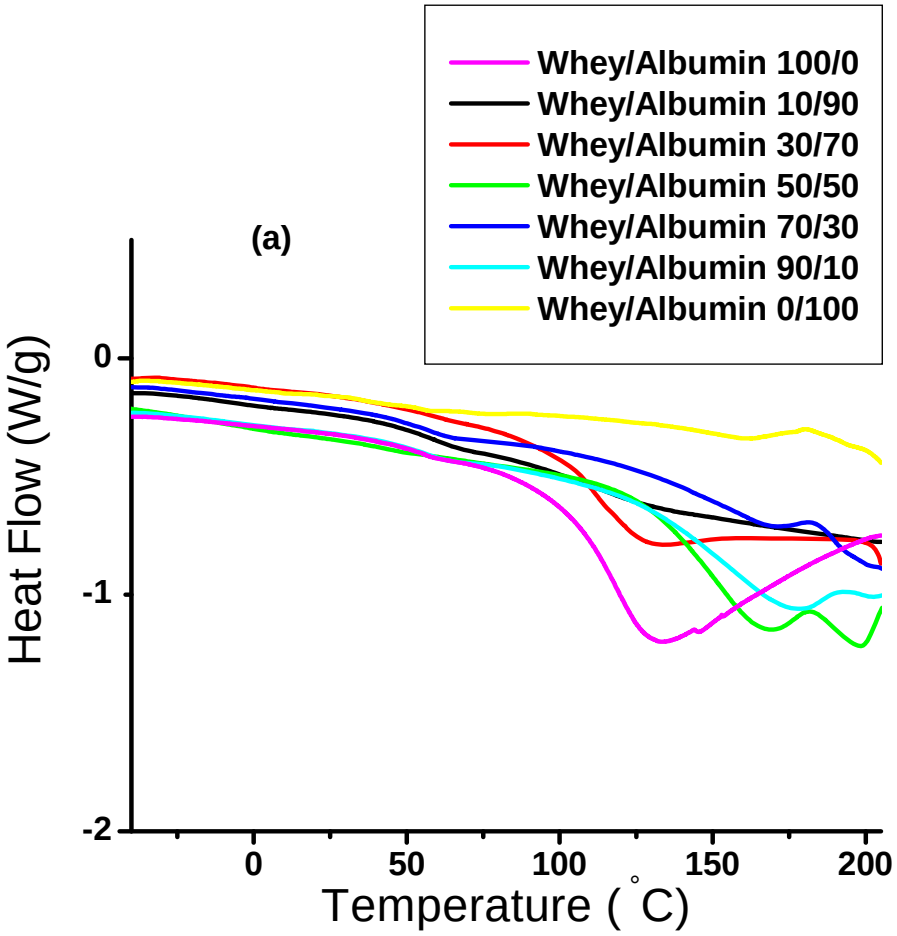

Figure 5.7(a). Thermal analysis of blends plastic samples produced at a temperature of 150°C and a pressure of 20 MPa, followed by ambient cooling and annealing overnight at 50°C: DSC thermograph.

Figure 5.8(d) shows the storage modulus obtained from dynamic mechanical testing. As this figure indicates, the storage modulus measured over a range of room temperature to 150°C increases as the whey component in the blend increased, probably because of increased crosslinks.

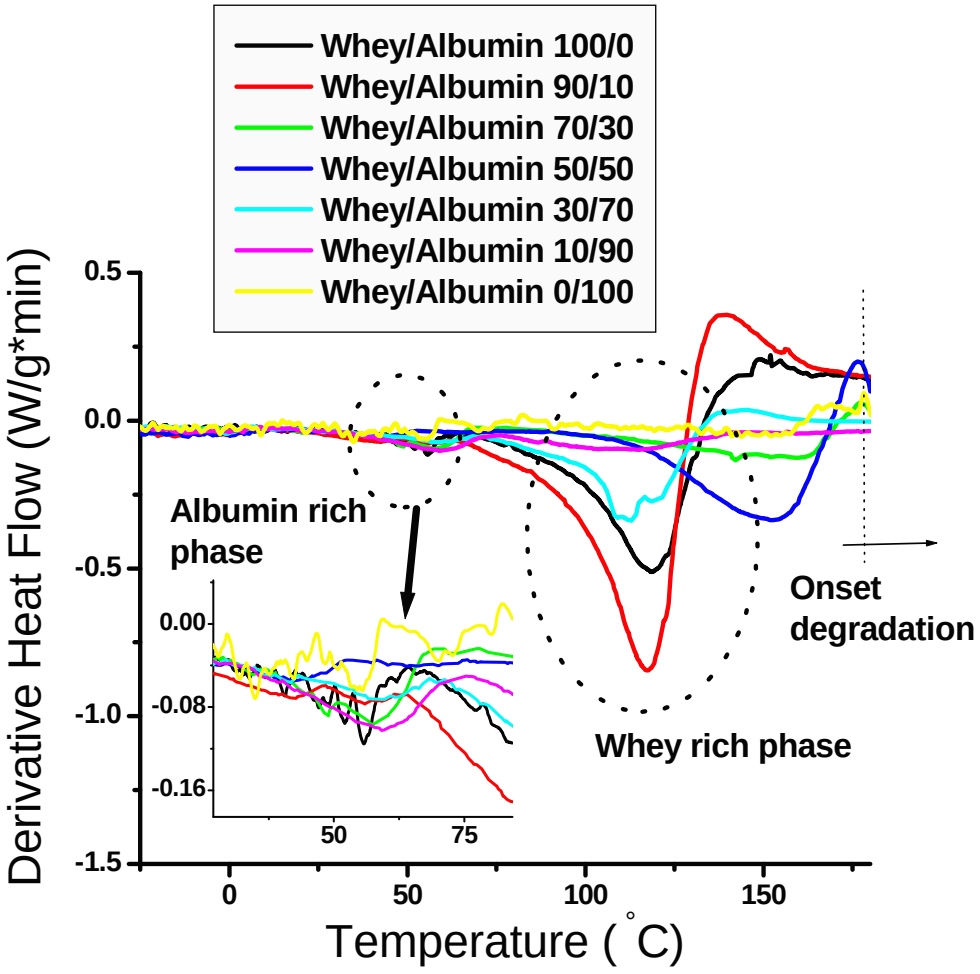

Figure 5.7(b). Thermal analysis of blends plastic samples produced at a temperature of 150°C and a pressure of 20 MPa, followed by ambient cooling and annealing overnight at 50°C: (b) DSC thermographs.

The Tan δ curves, the ratio of loss modulus to storage modulus shown in **Figure 5.8(e)**, peak at secondary transition or glass transition temperature (Tg). Increasing the whey component in blends leads to a shift in Tan δ peaks towards higher temperature values, indicating higher Tg and resulting in a decrease in the height of Tan δ peaks, implying an increase in stiffness (more elastic component).

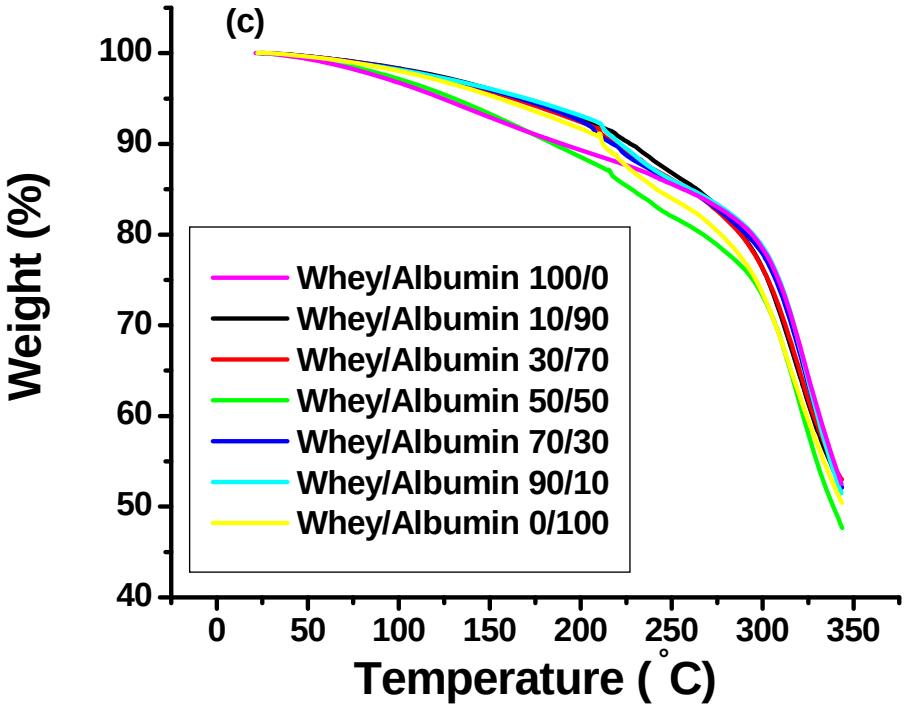

Figure 5.7(c). Thermal analysis of blends plastic samples produced at a temperature of 150°C and a pressure of 20 MPa, followed by ambient cooling and annealing overnight at 50°C: TGA thermograph.

5.4: Conclusion

Plastic samples were prepared from the blends of undenatured chicken egg albumin and whey proteins, and from the blends of whey protein and natural rubber latex, through the compression-molding process. It was observed that approximately 20% of natural rubber and 105% of water were optimal to process and improve the strength and elongation properties. However, these samples were molded using the modified molding

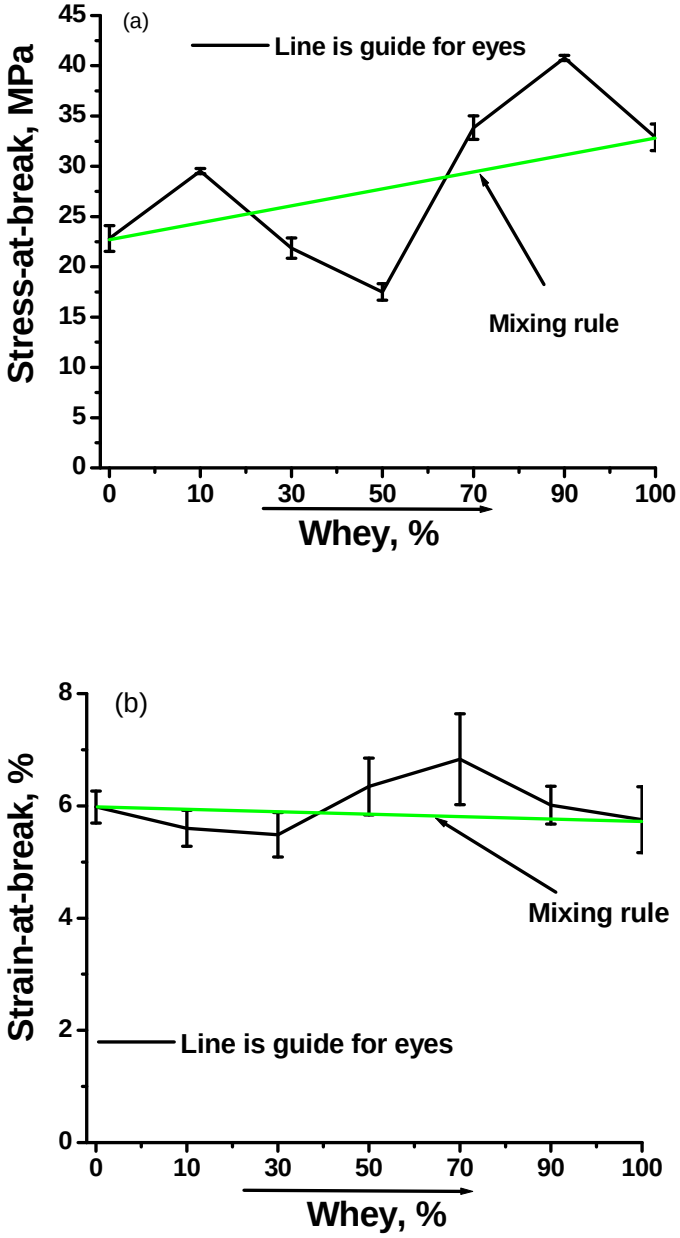

Figure 5.8(a,b). Static and dynamic mechanical properties of plastics produced from protein blends molded at a temperature of 150°C and a pressure of 20 MPa, followed by ambient cooling and annealing overnight at 50°C: (a) Strength; (b) Elongation.

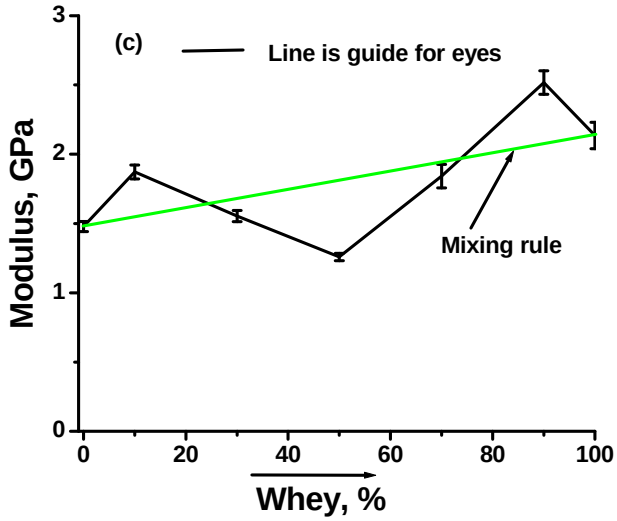

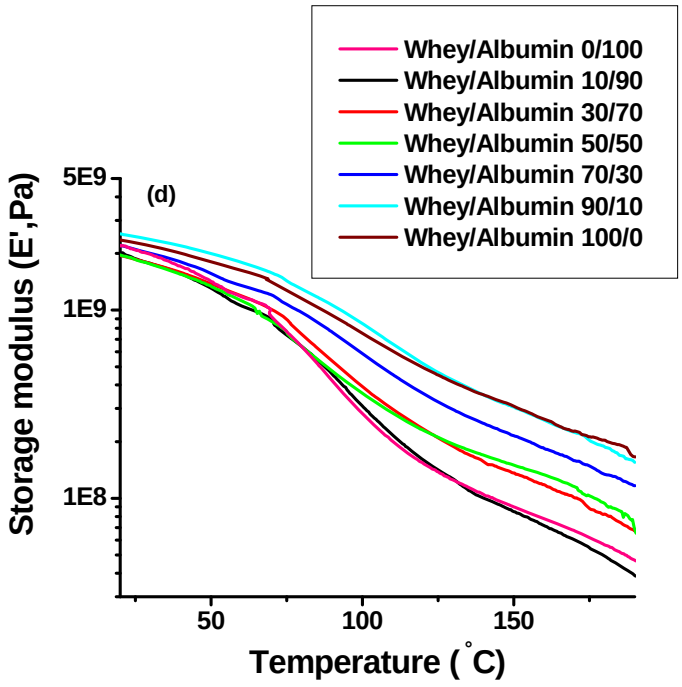

Figure 5.8(c,d). Static and dynamic mechanical properties of plastics produced from protein blends molded at a temperature of 150°C and a pressure of 20 MPa, followed by ambient cooling and annealing overnight at 50°C: (c) Modulus, (d) Storage modulus.

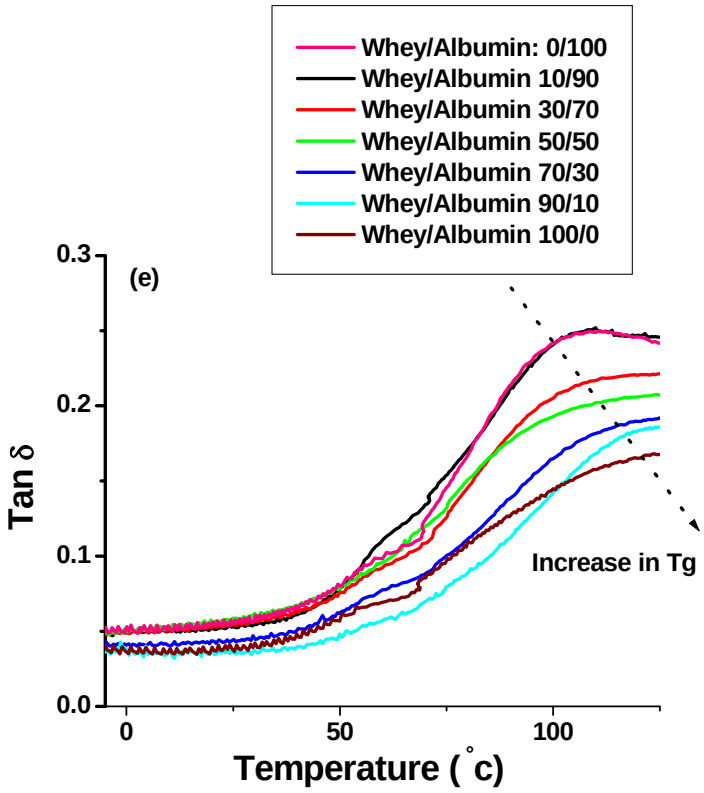

Figure 5.8(e). Static and dynamic mechanical properties of plastics produced from protein blends molded at a temperature of 150°C and a pressure of 20 MPa, followed by ambient cooling and annealing overnight at 50°C: Internal friction (Tan δ).

conditions: temperature--120°C, pressure--20MPa, holding time--5 minutes, followed by ambient cooling and subsequent annealing in an oven at 70°C for 3 days. In addition, the results from thermal analysis of these plastics indicated phase separation due to dispersed rubber particles and whey matrix; these phases were also confirmed by the loss factor graphs of dynamic mechanical analysis.

Dynamic mechanical and thermal analysis (DMTA) of whey-albumin blends confirmed the albumin and whey-rich phases. Properties of whey and albumin proteins blends followed mixing rule below 30% of either of these components. In the phase inversion region between 30 to 70%, plastics showed decreased tensile strength and modulus due to the significant contribution of either of these components, resulting in a mismatching of the mechanical properties.

5.5: References:

[1] Arvanitoyannis, I. S., J. Macromol. Sci.- Rev. Macromol. Chem. Phys. (1999), C39(2), 205.

[2] Koning, C., Duin, M. V., Pagnoulle, C., and Jerome, R., Prog. Polym. Sci. (1998), 23, 707.

[3] Salmoral, E. M., Gonzalez, M. E., Mariscal, M. P., and Medina, L. F., Ind. Crops Prod. (2000), 11, 227.

[4] Wu, Q., Selke, S., and Mohanty, A. K., Macromol. Mater. Engg. (2007), 292, 1149.

[5] Zhong, Z. and Sun, X. S., Polymer (2001), 42, 6961.

[6] Zhong, Z., and Sun, S. X., J. Appl. Polym. Sci., 88, 407.

[7] Aithani, D., and Mohanty, A. K. Ind. Eng. Chem. Res. (2006), 45, 6147.

[8] Mungara, P., Chang, T., Zhu, J., and Jane, J., J. Polym. Environ., (2002), 10,31.

[9] Wang, C., Carriere, C. J., Willett, J. L., J. Polym. Sci.: Part B: Polym. Phys. (2002), 40, 2324.

[10] Zhang, M., Reitmeier, C. A., Hammond, E. G., and Myers, D. J., Cereal Chem. (1997), 74, 594.

[11] Kumar, R., Choudhary, V., Mishra, S., Varma, I. K., and Mattiason, B., Ind. Crops Prod. (2002), 16, 155.

[12] Mohanty, A. K., Wu, Q., and Selke, S., US Patent Application No. US 2006/0041036 A1.

[13] Ezoe, S., US Patent No. 5,523,331 (1996).

[14] Carvalho, A. J. F., Job, A. E., Alves, N., Curvelo, A. A. S., and Gandini, A., Carbo. Polym. (2003), 53, 95.

[15] Greeve, H. H. Natural Rubber. In Ullmann's Encyclopedia of Industrial Chemistry (2005), Wiley-VCH, Weinheim.

[16] http://www.rcsb.org, Protein Data bank.

[17] Kramárová , Z., Alexy, P., Chodák, I., Špirk, E., Hudec, I., Košíková, B., Gregorová, A., Šúri, P., Feranc, J., Bugaj, P., and Ďuračka, M., Polym. Adv. Techno. (2007), 18, 135.

[18] Hart, H., Craine, L. E., Hart, D. J., and Hadad, C. M. Organic Chemistry: A Short Course, 12 ed.,2007, Houghton Mifflin Company, Boston.

[19] Zhang, J., Mungara, P., and Jane, J., Polymer (2001), 42, 2569.

[20] Cuq, B., Gontard, N., and Guilbert, S., Polymer (1997), 38, 4071.

[21] Rouilly, A., Orliac, O., Silvestre, L., and Rigal, L., Polymer (2001), 42, 10111.

[22] Matveev, Y. I., Grinberg, V. Y., Tolstoguzov, V. B., Food Hydrocolloids (2000), 14, 425.

[23] Nielsen, L. E., Mechancial Properties of Polymers and Composites (Vol. 2), 1974, Chap. 7, Pg. 379.

[24] Menard, K. P., Dynamic Mechanical Analysis: a practical introduction (1999), CRC Press LLC.

CHAPTER 6

BIODEGRADABLE PLASTICS FROM PARTIALLY DENATURED PROTEINS: FEATHERMEAL

6.1: Introduction

Synthetic polymers, almost without exception, are not biodegradable. Polymers such as polyethylene, polystyrene, and polypropylene can persist in the environment for many years after their disposal. Therefore, the significance of the depletion of petrochemical resources, and the need for eco-friendly/biodegradable materials based on easily renewable natural resources, has necessitated the development of polymers from agricultural processing products.[1] Indeed, the only truly biodegradable plastics are those that can be consumed by microorganisms and reduced to simple, eco-friendly compounds. Biodegradable plastics are especially important in the production of articles that are unlikely to be recycled.[2]

The straightforward method of producing biodegradable plastics is by using natural renewable and biodegradable polymers based on starch, proteins or cellulose.[3] In this respect, proteins are exceptionally versatile materials, both in the sources from which they can be obtained and in the wide variety of possible modifications, which can be helpful in tailoring their properties to the particular requirements of a specific application. They present significant advantages in that proteins are derived from a sustainable resource and can be processed in much the same way as conventional synthetic polymers. For instance, soy protein has been considered recently as an alternative to petroleum polymer in the manufacture of adhesives, plastics, and various binders.[4-7] It had been

shown that plastics and polymer blends that were made from soy protein had high tensile strength and good biodegradable performance. In another study, compression molding of blends that contained either protein isolates or defatted whole flour of chickpea produced plastic of acceptable properties.[3] Protein isolates from sunflower, along with glycerol and water, were also used in various research studies to make thermal injection-molded biodegradable thermoplastics with better mechanical properties.[8] Injection-molded biodegradable plastic made from blends of corn gluten meal (a byproduct of the corn-based ethanol industries) was also developed.[9] In this chapter, we are reporting on yet another novel plastic materials produced from proteins. Specifically, we will describe the properties of plastics made from proteins produced by the animal co-product (rendering) industry, and the process of fabricating those plastics.

Rendering, a process that involves both physical and chemical transformation, is the recycling of raw animal tissue from food animals and waste cooking fats and oils. As a result, a variety of value-added products, such as bone meal, meat meal, poultry meal, hydrolyzed feather meal, blood meal, and fishmeal, are produced. Without the continuing efforts of the rendering industry, the accumulation of unprocessed animal by-products would impede the meat industry and would pose a serious potential hazard to animal and human health.[10] Recently, the outbreak of "Bovine Spongiform Encephalopathy (BSE)", or "Mad Cow Disease", in Europe has led to prohibition of the use of various proteins (e.g., meat and bone meal) from co-product industries in ruminant feed in the United States and in any farm animal feed in the European Union. The excessive availability of these protein materials has encouraged the search for alternative uses of them, such as

fabrication of biodegradable plastics.[11]

6.2: Materials

Feathermeal protein was obtained from Fats and Proteins Research Foundation, VA. The reported protein content for feathermeal was 87.1% with additional 8.5% fatty contents (mainly saturated). Elemental analysis of carbon, hydrogen and nitrogen showed 49.8% carbon, 7.7% hydrogen, and 12.5% nitrogen content, respectively. A rubbery Random copolymer PGMA-Co-PBMA was synthesized by Dr. Viktor Klep.

6.3: Results and Discussion

6.3.1: Plastics from feathermeal protein

6.3.1.1: Plastics fabrication

Feathermeal protein can be described as an insoluble keratin protein containing high amounts of cysteine, a sulfur-containing amino acid. The biomacromolecule is stabilized by disulfide bonds through cross-links with other intra- or inter-molecular cysteine fragments.[12] Feathermeal is required to be processed by pressure and temperature to destroy the disulfide bonds in order to denature the protein. During the rendering process, clean, undecomposed feathers from slaughtered poultry are pressure-cooked with live steam, partially hydrolyzing the protein and breaking the beta-keratinaceous bonds that account for the structure of the feather fibers.

The as-received feathermeal had a moisture content of 5-6%, whereas the sieved defatted protein powder, after drying, had a moisture content of 9-10%. It was supposed

that the increase in the moisture content might be due to the removal of hydrophobic fatty contents (mostly saturated fats). The defatted feathermeal protein powder was analyzed by DSC and TGA. Even though the feathermeal protein was thermally treated via the rendering process; DSC data (**Figure 6.1(a))** indicated the presence of a denaturation (unfolding) temperature (~ 134°C) for the defatted feathermeal protein powder. Thus, the protein was not fully denatured during the rendering procedures, and further unfolding of the biopolymer took place upon heating.

In one study, protein was extracted out of meat and bone meal (MBM), a by-product of rendering industries, and found to have good adhesive properties. It can be calculated from their experimental data that around 60% of MBM (crude protein-56%) protein was soluble and had potential of pure proteins.[13]

The cooperative unfolding originates from disruption of the multiple small forces that maintain the secondary/tertiary protein structure.[14] Disruption of these forces alters the enthalpy of the system and causes the temperature to drop, because the unfolding process is generally endothermic. When a second DSC run was conducted for the feathermeal sample, no additional denaturation was observed. The results indicated that full denaturation was reached during the first DSC run. **Table 6.1** shows the denaturing temperatures of various plant and animal proteins, as obtained by DSC measurements. The data suggest that additional denaturation of the feathermeal occurs in the temperature range that is typical for denaturation of other protein biomacromolecules.

Table 6.1. Denaturing temperature of various plant and animal proteins from DSC studies

Protein	Denaturation temperature (°C)	Ref.
Corn zein isolate	~150°C	15
Wheat glutenin	65°C & 85°C	16
Soy protein isolate	80°C & 95°C	17
Fowl feather keratin (Dry)	170-200°C	18
Fowl feather keratin (Wet)	110-160°C	18
Cottonseed isolate	~140°C	19
Whey protein concentrate	~75°C	20
Ovalbumin from chicken egg white	~84°C	21

DSC measurements also provided important information on the nature of water incorporated into the feathermeal protein sample. In fact, an endothermic peak around 0°C, which would correspond to the melting of crystallizable (unbound) water, was not observed. Thus, it was concluded that the water molecules situated in the feathermeal were bound to the protein macromolecules.[22]

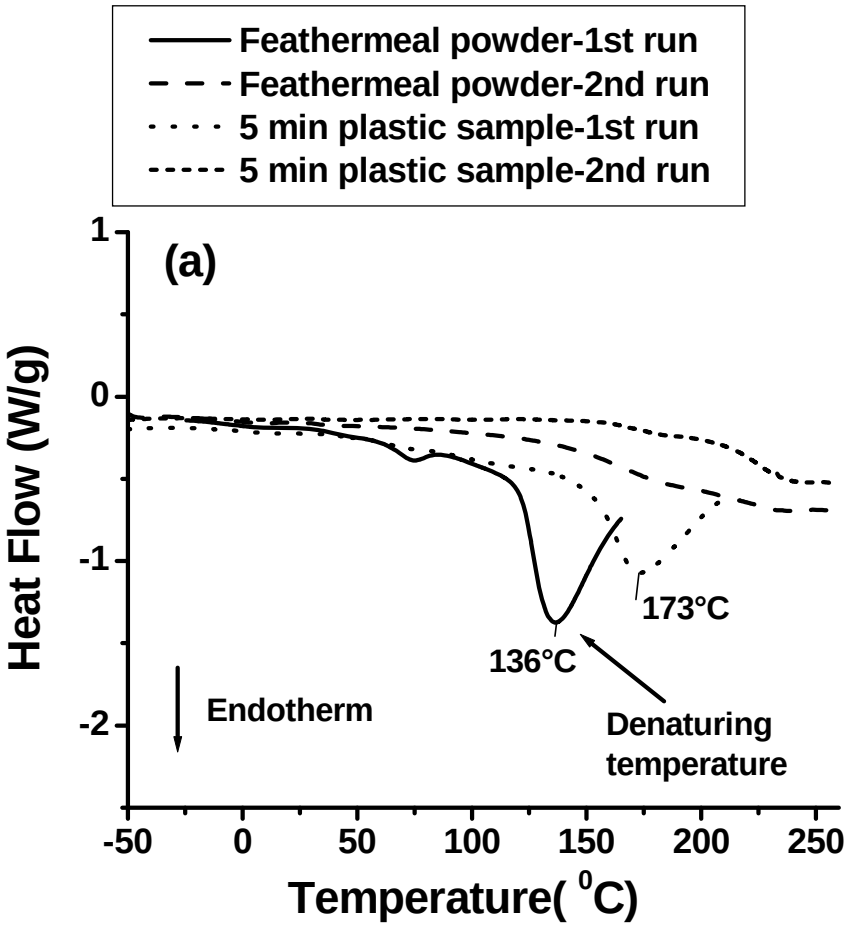

Figure 6.1(a). Thermal analysis of feathermeal protein powder and plastic samples produced at a temperature of 150°C and pressure of 20MPa, followed by cooling to 70°C under pressure at five minutes of pressing: (a) DSC thermograms.

Figure 6.1(b) shows the weight loss of the feathermeal sample. The first weight loss occurred from room temperature to about 100°C. The loss was mainly caused by the water evaporation during denaturation.[23] In addition, TGA results (second weight loss) suggested that significant degradation of the protein was initiated at approximately 220°C.

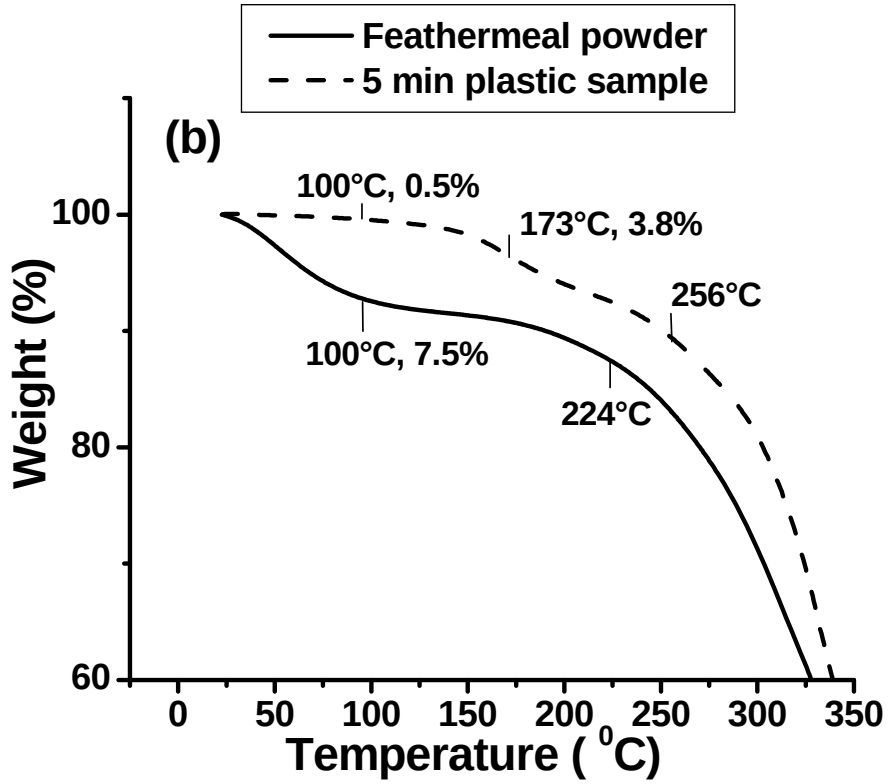

Figure 6.1(b). Thermal analysis of feathermeal protein powder and plastic samples produced at a temperature of 150°C and pressure of 20MPa, followed by cooling to 70°C under pressure at five minutes of pressing: (b) TGA thermograms.

Based on the results of the thermoanalysis, a certain molding cycle was accepted for the preparation of the plastic samples. Specifically, the defatted feathermeal protein powder was compression-molded using a Carver press at a temperature of 150°C (between denaturation temperature and degradation temperature) and molding pressure of 20 MPa for five minutes, and was then cooled to 70°C under pressure. The water content for the plastic obtained was on the level of 4%.

It was observed that, during the preparation of the plastic samples, the protein macromolecules denatured due to combined effect of heat, pressure and time as the

original endothermic peak due to the denaturation (~136°C) was not detected for the plastic samples obtained (**Figure 6.1(a)**). Conversely, an endothermic peak at roughly 173°C was found for the plastic specimens. The result indicates that another type of folded structure is formed during the plastic preparation. It was supposed that formation of multiple dispersive and hydrogen bonds between amino, carboxy, and hydroxy amino acid residuals are responsible for the structurization. Interestingly, the second DSC run (**Figure 6.1(a)**) shows no peak around 173°C for the feathermeal plastic, pointing to the conclusion that pressure might be responsible for the structurization of the protein material during the plastic fabrication.

TGA results showed that a different weight loss pattern was observed for the plastic samples (**Figure 6.1(b)**) in comparison with the original feathermeal material. Specifically, the first (water) weight loss occurred over a more extended temperature range: from room temperature to about 210°C. The slowdown of the water loss can be explained by the denser structure of the plastic sample as compared with the protein powder. The temperature of degradation, however, was virtually unaffected by the compression molding.

6.3.1.2: Mechanical Properties

Figure 6.2(a) shows the typical stress-strain diagram for the tested dog bone samples made from the feathermeal plastic. The first region, where stress (σ) increases linearly with strain (ε), is a region of elastic deformation; it is followed by plastic yield and strain hardening regions. In our opinion, the yield point may be attributed to the

break in hydrophobic interaction and hydrogen bonds of folded protein macromolecules. Remarkably, this phenomenon in the yield region is reversible in nature, as can be observed from the cyclic loading testing of plastic samples (**Figure 6.2(b)**).

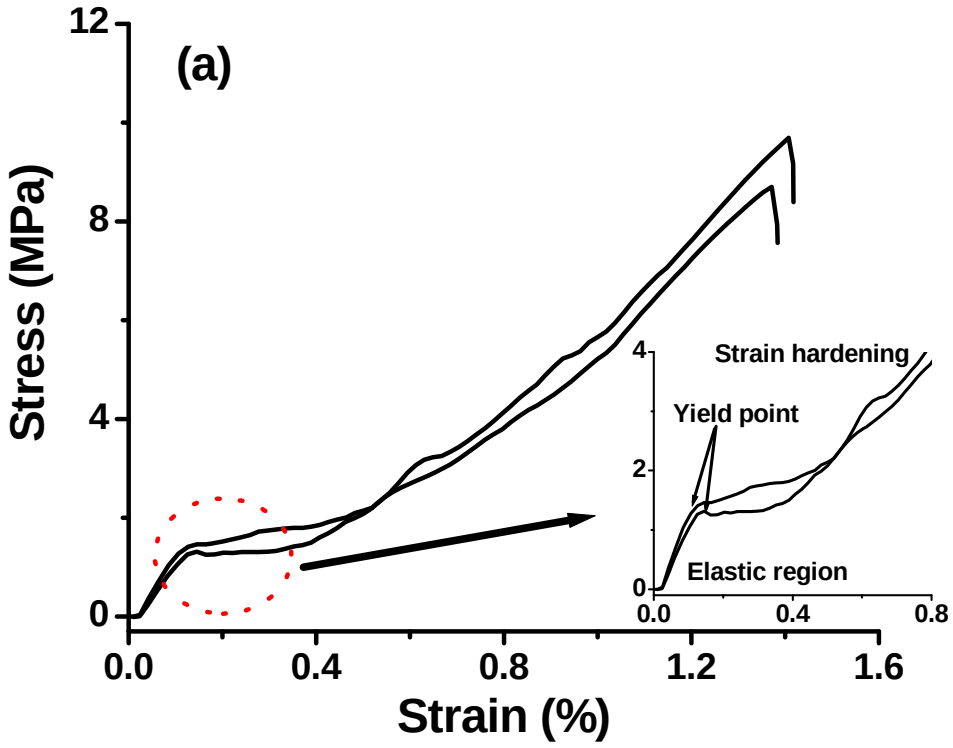

Figure 6.2(a). Stress-strain curve for the compression molded feathermeal plastic, produced at a temperature of 150°C and pressure of 20 MPa for 5 minutes, followed by cooling to 70°C under pressure.

It appears that biomacromolecules, which constituted the sample, fold back when the sample is unloaded prior to the break. This original mechanism of dissipating energy can be extremely useful if the plastic is subjected to a cycling loading during use.

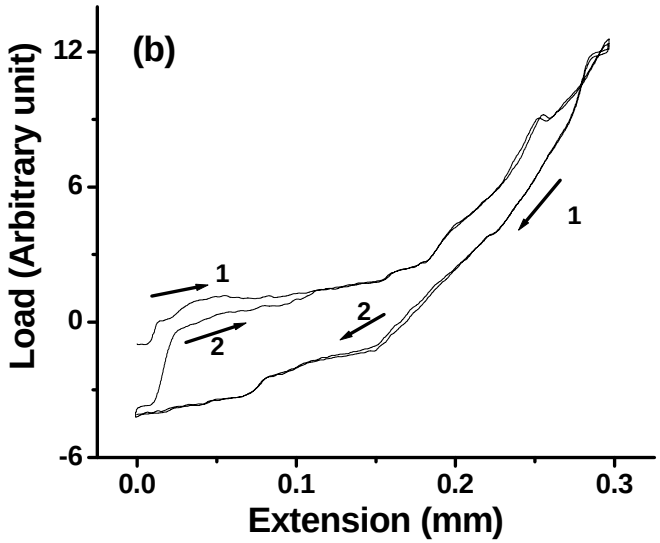

Figure 6.2(b). Cyclic loading testing of the feathermeal samples, produced at a temperature of 150°C and pressure of 20 MPa for 5 minutes, followed by cooling to 70°C under pressure.

Figure 6.3 shows the corresponding SEM micrograph of the fracture surfaces (from the tensile test), which indicate the brittle nature of the fracture. The stress at break, strain at break, and modulus were measured to be 9.2 MPa, 1.40%, and 2.20 GPa, respectively. The observed mechanical properties (high stiffness accompanied by low extensibility) are in the range of the values that are typically observed for bioplastics fabricated from unplasticized proteins. For instance, for plastic from soy protein, the stress at break, strain at break, and modulus were reported to be 35 MPa, 2.6%, and 1.63 GPa, respectively.[24] The properties of plastic made from soy protein are somewhat better in terms of strength and elongation. We associate this difference with the fact that protein plastics are typically prepared from biomacromolecules, which are thermally untreated and possess their native conformation. In this research, the protein had been subjected to

denaturation procedures before the fabrication of the plastics. Accordingly, to improve their properties, animal co-product proteins can be mixed with proteins that possess a lower level of denaturation and which demonstrate better properties.

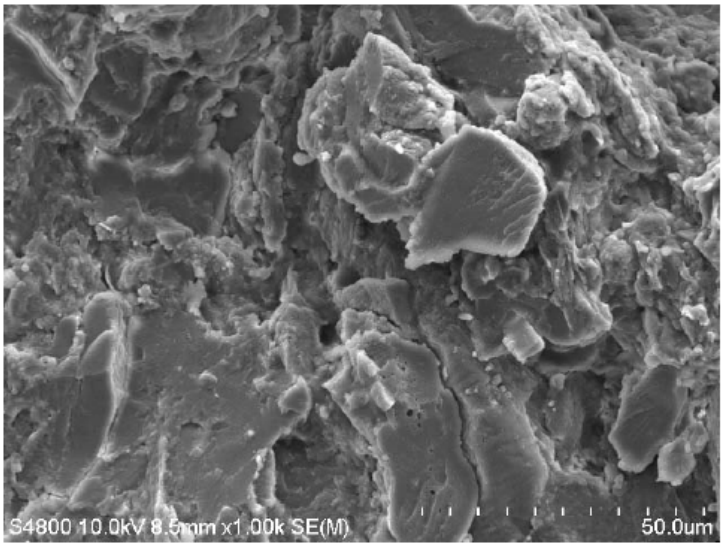

Figure 6.3. Scanning electron microscopy (SEM) micrograph of feathermeal plastic produced at a temperature of 150°C and pressure of 20 MPa, followed by cooling to 70°C under pressure.

6.3.2: Plastics from blends containing feathermeal protein

One of the most efficient routes for obtaining plastics with improved properties is polymer blending, in which two or more polymers are combined in one polymeric material. For instance, blends of synthetic polymers and natural polymers (polysaccharide and protein based) were utilized to produce totally and partially degradable blends.[25] For a polyblend, a weakness in one component can to a certain extent be camouflaged by strength in the other constituting part.[26] In general, the blends can be divided into homogeneous (miscible, one phase) and heterogeneous (more then one phase). In a

homogeneous blend, the components of the blend virtually lose part of their identity. The final properties of a miscible blend usually follow the so-called "mixing rule" (the arithmetical average of blend components). In a phase-separated blend, the properties of all blend components are present, and the final performance of the blend is very dependent on the size of structural elements and the adhesion at the interface. In general, a majority of immiscible blends are incompatible and demonstrate negative deviation from the "mixing rule" because of gross phase morphology and low interfacial adhesion. These blends are in many ways useless if they are not compatibilized.[26] In a few exceptional cases, (some) properties of a compatible blend may be better than those of the individual components. Namely, a synergistic effect, which is sometimes difficult to predict, is observed.

6.3.3: Blends of feathermeal with undenatured proteins

6.3.3.1: Fabrication of plastics

For the case of blending, as considered in this research work, where (partially denatured and non-soluble) feathermeal is blended with (non-denatured, water soluble) proteins, a heterogeneous polymer blend ought to be obtained. The protein/protein blend is supposed to be compatible, since the proteins possess complementary reactive functional groups such as amino, carboxy, and hydroxy. Owing to the reactions between the functionalities at the phase boundary, strong interfacial adhesion should be readily achieved after annealing of the samples at elevated temperatures.

Two commercially available non-denatured and pure natural proteins, such as albumin (chicken egg white) and whey, were selected for the blending experiments.

Whey and albumin proteins have already been used in various technical applications, such as adhesives and coatings.[27,28]

The stress-at-break, strain-at-break, and modulus were measured to be 19 MPa, 5.8%, and 1.4GPa and 16.7 MPa, 2.8%, and 2.4GPa for the whey and albumin plastics, respectively. In general, the plastics obtained showed higher strength and elongation than did the feathermeal materials. On another hand, the stiffness of the feathermeal plastic was somewhat higher. To compare the properties of the whey/albumin and feathermeal plastics directly, the procedure for preparation of the feathermeal samples was modified to include annealing overnight at 50°C.

The change in fabrication resulted in the alteration of mechanical properties of the feathermeal plastic. The stress-at-break, strain-at-break, and modulus were determined to be 5.7 MPa, 1.1%, and 2.87 GPa. The moisture content for the plastic was on the level of 4%. The annealing increased the modulus of the feathermeal plastic, but it caused a significant decrease in strength and elongation. Evidently, plastics obtained from the different biomacromolecules have complementary properties, and blending of the proteins should result in an improvement of the mechanical performance of the feathermeal polymeric materials.

Mixtures of feathermeal/albumin and feathermeal/whey proteins in 50%:50% w/w ratios were prepared to obtain polymer blends from the biomacromolecules. Specifically, the defatted feathermeal protein powder (moisture content of 10%) was dry-blended with the natural proteins using mechanical stirrer; water was then added to the mixture (up to 25% on dry weight of albumin and whey proteins) drop by drop. The mixture was kept

overnight for equilibration of water. A DSC study of the protein mixtures showed that there was practically no crystallizable (unbound) water in the samples. Therefore, the water molecules situated in the mixtures were bound to the protein. The blend samples were molded to form plastic samples at a temperature of 150° C and a pressure of 20 MPa for 5 minutes, and were then cooled to 70°C under pressure and dried in an oven at 50°C overnight.

6.3.3.1: Mechanical properties

The mechanical properties from the static testing showed significant improvement as compared to unmodified feathermeal protein samples, as shown in **Figure 6.4**. In general, addition of the non-denatured proteins to the feathermeal material improved the elongation at break and the stress-at-break of the plastics. In fact, strain-at-break for the blend increased more than 1.5 times as compared with plastic made from feathermeal alone at the same conditions. Significant improvement was found in the strength of the blended material. The stiffness of the polymer blend made with albumin was slightly lower than expected, since pure albumin plastic possessed lower stiffness than the pure feathermeal plastic.

The blend of feathermeal and whey proteins demonstrated the highest breaking stress and a Young's modulus of 12.6 Mpa and 3.34 GPa, respectively. This blend demonstrated a synergistic effect in terms of stiffness, since the elastic modulus of the blend was higher than the moduli of pure components (2.87 GPa for the feathermeal plastic and 1.4 GPa for the whey plastic).

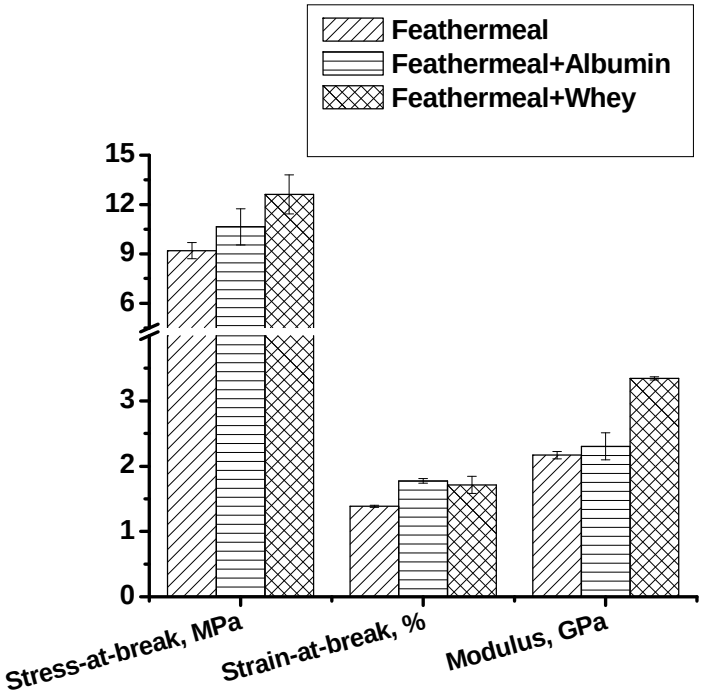

Figure 6.4. Mechanical properties of plastics produced from feathermeal and the blends of feathermeal/albumin and feathermeal/whey (50%:50% w/w ratios) proteins, molded at a temperature of 150°C and pressure of 20 MPa for 5 minutes, followed by cooling to 70°C under pressure and overnight drying in an oven at 50°C.

The obtained results indicated that blending of feathermeal with whey protein has definite potential. **Figure 6.5** shows the dynamic mechanical analysis (DMA) of these blends. This DMA analysis also demonstrated higher storage modulus with the blend of feathermeal and whey protein than with featherrmeal and albumin. To evaluate the properties of the blend further, plastics containing different ratios of biomacromolecular materials were prepared. Known relationships that have been used to predict properties of polymer blends were used to model the behavior of the blends. The relationships were developed for spherical inclusions distributed in a matrix, but as a first approximation are often used for systems, where inclusions are not spherical in shape.

Figure 6.6 shows that the stiffness of the blended plastics depends on the ratio between feathermeal and whey in the blend. With the increase in the (stiffer) feathermeal component, the elastic modulus of the plastic increases. The dependence deviates from the simple "mixing" (additive rule) in a positive way, indicating a clear synergistic effect in which the properties of the blend are better than those of the individual components. Interestingly, the effect is observed in the region of possible phase inversion, where the ratio between the components is close to 1:1.

For polymer blends containing nearly spherical particles of any modulus, a Kerner and Hashin equation has been used to model the level of stiffness. The well-established form of the Kerner equation, which considers the dispersed phase as spheroidal in shape, has the following form:[29]

$$E = E_1 \frac{\dfrac{\phi_2 E_2}{(7-5\nu_1)E_1 + (8-10\nu_1)E_2} + \dfrac{\phi_1}{15(1-\nu_1)}}{\dfrac{\phi_2 E_1}{(7-5\nu_1)E_1 + (8-10\nu_1)E_2} + \dfrac{\phi_1}{15(1-\nu_1)}} \qquad (6.1)$$

where E, E_1, E_2 are the moduli for the binary blend, the matrix and the dispersed phase, respectively; ϕ_1, ϕ_2 are the volume fractions of the matrix and the dispersed phase, respectively; ν_1 is the Poisson ratio for the matrix. (To estimate the volume fractions the density of protein material was considered to be 1g/cm^3). This equation is valid in case of an ideal stress transfer through the interface (strong adhesion between the phases). If no stress is transferred (i.e., there is no adhesion between the phases), the Kerner equation is simplified, since E_2 is then assumed to be zero:

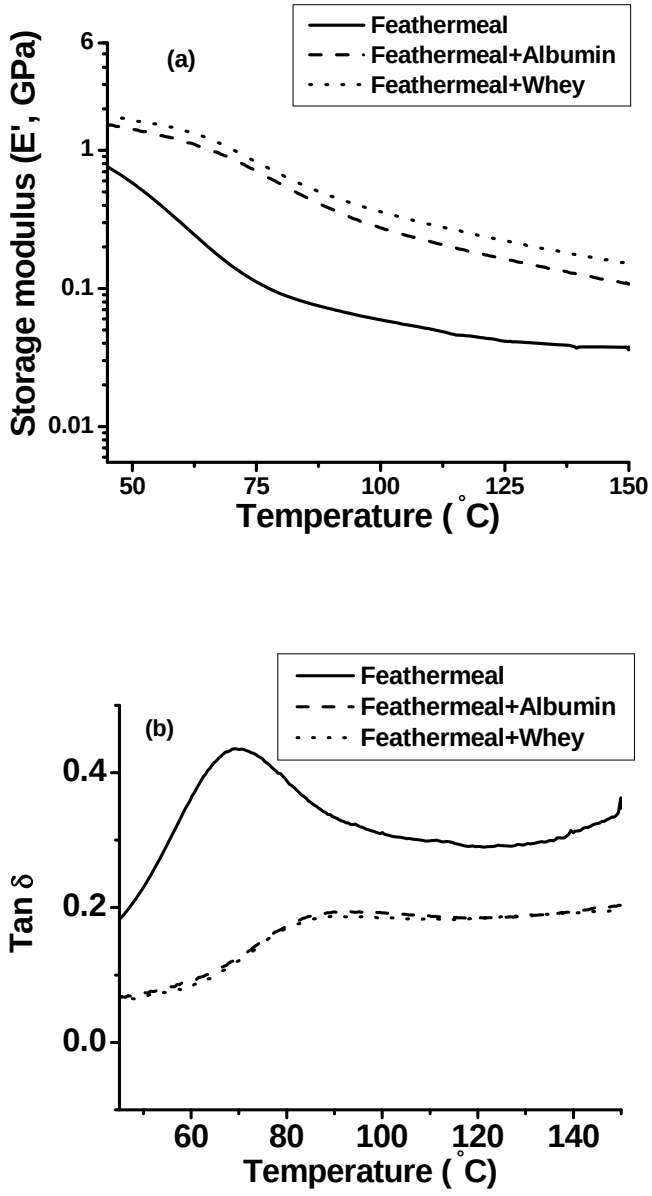

Figure 6.5. Dynamic properties of plastics from feathermeal and the blends of feathermeal/albumin and feathermeal/whey (50%:50% w/w ratios) proteins, molded at a temperature of 150°C and pressure of 20 MPa for 5 minutes, followed by cooling to 70°C and overnight conditioning at 50°C. (a) Storage modulus, (b) Internal friction (Tan δ).

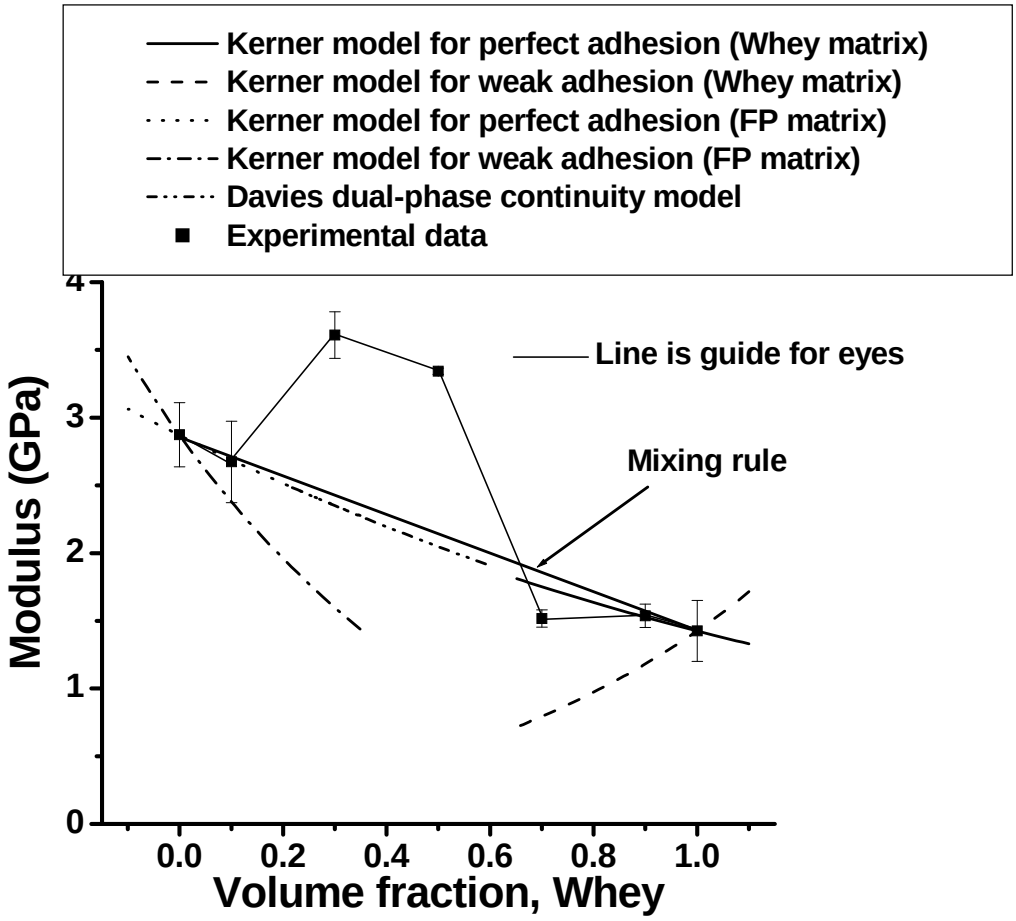

Figure 6.6. Tensile modulus of the feathermeal/whey blends and comparison with theoretical models with four replications at each volume fraction; error bars are ± one SD. Note: All samples were molded at a temperature of 150°C and pressure of 20MPa for 5 minutes, followed by cooling to 70°C under pressure, and overnight drying in an oven at 50°C. Note: FP- Feathermeal Protein.

$$E = E_1 \frac{1}{1 + (\phi_2 / \phi_1)[15(1 - \nu_1)/(7 - 5\nu_1)]} \tag{6.2}$$

Figure 6.6 shows that the theoretical prediction by **Equations 6.1 and 6.2** indicate that there is good adhesion between feathermeal and whey protein phases. This may be explained due to the functional compatibility between proteins (acid-basic interaction) and increased amide links from free COOH and NH_2 groups. The stiffness of the polymer blend in the phase inversion region, where dual-phase continuity is observed, can be approximated by the Davies equation[30], showing the moduli raised to the one-fifth power, as shown in **Equation 6.3**.

$$E^{1/5} = \phi_1 E_1^{1/5} + \phi_2 E_2^{1/5} \qquad (6.3)$$

For the projected phase inversion region, experimental results lie above the theoretically predicted ones from Davies dual-phase continuity model, suggesting presence of the synergistic effect.

Figure 6.7 shows the change in elongation (or % tensile strain at break) for the feathermeal/whey blend. There is a clear negative deviation from the "mixing"(additive rule). The elongation at break can be evaluated (for polymer composites and blends) using a Nielsen equation.[31] According to Nielsen, in general the introduction of a dispersed phase into a matrix causes a dramatic decrease in elongation to break. If there is good adhesion between the phases, the following equation is approximately correct:

$$\varepsilon_C = \varepsilon_0 \left(1 - \phi^{1/3}\right) \qquad (6.4)$$

where ε_C is the elongation to break of the blend and ε_0 is the elongation at break of polymer constituting the matrix. There is a clear indication of good adhesion between feathermeal protein and whey polymer, as the experimental data are in close agreement or

are higher than the values predicted by **Equation 6.4** (**Figure 6.7**). The obtained results are in accord with the elastic modulus calculations.

The presence of dispersed phase is also often expected to decrease the tensile strength of a matrix material. According to Nicolais and Narkis[32], the tensile (yield) strength (σ) of a composite with "uniformly" distributed spherical filler particles of equal radius can be estimated by E**quation 6.5**.

$$\sigma_C = \sigma_m (1 - a\phi^b) \qquad (6.5)$$

where σ_C is the composite tensile strength, σ_m is the polymer matrix tensile strength, *a* and *b* are constants, and ϕ is the volume fraction of filler. Constants '*a*' and '*b*' depend on stress concentration and dispersed phase geometry, respectively.

For the spherical fillers, if there is no adhesion with matrix and if the fracture goes through the filler-matrix interface, the above equation becomes:

$$\sigma_C = \sigma_m (1 - 1.21\phi^{2/3}) \qquad (6.6)$$

According to Piggot and Leidner, the strength at break can be described by first power law equation:

$$\sigma_C = \sigma_m (1 - \phi)S \qquad (6.7)$$

Where parameter S accounts for the weakness in structure due to stress concentration points at polymer-filler interphase. When S is unity, there is no stress concentration effect, implying better adhesion.

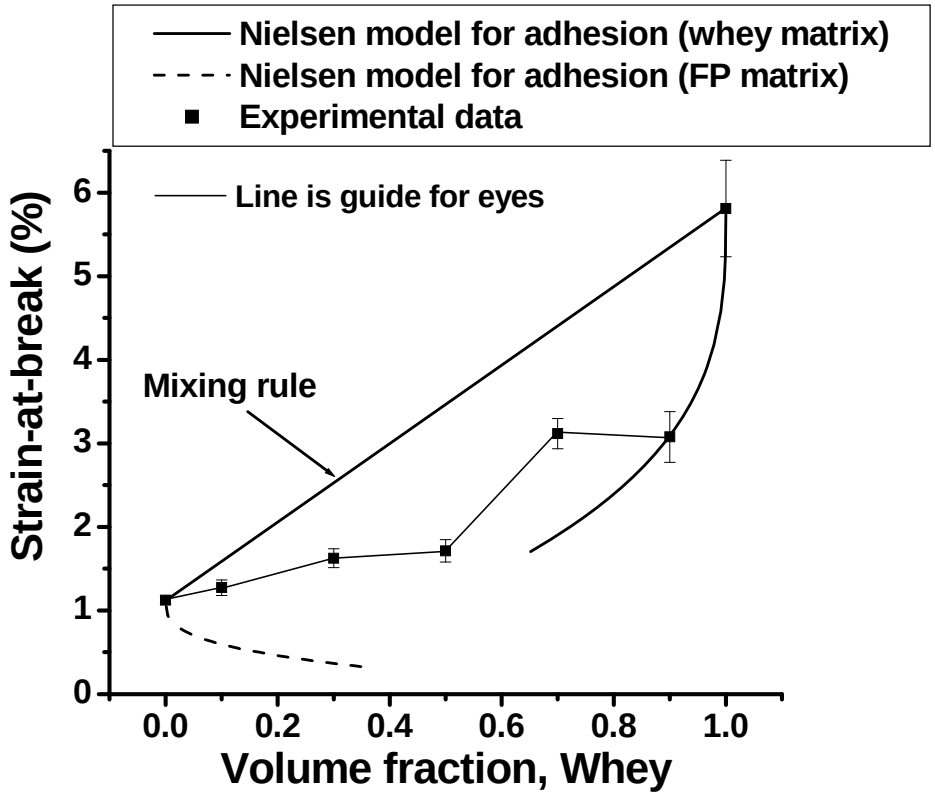

Figure 6.7. Tensile strain at break of the feathermeal/whey blends and comparison with theoretical models with four replications at each volume fraction; error bars are ± one SD. Note: All samples were molded at a temperature of 150°C and pressure of 20MPa for 5 minutes, followed by cooling to 70°C under pressure, and overnight drying in an oven at 50°C. Note: FP- Feathermeal Protein.

Figure 6.8 shows the tensile strength results for feathermeal/whey blends. The values of the stress-at-break are generally (beside one composition) significantly above those predicted by E**quations 6.6 and 6.7**. In fact, the strength of the blend is close to the "mixing" rule. The results once again indicate that there is strong interaction between the components of the blend.

6.3.4: Blends of Feathermeal with rubbery synthetic copolymer

Figure 6.9 shows the micrograph of the feathermeal protein powder. It shows a porous structure and can be filled with different impact modifiers or additives for improving the toughness properties. A synthetic random copolymer was synthesized from GMA (glycidyl methacrylate) and BMA (butyl methacrylate) monomers by Dr. V. Klep. Chemical structure of these monomers is shown in **Figure 6.10**. It was assumed that this copolymer might improve the toughness characteristics as long alkyl chains in BMA imparts flexibility and epoxy groups in GMA provides reactivity towards NH_2 and COOH groups in protein, forming chemical anchorage. Varying wt.-% of this copolymer was mixed with feathermeal protein according to procedure described in the experimental section of the Chapter 3.

Figure 6.11(a) shows the mechanical properties of plastics produced from different such percentages as 1%, 5%, 10%, & 15% of this copolymer. **Figures 6.11 (b,c,d)** represent these properties in comparison to some established theoretical models such as Kerner, Nielsen and Piggot-Leidner. These empirical models for composites and blends have been discussed in Section 6.3.3.1. In addition, Kunori and Geil[33] proposed **Equation 6.8** for systems having strong interfacial adhesion, assuming a strong adhesive force between the blend components, the disperse phase will contribute to the strength of the blend and the fracture will propagate through the matrix.

$$\sigma_C = \sigma_m (1 - \phi_d) + \sigma_d \phi_d \qquad (6.8)$$

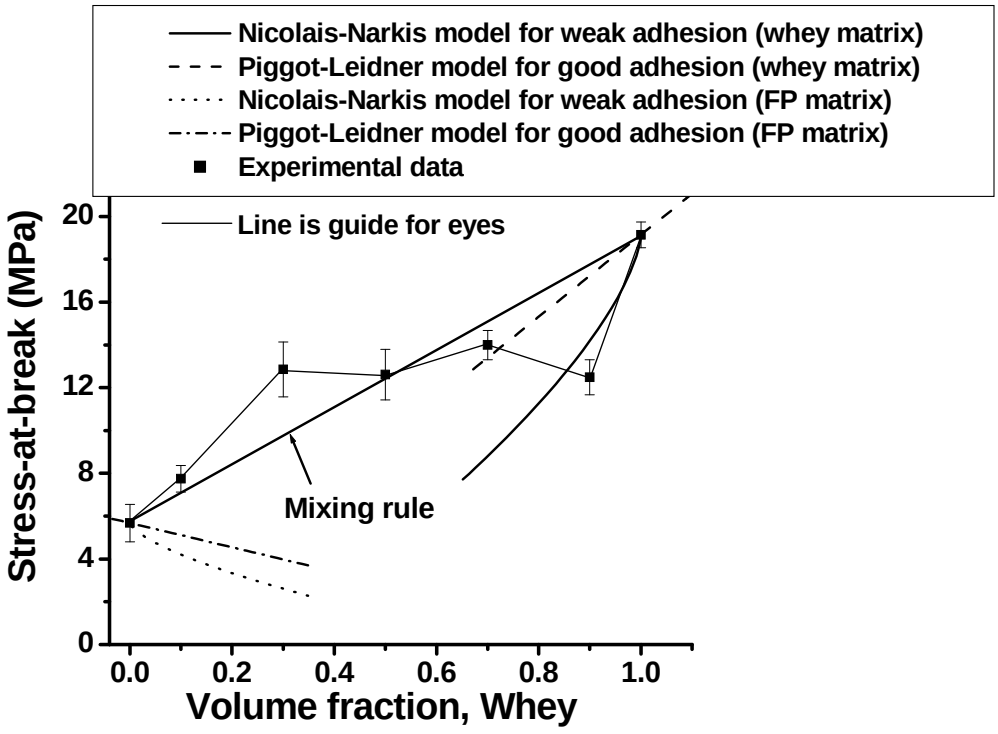

Figure 6.8. Tensile strength of the feathermeal/whey blends and comparison with theoretical models with four replications at each volume fraction; error bars are ± one SD. Note: All samples were molded at a temperature of 150°C and pressure of 20MPa for 5 minutes, followed by cooling to 70°C under pressure, and overnight drying in an oven at 50°C. Note: FP- Feathermeal Protein.

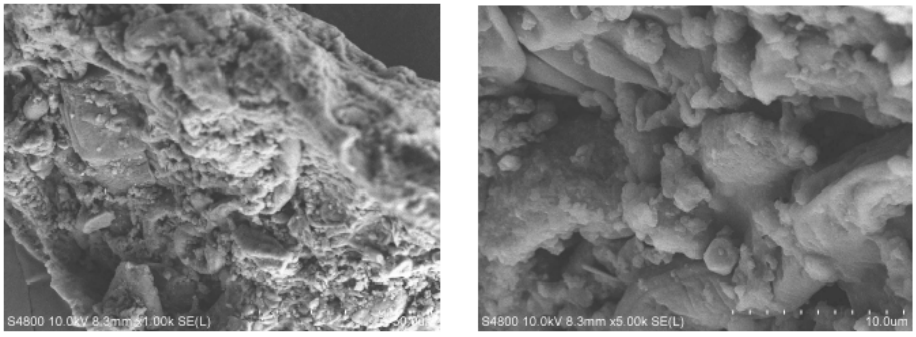

Figure 6.9. Scanning electron microscopy micrograph of the feathermeal protein powder.

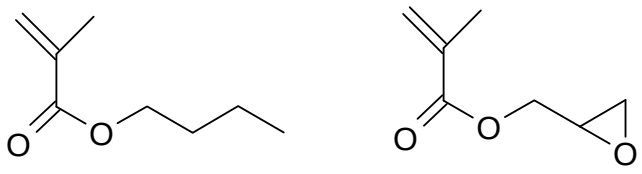

BMA GMA

Figure 6.10. Chemical structure of monomer for rubbery synthetic copolymer.

where σ_C is the composite tensile strength, σ_m is the polymer matrix tensile strength, and ϕ_d is the volume fraction of dispersed component.

The experimental results, shown in **Figure 6.11(b,c)** for tensile strength and elongation were having positive deviations from these models, indicating a strong adhesion between the blending components. This improvement in mechanical characteristics can be attributed to the formation of crosslinks between epoxy groups of copolymer and reactive functional groups of feathermeal protein such as carboxyl and amino at high temperature of plastic molding. Modulus results, represented in **Figure 6.11(d)**, showed a reducing trend, which is common with plastics modified with rubbery polymers. However, the control sample showed lower mechanical properties, confirming the positive effect of this copolymer. Therefore, depending on the percentage of copolymer, the mechanical properties of the feathemeal plastic samples could be tailored.

Figure 6.12 shows the fracture surfaces at different weight % of copolymer of PGMA-co-PBMA. All compositions of rubbery copolymer demonstrated uneven fracture surfaces, indicating more ductile behavior, compare to flat fracture surface of unmodified feathermeal sample, as shown in **Figure 6.3**.

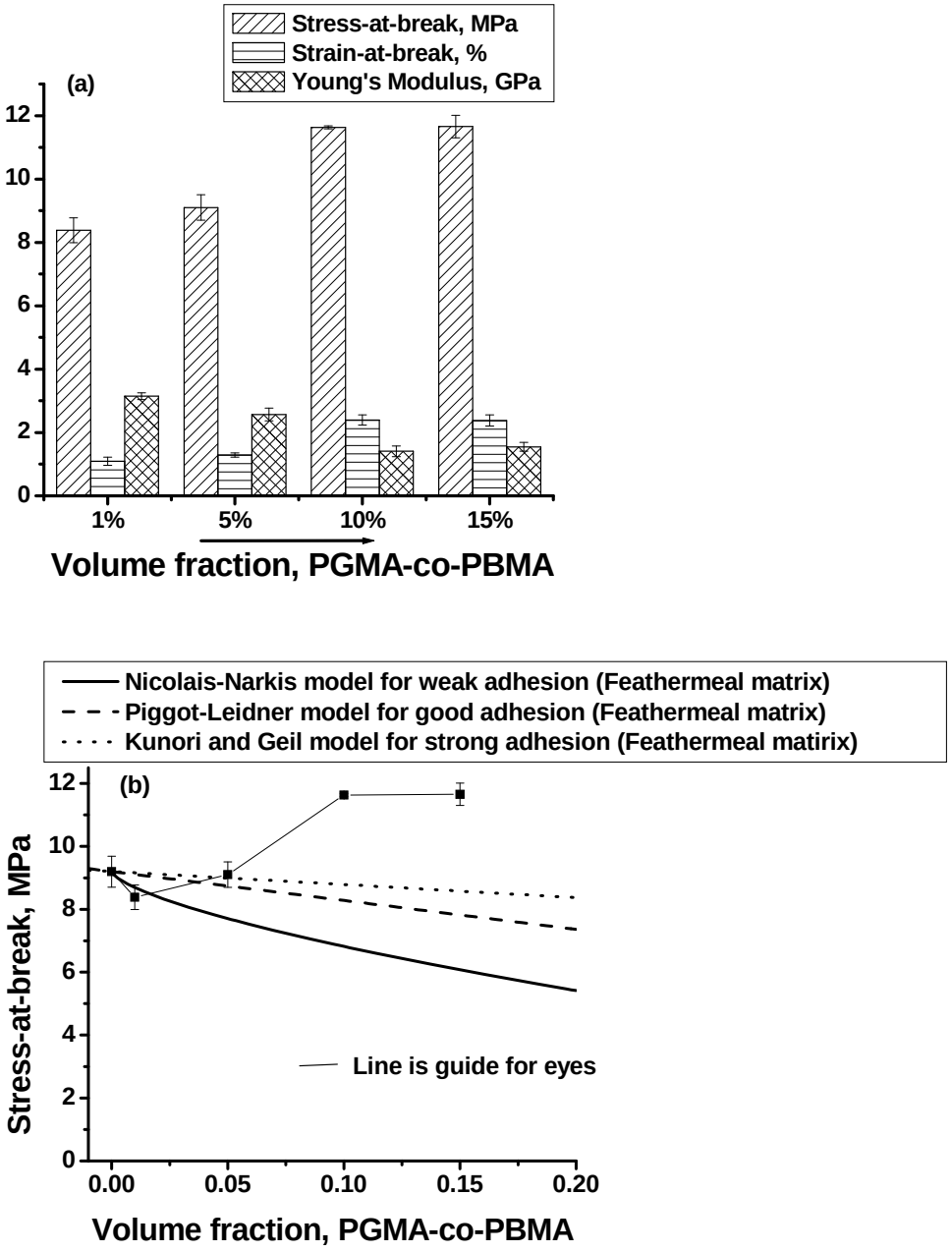

Figure 6.11(a, b). Mechanical properties of the feathermeal/PGMA-co-PBMA blends, molded at a temperature of 150°C and pressure of 20MPa for 5 minutes, followed by cooling to 70°C under pressure: (a) Mechanical properties, (b) Tensile strength.

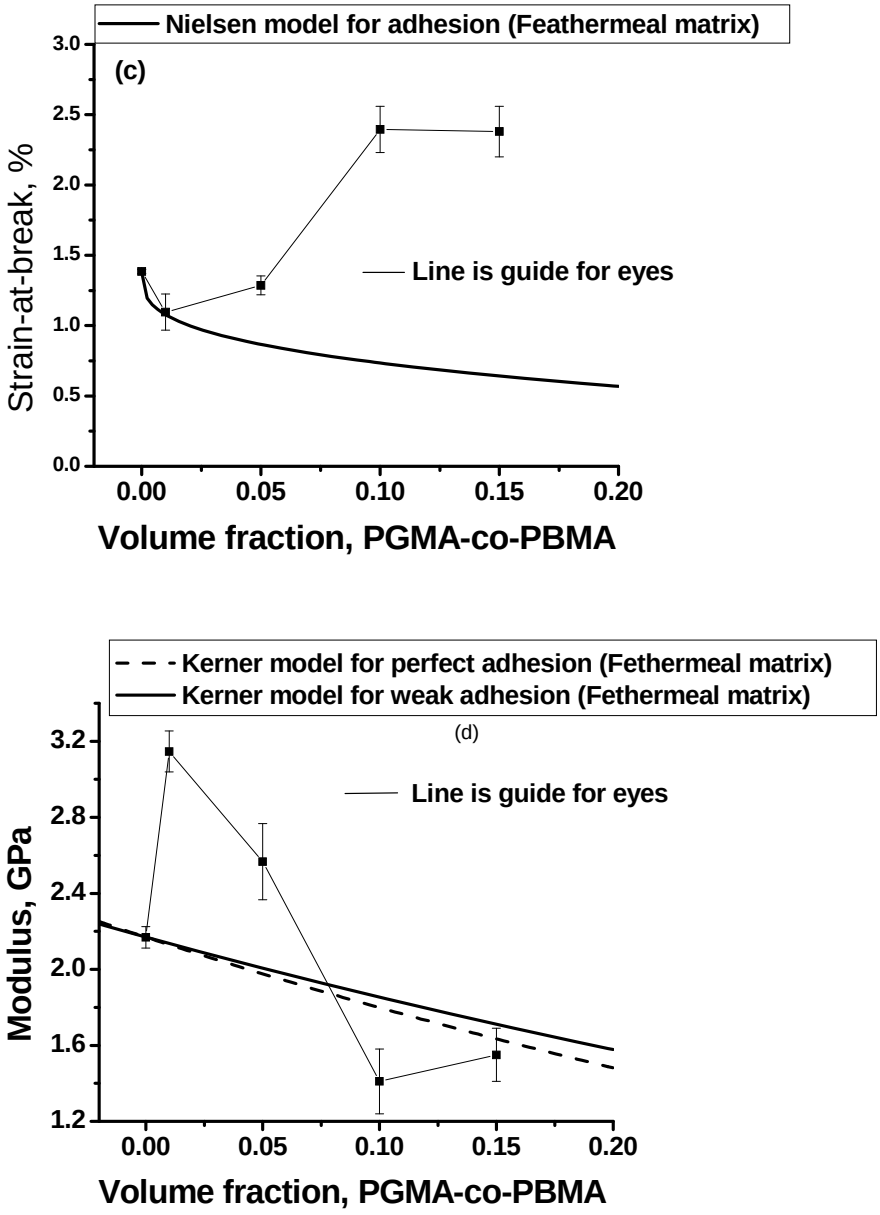

Figure 6.11(c, d). Mechanical properties of the feathermeal/PGMA-co-PBMA blends and comparison with empirical models. All samples were molded at a temperature of 150°C and pressure of 20MPa for 5 minutes, followed by cooling to 70°C under pressure.:(c) Strain-at-break, (d) Modulus.

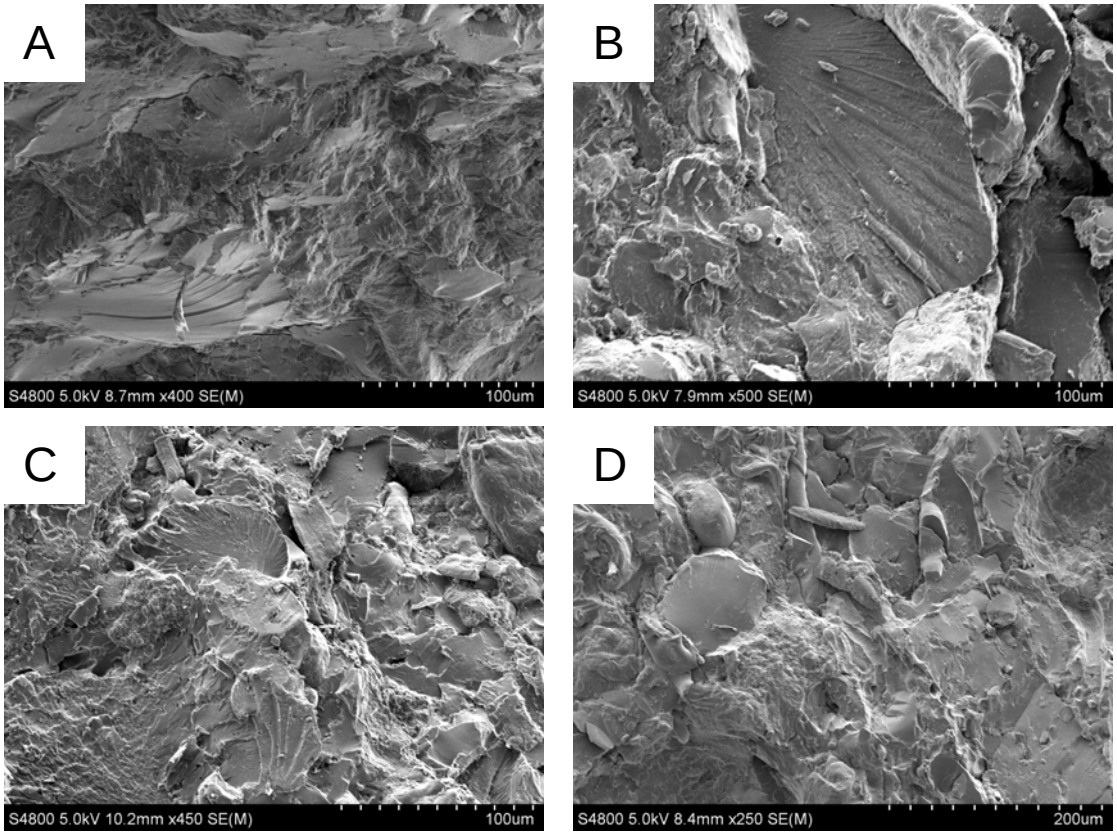

Figure 6.12. Scanning electron microscopy micrographs at different weight (%) of copolymer PGMA-co-PBMA: (A) 1% w/w; (B) 5% w/w; (C) 10% w/w; (D) 15% w/w. All samples were molded at a temperature of 150°C and pressure of 20MPa for 5 minutes, followed by cooling to 70°C under pressure.

6.4: Conclusions

Plastic samples from partially denatured feathermeal protein were successfully produced by the compression-molding process. The modulus (stiffness) for the material obtained was found to be comparable with that of commercial synthetic material but with lower toughness characteristics, which is a common phenomenon among plastics produced from animal and plant proteins. A reversible stress-strain property over the yield region was observed. Plastic forming conditions for undenatured animal proteins, such as albumin and whey proteins were also formulated for developing plastics out of

these protein's blends with feathermeal proteins. The resultant plastic samples made from these biomacromolecular blends demonstrated improved mechanical properties as compared to neat plastics from feathermeal proteins. The results were interpreted in terms of theoretical models to describe mechanical properties such as extensibility, tensile strength, and stiffness of the plastics made out of feathermeal/whey blends at various volume ratio. The values for the stiffness of the feathermeal/whey blends deviated from the simple mixing rule and showed a synergistic effect.

Plastic samples were also prepared from blends of synthetic rubber copolymer and feathermeal protein, demonstrating improved mechanical properties as compared to neat plastics from feathermeal proteins. In addition, these results were interpreted in terms of theoretical models, describing mechanical properties.

6.5: References

[1] Kumar, R., Choudhary, V., Mishra, S., Varma, I. K., and Mattiason, B., Ind. Crops Prod. (2002), 16, 155.

[2] Villar, M. A., Thomas, E. L., and Armstrong, R. C., Polymer (1995), 36, 1869.

[3] Salmoral, E. M., Gonzalez, M. E., Mariscal, M. P., and Medina, L. F., Ind. Crops Prod. (2000), 11, 227.

[4] Paetau, I., Chen, C., Jane, J., Ind. Eng. Chem. Res. (1994), 33, 1821. Zhang, J., Mungara, P., and Jane, J., Polymer (2001), 42, 2569.

[5] Zhong, Z., and Sun, X. S., Polymer (2001), 42, 6961.

[6] Liu, W., Misra, M., Askeland, P., Drzal, L. T., and Mohanty, A. K., Polymer (2005), 46, 2710.

[7] Huang, X., and Netravali, A. Comp. Sci. Tech. (2007), 67, 2005.

[8] Orliac, O., Silveste, F., Rouilly, A., and Rigal, L., Ind. Eng. Chem. Res. (2003), 42, 1674.

[9] Aithani, D., and Mohanty, A. K., Ind. Eng. Chem. Res. (2006), 45, 6147.

[10] Meeker, D. L., and Hamilton, C. R. In Essential Rendering: All About The Animal By-products Industry (2006), Meeker, D. L., Ed., Kirby Lithographic Company, Inc.: Arlington, Chap.1.

[11] Garcia, R. A., Onwulata, C. I., and Ashby, R. D., J. Agric. Food Chem. (2004), 52, 3776.

[12] Bielorai, R., Iosif, B., Neumark, H., and Alumot, E., J. Nutr. (1982), 112, 249.

[13] Park, S. K., Bae, D. H., and Hettiarachchy N. S., J. Amer. Oil. Chem. Soc. (2000), 77, 1223.

[14] Chowdry, B., and Leharne, S., J. Chem. Educ. (1997), 74, 236.

[15] Madeka, H., and Kokini, J. L., Cereal Chem. (1996), 73, 433.

[16] León, A., Rosell, C. M., and Barber, C. B., Eur. Food Res. Tech. (2003), 217, 13.

[17] Ortiz, S. E. M., and Aňón, M. C., J. Therm. Anal. Cal. (2001), 66, 489.

[18] Takahashi, K., Yamamoto, H., Yokote, Y., and Hattori, M., Biosc. Biotechnol. Biochem. (2004), 68, 1875.

[19] Grevellec, J., Marquie, C., Ferry, L., Crespy, A., and Vialettes, V., Biomacromolecules (2001), 2, 1104.

[20] Patel, M. T., Kilara, A., Huffman, L. M., Hewitt, S. A., and Houlihan, A.V., J. Dairy Sci. (1990), 73, 1439.

[21] Donovan, J. W., and Mapes, C. K., J. Sci. Food Agric. (1976), 27, 197.

[22] Muffett, D. J., and Snyder, H. E., J. Agric. Food Chem. (1980), 28, 1303.

[23] Liu, D., and Zhang, L., Macromol. Mater. Eng. (2006), 291, 820.

[24] Mo, X., and Sun, X. J., Polym. Environ. (2003), 11, 15.

[25] Arvanitoyannis, I. S., J. Macromol. Sci. Rev. Macromol. Chem. Phys. (1999), C39, 205.

[26] Koning, C., Duin, M. V., Pagnoulle, C., and Jerome, R., Prog. Polym. Sci. (1998), 23, 707.

[27] Audic, J-. L., Chaufer, B., and Daufin, G., Le Lait (2003), 83, 417.

[28] Jerez, A., Partal, P., Martínez, I., Gallegos, C., and Guerrero, A., J. Food Eng. (2007), 82, 608.

[29] Kerner, E. H., Proc.Phys.Soc. (1956), 69B, 808.

[30] Sperling, L. H. Polymeric Multicomponent Materials; John Wiley & Sons, Inc.: New York, 1997.

[31] Nielsen, L. E. Mechanical Properties of Polymers and Composites; Marcel Dekker: New York 1974.

[32] Nicolais, L., and Narkis, M., Polym. Eng. Sci. (1971), 1, 194.

[33] Nandan, B., Kandpal, l. D., and Mathur, G. N., Macromol. Mater. Eng. (2004), 289, 749.

CHAPTER 7

BIODEGRADABLE PLASTICS FROM PARTIALLY DENATURED PROTEINS: BLOODMEAL

7.1: Introduction

Rising oil prices and concerns over the dwindling availability of landfill sites have necessitated the development of polymers/biodegradable materials from agricultural processing by-products. A biodegradable material or green polymeric material can be obtained in various such forms as neat polymer, blended product, and composite.[1] Biodegradable plastics are especially important in articles that are unlikely to be recycled, such as trash and compost bags, mulch films, and disposable hygienic products.[2]

An important way to produce these plastics involves using natural polymers based on starch, proteins, and cellulose.[3] Several plant proteins, such as wheat and corn gluten, soy, pea, and potato, and animal proteins, such as casein, whey, collagen, and keratin are available for the development of biodegradable plastics.[4] The most relevant properties of proteins are good processability, good film forming characteristics, good adhesion to various substrates, and barrier properties.[5]

For example, Paetau et al.[6] studied the preparation and processing conditions of soy-plastic through a compression-molding process. These plastics exhibited tensile strength comparable to that of commercial polystyrene. In addition, it was observed that moisture, temperature, and pressure were important factors for the mechanical and water resistant properties.[6,7] Although plastics made from soy protein showed improved strength and good biodegradable performance, the brittleness problem of protein plastics

has not yet been solved. Therefore, blending methods have been extensively explored, producing plastics of desired properties. For example, compression molding of blends from chickpea protein isolates or defatted whole flour produced plastic materials of acceptable properties.[3] In addition, blends of cereal proteins (soybean and wheat gluten) and poly(hydroxyl ester ether) (PHEE) were produced through commercial extrusion and molding equipment, resulting in plastics of comparable properties to commercial thermoplastics such as polystyrene.[8]

To date, there has been only one reference regarding the development of plastics from animal protein co-products, especially from bloodmeal.[9] Verbeek[10] used chemically modified bloodmeal protein to produce plastic using injection molding process. Blood meal is produced from clean, fresh animal blood, exclusive of extraneous material, such as hair, stomach belchings, and urine, except as might occur unavoidably in good manufacturing processes.[11] A large portion of the moisture (water) is usually removed by a mechanical dewatering process or by cooking to a semi-solid state. The semi-solid blood mass is then transferred to a rapid drying facility where more tightly bound water is rapidly removed.

Excessive availability of bloodmeal protein on a renewable basis has forced rendering industries to explore alternative uses, such as fuel, fertilizers, and plastics in addition to the traditional use as an ingredient for animal feed. Therefore, the primary objective of this part of the research was to develop bioplastics from partially denatured bloodmeal protein. Another important objective of this research was to investigate the thermal and mechanical characteristics of these plastics in order to understand the

fabrication process. In addition, other less important objectives were to develop blends from bloodmeal and undenatured whey and albumin proteins and to develop biocomposites reinforced with natural fiber.

7.2: Materials

Partially denatured bloodmeal, pure undenatured proteins (whey and chicken egg whites albumin), and hemp fiber were used to develop plastics and composites. Bloodmeal protein was supplied by Fats and Proteins Research Foundation (FPRF), VA, containing 86-89% of crude protein with no saturated fatty content. Whey protein isolates (BiPro, Davisco Foods Intl.) and chicken egg whites albumin (A5253, Sigma-Aldrich) were composed of 91% and at least 90% protein, respectively. Chopped hemp fibers were supplied by Hempline, Inc., Canada.

7.3: Results and Discussion

7.3.1: Plastics from bloodmeal protein

The bloodmeal contained a moisture content of approximately 8-9% and was analyzed using DSC and TGA to determine the denaturation and thermal stability. Even though the bloodmeal protein was thermally treated via the rendering process; DSC data in **Figure 7.1(a)** indicated the presence of the denaturation (unfolding) temperature (~ 150°C) for the protein powder. Thus, the protein was not fully denatured during the rendering procedures, and further unfolding of the biopolymer occurred upon heating. The cooperative unfolding of the biopolymer originates from disruption of the multiple

small forces that maintain the secondary/tertiary protein structure.[12] The denaturation of the bloodmeal occurs in the temperature range that is typical for denaturation of other protein biomacromolecules. DSC measurements also provided important information about the nature of water incorporated into the bloodmeal protein. In fact, an endothermic peak around 0°C, which would correspond to the melting of crystallizable (unbound) water, was not observed. Thus, the water was hydrogen bonded between protein macromolecules.

Figure 7.1(b) shows the weight loss of the bloodmeal sample. The first weight-loss occurred from room temperature to about 100°C, and was mainly due to by water evaporation.[13] In addition, TGA results (second weight loss) suggested that significant degradation of the protein was initiated at 265°C. Based on the analysis from DSC and TGA, the bloodmeal protein powder was compression-molded using a Carver press at a temperature of 180°C (between denaturation temperature and degradation temperature) and a pressure of 40 MPa for five minutes, and was then cooled to 70°C under pressure. The water content for the plastic obtained was on the level of 4%.

It can be observed from **Figure 7.1(a)** that the original endothermic peak because of denaturation (~150°C) was not observed in plastic samples due to denaturing resulting from heating and pressing. TGA results in **Figure 7.1(b)** showed a different weight-loss pattern for these plastics in comparison to the original bloodmeal powder. Specifically, the first (water) weight loss occurred over a more extended temperature range. The slowdown of the water loss can be attributed to the denser structure of the plastic sample as compared to the protein powder. The temperature of degradation, however, was

virtually unaffected by the compression-molding.

7.3.2: Mechanical properties

Figure 7.2 shows the stress-strain diagram for the plastic samples made from the bloodmeal protein, and it is comprised of three regions: initial elastic deformation, plastic yield, and strain hardening. The behavior of the yield point can be due to the breaking of hydrophobic interactions and hydrogen bonds of folded protein macromolecules. **Figure 7.3** shows the SEM micrograph of the fracture surfaces (from the tensile test) of this plastic, indicating the brittle nature of the fracture. The stress-at-break, strain-at-break, and modulus of bloodmeal plastics were measured to be 16.5 MPa, 1.65%, and 4.7 GPa, respectively.

To observe the effect of molding pressure, trials were conducted at 20, 40, 50, 60 and 70 MPa. **Figure 7.4** shows the resulting mechanical properties of these plastics. It can be observed that the molding pressures of more than 40 MPa did not cause a significant improvement in tensile properties. Therefore, a pressure of 40 MPa was selected for the development of bloodmeal plastic samples.

However, modulus increased with increasing pressures. This increased stiffness (or modulus) of plastic may have potential for developing such products as shooting discs and bullets for hunting. Overall, the observed mechanical properties (high stiffness accompanied by low extensibility) are in the range of the values that are typically observed for bioplastics fabricated from unplasticized undenatured proteins. The properties of plastic from undenatured proteins are somewhat better than the ones from

partially denatured proteins in terms of strength and elongation. This behavior can be associated with the fact that undenatured protein plastics are typically prepared from biomacromolecules, which are thermally untreated and possess their native conformation. Accordingly, to improve the properties of plastics, bloodmeal protein can be mixed with proteins that possess a lower level of denaturation and may demonstrate better properties.

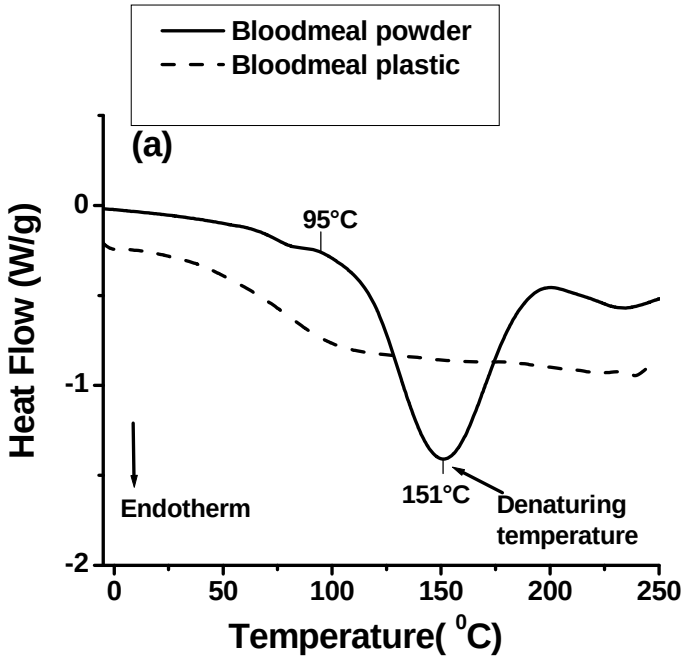

Figure 7.1(a). Thermal analysis of bloodmeal protein powder and plastic samples produced at a temperature of 180°C and a pressure of 40MPa for 5 minutes, followed by cooling to 70°C under pressure: (a) DSC thermograms.

7.3.3: Fabrication of plastics from blends containing bloodmeal protein

One of the most efficient ways to obtain plastics with improved properties is to combine two or more polymers in a polyblend where weakness in one component can, to

a certain extent, be masked by the strength of the other component.[14] The protein/protein blend is supposed to be compatible because of the complementary reactive functional groups such as amino, carboxy, and hydroxy. Owing to the reactions between the functionalities at the phase boundary, strong interfacial adhesion should be readily achieved after molding the samples at higher temperatures.

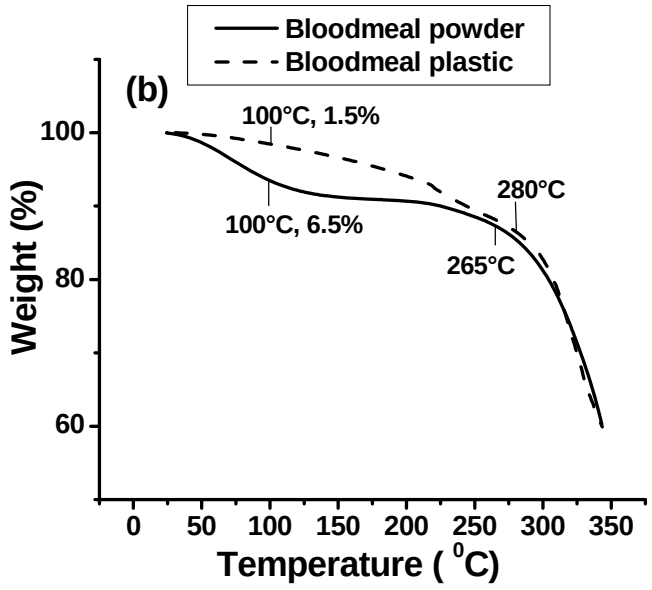

Figure 7.1(b). Thermal analysis of bloodmeal protein powder and plastic samples produced at a temperature of 180°C and a pressure of 40MPa for 5 minutes, followed by cooling to 70°C under pressure: (b) TGA thermograms.

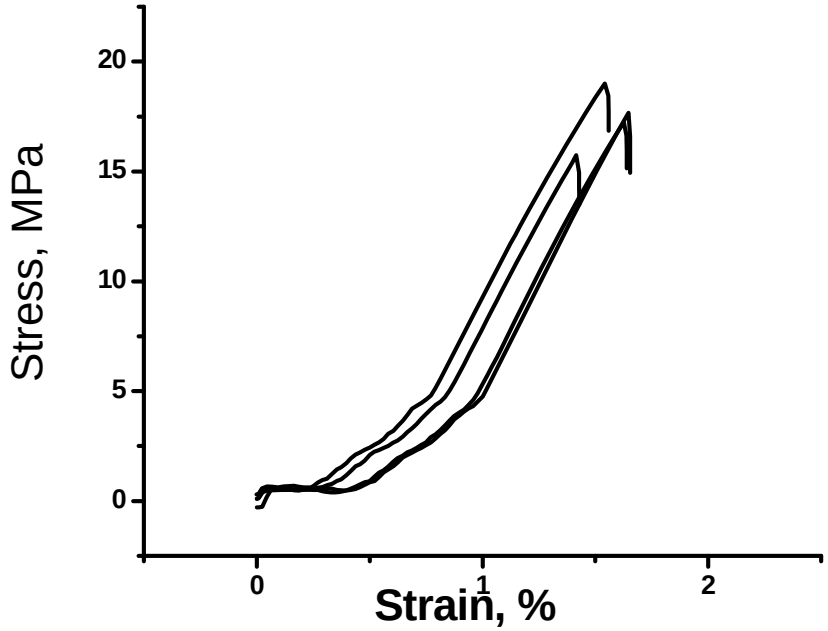

Figure 7.2. Stress-strain curve for the bloodmeal plastic, molded at a temperature of 180°C and a pressure of 40MPa for 5 minutes, followed by cooling to 70°C under pressure.

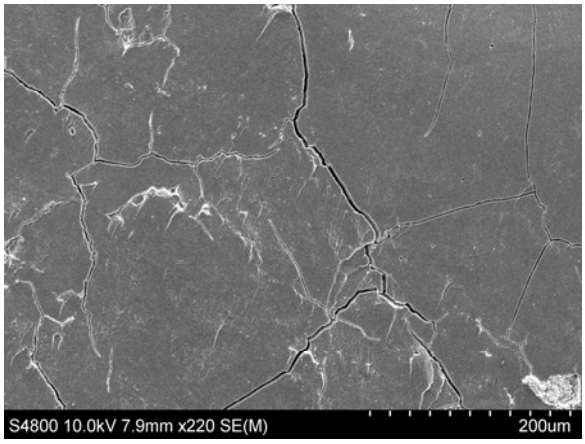

Figure 7.3. SEM (Scanning Electron Microscopy) micrograph of bloodmeal plastic, molded at a temperature of 180°C and a pressure of 40MPa, followed by cooling to 70°C under pressure.

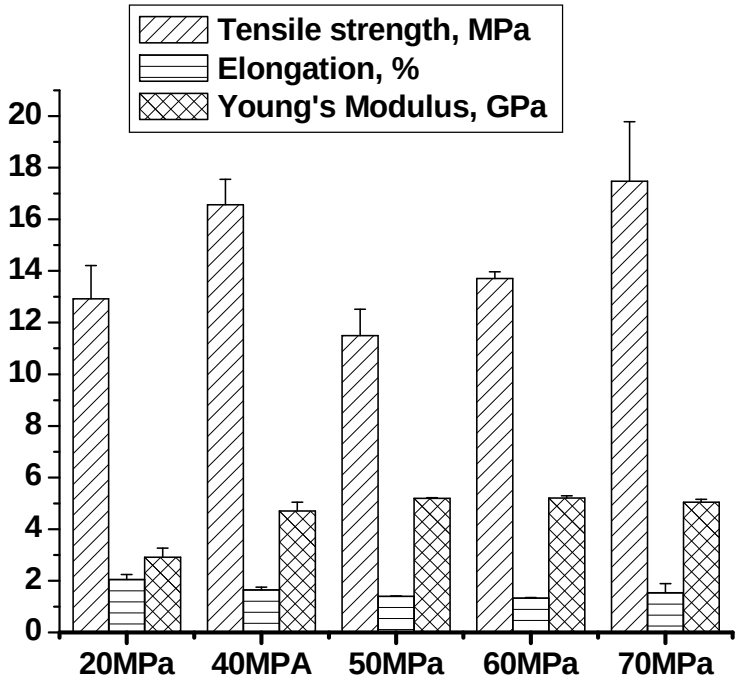

Figure 7.4. Comparison of mechanical properties of bloodmeal plastic samples molded at a temperature of 180° C under different molding pressures for 5 minutes, followed by cooling to 70°C under pressure.

Two commercially available, undenatured or pure natural proteins, chicken egg whites albumin and whey, were considered for the blending experiments. The stress-at-break, strain-at-break, and modulus were measured to be 32.3 MPa, 5.7%, and 2.1 GPa and 22.8 MPa, 5.98%, and 1.5 GPa for the whey and albumen plastics, respectively. On the contrary, bloodmeal plastic exhibited stress-at-break, strain-at-break, and modulus of 16.5 MPa, 1.65%, and 4.7 GPa, respectively. In general, the plastics from the egg albumin and whey proteins showed higher strength and elongation properties than the plastic from the bloodmeal protein itself. To compare the properties of the whey/albumin

and bloodmeal plastics directly, the procedure for preparation of the bloodmeal samples was modified to include the addition of 25% water and an overnight annealing at 50°C. The change in fabrication method altered the mechanical properties of the bloodmeal plastic as well, and the stress-at-break, strain-at-break, and modulus were determined to be 3.1MPa, 1.1%, and 1.85GPa, respectively. The annealing caused a significant decrease in strength, elongation, and modulus of bloodmeal plastic. Mixtures of bloodmeal/albumin and bloodmeal/whey proteins in 50%:50% w/w ratios were prepared to obtain polymer blends. A DSC study of these protein blends did not show any crystallizable (unbound) water. Therefore, the water molecules situated in the mixtures were bound to the protein macromolecules.

7.3.3.1: Mechanical properties of bloodmeal plastics

The mechanical properties of these plastics, shown in **Figure 7.5,** represented a significant improvement compared to the unmodified bloodmeal plastic samples. The blend of bloodmeal and albumin proteins showed the highest breaking stress and elongation of 18.7 MPa and 2.9%, respectively. Moreover, the dynamic mechanical analysis of these plastics, shown in **Figure 7.6**, also demonstrated higher storage modulus and loss factor (internal friction) peak compared to neat bloodmeal plastic, confirming the compatibility between these proteins. However, the blend of bloodmeal/albumin exhibited improved dampening (height of tan δ peak) compared to the blend of bloodmeal/whey proteins. These improved mechanical properties may be attributed to the same native albumin protein, constituting the bloodmeal and chicken egg whites. Overall,

the mechanical properties demonstrated that blending of bloodmeal with albumin protein has definite potential.

7.3.3.2: Modeling of mechanical properties of plastics from blends

To further evaluate the properties of blends, plastics containing different ratios of bloodmeal and albumin proteins were prepared. Known relationships that have been used to predict properties of polymer blends and composites were used to model the behavior of these blends. These empirical relationships were developed for spherical inclusions distributed in a matrix, but as a first approximation are often used for systems where inclusions are not spherical in shape. **Figure 7.7** shows that the stiffness of these plastics deviated from the simple "mixing" additive rule in a positive way, indicating a clear synergistic effect, where the properties of blends are better than those of the individual components.

For polymer blends, the well-established Kerner equation considers the dispersed phase as spheres having the following form:[15]

$$E = E_1 \frac{\dfrac{\phi_2 E_2}{(7-5\nu_1)E_1 + (8-10\nu_1)E_2} + \dfrac{\phi_1}{15(1-\nu_1)}}{\dfrac{\phi_2 E_1}{(7-5\nu_1)E_1 + (8-10\nu_1)E_2} + \dfrac{\phi_1}{15(1-\nu_1)}} \qquad (7.1)$$

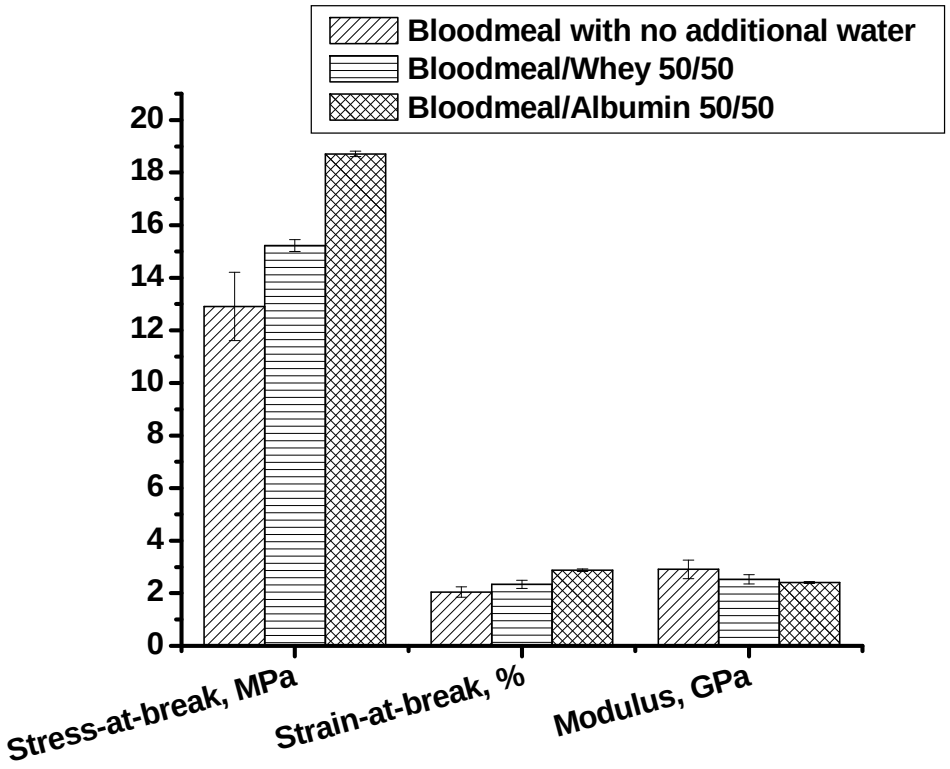

Figure 7.5. Mechanical properties of plastics from bloodmeal and the blends of bloodmeal/albumin and bloodmeal/whey (50%:50% w/w ratios), molded at a temperature of 150°C and a pressure of 20MPa for 5 minutes, followed by cooling to 70°C under pressure and subsequent overnight drying in an oven at 50°C.

where E, E_1 ,E_2 represent the moduli for the binary blend, the matrix and the dispersed phase, respectively; ϕ_1, ϕ_2 the volume fractions of the matrix and the dispersed phase, respectively; and ν_1 represents the poisson r**a**tio for the matrix. (To estimate the volume fractions the density of protein material was considered to be 1g/cm^3).

Equation 7.1 is valid for an ideal stress transfer through the interface, indicating strong adhesion between the phases. If no stress is transferred, i.e., there is no adhesion between

the phases, the Kerner equation is simplified in the following form:

$$E = E_1 \frac{1}{1 + (\phi_2 / \phi_1)[15(1 - \nu_1)/(7 - 5\nu_1)]} \qquad (7.2)$$

E_2 is assumed to be zero.

Figure 7.7 shows that the theoretical prediction by **Equations 7.1 & 7.2** indicate good adhesion between the bloodmeal and albumin protein phases. This may be explained by the functional compatibility between proteins and increased amide and ester links from free COOH, NH_2 and OH groups. The stiffness of the polymer blend in the phase inversion region, where dual-phase continuity is observed, can be approximated by the Davies equation:[16]

$$E^{1/5} = \phi_1 E_1^{1/5} + \phi_2 E_2^{1/5} \qquad (7.3)$$

For the projected phase inversion region (volume fraction 0.35 to 0.65), experimental results lie above the ones theoretically predicted by the Davies dual-phase continuity model, suggesting also a synergistic effect. The Takayanagi model for a two phase system, which assumes different morphological structures in the blend or composites, was also used to predict the modulus results. **Equations 7.4 & 7.5** show the Young's modulus for a system with two continuous phases (upper bound) and two discontinuous phases (lower bound), respectively. This model also predicted the strong adhesion between two protein phases.

$$E = (1 - \phi_2)E_1 + \phi_2 E_2 \qquad (7.4)$$

$$E = \left(\frac{\phi_2}{E_2} + \frac{1-\phi_2}{E_1} \right) \tag{7.5}$$

Figure 7.8 shows the change in elongation (or % tensile strain at break) for the bloodmeal/albumin blend. There is a clear negative deviation from the "mixing" additive rule. According to Nielsen[17], in general, the introduction of a dispersed phase into a matrix causes a dramatic decrease in elongation to break. If there is a good adhesion between the phases, the following equation is approximately correct:

$$\varepsilon_C = \varepsilon_0 \left(1 - \phi^{1/3} \right) \tag{7.6}$$

where ε_C represents the elongation to break of the blend, and ε_0 the elongation to break of polymer constituting the matrix.

The experimental data from **Figure 7.8** are in close agreement or are higher than the values predicted by **Equations 7.6** that clearly indicates the good adhesion between bloodmeal and albumin biopolymers.

Presence of the dispersed phase is also often expected to decrease the tensile strength of a matrix material. According to Nicolais and Narkis[18], the tensile strength (σ) of a composite, reinforced with "uniformly" distributed spherical filler particles of equal radius, can be estimated by **Equation 7.7**.

$$\sigma_C = \sigma_m (1 - a\phi^b) \tag{7.7}$$

where σ_C represents the composite tensile strength; σ_m is the tensile strength of polymer matrix; *a* and *b* the constants; and ϕ the volume fraction of filler. Constants '*a*' and '*b*' depend on stress concentration and dispersed phase geometry, respectively.

For the spherical fillers, if there is no adhesion with matrix and if the fracture goes through the filler-matrix interface, **Equation 7.7** becomes:

$$\sigma_C = \sigma_m (1 - 1.21\phi^{2/3}) \qquad (7.8)$$

According to Piggot and Leidner, the strength at break can be described by first power law equation:

$$\sigma_C = \sigma_m (1 - \phi) S \qquad (7.9)$$

where parameter S accounts for the weakness in structure due to stress concentration points at polymer-filler interphase. When S is unity, there is no stress concentration effect, implying better adhesion. **Figure 7.9** shows the tensile strength results for blends of bloodmeal/albumin. The experimental values of the stress-at-break lie above those predicted by **Equations 7.8 & 7.9**. The results once again indicate that there is a strong interaction between the components of the blend.

7.3.3.2 Dynamic mechanical properties of plastics from blends

Figures 7.10(a) & 7.10(b) show the storage modulus and the loss factor (internal friction) of the plastics from blends of bloodmeal/albumin through dynamic mechanical analysis (DMA). It can be observed that the increased portion of the albumin protein in blends exhibit a shift of Tan δ peak (glass-transition) towards lower temperatures and increase in the Tan δ height, indicating the improvement of the dampening (or toughening) characteristics of bloodmeal plastics. The trend of Tg's is shown in **Figure 7.10(c)** and compared with the Fox equation (**Equation 7.10**) for miscible polymer blends.

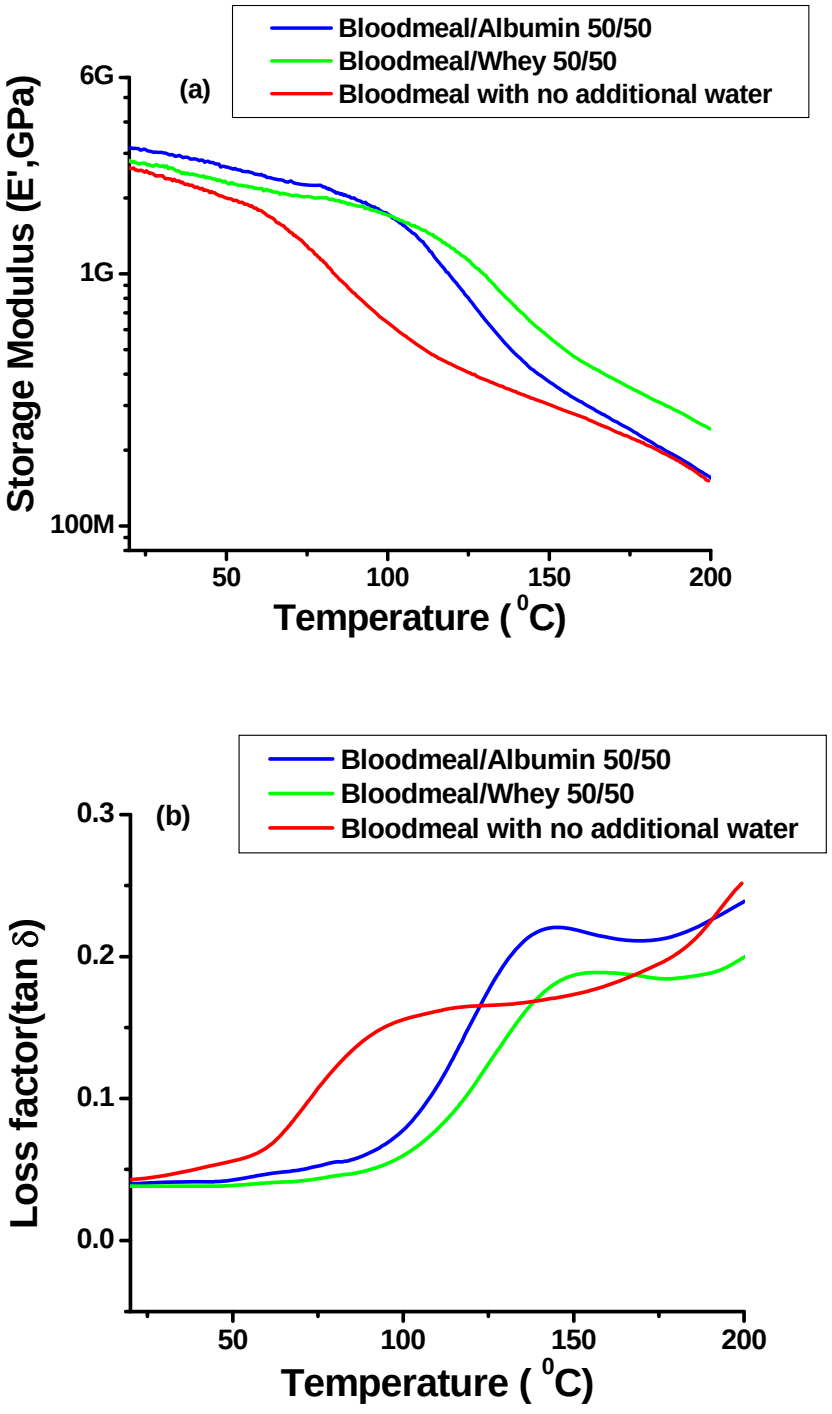

Figure 7.6. Dynamic properties of plastics from bloodmeal and its blends, molded at a temperature of 150°C and a pressure of 20 MPa for 5 minutes, followed by cooling to 70°C and overnight conditioning at 50°C: (a) Storage modulus, (b) Loss factor (tan δ).

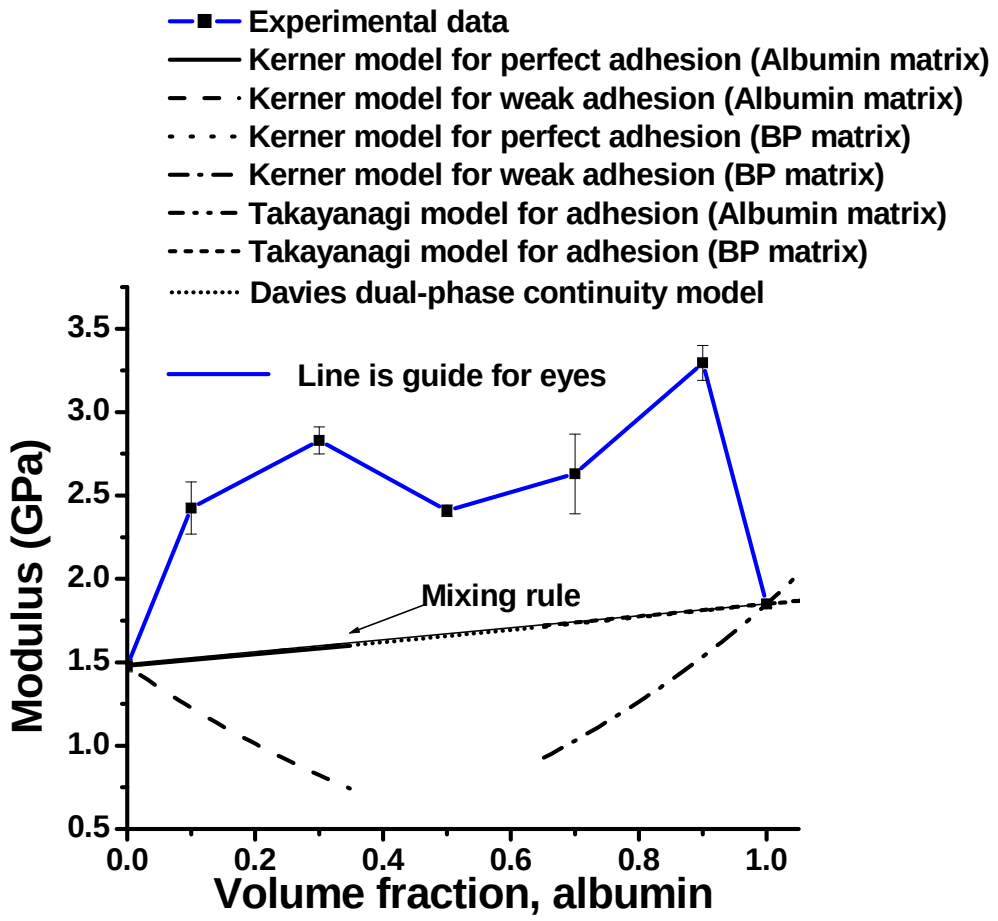

Figure 7.7. Tensile modulus of the plastics from blends of bloodmeal/albumen and their comparison with theoretical models. Note: All samples were molded at a temperature of 150°C and pressure of 20 MPa for 5 minutes, followed by cooling to 70°C under pressure and overnight drying in an oven at 50°C. Note: BP- Bloodmeal Protein.

$$\frac{1}{T_g} = \frac{W_1}{T_{g^1}} + \frac{W_2}{T_{g^2}} \qquad (7.10)$$

where T_{g^1} and T_{g^2} represent the glass-transitions of the component polymers, and W_1

and W_2 the weight fractions.

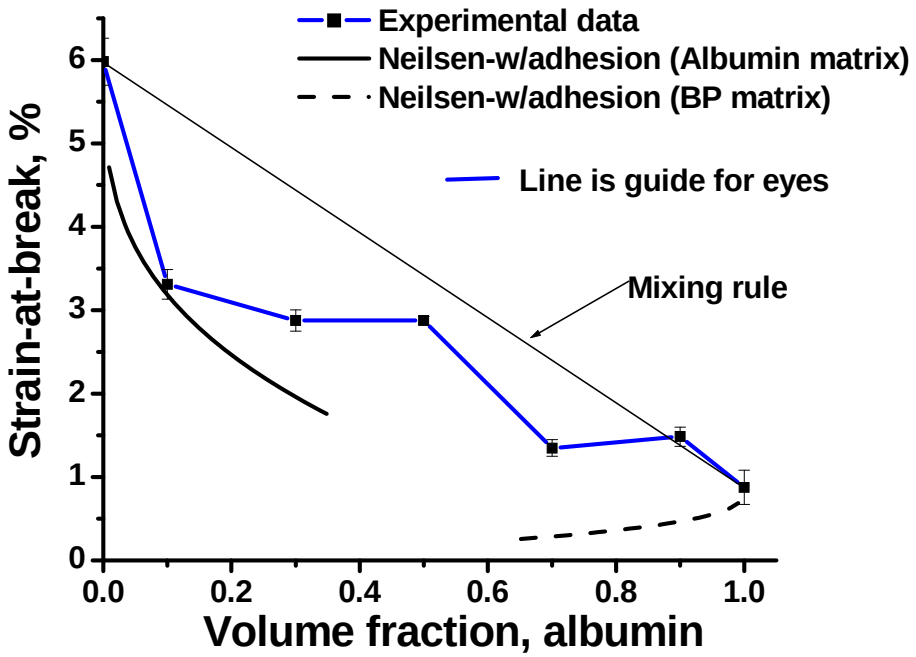

Figure 7.8. Tensile strain at break of the plastics from blends of bloodmeal/albumen and their comparison with theoretical models. Note: All samples were molded at a temperature of 150°C and a pressure of 20 MPa for 5 minutes, followed by cooling to 70°C under pressure and overnight drying in an oven at 50°C. Note: BP- Bloodmeal Protein.

The T_g for mixtures is repeatedly higher than the one predicted by the Fox equation. This result indicates that the level of mobility of protein chains in the blends is lower than in one-component protein plastics. We suggest that this effect originates from strong interaction between the components in the blends.

7.3.4: Technical applications of bloodmeal plastics

Bloodmeal plastics have potential in the development of biodegradable items such as flowerpots, golf tees, and mulch film holding nails. A special mold and plunger from stainless steel was designed to manufacture rectangular bars of bloodmeal plastics using standardized conditions for developing dogbone samples. These bars, strong enough to withstand the stresses of machining, were machined into golf tees, as shown in **Figure 7.11**.

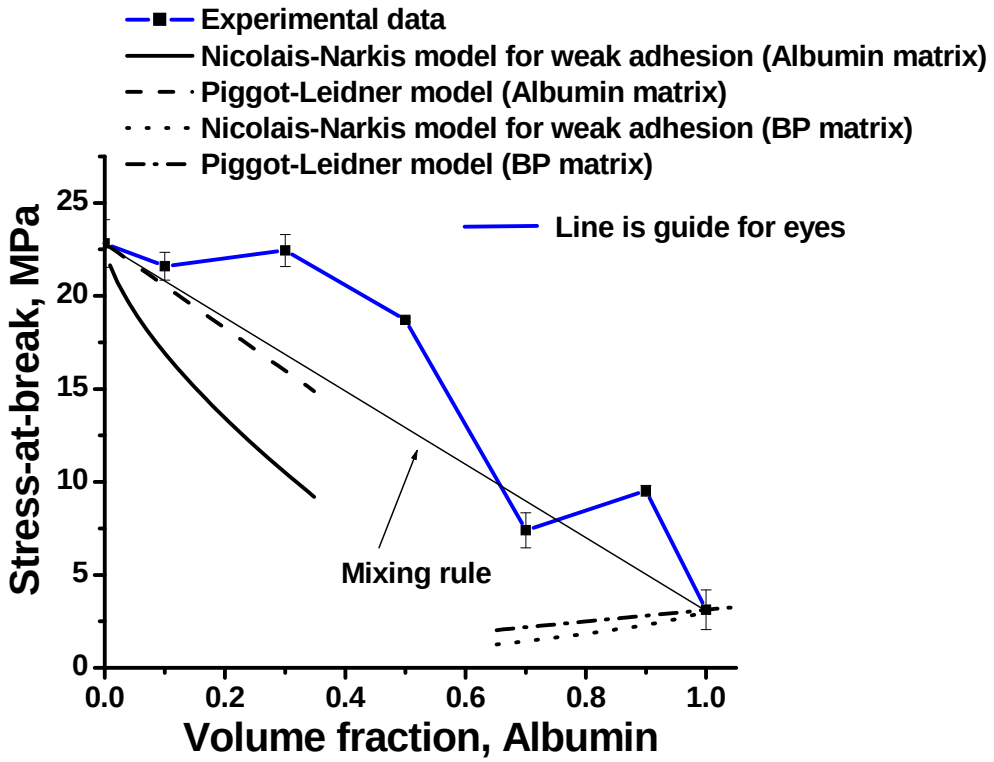

Figure 7.9. Tensile strength of plastics from blends of bloodmeal/albumin and their comparison with theoretical models. Note: All samples were molded at a temperature of 150°C and a pressure of 20 MPa for 5 minutes, followed by cooling to 70°C under pressure and overnight drying in an oven at 50°C. Note: BP- Bloodmeal Protein.

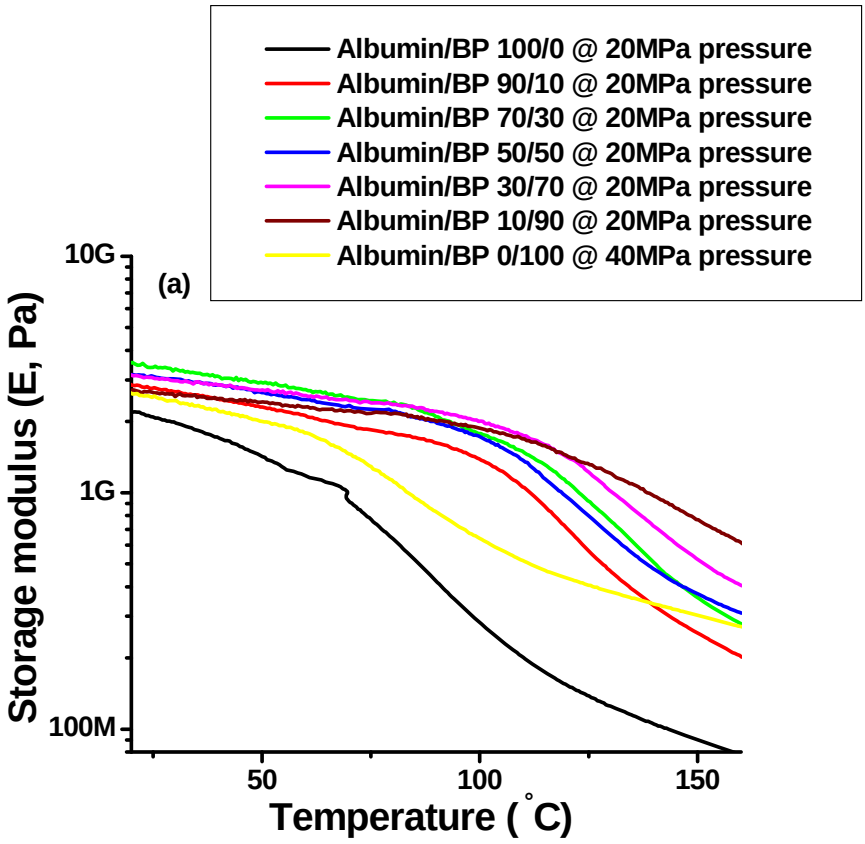

Figure 7.10(a). Dynamic mechanical properties of the plastics from blends of bloodmeal/albumen. All samples were molded at a temperature of 150°C and a pressure of 20MPa for 5 minutes, folloed by cooling to 70°C under pressure and overnight drying in an oven at 50°C: (a) Storage modulus. Note: BP- Bloodmeal Protein.

7.3.5: Preparation of biocomposite from bloodmeal protein and hemp fiber

Natural fibers, available on a renewable basis, have been considered recently as reinforcements in producing various biodegradable composites for improving the mechanical properties of protein-based plastics.[19] Moreover, these fibers have low cost, low density, acceptable mechanical properties, ease of separation, carbon dioxide

sequestration, biodegradability, and thermal and sonic insulation properties. Past studies have shown that these fibers can be processed through such common methods as sheet molding compound (SMC) or bulk molding compound (BMC) into a variety of composites for door panels, car roofs, and grain elevators. **Table 7.1**[1] shows the mechanical properties of various natural fibers, including hemp, for developing biocomposites for technical applications.

Hemp fiber is a natural fiber produced from the stalks of the Cannabis sativa plant and is considered biodegradable. In this part of the research, hemp fibers were milled into short fibers through a Wiley mill having mesh of size 20. These chopped fibers were dried overnight in an oven at 50ºC, and later immersed in a 3%w/v whey solution in water. After 30 minutes of sonication, these fibers were kept in solution for three days. Subsequently, excess liquid was centrifuged, and modified hemp fibers were dried at 50ºC. **Figure 7.12** shows the UV-vis spectra of protein solutions before and after the modification of hemp fibers. Proteins have a characteristic peak at 280nm due to phenyl groups in various amino acid residues. A decrease in the intensity of this peak indicates the protein absorption of hemp fibers. However, the control sample did not show the characteristic peak of protein.

A mixture of bloodmeal/whey modified hemp fibers in 90%:10% w/w was prepared and compression molded using the similar processing conditions of bloodmeal plastic. **Figure 7.13** shows the mechanical properties of the bloodmeal/whey composites, and it can be observed that the addition of whey-modified hemp fibers improved the elongation and reduced the modulus (good for impact and energy absorption

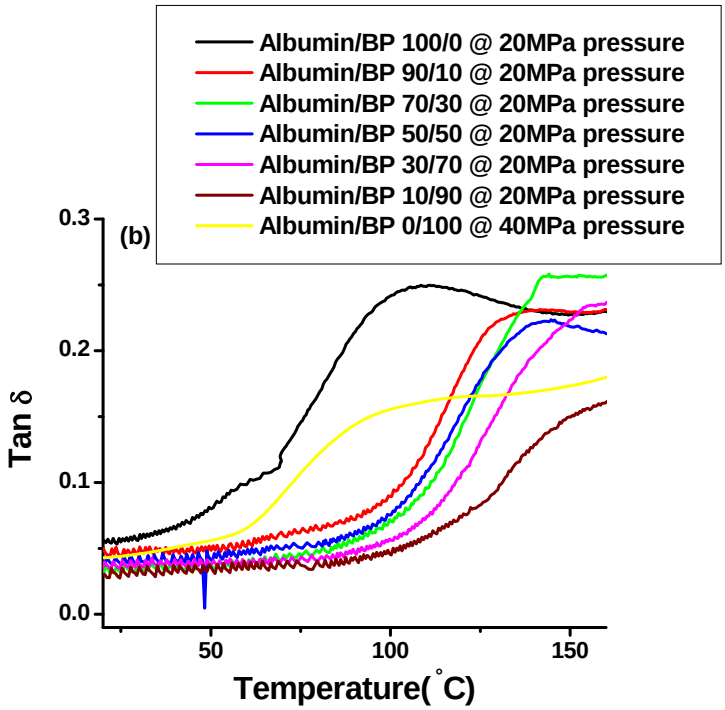

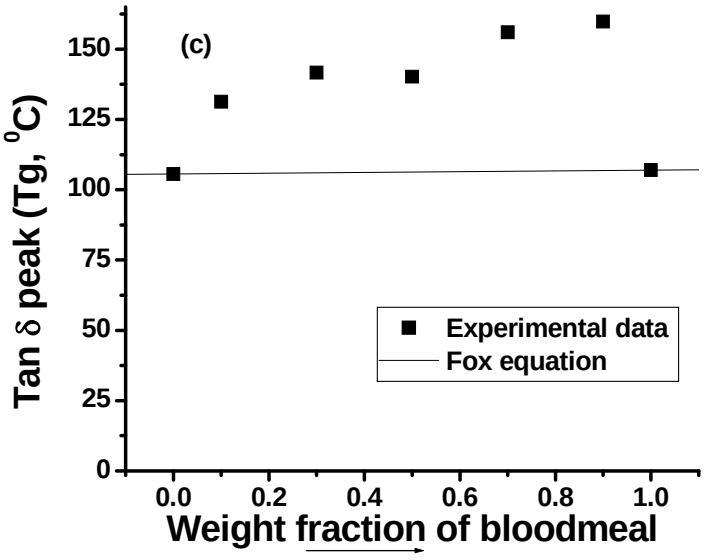

Figure 7.10(b, c). Dynamic properties of the plastics from blends of bloodmeal/albumen, molded at a temperature of 150°C nd a pressure of 20MPa for 5 minutes, followed by cooling to 70°C and overnight conditioning at 50°C: (b) Loss factor, (c) Tg.

Figure 7.11. Different machined products from the bar of bloodmeal plastics.

Table 7.1. Mechanical properties of vegetable and synthetic fibers.[1]

Fiber	**Density (g/cm^3)**	**Elongation (%)**	**Strength (MPa)**	**Modulus (GPa)**
Cotton	1.5-1.6	7.0-8.0	287-597	5.5-12.6
Indian grass	1.25		264	28
Hemp	1.29	1.6	695	42-70
Ramie	-	3.6-3.8	400-938	61.4-128
Sisal	1.5	2.0-2.5	511-635	9.4-22.0
Coir	1.2	30.0	175	4.0-6.0
Kenaf	1.4	-	284-800	21-60
Henequen	1.57	-	372	10
Pineapple leaf fiber	1.44	-	413-1627	35-83
Jute	1.3-1.45	1.5-1.8	393-773	13-27
Flax	1.5	2.7-3.2	345-1100	28-80
Carbon (standard)	1.4	1.4-1.8	4000	230.0-240.0
Aramid (normal)	1.4	3.3-3.7	3000-3150	63.0-67.0
E-glass	2.5	2.5	2000-35000	70

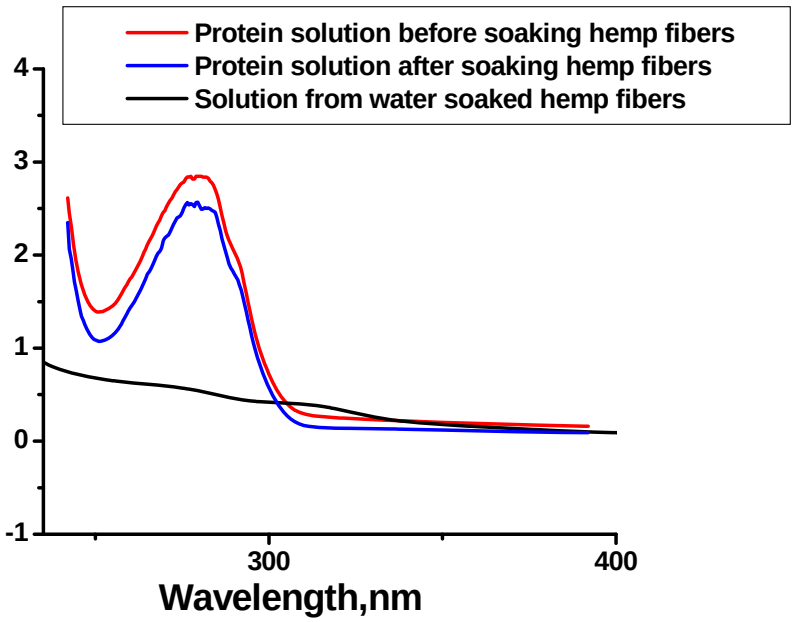

Figure 7.12. UV-vis spectra of whey protein solution before and after soaking hemp fibers.

applications) compared to neat bloodmeal plastic or bloodmeal plastic reinforced with unmodified hemp fibers. This may be attributed to protein-protein interaction at the interfaces of modified hemp fibers and bloodmeal matrix. Therefore, tensile strength and elongation of the resulting composites was higher than the composites reinforced with unmodified hemp fibers.

7.4: Conclusions

Plastic samples from partially denatured bloodmeal protein were successfully produced through a compression-molding process. These plastics exhibited comparable modulus and lower strength and elongation than conventional synthetic plastics such as

polystyrene and polymethylmethacrylate. This is a common phenomenon for plastics

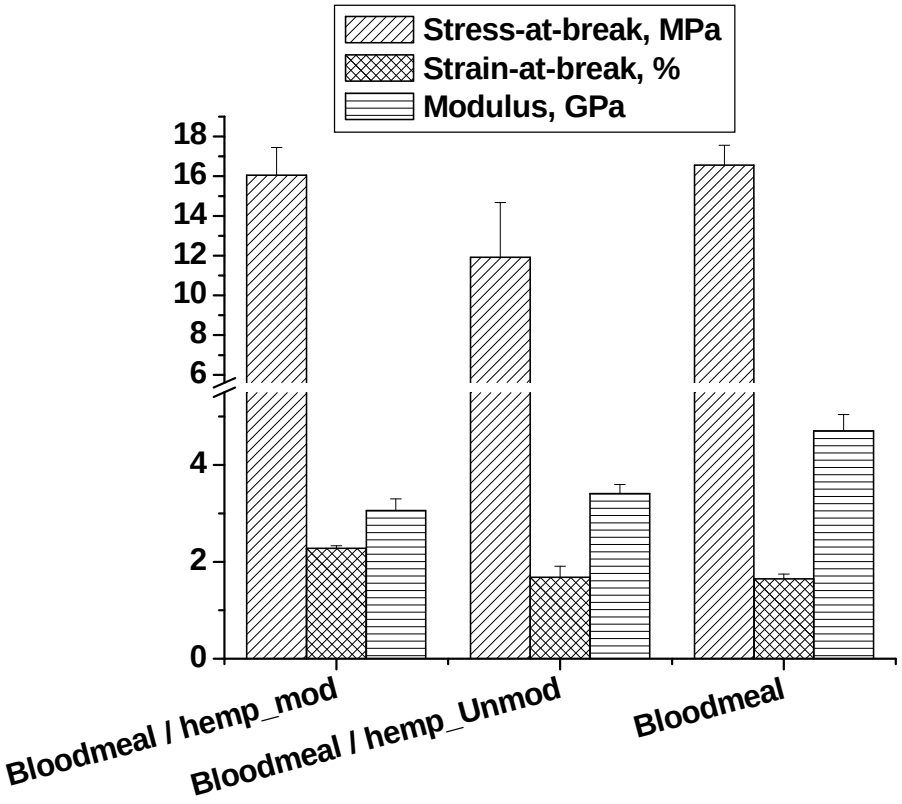

Figure 7.13. Mechanical properties of bloodmeal composites reinforced with hemp fibers (10%wt.-), molded at a temperature of 180°C and a pressure of 40MPa for 5 minutes, followed by cooling to 70°C under pressure.

produced from animal and plant proteins. Plastic forming conditions for undenatured animal proteins, chicken egg whites albumin and whey, were also investigated for the development of plastics from blends of undenatured and bloodmeal proteins. The resulting plastic samples, made from these biomacromolecular blends, exhibited improved mechanical properties as compared to neat bloodmeal plastics. Extensibility,

tensile strength, and stiffness from the mechanical analysis of bloodmeal/albumin blends at various volume fractions were interpreted in terms of theoretical models and showed better adhesion. Bloodmeal protein also showed potential in the development of composites reinforced with hemp fibers.

7.5: References

[1] Mohanty, A. K., Misra, M., and Hinrichsen, G., Macromol. Mater. Eng. (2000), 276/277, 1.

[2] Villar, M. A., Thomas, E. L., and Armstrong, R. C., Polymer (1995), 36 , 1869.

[3] Salmoral, E. M., Gonzalez, M. E., Mariscal, M. P., and Medina, L. F., Ind. Crops Prod. (2000), 11, 227.

[4] Lim, L.T., Mine, Y., and Tung, M. A., J. Agric. Food Chem. (1998), 46, 4022.

[5] de Graaf, L. A., and Kolster, P., Macromol. Symp., 1998, 127, 51.

[6] Paetau, I., Chen, C.- Z., and Jane, J., Ind. Eng. Chem. Res. (1994), 33, 1821.

[7] Mo, X., Sun, X., and Wang, Y. J., J. Appl. Polym. Sci. (1999), 73, 2595.

[8] Wang, C., Carriere, C. J., and Willett, J. L., J. Polym. Sci.: Part B: Polym. Phy., 40, 2324.

[9] Pickering, K. L., Verbeek, C. J. R., Viljoen, C., and Everett, L., Plastic Material, World Intellectual Property Organization, WO/2008/063088.

[10] http://www.theengineer.co.uk/Articles/306409/Waste+into+plastic.htm.

[11] Meeker, D. L., and Hamilton, C. R. In Essential Rendering: All About The Animal By-products Industry (2006), Meeker, D. L., Ed., Kirby Lithographic Company, Inc.: Arlington, Chap.1.

[12] Chowdry, B., and Leharne, S. J., Chem. Educ. (1997), 74, 236.

[13] Liu, D., and Zhang, L. Macromol. Mater. Eng. (2006), 291, 820.

[14] Koning, C., Duin, M. V., Pagnoulle, C., and Jerome, R., Prog. Polym. Sci. (1998), 23, 707.

[15] Kerner, E. H. Proc.Phys.Soc. (1956), 69B, 808.

[16] Sperling, L. H. Polymeric Multicomponent Materials (1997), John Wiley & Sons, Inc.: New York.

[17] Nielsen, L. E. Mechanical Properties of Polymers and Composites (1974), Marcel Dekker: New York.

[18] Nicolais, L., and Narkis, M., Polym. Eng. Sci. (1971), 1, 194.

[19] Liu, W., Misra, M., Askeland, P., Drzal, L. T., and Mohanty, A. K., Polymer (2005), 46, 2710.

CHAPTER 8

PLASTICS FROM EPOXIDIZED VEGETABLE OIL VIA THERMAL AND ULTRASONIC CURING

8.1: Introduction

Biodegradable materials are receiving increased attention due to their availability on a renewable basis and environmental advantages. The depletion of non-renewable resources and the dependence on petroleum-based polymers has caused growing urgency to develop and commercialize new environmentally compatible biobased polymers.[1] In this context, natural oils from agricultural resources, such as linseed oil and soybean oil, are useful in polymer material synthesis.[2] These natural oils can be functionalized by epoxidation with organic peracids or H_2O_2 (hydrogen peroxide), and are considered an inexpensive renewable material for the generation of thermoset epoxy resins.[3]

Thermoset composites from epoxy resins are often used in high-performance structural applications because they generally possess excellent properties such as toughness and dimensional stability.[4,5] These resins are generally used as the binding agent, offering attractive combinations of strength, ease of processing, and cost. For example, epoxy resin is used as the binder in composites reinforced with carbon fibers for aerospace applications.[6] To acquire the desired mechanical performance, epoxy-based composites need to be heated (curing process) in an autoclave, a pressurized vessel, throughout the curing procedure; this adds to the cost of manufacturing.[6,7] In addition, and equally significantly, the autoclave process can limit the size and shape of the parts,

and can affect factory logistics and manufacturing lead times. This motivation is the major driving force for the intense interest in alternative methods and procedures for manufacturing these composites. As a result, alternative techniques such as ultrasonic heating, radio-frequency heating, and microwave heating have been studied.[8,9,10]

The traditional autoclave process of epoxy curing employs heating from the outside-in and relies on thermal conduction; the heating time is strongly dependent on the geometry and the dimensions of the structure.[8] Research has been conducted to investigate several unconventional epoxy-curing methods to accelerate the curing process and reduce the total curing time.[11,12] These processes can be classified as radiation curing using UV, gamma rays and electron beams; induction curing; dielectric curing using radio frequency and microwaves; and ultrasonic curing. However, ultrasonic curing, due to the heat generated within the sample by intermolecular friction, may be distinguished from the other curing techniques due to its beneficial non-thermal effects.[9,13,14,15,16,17,18]

Ultrasonic treatment (besides volumetric heating) leads to the higher mobility of the epoxide oligomeric molecules during the curing process, an increase in the homogeneity of the curing composition, a decrease in the composites' porosity due to removal of the air bubbles, an improvement in resin and fiber (filler) interactions at the interface because of better wettability, an increase in contact area, and a decrease in border defects. In addition, other technological advantages of ultrasonic energy have been reported:[15] (a) reduced resin viscosity exhibits good consolidation without resin advancement; (b) the time to finish curing is decreased by at least a factor of two; and (c)

the sonic energy adsorption tends to be self-limiting, reducing the risk of damage due to overcuring.

Curing agents (hardeners) have an important role in determining the storage and handling requirements of epoxy formulations. Various curing agents such as amines, anhydrides and dicyandiamide (DDA), a latent curing agent, have been used for epoxy systems in adhesives, composites, printed circuit boards, and powder coatings.[19] It has been found that a one-part epoxy system, consisting of DGEBA (Diglycidyl Ether of Bisphenol A) and DDA, can be cured at a temperature of 180ºC-200ºC.[20] However, the addition of accelerators such as aryldimethyl urea compounds (e.g., Monuron, Diuron, Fenuron, and TDI-uron) would allow this system to cure at a temperature of less than 130ºC.[21] In a study by Laliberte et al.[20] using DSC, the epoxy/DDA/Monuron system exhibited a lower activation energy than both the epoxy/DDA and epoxy/Monuron systems, primarily due to the formation of the by-product dimethylamine.

During polymerization or the curing reaction, epoxy groups open due to the active hydrogen of the curing agents, resulting in a cross-linked network structure. Several techniques, in addition to the traditional DSC technique, have been studied to determine the degree of epoxy curing; these techniques include the NIR (near-infrared) and MIR (mid-infrared),[22] HPLC (high-performance-liquid-chromatography), [22] dielectric, raman, [23] and gravimetric methods.[24]

Various natural epoxies, such as ELO (epoxidized linseed oil) and ESO (epoxidized soybean oil), have been used for coatings and printing inks and as an additive in thermoplastics to improve stability and flexibility, respectively.[1] Vegetable oil based

epoxy is composed of fatty acid residues, which can be readily attacked by lipase secreting bacteria and fungi, allowing them to biodegrade.[25]

Various curing agents, such as anhydrides[2,26,27] and amines are available to cure epoxidized vegetable oils, but are toxic, require long curing processes at high temperatures, and have low heat resistance.[3] Moreover, stochiometric ratios of these resins and curing agents are required for acquiring the desired properties.[28] Recently, Kim et al.[29] have synthesized latent catalytic initiator benzylpyrazinium salts with complex metal halide anions, which were found to be effective curing agents for various petroleum-based epoxy resin systems. Park et al.[3] also used only 1% N-benzyl pyrazinium hexafluoroantimonate (BPH) to cure epoxy resin systems, which exhibited improved thermal-oxidative resistance and mechanical properties. They also showed that this curing agent did not propagate the reaction at a lower temperature (50°C), compared to rapid conversion at a higher temperature (180°C), indicating its latency at room temperature.[30] Therefore, it is expected that the use of this latent catalyst would increase the storage stability and handling of thermosetting epoxy resins. To date, only Lligadas et al.[31] have used a BPH curing agent to develop a bionanocomposite from ELO-polyhedral oligomeric silesequioxane hybrid materials with improved mechanical properties.

However, petroleum-derived epoxy resins are well known for their easy processability, compositional versatility, superior tensile strength, solvent resistance, good heat and chemical resistance; despite these advantages, the costs involved in curing these resins are high. In this respect, epoxidized vegetable oils can replace and/or substitute traditional epoxy resins to produce tougher and flexible crosslinked material.[1]

For example, Miyagawa et al.[26] used nanoscale reinforcements from organoclay and alumina nanowhiskers with ELO or ESO in conjunction with synthetic epoxy, producing a tough material that could be applicable for automotive, electronic packaging and aeronautic structures. In another study, Crivello et al.[32] used a photochemical route to fabricate fiberglass-reinforced composites using the ultraviolet and visible (solar) irradiation of epoxidized vegetable oils. Bouquillon[27] used natural hemp fibers to develop composites from thermosetting vegetable oil-based resin.

The primary objective of this phase of research was to investigate the thermal and ultrasonic curing of natural, vegetable-based epoxy in order to determine its plastic forming ability using the least amount of an appropriate curing agent. Moreover, to understand these curing methods, a one-part model epoxy system, consisting of a latent curing agent, was studied, including the optimization of the ultrasonic curing variables, resulting in the development of rapid and cost effective out-of-autoclave composites. The other important objective was to develop a chemical model for differentiating the thermal and non-thermal effects of ultrasonic curing. Another objective was to investigate the effectiveness of FTIR as a rapid technique for determining the degree of curing.

8.2: Materials

A one-part epoxy system was used to study the ultrasonic curing process. Epoxy adhesive system 2214 was supplied by 3M. This resin was mainly composed of the bi-functional epoxy diglycidyl ether of bisphenol-A (DGEBA), the curing agent dicyandiamide (DDA) and the accelerator 3-(p-chloro phenyl)-1,1-dimethyl urea

(Monuron). The chemical structures of the Epoxy/DDA/Monuron system are shown in **Figure 8.1**.

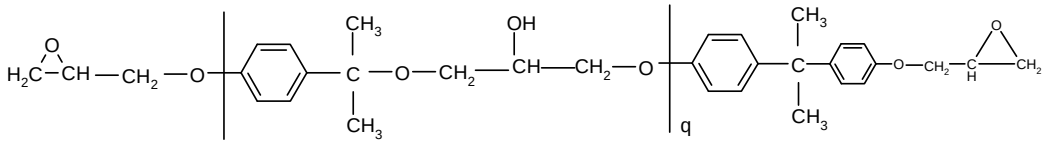

Diglycidyl ether of bisphenol A (DGEBA)

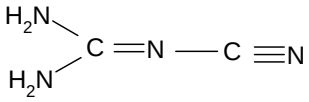

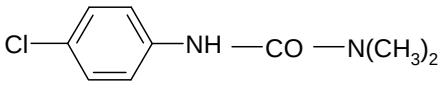

Dicyandiamide (DDA) 3-(p-chlorophenyl)-1, 1-dimethylurea (Monuron)

Figure 8.1. Chemical structures of the Epoxy/DDA/Monuron system.

Epoxidized vegetable oils ESO and ELO, curing agent BPH and thixotropic agent Aerosil R805 were used to develop plastic through thermal and ultrasonic curing methods. ELO and ESO are mainly composed of triglyceride molecules containing three fatty acid chains joined by a glycerol center. The fatty acid chains have 0-3 double bonds and vary in length from 16-22 carbon atoms.[33] The typical chemical structure of an epoxidized oil is shown in **Figure 8.2.**

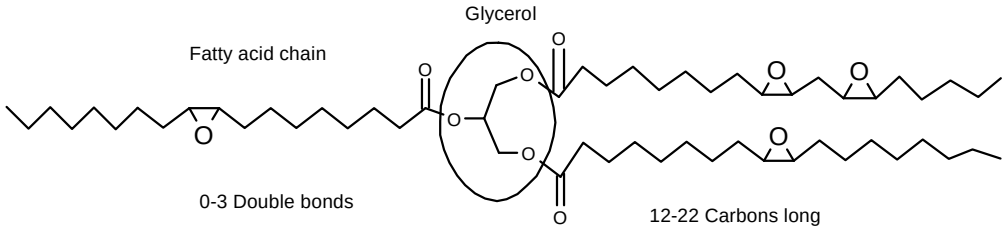

Figure 8.2. General chemical structure of epoxidized oil.

Epoxidized soybean oil, Vikoflex® 7170, and epoxidized linseed oil, Vikoflex® 7190,

were supplied by Arkema, Inc., MN. The physical and chemical properties of these epoxidized oils are given in **Table 8.1.**[34]

Table 8.1 Physical and chemical properties ESO and ELO.[34]

Properties	**ELO7190**	**ESO7170**
Appearance/odor	Light yellow viscous liquid, slight vegetable odor	Light yellow viscous liquid, slight vegetable odor
Sp. Gravity	1.03	0.994
Vapor pressure	<0.1mmHG@25C	Very low
Boiling point	decomposes	decomposes
Freezing point	0°C	0°C
Solubility in water	0.011%by wt	Insoluble
Oxirane %	9.18	7.02
Iodine value	3	0.89
Acid value	0.24	0.12
Viscosity stokes @ 25C (Cp)	114	4.1
Molecular weight	~950 g/mol	~900-1000 g/mol
EEW (epoxide equivalent weight)	176	227-231

For synthesis of the latent curing agent BPH (N-Benzylpyrazinium Hexafluoroantimonate), a known method from the literature[29] was used. Dr. Viktor Klep assisted in the synthesis. Benzyl bromide, pyrazine, and sodium hexafluoroantimonate (technical grade) were supplied by Sigma-Aldrich; these were not purified further. Pyrazine (11.9g) was mixed with benzyl bromide (220g) at room temperature. The

mixture was stirred for 48 h and the precipitated product was filtered and rinsed with toluene several times and left in a fume hood to remove any residual benzyl bromide via evaporation. The aqueous solution of this precipitate was mixed with an aqueous solution of sodium hexafluoroanitmonate (0.15%w/v), which resulted in a white precipitation. This white precipitation was filtered, vacuumed, rinsed several times with ether, and recrystallized from methanol to yield 25g of white crystals of BPH. The chemical structure of BPH is shown in **Figure 8.3.** It illustrates a melting endothermic peak at 136°C, which is in close agreement with Kim et al.'s [29,35] work. Aerosil R805 was supplied by Evonik Degussa.

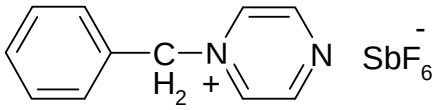

Figure 8.3. Chemical structure of BPH (N-Benzylpyrazinium Hexafluoroantimonate).

8.3: Results and discussion

8.3.1: Thermal curing of one-part model epoxy

Traditionally, DSC has been considered an effective off-line tool to determine the extent of curing for thermoset polymers. To determine the curing kinetics, samples were thermally cured in an oven at a temperature of 100ºC (an optimal preheating temperature for ultrasonic curing, as discussed below) for different time intervals. The residual heat of curing, and thereby degree of curing from **Equation 8.1,** was determined using DSC, as represented in **Figure 8.4.** A latent period of 20 minutes for activating the DDA was

observed during curing. However, after 40 minutes into the activation period, a rapid acceleration in the curing process was observed.

The extent of curing can also be substantiated by the decreased intensity of the epoxy band (916 cm^{-1}) and the increased intensity of the hydroxyl band (3364 cm^{-1}) due to the opening of epoxide groups identified in the FTIR analysis of uncured and fully cured samples, as shown in **Figure 8.5**. [19,36,37,38] Degree of curing (disappearance of the epoxy band) from FTIR was determined using **Equation 8.1**:[37]

$$\text{Degree of cure (diminishing of epoxy group)} = \alpha = 1 - \frac{\left(A_{epoxy,t}\right)\left(A_{ref,0}\right)}{\left(A_{epoxy,0}\right)\left(A_{ref,t}\right)} \qquad (8.1)$$

where A_{epoxy} represents the area under the Gaussian peak of the epoxy fundamental band at 916 cm^{-1}, and A_{ref} the area under the Gaussian peak of the phenyl group (reference) band at 831cm^{-1}.[19,37,39] The degree of curing assessed by both DSC and FTIR are compared in **Figure 8.6**. It can be observed that there is a good correlation between the results from these techniques. Thus, both techniques can be used for evaluating the degree of epoxy curing.

8.3.2: Ultrasonic curing of one-part model epoxy

To achieve rapid curing through the ultrasonic curing process, different variables such as wave amplitude, pulse duration and preheating temperature were investigated and optimized. The amplitude of the horn vibration (or wave vibration) determines the horn output power. Ultrasonic energy may be applied continuously or in pulse mode, influencing the amount of energy put into the epoxy system. Kwan and Benatar[13] used

pulsed ultrasound with a two second ON/OFF pulse condition.

The preheating temperature depends on the latency of the curing agent of a one-part epoxy system, and even with ultrasonic curing, there is a need of some initial energy to activate the curing agents, which results in the propagation of curing reaction. First, trials were conducted to achieve optimal conditions of ultrasonic curing in a shorter amount of time. **Figure 8.7** shows the temperature history of the epoxy system over a period of 20 minutes cured by the pulsed-ultrasound under different pulse (one second) durations such as 10%, 30% and 50%, while keeping the amplitude and the preheating temperature constant at 21μm and 100ºC, respectively. It can be observed from **Figures 8.7 and 8.8** that with 10% and 30% pulses, the temperature rose to approximately 100ºC, achieving a maximum degree of curing of 46%. In contrast, a 50% pulse raised the temperature to approximately 150ºC and produced full curing. Therefore, a pulsed ultrasound was superior to a continuous one.

Benatar[8], through a study of the ultrasonic curing of a two-part epoxy system, also observed the positive effect of pulsed mode rather than continuous mode of ultrasonic curing. In addition, increasing the pulse to more than 50% (e.g. 60%) caused damage to the samples due to the excessive accumulation of ultrasonic energy. The preheating temperature is also important in activating and propagating the curing reaction. **Figures 8.9 (a, b)** show the temperature history and corresponding degree of curing for different preheating temperatures under a constant amplitude of 21μm and a pulse duration of 50%.

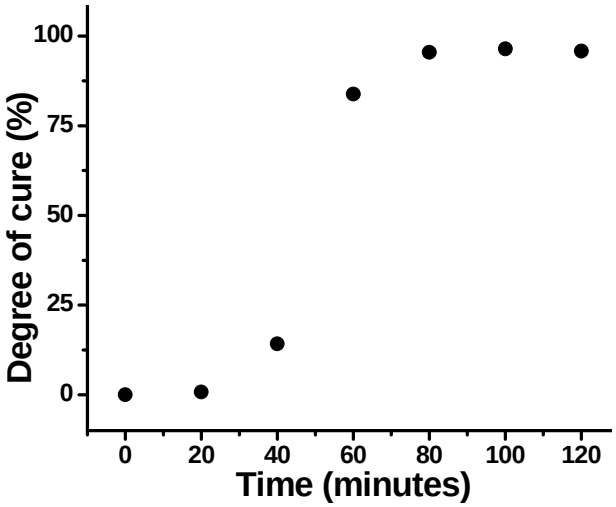

Figure 8.4. Epoxy curing from DSC analysis for an isothermal curing at 100ºC in an oven.

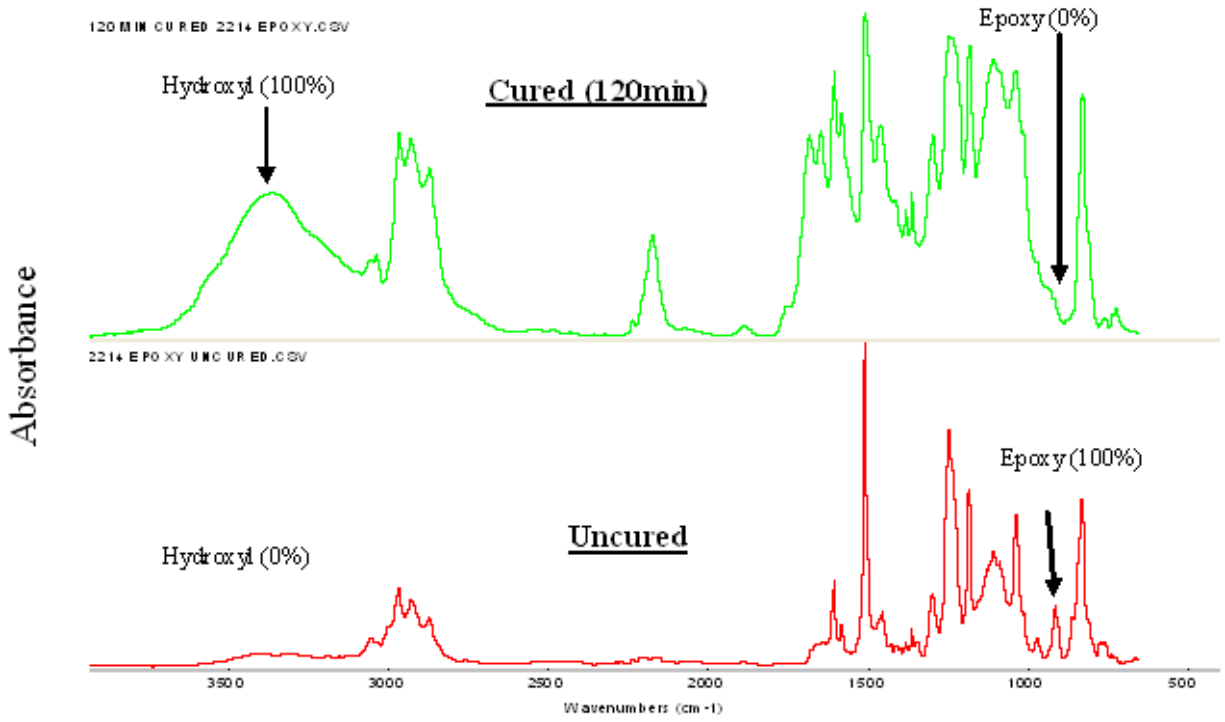

Figure 8.5. FTIR spectra for epoxy curing for an isothermal curing at 100ºC in an oven.

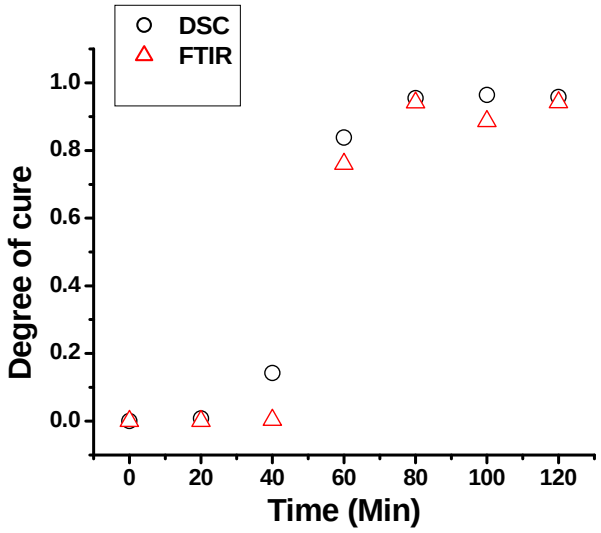

Figure 8.6. Comparison of degree of curing from FTIR due to epoxy band disappearance and from DSC for isothermal curing at 100ºC in an oven.

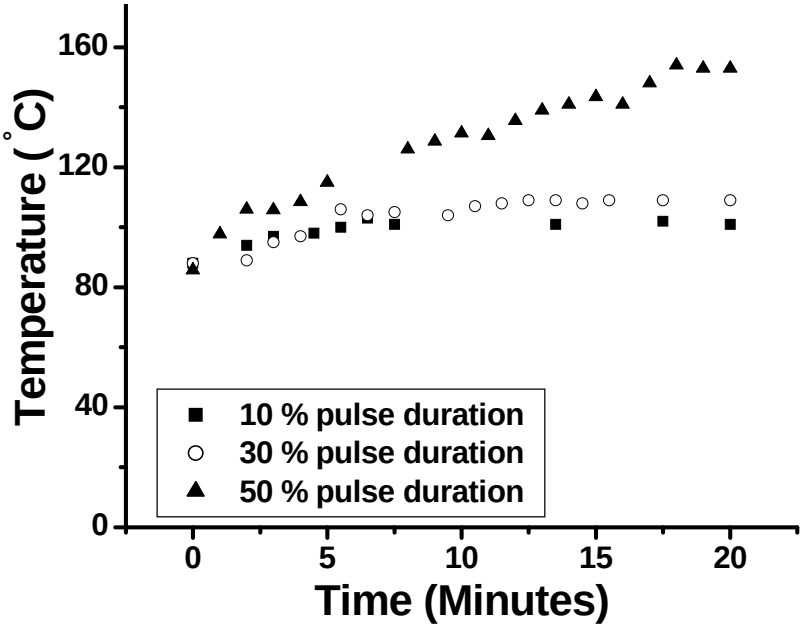

Figure 8.7. Temperature profile of the one-part model epoxy system at various pulse durations.

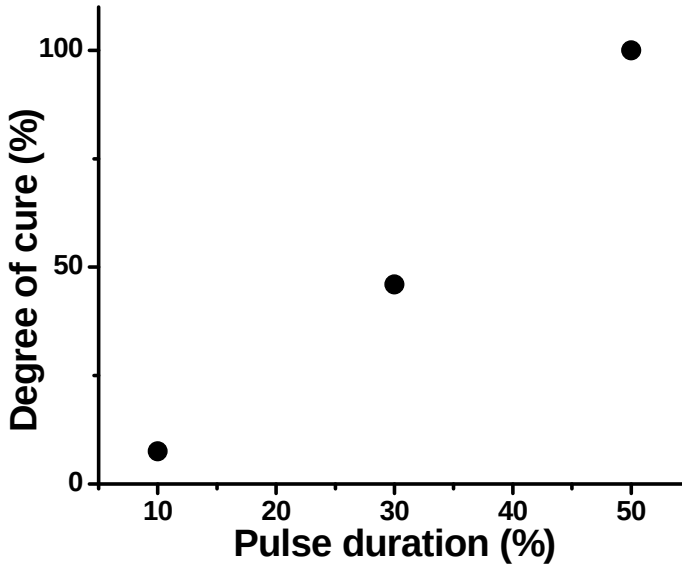

Figure 8.8. Degree of cure with different pulse durations for 20 minutes ultrasonic curing.

It can be seen that at a low preheating temperature of 40°C, ultrasonic energy could not produce sufficient activation energy to begin the curing reaction. However, at a preheating temperature of 60°C, the temperature during curing did not rise when the ultrasound was applied. The sample could achieve a degree of curing of 30%, possibly due to non-thermal effects such as streaming from the cavitations, lower viscosity, and a higher diffusion rate. At a preheating temperature of 80°C, the application of ultrasound raised the temperature to 120°C and a degree of curing of 90% was achieved due to combined thermal and non-thermal effects of ultrasonic curing. However, at a preheating temperature of 100°C, the ultrasonic treatment raised the temperature to approximately 150°C from the curing reaction, producing full curing. Therefore, the samples were ultrasonically cured under optimal conditions (i.e., amplitude--21μm, pulse duration--

50%, and preheating temperature--100ºC) to investigate the curing kinetics.

The resulting degree of curing at different time intervals is shown in **Figure 8.10**. A short latent period of 5 minutes, compared to 20 minutes with thermal curing, was observed due to combinations of the thermal (ultrasonic heating) and non-thermal effects of ultrasonic curing. It can be seen that full curing was achieved in 20 minutes, compared with the 120 minutes necessary for thermal curing. Moreover, a micrograph of the fully ultrasonically cured sample from SEM (**Figure 8.11**) did not reveal porosity, indicating a well consolidated material.

FTIR was conducted to observe the curing trend, as this analysis is faster than traditional DSC analysis. FTIR analyses of samples cured at various time intervals are shown in **Figure 8.12**. It can be seen that ultrasonic treatment over time caused a change in the epoxy (916 cm^{-1}) and hydroxyl (3364 cm^{-1}) bands, while not affecting the band due to phenyl groups (831 cm^{-1}). Therefore, the progression of curing can be confirmed by the decreased intensity of the epoxy band (916 cm^{-1}) and the increased intensity of the hydroxyl band (3364 cm^{-1}) due to the opening of epoxide groups.[19]

8.3.3: Thermal and non-thermal effects of ultrasonic curing

The interaction of the sonic energy with the uncured resins can produce both thermal and non-thermal effects due to micro-mixing, lower viscosity and higher diffusion rates. For instance, Kwan and Benatar[13]studied the reaction kinetics of a two-part structural epoxy adhesive through DSC analysis. They developed a four parametric semi-empirical equation to separate the non-thermal effects resulting from ultrasonic

vibration, and the thermal effects resulting from ultrasonic heating. They demonstrated that in the initial 50 seconds of pulsed ultrasonic curing (both non-thermal and thermal), the curing was three times higher than with ultrasonic heating alone. The degree of curing was determined using the modified autocatalytic equation by plugging in the temperature history. This difference between thermal and non-thermal effects decreased to a minimum as the time increased above 100 seconds. The DSC technique in the dynamic and isothermal modes has been used to study the kinetics of epoxy curing.[40] If the curing reaction is the only thermal event, then the rate of heat released during curing $\left(\frac{dH}{dt}\right)$ will be directly proportional to the rate of reaction, $\frac{dc}{dt}$ by **Equation 8.2:**

$$\frac{dc}{dt} = \frac{1}{\Delta H}\left(\frac{dH}{dt}\right) \tag{8.2}$$

where c represents the extent of reaction, (ΔH_t) the heat evolved at a certain time, and (ΔH) the total heat of reaction.

Therefore, the DSC technique can be used to determine the curing kinetics of epoxy curing, representing by the nth order (**Equation 8.3**) or the autocatalytic form (**Equation 8.4**), respectively:

$$\frac{dc}{dt} = k(1-c)^n \tag{8.3}$$

$$\frac{dc}{dt} = k(1-c)^n c^m \tag{8.4}$$

where k represents the Arrhenius rate constant, and m and n the orders of the reaction.

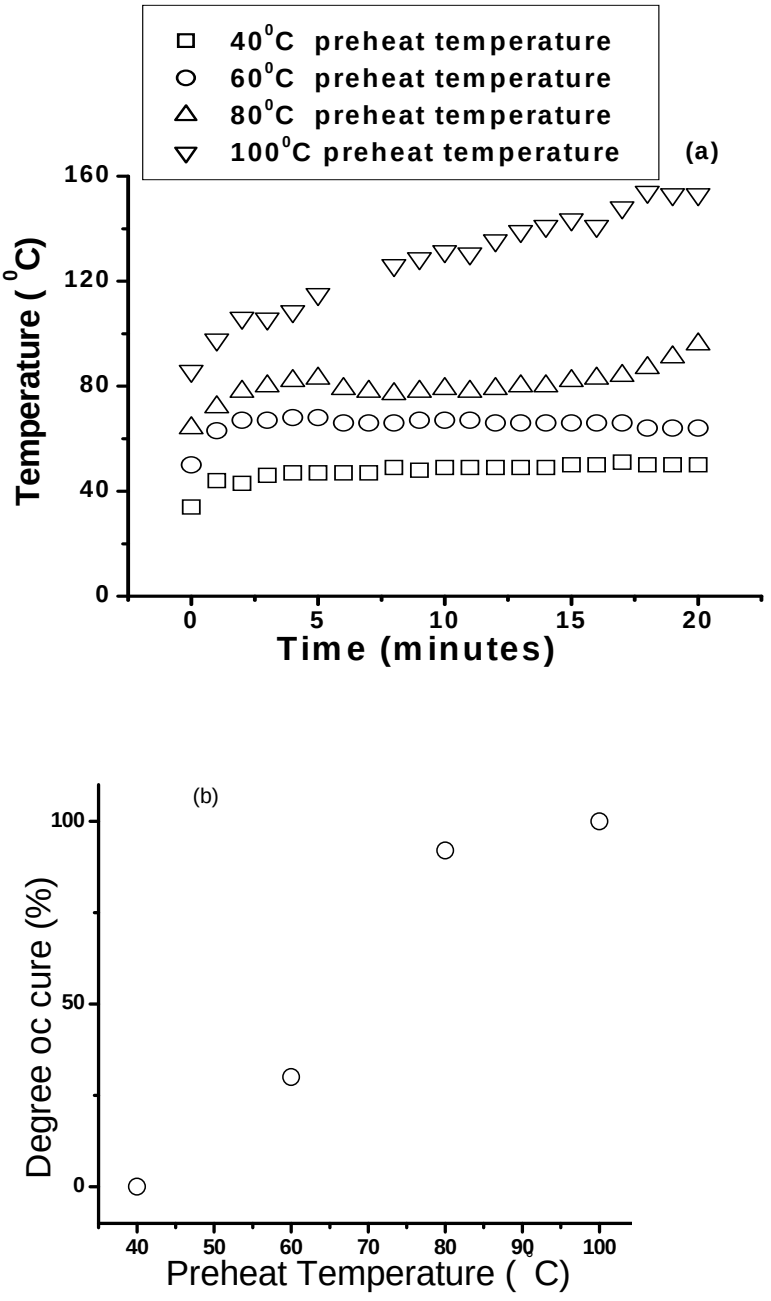

Figure 8.9. (a) Temperature history of one-part model epoxy system at different preheating temperatures for 20 minutes of ultrasonic curing, (b) Corresponding degree of curing.

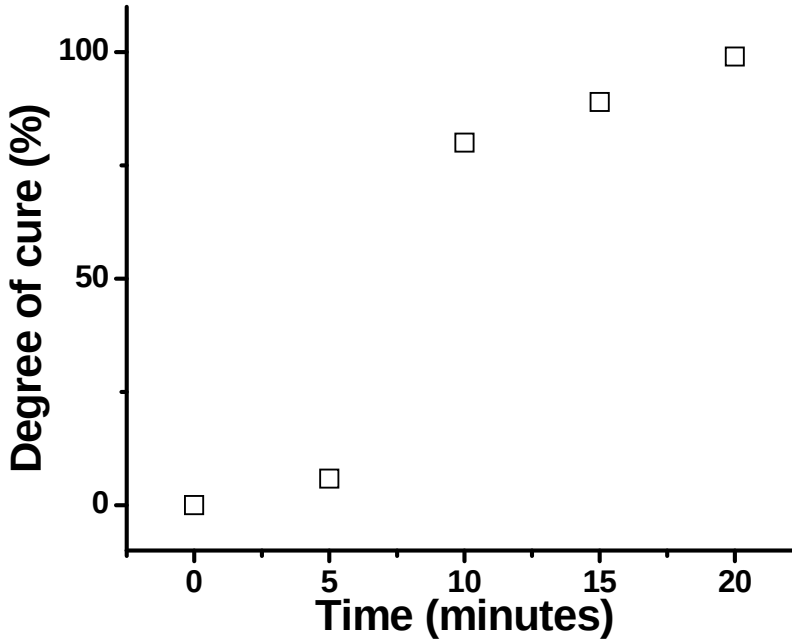

Figure 8.10. The degree of cure for the one-part model epoxy system cured using the pulsed ultrasonic process.

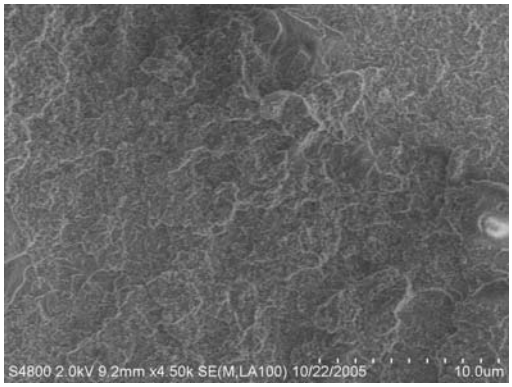

Figure 8.11. SEM micrograph of fully ultrasonically cured sample.

According to n^{th} order, the reaction rate is maximal at time t=0, while for the autocatalytic form, it is maximal at some intermediate conversion, but the initial rate is zero.[40]

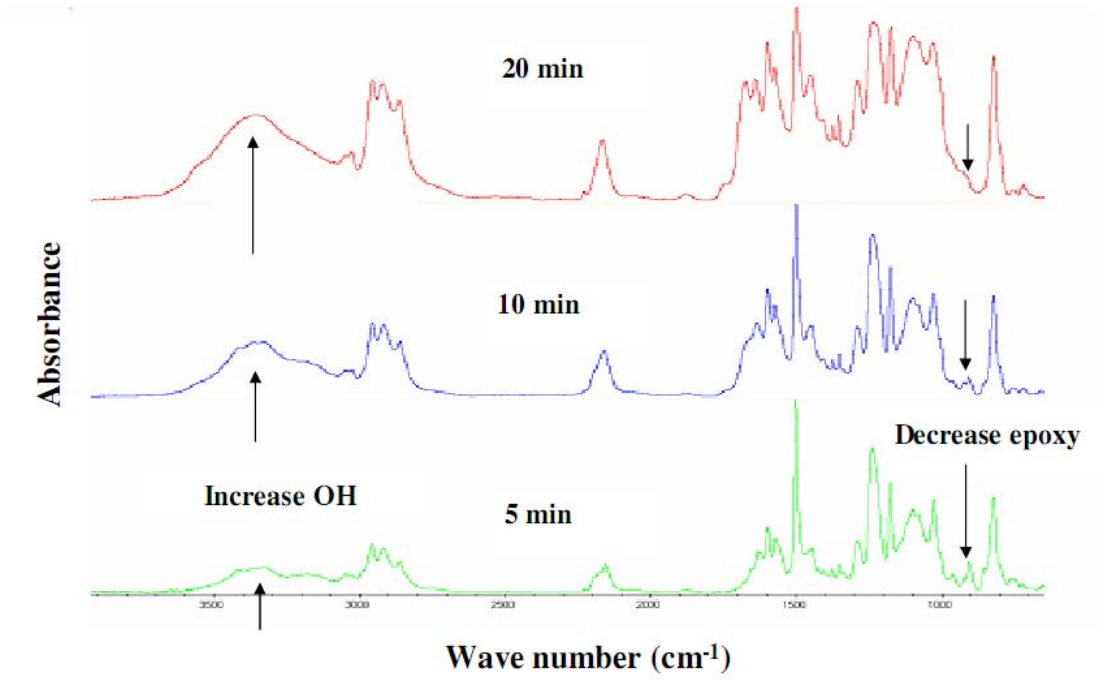

Figure 8.12. Mid-infrared spectra for one-part model epoxy, cured using pulsed ultrasonic curing (amplitude-21μm; pulse duration=50%) for different times.

To differentiate between the non-thermal and thermal effects of ultrasonic curing, isothermal kinetics using DSC was conducted to develop the chemical model. A study by Kamal[41] showed that during the isothermal curing of an epoxy system, the curing reaction exhibited a marked autocatalytic behavior. Kwan and Benatar[13] stated that the high and rapidly changing heat rate produced by ultrasonic curing makes it impossible to simulate the heating profile by conventional heating methods. Therefore, they developed a chemical model through isothermal studies in DSC to determine the thermal effect on the reaction kinetics of epoxy. **Figure 8.13** shows the typical thermograph of isothermal curing from the DSC instrument, comprising an initial baseline, an exothermic peak, and a final baseline. When the initial baseline and final baseline are at the same level, the

curing is assumed to be complete.

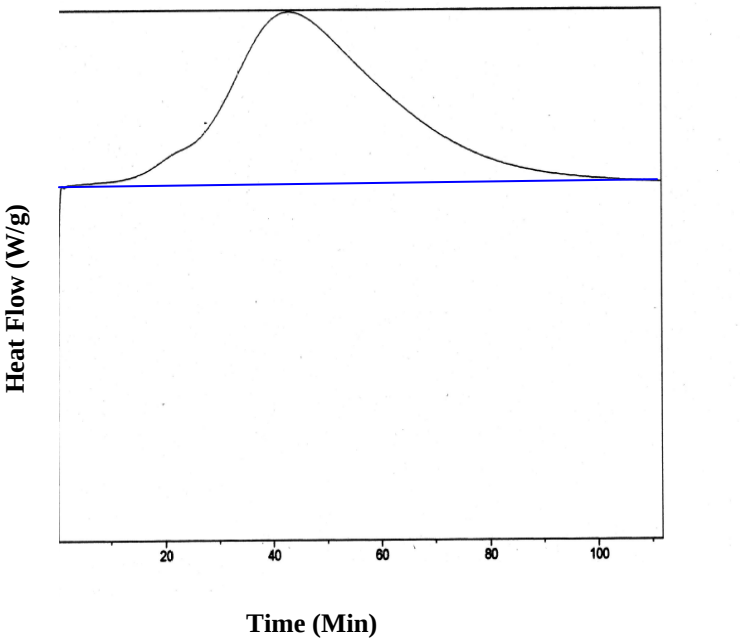

Figure 8.13. Isothermal curing of the one-part model epoxy system at 100ºC.

An isothermal curing study was conducted at various isothermal temperatures such as 100ºC, 115ºC, 125ºC and 135ºC, as these temperatures were observed during ultrasonic curing under optimal conditions. According to **Equation 8.2**, the rate of reaction is proportional to the evolved rate of heat in DSC analysis. Therefore, the reaction rate $(\frac{dc}{dt})$ was determined for different degrees of curing at these isothermal temperatures, as shown in **Figure 8.14**. This graph clearly shows the autocatalytic behavior of epoxy curing, as the reaction rate exhibits the maximum at some intermediate value (approximately 40%) of curing. In addition, the reaction rate is found to increase with

increased isothermal temperature.

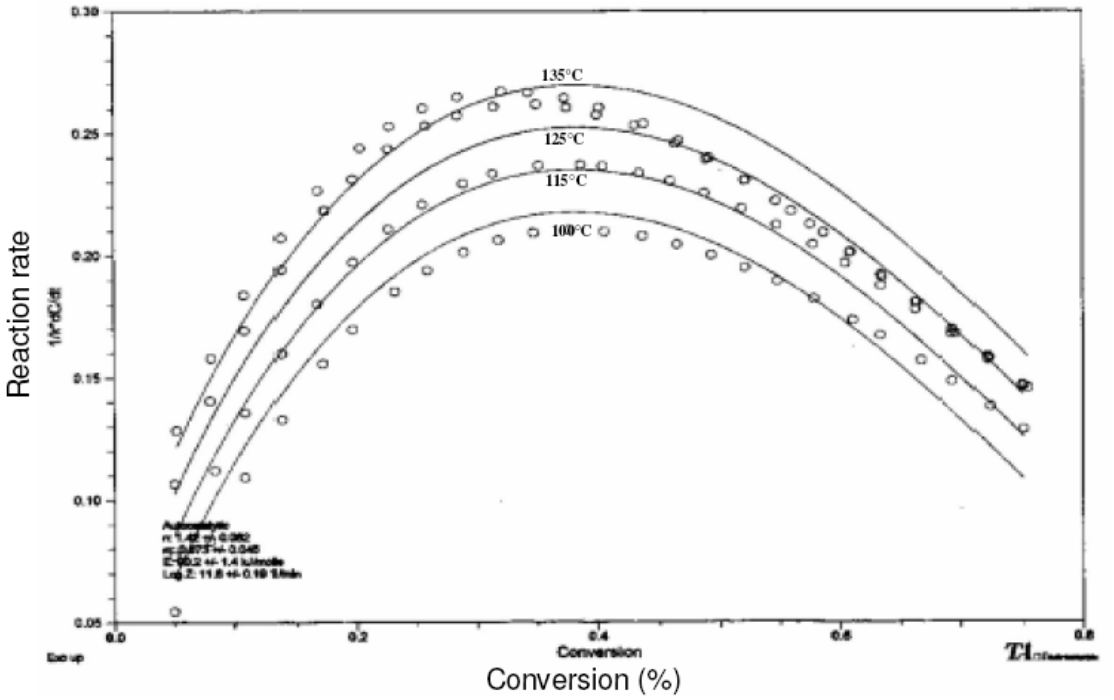

Figure 8.14. Comparison between the model predictions and experimental results of the reaction rate and conversion (degree of curing) observed in DSC at various isothermals.

A good agreement to experimental data was observed using the autocatalytic equation (**Equation. 8.4**), leading to n of 1.42±0.082, m of 0.873±0.045, and activation energy (E) of 90.2 ±1.4 kJ/mole. Therefore, the chemical model (autocatalytic **Equation 8.4**) can predict the curing kinetics of the epoxy system for non-isothermal conditions and can determine the pure thermal effects of ultrasonic curing to differentiate the thermal and non-thermal effects.[14]

Figure 8.15 shows the temperature history of the epoxy system cured using the ultrasonic curing process under optimal conditions (i.e., pulse duration of 50%, amplitude of 21μm and preheating temperature of 100ºC). This temperature history, due to the

thermal effect of ultrasonic curing, was then plugged into the chemical model for determining the degree of curing, as shown in **Figure 8.16**.

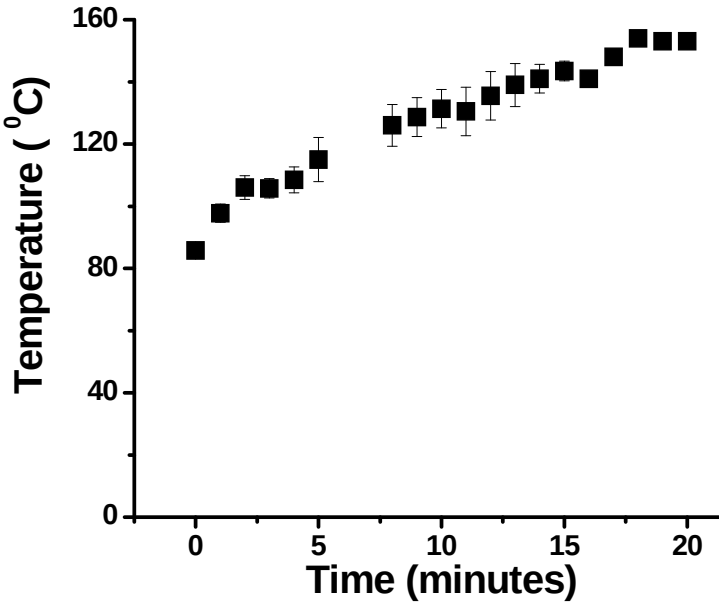

Figure 8.15. Temperature profile of the one-part model epoxy system at different times under optimum ultrasonic conditions.

The degree of curing due to the combined thermal and non-thermal effects was determined using DSC for various time intervals such as 5, 10, 15 and 20 minutes. **Table 8.2** summarizes the degree of curing, and the results for both non-thermal and thermal effects are represented in **Figure 8.16**. There are no non-thermal effects that influence curing. Thus, the resulting curing is due to ultrasonic heating.

Table 8.2. The residual heat and corresponding conversion of epoxy samples cured by pulsed ultrasonic heating for different heating times.

Ultrasonic-heating time (min)	Residual heat (joules/g)	Degree of Curing (%)
5	397.3	5.9
10	83.79	80
15	45.9	89.13
20	4	99

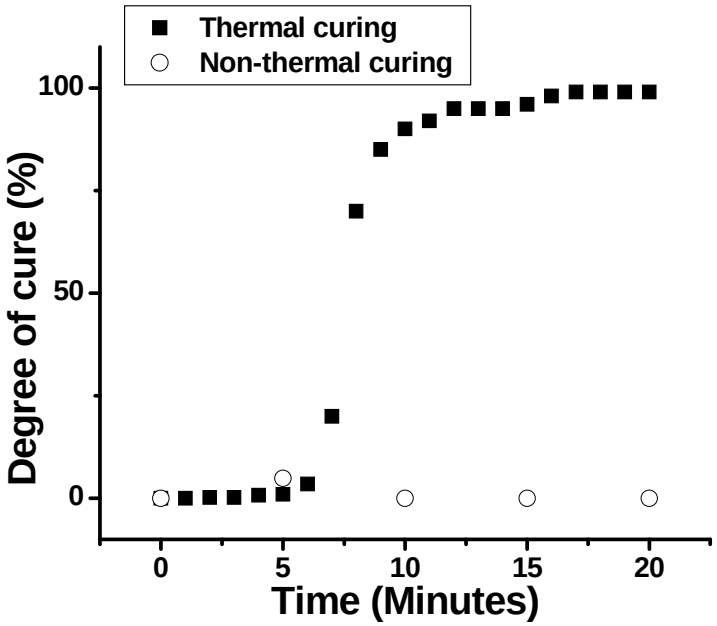

Figure 8.16. Comparison between the degree of cure produced by pulsed ultrasonic curing and predictions from the autocatalytic model for different times.

Moreover, the temperature profiles of **Figure 8.9 (a)** at different preheating temperatures were substituted in the autocatalytic model **Equation 8.4** to differentiate between any possible thermal and non-thermal effects. This equation determined the degree of curing due to the thermal effect of ultrasonic curing, as shown in **Figure 8.17**. In addition, the degree of curing due to the combined thermal and non-thermal effects was determined using DSC for these preheating temperatures, as shown in **Figure 8.17**. It can be seen that a preheating temperature of 80ºC produced significant curing due to the non-thermal effects of ultrasonic curing; thus, the curing may be attributed to streaming from the cavitations, lower viscosity, and a higher diffusion rate. It has been previously observed that the liquid motion in the vicinity of cavitation bubbles generate large shear and strain gradients due to the rapid streaming of the molecules around the cavitation bubble and the intense shock waves emanating from the collapse of the bubbles.[42] Moreover, ultrasonic vibration assists secondary amines (produced during crosslinking reaction and less reactive due to their steric hindrances) to absorb sufficient energy in a short time to promote the reaction.[13] However, as the preheating temperature increases (for example 100°C), the difference due to non-thermal effects no longer prevails over thermal effects.

8.3.4: Mechanical properties of samples cured using ultrasound

Polymers, being viscoelastic, can store mechanical energy as potential energy and have the capacity to dissipate energy as heat.[43] The DMA (dynamic mechanical analysis)

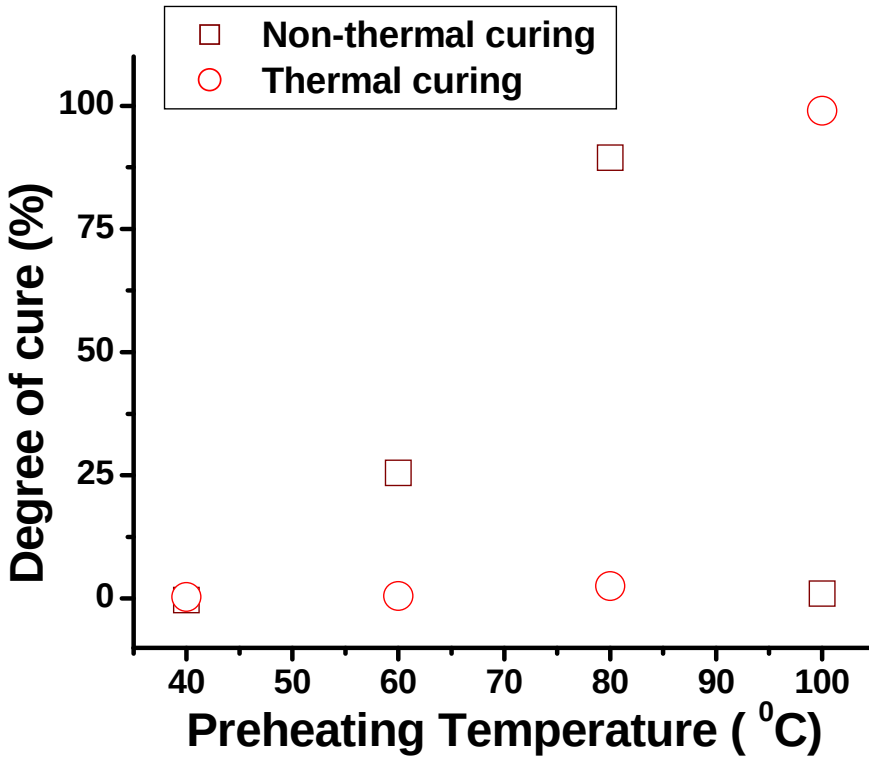

Figure 8.17. Comparison between the degree of cure produced by pulsed ultrasonic heating and predictions from the autocatalytic model for different preheating temperatures.

instrument measures the deformation of a material in response to vibrational forces, and determines the dynamic modulus (E', stiffness of material), the loss modulus (E") and mechanical damping or internal friction ($\tan\delta = \frac{E''}{E'}$ energy dissipation). These dynamic parameters have useful implications in determining the glass transition region, relaxation spectra, degree of crystallinity, crosslinking, phase separation, etc.

DMA was conducted to compare the mechanical properties of the samples

produced through both the thermal and ultrasonic curing processes. The results of storage (or elastic) modulus and glass-transition temperatures are shown in **Figure 8.18**. Samples from ultrasonic curing, under optimal conditions, exhibited similar or better properties than those from thermal curing.

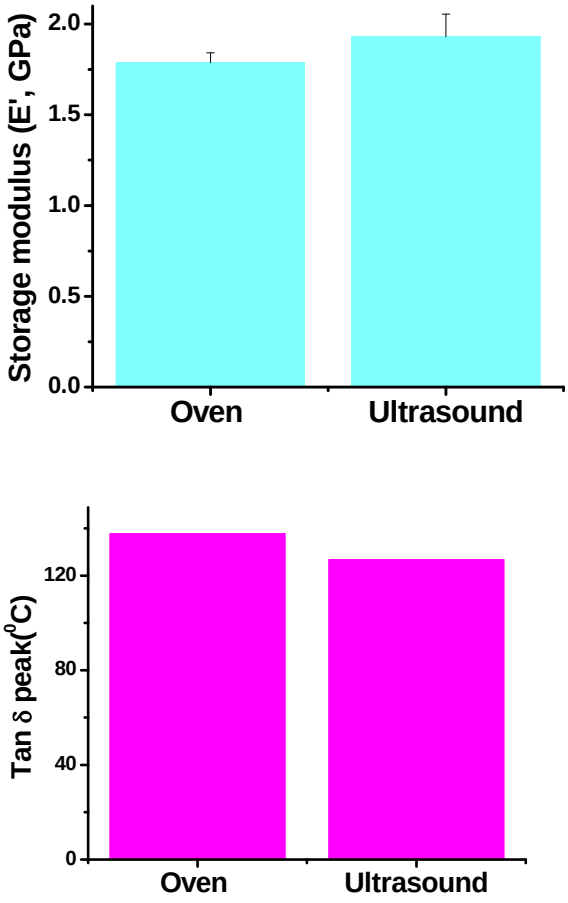

Figure 8.18. Storage modulus (a) and glass-transition temperature (b) of samples cured using ultrasonic and thermal (oven) curing processes.

8.3.5: Thermal curing of epoxidized vegetable oil

After studying the positive effects of ultrasonic curing on a traditional model one-

part epoxy system, the next phase of research was conducted to investigate the thermal and ultrasonic curing of natural epoxy. **Figures 8.19 (a, b)** shows the DSC thermographs of ESO and ELO curing using 1wt.-% of curing agent BPH, which acts as a thermally latent cationic initiator in the curing reaction. It can be seen that the onset temperature of the curing reaction is approximately 130°C, which matches with the dissociation temperature of BPH, a latent curing agent. In addition, the exothermic curves consist of an initial shoulder (initiation) and main exothermic peaks (curing reaction). Boquillan et al.[35] found that the polymerization of a cationic epoxy system leads to a Lewis acid process with two separate initiation reactions:

$$BPH + Epoxide \xrightarrow{\Delta} Ph - CH_2 - (O^+ of\ \ Epoxide) - SbF_6^- + pyrazine \qquad (1)$$

$$BPH + R - OH \xrightarrow{\Delta} Ph - CH_2 - OR + pyrazine + H^+ SbF_6^- \qquad (2)$$

These two reactions are responsible for the initial shoulder of the exothermic curves in **Figures 8.19(a, b),** indicating the initiation of the curing reaction and, subsequently, the main exothermic peak due to the catalytic action of $HSbF_6$, a protic or Lewis acid. It was observed that only 1% of BPH was sufficient to cure both ELO and ESO fully. BPH exhibited a sharp endothermic peak at a temperature of 136°C, resulting in its dissociation and thereby activating the epoxy curing reaction. The exothermic heat of curing was found to be 264.6 J/g for the ELO system, and 117.8J/g for the ESO system. This difference in the heat of curing can be attributed to the higher number of epoxy groups in ELO than ESO due to the higher degree of unsaturation, due to the constituent esterfied linolenic acid, which contains three double bonds. Moreover, neither ELO nor ESO cured in the absence of the curing agent.

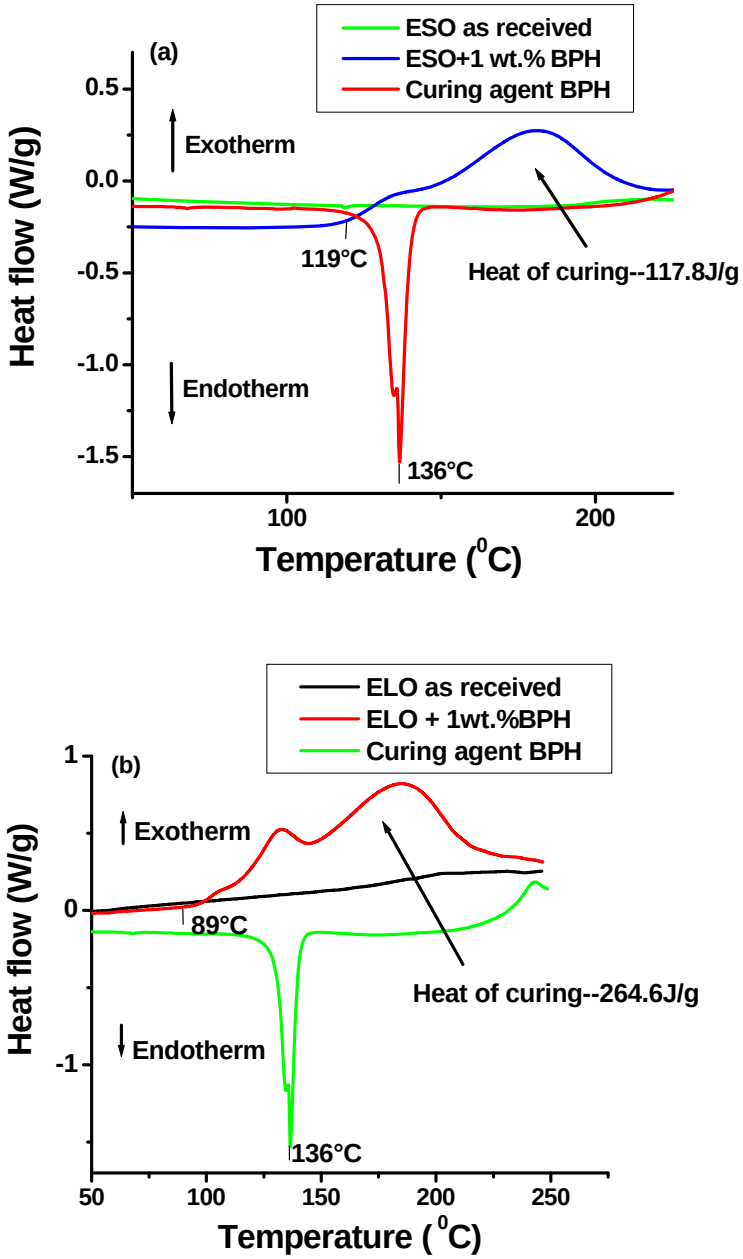

Figure 8.19. DSC thermographs of thermal curing. (a) ESO/BPH system, (b) ELO/BPH system.

Figure 8.20 shows the TGA thermograph for ELO and ESO in the absence of the curing agent. They showed good thermal stability, as they begin degrading at

approximately 300°C. Moreover, the amount of volatiles is less than 1% until at temperature of approximately 200°C. Therefore, this thermal stability would produce minimum volatiles and thereby less shrinkage during epoxy curing.

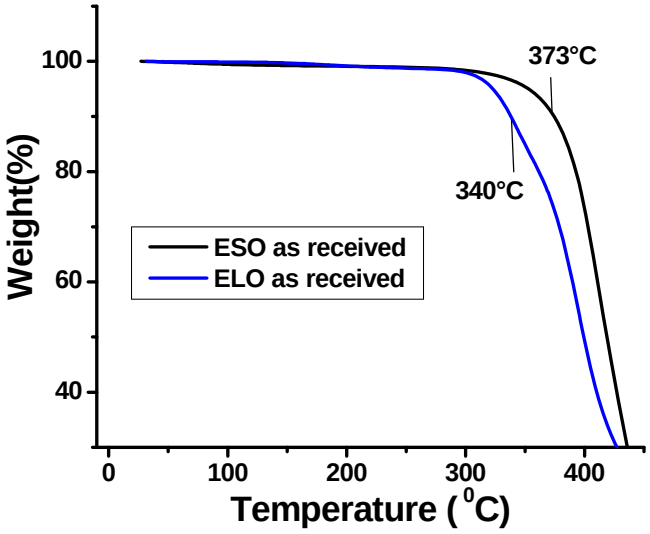

Figure 8.20. TGA thermographs of the as-received natural epoxies ELO and ESO.

It was observed that the plastic from ESO lacked integrity and crumbled compared to ELO plastic, which demonstrated good integrity and showed the dynamic mechanical characteristics of a rubbery material. DMA analysis provides information about the viscoelasticity, crosslinking density and thermal stability of polymer networks. Crosslinking density can be obtained from the following equation for rubber elasticity in a plateau region of the DMA curve:[44]

$$\rho = \frac{E'}{\varphi RT}; \qquad \frac{mol}{m^3} = \left(\frac{N}{m^2}\right)\left(\frac{mol-K}{8.319N-m}\right)\left(\frac{1}{K}\right)$$

where E' represents the rubber modulus, ρ the density of network or crosslinking density (mol/m^3), φ the front factor (usually equal to unity), R the gas constant, and T the absolute temperature in the rubbery region.

Figure 8.21 shows the DMA spectra of the ELO system cured using 1wt.-% of BPH. The rubbery storage modulus and glass transition temperature were 55MPa and 54.3°C, respectively, resulting in a crosslinking density of 18.5×10^{-3} mol/cm^3.

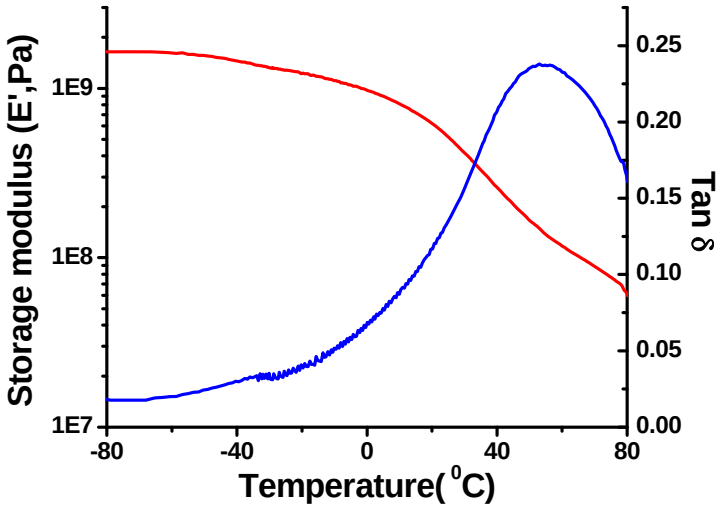

Figure 8.21. Dynamic mechanical properties of ELO/BPH plastic.

8.3.6: Ultrasonic curing of epoxidized vegetable oil

It was found in the initial phase of this research that ELO can be an important biodegradable polymer to develop plastics and reinforced composites for various industrial applications. Recently, non-traditional methods of curing such as electron beam, ultrasonic and infrared curing have been studied to develop composites at reduced time and costs. Ultrasound curing has definite advantages, such as non-thermal and

thermal benefits, self-limiting, and better consolidation. Therefore, the ELO/BPH system was investigated through the ultrasonic curing method. To prevent the problem of ELO advancement (leading to migration of the epoxy resin out of mold) during ultrasonic treatment, it was found that 10wt.-% of thixotropic agent R805 (silica powder) produced a viscous consistency, resulting in a minimum advancement of ELO during curing.

Figure 8.22 shows the residual heat of curing for samples using DSC, produced at 5 and 20 minutes through both thermal and ultrasonic curing process. Thermal curing of epoxy oil requires sufficient time to accumulate energy, which propagates the reaction. It was observed that, for the initial 5 minutes, thermal energy is not enough to initiate the curing reaction, as evidenced by the presence of the shoulder in the exothermic curve due to the latency of BPH. Moreover, the degree of curing rose to 36% after 20 minutes. However, the thermal and non-thermal effects of ultrasonic curing caused a rapid initiation of the reaction (absence of initial shoulder), and the degree of curing rose to 81% after 20 minutes of treatment. These results are summarized in **Table 8.3**, indicating the benefits of ultrasonic curing.

To observe the effect of ultrasonic curing on the mechanical properties of cured plastic, samples were first thermally cured at a preheating temperature of 100°C for 10 minutes, followed by 20 minutes of ultrasonic curing. The initial thermal curing for 10 minutes yields the integrity of the material and prevents oil advancement during ultrasonic curing.

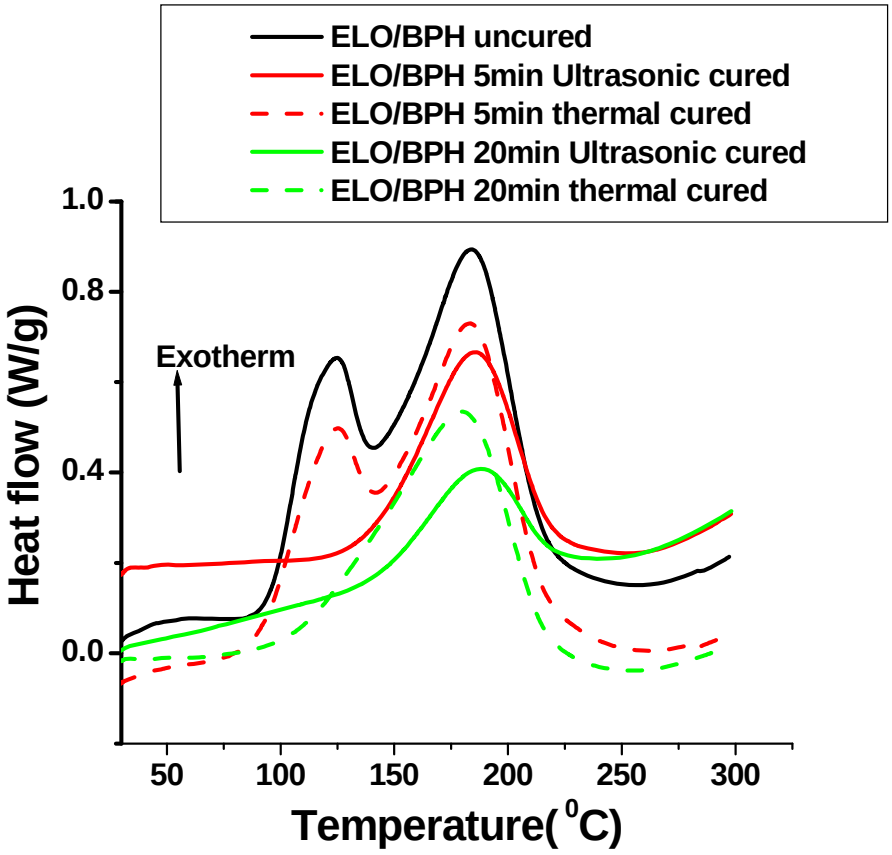

Figure 8.22. DSC thermographs of ultrasonic cured samples of the ELO/Silica/BPH system.

Figure 8.23(a) shows the corresponding DSC analysis, indicating a higher degree of curing for sonicated samples. Moreover, the extent of ELO curing can also be followed using FTIR, as shown in **Figure 8.23(b)**. The presence of epoxide moieties in ELO can be characterized through the band at 817cm^{-1}. New band at 1070cm^{-1} corresponds to the aliphatic ether groups produced during epoxy ring opening.[45] It can be seen in **Figure 8.23(b)** that the ultrasonic cured samples exhibited a higher number of ether links (higher intensity of peak) due to the opening of epoxide groups.

Table 8.3. Residual heat of curing and degree of curing for the ELO/Silica/BPH system.

Sample	Ultrasonic Curing		Thermal Curing	
	Residual heat of curing (J/g)	Degree of curing (%)	Residual heat of curing (J/g)	Degree of curing (%)
Uncured	383	0	383	0
5 min	149.2	61	379.7	10
20 min	71.6	81	246.1	36

To examine the stiffness of the samples, TMA (Thermomechanical Analysis) was used to measure the penetration depth between room temperature and 180°C, as shown in **Figure 8.24**. It can be observed that the ultrasonic cured samples exhibited less penetration due to having more crosslinks than the samples from thermal curing.

8.4: Conclusions

Natural epoxy ELO exhibited the potential for developing plastics and composites. Moreover, for the first time, an ultrasonic process was used to accelerate the curing of ELO. An induction period (latency) was observed during the isothermal oven curing of one-part model epoxy at 100ºC, corresponding to time required for the dissociation of monuron into isocyanate and dimethyl amine, which, after exceeding a critical concentration, catalyzes the reaction. Similarly, latency was also observed during ultrasonic curing, although less than with thermal curing due to combined non-thermal

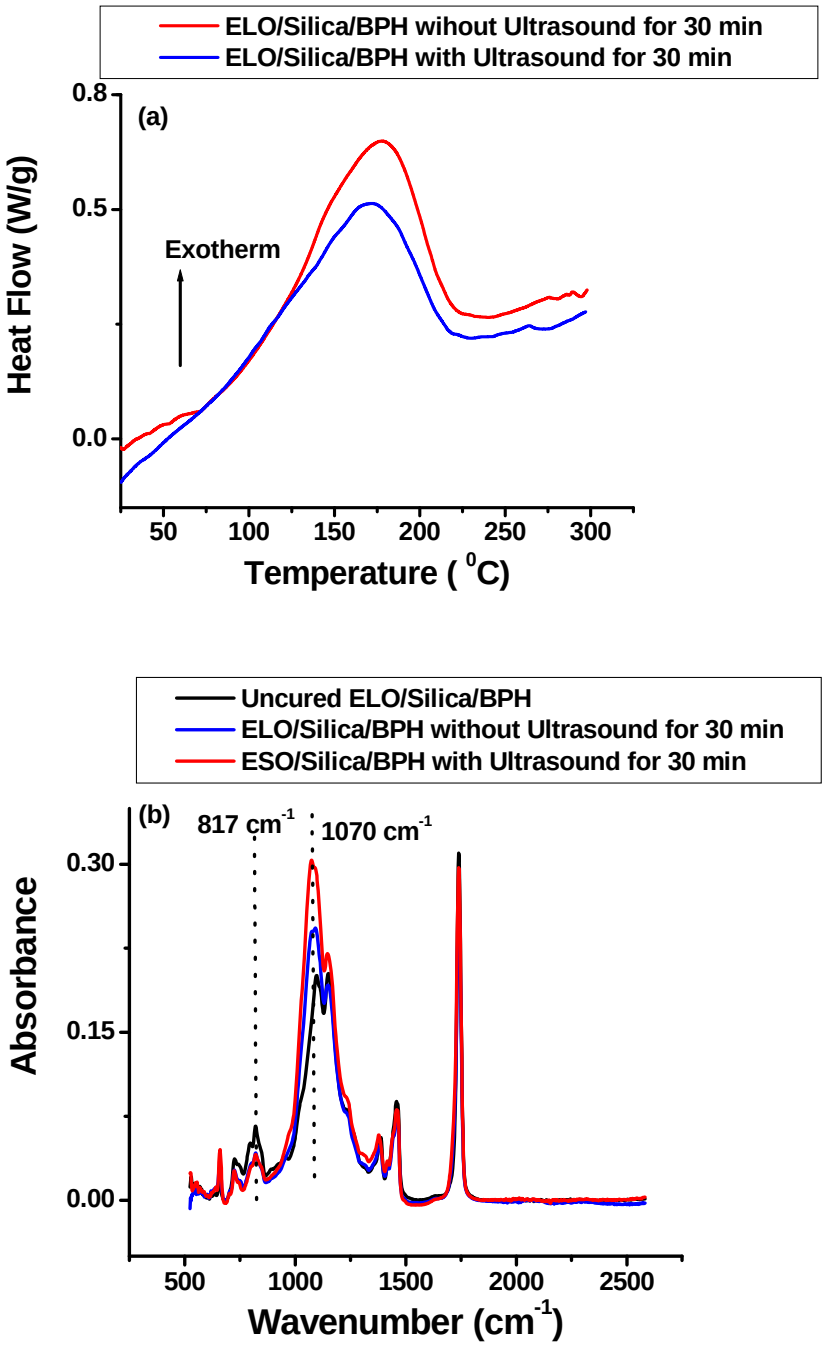

Figure 8.23. Comparison between the samples from ultrasonic and thermal curing processes: (a) DSC thermographs, (b) FTIR.

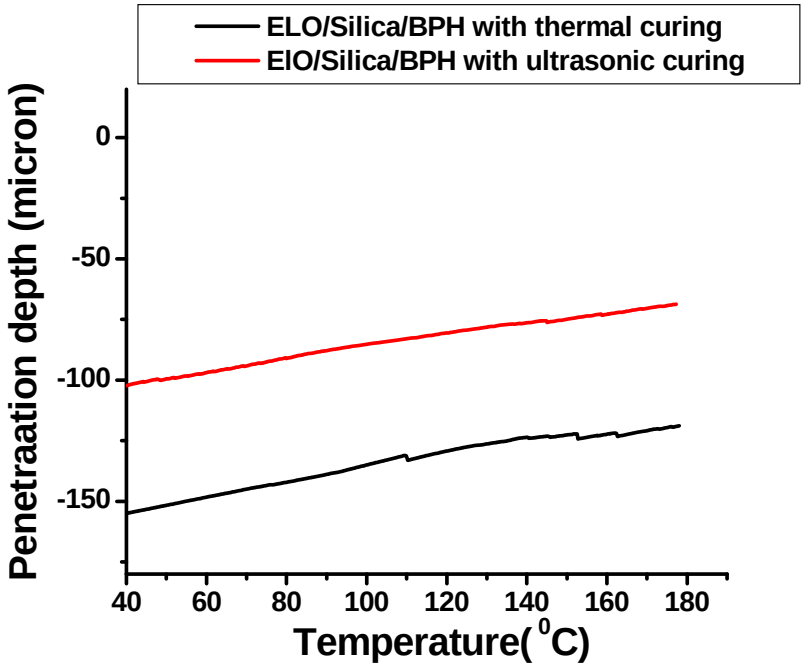

Figure 8.24. TMA graph for ultrasonic and thermal cured samples.

and thermal effects. From DSC analysis, a preheating temperature of 100ºC was found to be optimal for the progression of the curing reaction; however, the maximum difference between non-thermal and thermal effects was observed at a preheating temperature of 80ºC. The full curing time was found to be reduced by a factor of six with pulsed ultrasonic curing. The curing level from pure thermal effects, produced by pulsed ultrasonic curing, could be determined by incorporating the curing temperature history into the autocatalytic equation. There was a good agreement for the degree of curing between the experimental results and those predicted by the autocatalytic equation. The results for curing at a preheating temperature of 100 ºC could not differentiate between

non-thermal and thermal effects. However, a distinguishable difference between these effects was observed at a preheating temperature of 80 ºC.

ELO was found to be an appropriate functionalized vegetable oil to produce plastics and reinforced composites. The latent curing agent BPH seemed to be a more eco-friendly hardener since it required a very small amount to cure the epoxy material completely. The non-traditional ultrasonic curing method demonstrated the advantage of rapid curing over the traditional thermal curing method for developing plastics or composites from natural epoxy ELO.

8.5: References:

[1] Miyagawa, H., Mohanty, A. K., Drzal, L., and Misra, M., Nanotechnology (2005), 16, 118.

[2] Boquillon, N., and Fringant, C., Polymer (2000), 41, 8603.

[3] Park, S-., Jin, F-., and Lee, J-., Macromol. Rapid Commun. (2004), 25, 724.

[4] Mezzenga R., Boogh L., and Manson J. A. E., Comp. Sci. Tech. (2001); 61: 787.

[5] Adachi T., Araki W., Nakahara T., Yamaji A., and Gamou M., J. Appl. Poly. Sci. (2002), 86: 2261.

[6] Williamson A., Encyclopedia of Materials Science & Technology, Elsevier Sc. Ltd., 2001. pp. 90.

[7] Plummer C. J. G., Bourban P. E., and Manson J. A. E., Encyclopedia of Materials Science & Technology, Elsevier Sc. Ltd., 2001. pp. 7388.

[8] Kwan K. M., Cheng K., and Benatar A., Proc. Annual Tech. Conf.-Soc. Plas. Eng. (1998), 56, 1089.

[9] Whitney T. M., and Green R. E., Mater. Sci. Forum (1996); 210/213, 695.

[10] Fukui, H., Rapid curing of resins by ultrasound irradiated via metal media without heater, Jpn. Kokai Tokyo Koho 1995; JP 07137042 (in Japanese).

[11] Hahn O., Ewerszumrode A., Weld. World (1998), 41, 149.

[12] Berlan J., Rad. Phys. Chem. (1995), 45, 581.

[13] Kwan K. M., and Benatar A., Proc. Annual Tech. Conf.-Soc. Plas. Eng. (2001), 59, 1234.

[14] Kwan K. M., and Benatar A. Proceedings of Annual Meeting of the Adhesion Society (2001), 24, 245.

[15] Graham L. J., and Ahlberg L. A., Cohen-Tenoudji F., and Tittmann B. R., Ultra. Symp. Proc. (1986), 2, 1013.

[16] Khozin V. G., Karimov A. A., Cherevatski, A. M., Murafa, A. V., Polyanskii, A. A., Murashov, B. A., and Pimenov, N., Mekhanika Kompozitnykh Materialvo (in Russian) (1984), 4, 702.

[17] Vishnevetskaya, L. P., Moskalev, E. V., and Timofeeva, T. G., Stroitel'nye Materialy (in Russian) (1984), 10, 22.

[18] Karimov, A. A., Kolosov, A. E., Khozin, V. G., and Klyavlin, V. V. Mekhanika Kompozitnykh Materialvo (in Russian) (1989), 1, 96.

[19] Guthner, T., and Hammer, B., J. Appl. Polym. Sci. (1993), 50, 1453.

[20] Laliberte, B. R., Bornstein, J., and Sacher, R. E., Ind. Eng. Chem. Prod. Res. (1983), 22, 261.

[21] Hagnauer, G. L., and Dunn, D. A., J. Appl. Polym. Sci. (1981), 26, 1837.

[22] Mijovic, J., and Andjelic, S., Macromolecuels (1995), 28, 2787.

[23] DeBakker, C., Georges, G. A., and St John, N. A. Spectro. Acta. (1993), 49, 739.

[24] Min, B. G., Shin, D. K., Stachurski, Z. H., and Hodgkin, J. H., Polym. Bull. (1994), 33, 465.

[25] Xu, J., Liu, Z., Erhan, S. Z., and Carriere, C. J., J. Amer. Oil Chem. Soc. (2004), 81, 813.

[26] Miyagawa, H., Mohanty, A., Drzal, L. T., and Misra, M., Ind. Eng. Chem. Res. 2004, 43, 7001.

[27] Boquillon, N., J. Appl. Polym. Sci. (2006), 101, 4037.

[28] Miyagawa, H., Mohanty, A. K., Misra, M., and Drzal, L. T., Macromol. Mater. Eng. (2004), 289, 629.

[29] Kim, M.., Lee, K. W., Endo, T., and Lee S. B., Macromolecules (2004), 37, 5830.

[30] Park, S-., and Seo, M-., Macromol. Mater. Eng. (2003), 288, 894.

[31] Lligadas, G., Ronda, J. C., Galià, M., and Cádiz, V., Biomacromolecules (2006), 7, 3521.

[32] Crivello, J. V., Narayan, R., and Sternstein, S. S., J. Appl. Polym. Sci. (1996), 64, 2073.

[33] Dweib, M. A., Hu, B., O'Donnell, A., Shenton, H. W., and Wool, R. P., Comp. Struct. (2004), 63, 147.

[34] Certificate of Analysis, Arkema Inc., MN.

[35] Kim, Y. C., Park, S-., and Lee, J-., Polymer (1997), 29(9), 759.

[36] Zhang, Z., Beatty, E., and Wong, C. P., Macromol. Mater. Eng. (2003), 288, 365.

[37] Poisson, N., Lachenal, G., and Sautereau, H., Vib. Spect. (1996), 12, 237.

[38] Caňavate, J., and Colom, X., Polym., Plast. Tech. Eng. (2000), 39, 937.

[39] Eidelman, N., Raghavan, D., Forster, A. M., Amis, E. J., and Karim, A., Macro. Rapid Comm. (2004), 25, 259.

[40] Ghaemy, M, Barghamadi, M, Behmadi, H., J. Appl. Polym. Sci. (2004), 94, 1049.

[41] Kamal, M. R., Polym. Eng. Sci. (1974), 14, 231.

[42] Suslic, K. S., and Price, G. J., Annu. Rev. Mater. Sci. (1999), 29, 295.

[43] Murayama, T., Dynamic Mechanical Analysis of Polymeric Material, 1978, Elsevier Scientific Publishing Company, Amsterdam- Oxford- New York.

[44] Park, S-. J., Lee, H-. Y., Han, M., and Hong, S-. K., J. Coll. Interface Sci. (2004), 270, 288.

[45] Lligadas, G., Ronda, J. C., Galià, M., and Cádiz, V., Biomacromolecules (2006), 7, 3521.

CHAPTER 9

SUMMARY

This research has demonstrated the fabrication and characterization of polymer blends and composites from biopolymers, especially animal co-product proteins and natural vegetable oil-based epoxy. Model animal proteins, whey and chicken egg whites albumin, were used to understand the plastic fabrication process. Through these studies, different approaches were developed for preparing pure or blend plastics from partially denatured or undenatured proteins. These proteins showed complimentary properties to address the issue of toughness. The compression molding process used here can be commercialized in developing various articles of desire in an easy way. The conclusions based on this research are summarized below according to the respective chapters.

9.1: Biodegradable Plastics from Undenatured Proteins: Animal and Human

This research into developing plastics from animal and human proteins has provided, for the first time, a foundation on which to design various medical devices and implants with increased biocompatibility.

Plastic samples made from pure, undenatured animal and human proteins were successfully produced through the compression-molding process in order to better understand the plastic fabrication process. These plastics were prepared under optimal conditions: molding temperature of 150°C, molding pressure of 20MPa, holding time of 5mins, followed by ambient cooling and overnight drying in an oven at 50°C. The water content in the protein material during thermal processing played a vital role. In addition,

ageing (water evaporation) during storage led to an increase in the plastic's mechanical properties of strength and stiffness (modulus). A reversible stress-strain over the yield region was observed. These plastics showed viscoelastic characteristics.

Plastic samples produced from chicken egg whites albumin and human serum albumin (HSA) demonstrated antimicrobial properties. HSA plastics exhibited increased strength, elongation, and modulus compared to egg white plastics. In addition, HSA plastics swelled to 83% in water. A significant drop in swelling of HSA plastics due to modification with calcium ions as crosslinks was found.

9.2: Biodegradable Plastics from Blends of Undenatured Proteins

The research reported here explored blending to develop plastics of desired properties, which are difficult to achieve using single components. Therefore, to address the issue of toughness, plastic samples were prepared from blends of undenatured chicken egg whites albumin and whey proteins, and from the blends of whey protein and natural rubber latex, through compression-molding. It was observed that approximately 20% of natural rubber and 105wt.-% of water were optimal to process and improve the strength and elongation properties. The results from the dynamic mechanical and thermal analysis (DMTA) of these plastics indicated phase separation when dispersed rubber particles were formed in the whey matrix; the presence of the two phases were also confirmed by the loss factor graphs of dynamic mechanical analysis.

Thermal analysis of whey/albumin blends confirmed the presence of albumin and whey rich phases. Properties of whey/albumin protein blends followed mixing rule below

30% of either of these components. In the phase inversion region between 30 to 70%, plastics showed decreased tensile strength and modulus due to the significant contribution of either of these components, resulting in a mismatching of the mechanical properties. Overall, the addition of whey protein increases the stiffness of the material due to its higher number of complimentary reactive groups.

9.3: Biodegradable Plastics from Partially Denatured Proteins: Feathermeal

The research reported here, for the first time, studied the animal co-product protein feathermeal, which is used mostly as an ingredient in animal feed, to develop plastic. This partially denatured protein exhibited strong potential for various technical applications that are difficult to recycle.

Thus, plastic samples from partially denatured feathermeal protein were successfully produced by the compression-molding process. The modulus (stiffness) for the material obtained was found to be comparable with that of commercial synthetic material but with lower toughness characteristics, which is a common phenomenon among plastics produced from animal and plant proteins. A reversible stress-strain property over the yield region was observed. The resultant plastic samples made from these biomacromolecular blends of partially denatured and undenatured proteins demonstrated improved mechanical properties as compared to neat plastics from feathermeal proteins. The results were interpreted in terms of theoretical models to describe mechanical properties such as extensibility, tensile strength, and stiffness of the plastics made from feathermeal/whey blends at various volume ratios. The values for the

stiffness of the feathermeal/whey blends positively deviated from the simple mixing rule and showed a synergistic effect.

Plastic samples were also prepared from blends of synthetic rubber copolymer and feathermeal protein, which demonstrated improved mechanical properties compared to plastics from feathermeal proteins. In addition, these results were interpreted in terms of theoretical models to describe mechanical properties.

9.4: Biodegradable Plastics from Partially Denatured Proteins: Bloodmeal

Plastic samples from another partially denatured bloodmeal protein, which is primarily used as an ingredient in animal feed, were successfully produced for the first time through the compression-molding process. These plastics exhibited comparable modulus but lower strength and elongation than conventional synthetic plastics. To address the issue of toughness, polymers blends were prepared from bloodmeal and pure undenatured proteins. Extensibility, tensile strength, and stiffness from the mechanical analysis of bloodmeal/albumin blends at various volume fractions were interpreted in terms of theoretical models and showed better adhesion. Bloodmeal protein also showed potential in the development of biocomposites reinforced with natural hemp fibers.

9.5: Plastics from Epoxidized Vegetable Oil via Thermal and Ultrasonic Curing

This research reports that vegetable oil-based epoxy, especially epoxidized linseed oil, showed significant potential to replace petroleum-derived resins to be used as a matrix for composites in structural applications. Furthermore, the research showed the

benefits of ultrasonic curing, which can help in preparing the out-of-autoclave composites.

Initially, this research used a traditional one-part epoxy system as a model to investigate both thermal and ultrasonic curing processes. An induction period (latency) was observed during the isothermal oven curing of this epoxy system at 100ºC. Similarly, latency was also observed during ultrasonic curing, although lesser compared to thermal curing due to combined non-thermal and thermal effects. From DSC analysis, a preheating temperature of 100ºC was found to be optimal for the progression of curing reaction; although, maximum difference between non-thermal and thermal effects was observed at a preheating temperature of 80ºC. The time of full curing was found to be reduced by a factor of six with pulsed ultrasonic curing. The curing level from pure thermal effects, produced by pulsed ultrasonic curing, could be determined by incorporating the curing temperature history into the chemical model. There was good agreement between the degree of curing from the experimental results and the one predicted by the autocatalytic equation.

ELO was found to be appropriate functionalized vegetable oil, which has potential to produce plastics and reinforced composites. The latent curing agent BPH seemed to be a more eco-friendly hardener and required a very small amount in natural epoxy system to cure completely. A non-traditional ultrasonic curing method demonstrated the advantage of rapid curing over the traditional thermal curing method for developing plastics or composites from natural epoxy ELO.

CHAPTER 10

FUTURE STUDY

The depletion of petroleum resources along with environmental regulations has spurred efforts to find new biocompatible and environmental friendly materials and products. Bio-based materials, such as agricultural and animal co-product/byproduct, offer a potential solution to this problem. The research in this dissertation sought the possibilities of utilizing biopolymers, such as proteins and natural epoxy for developing plastics/composites. Following list of future study can be conducted.

- Development of biocomposites and bioplastics from rendering proteins (bloodmeal and feathermeal) modified with various additives, such as natural rubber latex and PEG (poly ethylene glycol) using a spray-drying process. Subsequently, plastic from these modified proteins can be reinforced with lignocellulosic reinforcements (wood and natural fibers) to improve toughness, and water resistance.
- Development of polymer blends from rendering proteins and thermoplastic starch (TPS).
- Biodegradability study of plastics made from animal co-product proteins and their derivatives.
- Wound healing response of plastics produced from human serum and egg white albumins.
- Development of epoxidized linseed oil- based composites.

APPENDIX

ULTRASONIC CONSOLIDATION OF EPOXY COMPOSITES

A-I.1: Introduction

Current high performance composites are made by hansd lay-up of prepreg tapes (sheets of unidirectional fibers coated with a partially cured thermoset resin), followed by vacuum bagging, and autoclave or compression curing at slow heating rate (approximately 1-2°C).[1] On the contrary, ultrasonic consolidation has several promising features that differs this method from other established techniques of the epoxy composite fabrication. The beneficial effects of ultrasonic curing have been investigated for various epoxy resins and composites, including AS1/3501-5A graphite/epoxy prepreg tape,[2] AS4/3501-6 carbon/epoxy composite,[3] B7809 epoxy adhesive (PPG), 2214 epoxy adhesive (3M) ,[4] and EPO1441-30 epoxy resin (Shell).[5]

All published investigations about ultrasonic curing have been focused on relatively small, cured, well consolidated, and pore-free samples. According to Graham et al.[2], desired distribution of ultrasonic energy is necessary to extend this technique for producing larger specimens. They studied different possibilities to equalize sonic energy distribution over the bigger part and were able to cure a sample of 6" × 6" in dimension with variable thickness.

Ultrasonic curing promises a great potential to develop epoxy based composites reinforced with high-performance fibers or fillers. However, this approach has not yet

been employed for relatively large structures. One of the main reasons for this limitation was the unavailability of ultrasonic equipment to develop large structural parts. Recently, Form-ation 2030, ultrasonic consolidation machine from Solidica, Inc., has shown potential for developing metal matrix composites reinforced with high performance fibers.[6] This machine can apply ultrasonic vibrations with a specific accuracy within 0.002-0.005 inch over the machine envelope of 20" ×30". In addition, the ultrasonic consolidation parameters can be precisely controlled by an advanced control, drive, and application software. Therefore, the primary objective of the research was to optimize the ultrasonic curing variables using a model epoxy/carbon prepreg system on a Solidica ultrasonic consolidation machine. The outcome of this investigation would help in developing relatively large composite samples from bio-based epoxy and/or its blend with petroleum-based epoxy.

A-I.2: Materials

Carbon/one-part epoxy prepreg system was used to develop laminates/composites through ultrasonic consolidation process. The prepreg tape (DA409U/G35) was supplied by APCM Company, CT. It contained 42% unidirectional carbon fiber and 58% one-part epoxy system (DGEBA/DDA/Uron). The Teflon™ coated aluminum sheet (5.5 mil thick, alloy 3003, and 0.5 mil TEFLON coating) was supplied by McMaster-Carr.

A-I.3: Experimental

A-I.3.1: Specimen preparation

Figure A-I.1 shows the schematic representation of carbon/epoxy composite curing using ultrasonic consolidation process. After laying and assembling the two-ply laminate using Teflon coated aluminum sheet, the whole assembly was cold pressed to make it flat. Subsequently, it was tacked on heated platen of UTL and equilibrated at desired preheating temperature before subjecting to vibrating ultrasonic vibrations.

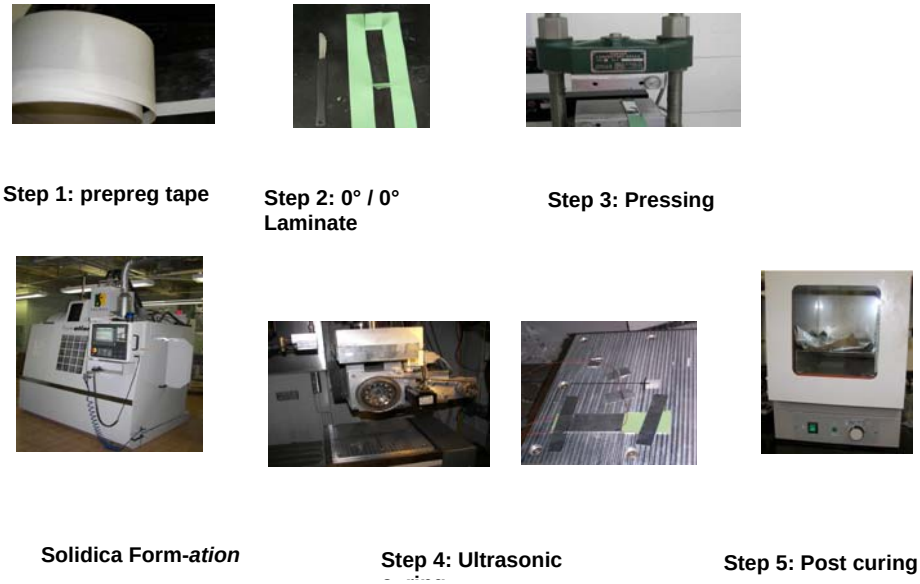

Figure A-I.1. Schematic representation of carbon/epoxy composite production using ultrasonic consolidation.

Figure A-I.2 shows the basic principal of ultrasonic consolidation process. A horn, oscillating at a constant frequency of 20 kHz, transfers ultrasonic vibrations to the composite assembly and induce curing reaction due to thermal and non-thermal effects of ultrasound. For this ultrasonic curing, Formation 2030 UTL machine from Solidica, Inc. was used. It was equipped with advance CAD software to manipulate the horn position

over an envelope of 13" × 13". CALCOMMS^{TM} software, coupled with CALCONTROL^{TM} thermal controllers and thermocouples, was used to acquire temperature data during ultrasonic curing.

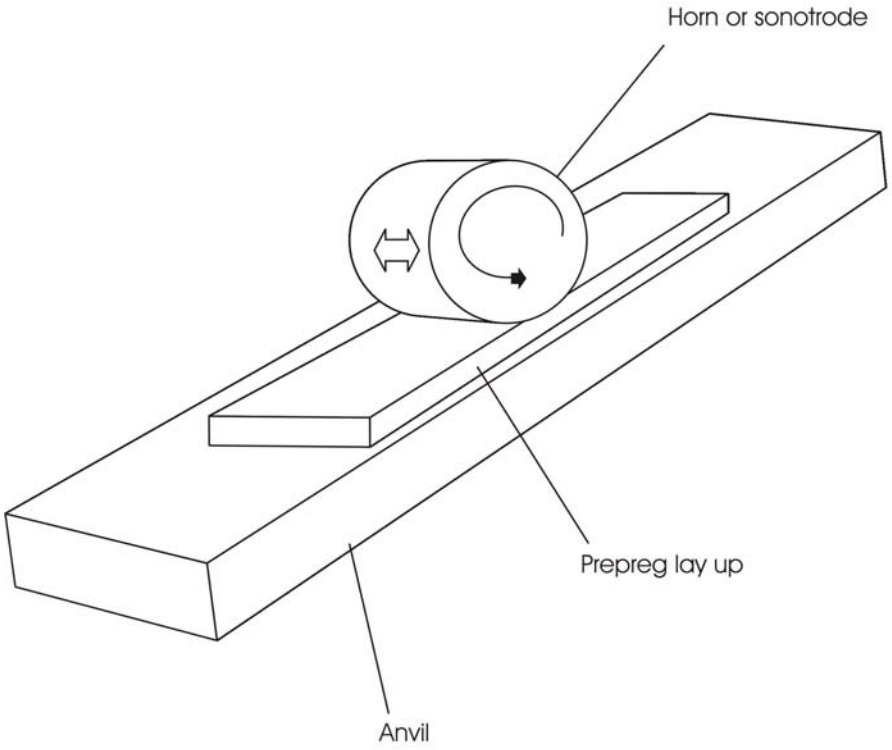

Figure A-I.2. Basic principle of ultrasonic consolidation.

A-I.3.2: Thermal analysis

A TA Instrument differential scanning calorimeter (DSC 2920) was used to determine the degree of conversion using **Equation A-I.1** at a heating rate of 10°C min^{-1}.

$$\text{Degree of cure} = \alpha = \left(1 - \frac{\Delta H_r}{\Delta H_T}\right) \Big/ a \qquad \textbf{(A-I.1)}$$

where ΔH_r represents the residual heat (J/g); ΔH_T the total heat for uncured sample (J/g); and a the fraction of epoxy content (1.0 if no fiber content). **Figure A-I.3** shows a dynamic DSC run for uncured carbon/epoxy prepreg.

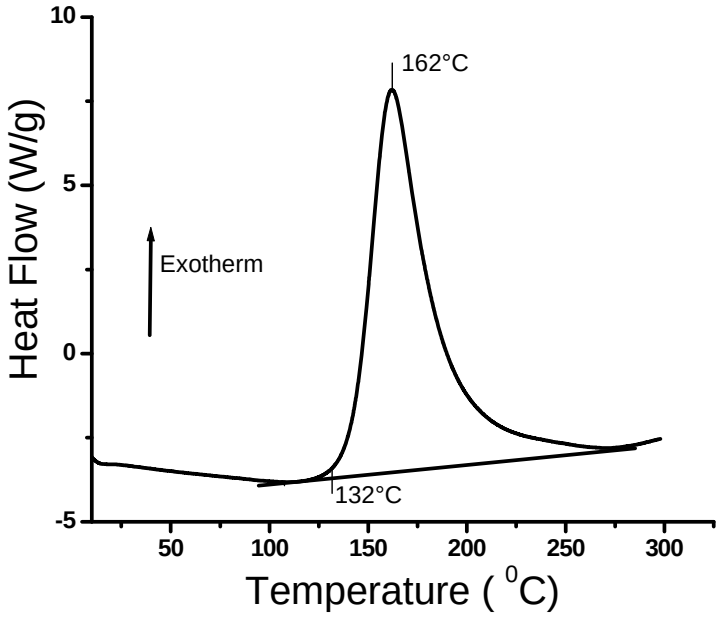

Figure A-I.3. DSC thermogram of as received uncured carbon/epoxy prepreg at a heating rate of 20°C min^{-1}.

To determine the fraction of epoxy content (a), TGA analysis was conducted at a heating rate of 20°Cmin^{-1} under both nitrogen and air environment to calculate the amount of carbon fibers, as shown in **Figure A-I.4**.

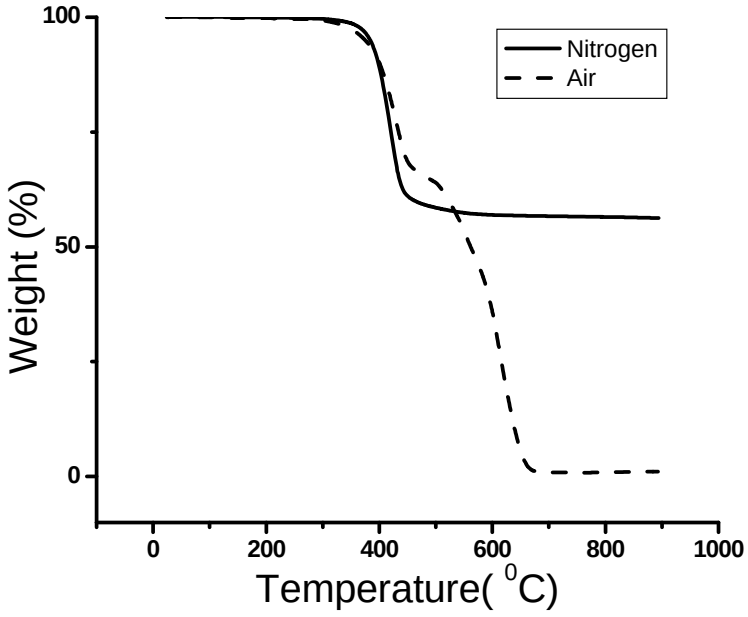

Figure A-I.4. TGA thermogram of uncured as received carbon/epoxy prepreg at a heating rate of 20°C min^{-1}.

Dynamic mechanical properties storage and loss factor of the cured samples were analyzed using DMTA instrument (Model DMS 210, Seiko Instruments). DMA was conducted on samples of dimension $20 \times 10 \times 2\ mm^3$, using a tensile fixture at a frequency of 1 Hz and a heating rate of 2°C min^{-1}. Under ideal conditions, the glass transition region is marked by a rapid decrease in the storage modulus and a rapid increase in loss modulus.

A-I.4: Results and discussion

A-I.4.1: Ultrasonic curing of samples

There are primarily four process parameters that can determine the time and extent of curing: horn oscillation amplitude (4.2-28.9 μm); normal force (20N- 1800N with a contact area of 1” × 0.6”) and traverse speed (3 to 100 inches/min); and temperature of platen, i.e., preheating temperature. Successful curing is dependent on the proper setup of these parameters. Amplitude determines the power (energy produced) of ultrasonic vibrations, while normal force affects the resin advancement during ultrasonic curing. Horn traverse relative to sample determines the sample-horn interaction time, affecting the degree of curing. It has been studied in Chapter 8 that one-part epoxy system requires certain activation energy to propagate the epoxy polymerization, and it was found to be at a preheating temperature of 100°C.

It was observed that lowest horn traverse speed (3 inches/min) allowed enough time of interaction between the sample and the ultrasound to produce highest degree of curing. In addition amplitude exhibited significant influence on ultrasonic intensity as well. Effect of amplitude on temperature rise can be seen in **Figure A-I.5.** It is evident that an increase in amplitude raised the temperature to facilitate the epoxy curing. Moreover, the amplitude more than 20.0 μm caused cracks in the interfacing aluminum sheet of carbon/epoxy samples possibly due to excessive ultrasonic energy. Therefore, amplitude of 20 μm and a traverse speed of 3”/min were found to be optimal for curing the samples.

After studying the effect of various ultrasonic parameters on curing, experiments were conducted to observe the spatial distribution of ultrasonic energy in the vicinity of the contact zone of horn and sample. To determine temperature from ultrasonic energy,

three thermocouples were embedded during prepreg laying up process according to schematics shown in **Figure A-I.6**.

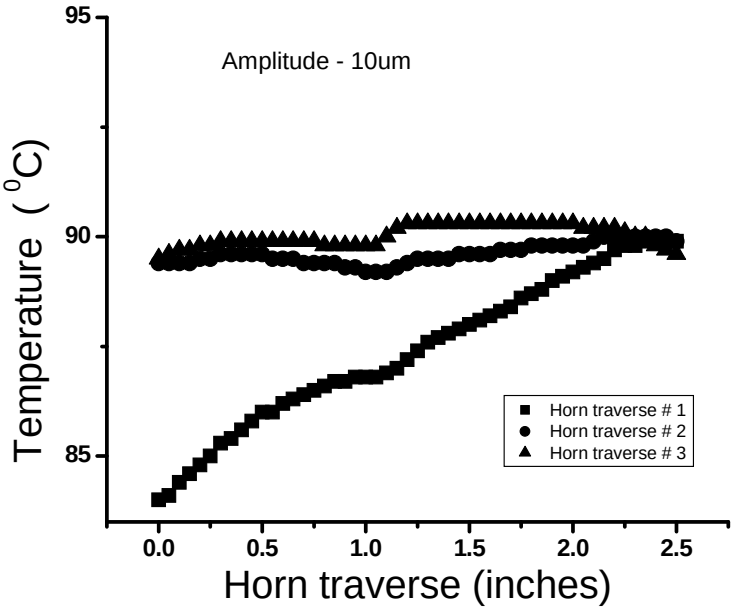

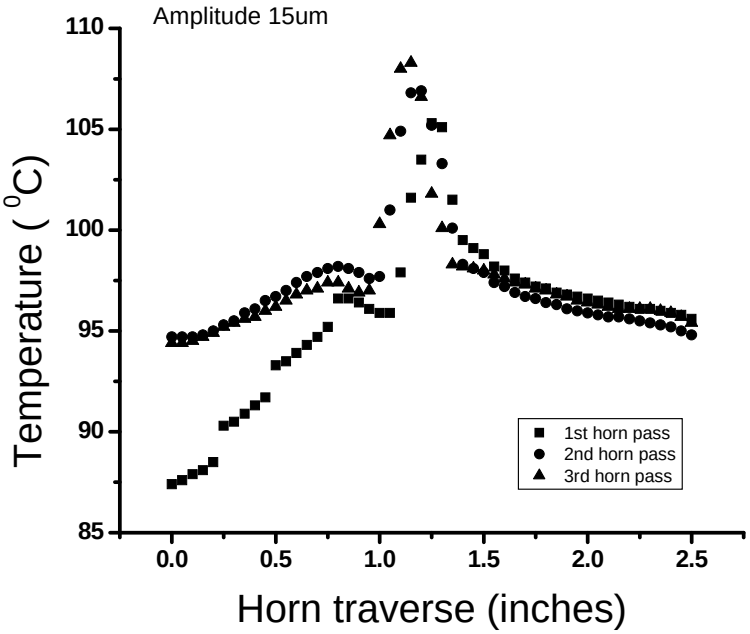

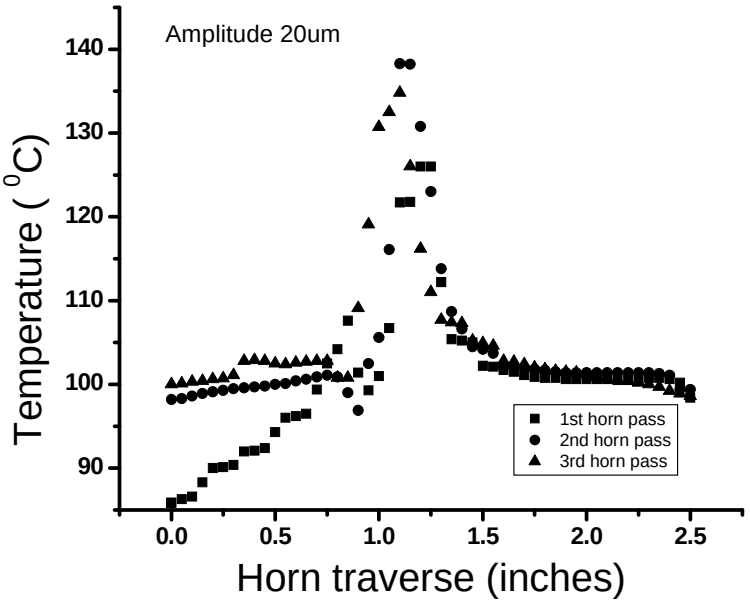

Figure A-I.5. Temperature profile under ultrasonic consolidation at various amplitudes with sample length--2.5 inch, preheating temperature--100°C, and horn traverse speed--3 inch min^{-1}.

The corresponding bell-shaped temperature profile due to ultrasonic curing can be seen in **Figure A-I.7** for 10 successive horn traverses. The short burst of temperature extended for approximately 10-14 seconds of horn single traverse time. This is similar to a pulsed (20-30% pulse duration) ultrasonic curing due to the stationary horn studied in Chapter 8, resulting insufficient time for heating and cooling.

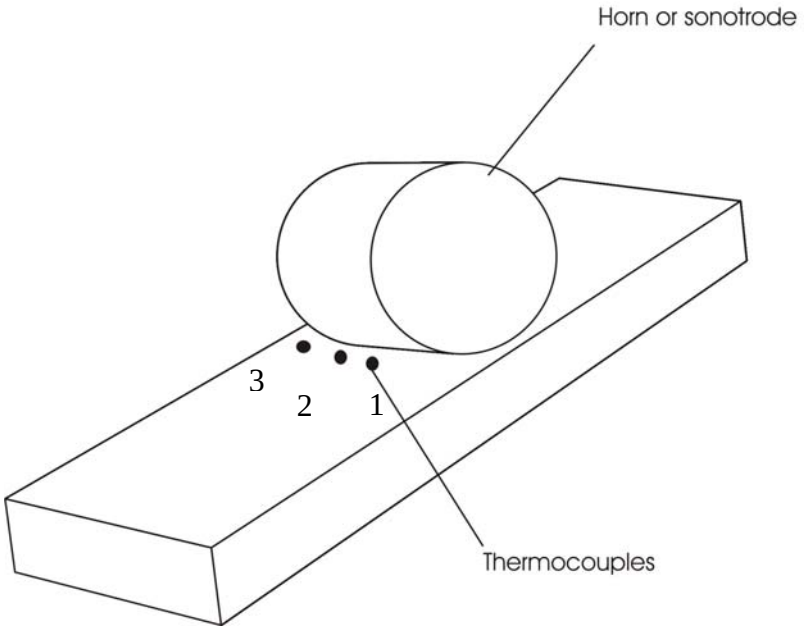

Figure A-I.6. Set up for monitoring the temperature profile at following ultrasonic conditions: amplitude--20um; horn traverse speed--3 inch/min; normal force--20N; temperature--100ºC; and length of the sample-- 2.50 inch.

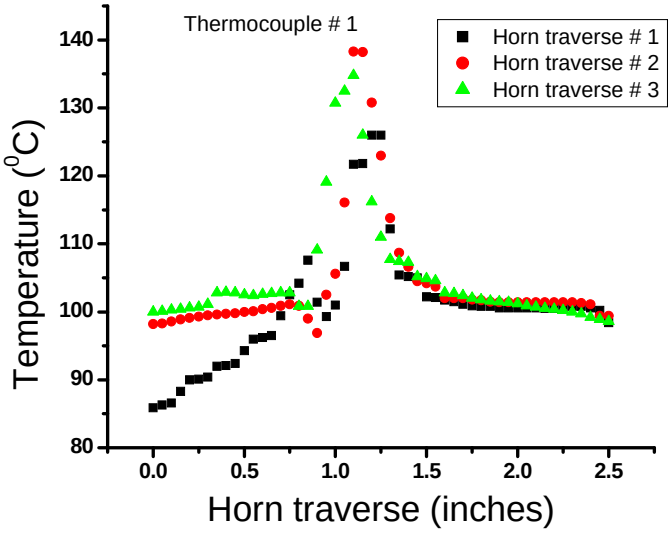

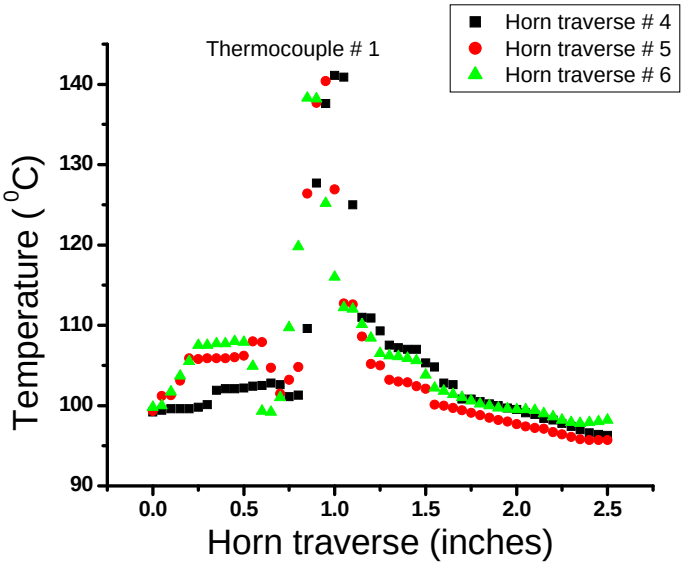
Thermocouple # 1
Horn traverse # 4
Horn traverse # 5
Horn traverse # 6
Temperature (^{0}C)
Horn traverse (inches)
90
100
110
120
130
140
0.0
0.5
1.0
1.5
2.0
2.5

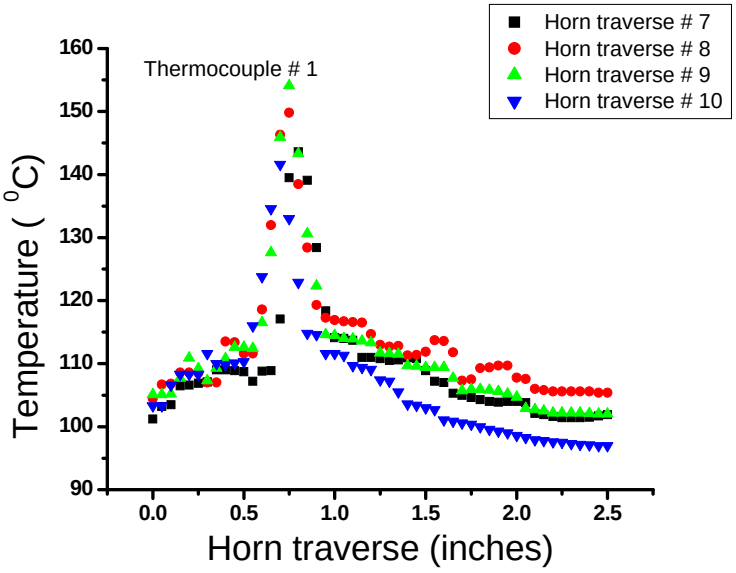
Thermocouple # 1
Horn traverse # 7
Horn traverse # 8
Horn traverse # 9
Horn traverse # 10
Temperature (^{0}C)
Horn traverse (inches)
90
100
110
120
130
140
150
160
0.0
0.5
1.0
1.5
2.0
2.5

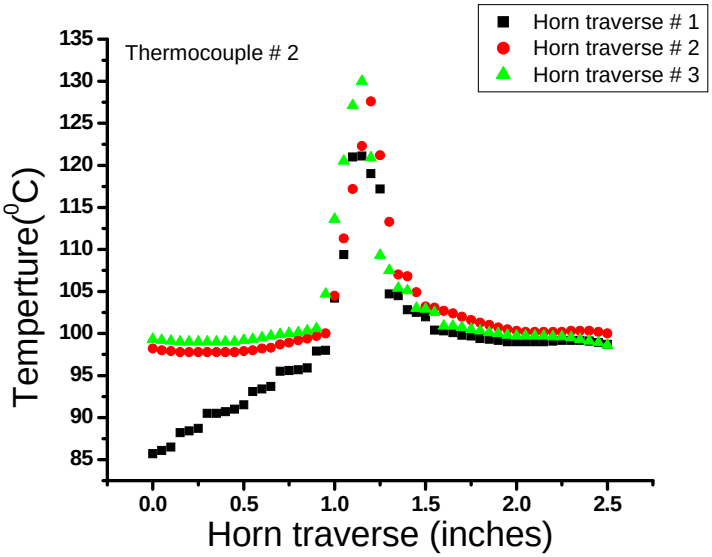
Thermocouple # 2
Horn traverse # 1
Horn traverse # 2
Horn traverse # 3
Temperture(0C)
Horn traverse (inches)

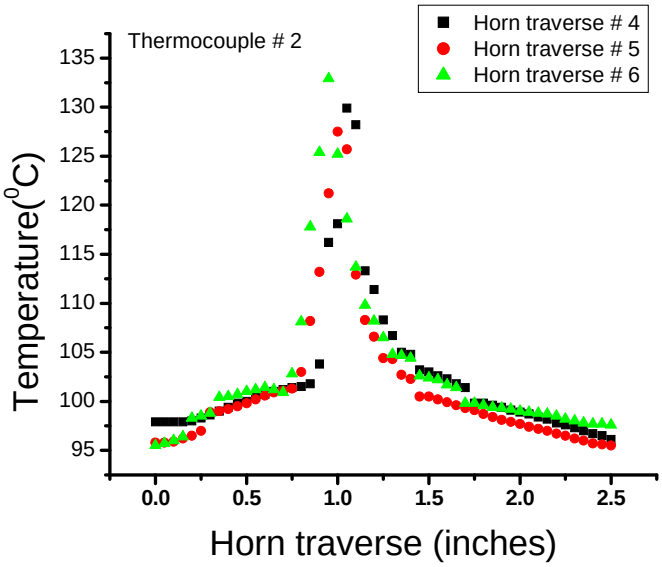
Thermocouple # 2
Horn traverse # 4
Horn traverse # 5
Horn traverse # 6
Temperature(0C)
Horn traverse (inches)

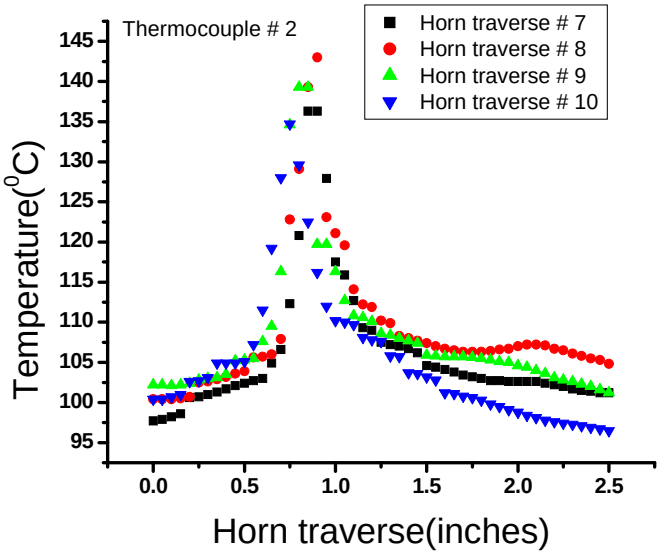
Thermocouple # 2
Horn traverse # 7
Horn traverse # 8
Horn traverse # 9
Horn traverse # 10
Temperature(°C)
Horn traverse(inches)
145
140
135
130
125
120
115
110
105
100
95
0.0
0.5
1.0
1.5
2.0
2.5

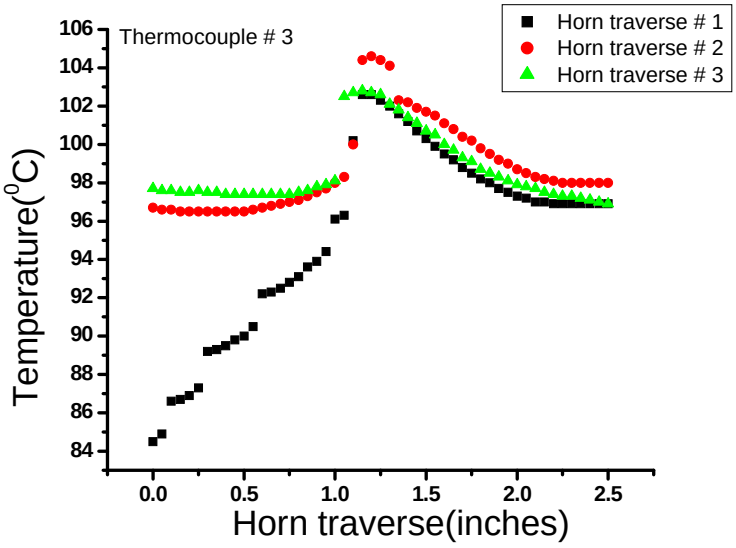
Thermocouple # 3
Horn traverse # 1
Horn traverse # 2
Horn traverse # 3
Temperature(°C)
Horn traverse(inches)
106
104
102
100
98
96
94
92
90
88
86
84
0.0
0.5
1.0
1.5
2.0
2.5

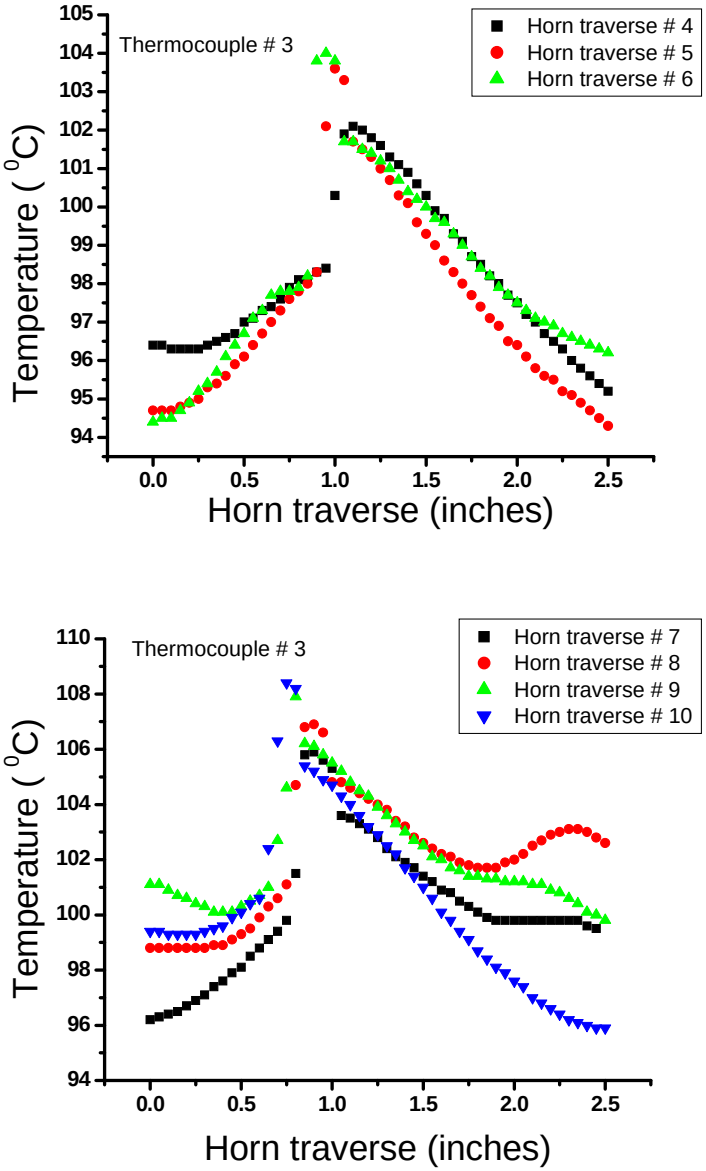

Figure A-I.7. Temperature profile under following ultrasonic conditions: amplitude—20 µum; horn traverse speed--3 inch/min; normal force--20N; temperature--100ºC; and length of the sample-- 2.50 inch.

In addition, it has been observed through the research reported in Chapter 8 that pulse ultrasonic process was more beneficial than continuous one to cure one-part epoxy

system. Moreover, this spike in temperature was enough to start epoxy polymerization without overheating the samples. However, temperature profile from the third thermocouple placed outside the edge of horn did not show this spike, suggesting a mild intensity of ultrasonic energy at the edges of the horn. Moreover, a dummy sample (fully oven cured sample) did not show any rise or spike in temperature, indicating a self-limiting effect of ultrasound. Subsequently, samples were produced at different number of repeating horn traverses to determine the kinetics of curing as shown in **Figure A-I.8.**

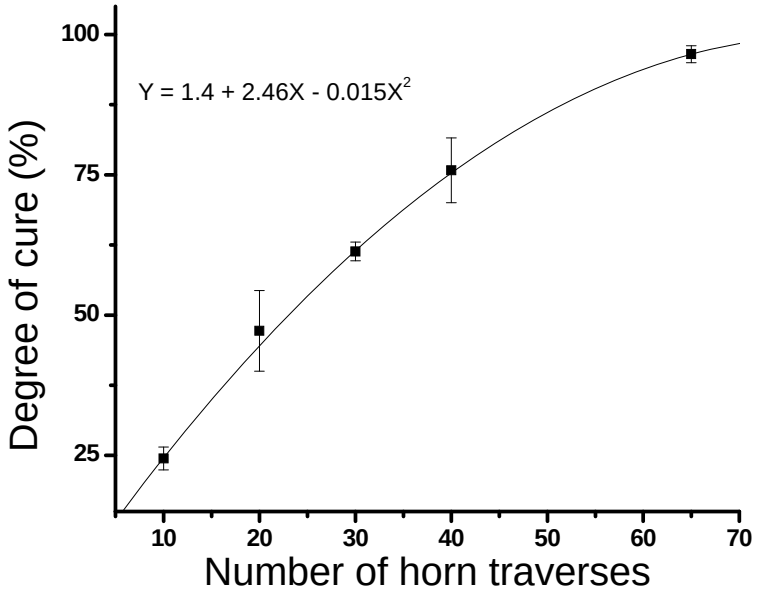

Figure A-I.8. Curing kinetics under following ultrasonic conditions: amplitude-20 μm; horn traverse speed--3 inch/min; normal force--20N; temperature--100ºC; and length of the sample-- 2.50 inch.

It can be seen that the degree of curing increased virtually linearly with the number of horn traverses till 40 traverses. During this time period, epoxy matrix

transforms to a gel state and subsequently to a densely crosslinked network. It has been observed by previous research that as the glass-transition temperature of the crosslinked network approaches to the curing temperature, material vitrifies, where uncured resin entraps in a glass state. The reaction at vitrification is controlled by the diffusion mechanism, making high energy ultrasound difficult to propagate the polymerization reaction at the same rate.[7] Because of this vitrification effect, the curing curve in **Figure A-I.8** deviated from the linear trend above 40 traverses. Therefore, once a good consolidated and crosslinked material is produced under ultrasound for smaller number of traverses (below 40), it would be prudent to go for post curing to develop final properties.

A-I.5: Conclusions

During this phase of the research, ultrasonic curing conditions horn amplitude, traverse speed and horn normal force, and preheating temperature were investigated to observe the curing kinetics. Bell shaped temperature spikes (maximum 150ºC) were observed during ultrasonic consolidation while going for repeating horn traverses. Based on this study, the application of the Solidica machine in its present configuration is limited by its relatively high normal force and minimum horn traverse speed.

A-I.6: References

[1] Zhou, G., PhD Dissertation (2007), The Ohio State University, Chapter 3, 111.

[2] Graham, L. J., Ahlberg, L. A., Cohen-Tenoudji, F., and Tittmann, B. R., Ultra. Symp. Pro. (1986), 2, 1013.

[3] Whitney, T. M., and Green, R. E., Mater. Sci. Forum (1996), 210/213, 695.

[4] Sharma, S., and Luzinov, I., PMSE Preprints (2006), PMSE-277.

[5] Liu, L., Huang, Y. D., Zhang, Z. Q., Jiang, B., and Nie, J., J. Appl. Polym. Sci. (2001), 81, 2764.

[6] http://www.solidica.com/technology_overview1.htm

[7] Kwan, K. M., and Benatar, A., Proceedings of Annual Meeting of the Adhesion Society (2001), 24, 245.